Chironomid-inferred summer temperature and lake development during the last interglacial-glacial cycle in central Europe

Inauguraldissertation
zur
Erlangung der Würde eines Doktors der Philosophie
vorgelegt der
Philosophisch-Naturwissenschaftlichen Fakultät
der Universität Basel
von

Alexander Bolland

2021

Genehmigt von der Philosophisch-Naturwissenschaftlichen Fakultät auf Antrag von

Oliver Heiri, Nikolaus Kuhn and Stefan Engels

Basel, 30.3.2021

The Dean of Faculty

Prof. Dr. Marcel Mayor

Table of Contents

Abstract

The last interglacial-glacial cycle represents an interval in which a broad range of climatic conditions forced landscape and ecosystem development in central Europe, and to date there is a sparsity of long, millennial scale, continuous palaeoclimatic records from the region. Palaeoclimatic reconstructions are essential to develop our understanding of how climatic forcing from internal and external variables, as well as associated climatic feedbacks, produced those landscape and ecosystem developments. This thesis aims to develop new mean July air temperature records covering large sections of the last interglacial-glacial cycle from central Europe in the pursuit of better understanding past climate development and climatic forcing by utilising the biotic proxy Chironomidae. Using sediment records from Burgäschisee, Swiss plateau, and Füramoos, southern Germany, records of chironomid assemblage change were developed, used to assess changes in the lake ecosystems and environments, and then implemented in a transfer function to quantitatively estimate change in July air temperature. For the Füramoos record this was achieved for the interval from ca. 127 to 49 ka while the Burgäschisee record covered the interval from ca. 18 to 14 ka. The chironomid assemblage as well as other associated chitinous invertebrate remains were utilised to qualitatively assess changes in temperature, nutrient state and organic content, and to a lesser extent changes in lake level. Further analysis using a transfer function enabled the quantitative estimation of mean July air temperature from the chironomid assemblages for the study intervals. The largest changes in mean July air temperature were associated with changes in northern hemisphere July insolation and major reorganisations of the local vegetation. These changes were at the mid to late Eemian transition at ca. 115–125 ka, the transition from MIS 5 to MIS 4 at ca. 84–76 ka. and the onset of the Bölling interstadial at ca. 16–14 ka. Furthermore, Stadials A and B in the Würmian, which are characterized by forest openings, were not found to be associated with major July air temperature changes and probably a result of decreases in mean temperature of the coldest month or precipitation.

List of Papers

The following doctoral thesis contains three papers, referred to by respective Roman numerals in text, and an introduction to and a summary of the work therein. At the time of submission Paper I (Bolland et al, 2020) was published, paper II was submitted and paper III was in the final stages of development with co-authors immediately prior to submission.

I Bolland, A., Rey, F., Gobet, E., Tinner, W. and Heiri, O., 2020. Summer temperature development 18,000–14,000 cal. BP recorded by a new chironomid record from Burgäschisee, Swiss Plateau. *Quaternary Science Reviews*, *243*, p.106484.

II Bolland, A, Kern, O., Allstädt, F., Koutsodendris, A., Pross, J., Peteet., D., and Heiri, O. Summer temperatures during the Last Glaciation (MIS 5c to MIS 3) inferred from a 50,000-year chironomid record from Füramoos, southern Germany. Submitted to *Quaternary Science Reviews* on 25/1/2021.

III Bolland, A, Kern, O., Becker, C, M., Koutsodendris, A., Pross, J., and Heiri, O. Climatic development of the Late Eemian and transition into the last glacial period described by a new chironomid record from Southern Germany. To be submitted to *Boreas*.

Contributions of first author, Alexander Bolland, and co-authors to individual thesis chapters.

Burgäschisee sediments used in Paper I were collected and stored by Willy Tinner, Erika Gobet, Fabian Rey and affiliates. Füramoos sediments were collected by Jörg Pross and affiliates. Sediment cores FU1/3 and Fu15-1/2 were stored at Heidelberg University under curation of Jörg Pross, Andreas Koutsodendris, Oliver Kern and Frederik Allstädt. The FURA cores were stored and curated at Lamont Doherty Earth Observatory and returned to Heidelberg by Dorothy Peteet and affiliates. Correlation and dating in Paper I was conducted by Fabian Rey. Oliver Kern correlated the FU1/3 and FURA cores to produce the new Füramoos composite core. Oliver Kern also correlated the composite to the record of Müller et al., (2003) and correlated the Fu15-1/2 cores to the composite core. Alexander William Bolland adjusted the correlations of Fu15-2 790-890cm core segment to the Füramoos composite core and the correlation of the Füramoos composite core to Müller et al., (2003). Alexander William Bolland developed the age depth model presented in this thesis that was used in Papers II and III. Project development in all papers was conducted by Alexander William Bolland and Oliver Heiri. Chironomid analysis and associated numerical analysis was conducted by Alexander William Bolland in all papers, as was the associated numerical analysis, excepting the total phosphorus reconstruction and reconstruction diagnostic statistics published in Paper I, which was conducted by Oliver Heiri. Oliver Heiri also produced the temperature reconstruction for Paper I, however it was replicated by Alexander William Bolland prior inclusion in the manuscript. Pollen analysis for paper I was conducted by Fabian Rey; Paper II, Oliver Kern and Frederik Allstädt and paper III, Oliver Kern. Loss on ignition data was produced by Oliver Kern and Frederik Allstädt (Paper II) and Alexander William Bolland (Paper III). X-Ray Fluorescence data and interpretation was developed by Oliver Kern (Paper II). Alexander William Bolland led the palaeoenvironmental interpretation of data, writing of all papers and developed all figures. Oliver Heiri applied for and received the funding for this PhD project supported by the Swiss National Science Foundation (SNF grant 200021_165494). All co-authors are acknowledged for reading and commenting on the manuscripts that they co-authored.

Co-authors of individual thesis chapters:
Andreas Koutsodendris (AK); Dorothy Peteet (DP); Erika Gobet (EG); Frederik Allstädt (FA); Fabian Rey (FR); Jörg Pross (JP); Oliver Heiri (OH); Oliver Kern (OK); Willy Tinner (WT).

1. Introduction to the thesis topic

Role of Proxy data in Palaeoclimatic Research

Understanding past climatic change is a fundamental component of the prediction of future climate. In the list of four World Climate Research Project scientific Objectives, Objective 1 is to advance fundamental understanding of the climate system and Objective 3 is to understand the long-term response of the climate system with an emphasis on climate dynamics (WCRP, 2019). This is essential as it places the phenomenon of anthropogenic climatic change in the context of long-term natural variability and highlights deviation from it (Kaufman et al, 2020a). Therefore, it is essential to develop understanding of how climatic changes are forced by internal and external variables and the responses of climatic feedbacks both regionally and globally. Furthermore, it is essential to assess how the climate system has as modulated the development of landscape, ecosystems and culture. For this reason, the development of climatic reconstructions from a range of climatic and environmental conditions are a necessity, however those conditions do not necessarily exist in the present, highlighting the utility of archives of past environmental and climatic change.

Proxy-based reconstructions of past climates are essential for understanding how our climate system was forced in the past and how it developed, as well as for describing its long-term variability (Clark et al, 2001; 2012; Kaufmann et al, 2020b). The results of proxy-based palaeoclimatic reconstructions have previously been used to assess the results of climatic models (Renssen and Isarin, 2001; Heiri et al, 2014a; van Meerbeeck et al, 2011; Marlon et al, 2016) and also incorporated into model simulations of past climate change (Hubbard et al, 2006; Lischke et al, 2013; Seguinot et al, 2018). In order for proxy-based reconstructions to be used in the development of model simulations of global climatic change, large and geographically extensive datasets encompassing regional temperature patterns are necessary for the evaluation of model performance against climate reconstructions (Heiri et al, 2014b). In a recent publication a database of 1319 high resolution, well dated Holocene temperature records (Kaufmann et al, 2020a) was used to develop a global mean surface temperature (GMST) reconstruction for that interval (Kaufmann et al, 2020b). In doing so the GMST reconstruction confirmed and highlighted the discrepancy between global climate models and proxy-based reconstructions for the Holocene, earlier referred to as the "Holocene temperature conundrum" (Liu et al, 2014) highlighting the power of multi-proxy reconstructions. The example of Kaufmann et al., (2020a; 2020b) sets a target to work towards when developing similar studies that aim to cover the entire last interglacial-glacial cycle.

In order to work towards developing regional or even global reconstructions of climatic change for the last interglacial-glacial cycle such as the Kaufmann et al., (2020b) GMST reconstruction, far more records need to be produced for the interval on both a local and regional level. Heiri et al., (2014a) highlight six strategies for the development of major advancements for quantitative climate reconstructions in the Austrian and Swiss alpine region for the late Quaternary period, overlapping the geographical range of study sites to be incorporated into this thesis. Of these strategies this thesis will address two in particular, strategies 2. replication and the production of regional reconstructions of past climatic change and to a lesser extent, 3. cross-validation of different proxy types and approaches. This is achieved herein by the development of new palaeoclimatic records of chironomid-based July air temperature change for the last interglacial-glacial cycle. The new records are compared with existing records of summer temperature change based primarily on beetle assemblages and pollen assemblages, previously published within the same study region.

Regional and temporal setting

The last interglacial-glacial cycle represents an interval in which there were major changes in climatologically relevant variables including ocean circulation (Bauch et al, 2012), insolation (Berger and Loutre, 1991) and greenhouse gas concentrations (Petit et al, 1999; Spahni et al, 2005). Encompassed within this variability is a broad range of climatic conditions from full interglacial to full glacial climate. This interval is globally defined by Marine Isotope Stages (MIS), spanning from the beginning of MIS 5e dated to 130 ka to the end of MIS 2 dated to 14 ka, based on a stack of 57 globally distributed benthic $\delta^{18}O$ records marine sediment cores (Lisiecki and Raymo, 2005). The onset of MIS 5e, the last interglacial interval (Past Interglacials Working Group of PAGES, 2016), was initiated by large scale deglaciation and ice sheet collapse (McKay et al, 2011) associated with increasing northern hemisphere summer insolation (Berger and Loutre, 1991) and CO_2 and CH_4 concentrations rising on the global scale (Petit et al, 1999) culminating in peak interglacial warmth 1-2°C higher than pre-industrial values globally (Turney and Jones, 2010; Masson-Delmotte et al, 2013; Otto-Bliesner et al, 2013). The subsequent transition from full interglacial conditions to the beginning of the glacial period is globally associated with the transition from MIS 5e to MIS 5d at ca. 116 ka with glacial conditions prevailing globally until the onset of MIS 1 at ca. 14 ka (Lisiecki and Raymo, 2005; Past Interglacials Working Group of PAGES, 2016). The glacial interval was characterised by major continental glaciation (Hughes et al, 2013; Hughes and Gibbard, 2018) and decreasing sea levels (Waelbroeck et al, 2002; Spratt and Lisiecki, 2016) culminating in the Last Glacial Maximum (LGM) dated globally to ca. 18 to 24 ka (Mix et al, 2001) after which ice sheets began to collapse (Lambeck et al, 2000).

Within the north Atlantic region there were dynamic changes of the climate system during the last interglacial-glacial cycle. These include variations in Atlantic Meridional Overturning Circulation (AMOC; Clark et al, 2012; Stern and Lisiecki, 2013), ice-rafting events (Bond et al, 1997; Chapman and Shackleton, 1999, Hibbert et al, 2010), sea surface temperature changes (Martrat et al, 2007; Sánchez Goñi et al, 2008) and air temperature changes (Johnsen et al, 2001). Regional climatic changes in the North Atlantic Ocean are often reflected both marine and terrestrial records of vegetation change in the circum-north Atlantic region (Sánchez Goñi et al, 2008; Fletcher et al, 2010). For central and north western Europe, the last interglacial (the Eemian; ca. 126 - 110ka; Shackelton et al, 2003), is locally identified as a heavily forested interval between the more open landscapes of the penultimate glaciation (in central Europe called the Rissian) and the first forest opening phase of the following glacial period (Turner and West, 1968). The last glacial period (in central Europe named the Würmian; 11.7 - 110ka, Shackelton et al, 2003; Rasmussen et al, 2014) is divided into a series of stadial and interstadial intervals that can often be observed in central Europe as intervals forest opening and forest closing respectively (Woillard, 1978; de Beaulieu and Reille, 1984; Müller et al, 2003; Fletcher et al, 2010). However there is a general trend of increased continentality (Caspers and Freund, 2001) throughout the Würmian.

For Europe, north of the Alps, long continuous palaeotemperature records based on biological proxies covering the entire last interglacial-glacial cycle are rare. Sites in areas that were glaciated during the Last Glacial Maximum (LGM) have chronological constraints of ca. 14,500-18,000 calibrated radiocarbon years BP (cal. BP) for their lowermost dates (Magny et al, 2006; Wehrli et al, 2007; Millet et al, 2012). Furthermore, in many sites in central and northwest Europe that were not glaciated, a dry climate (Hoek and Bohncke, 2001) limited the number of lakes and therefore the number of palaeolimnological records that are currently available. Therefore, long continuous reconstructions covering the entire interval are extremely valuable such as the long, millennial-scale pollen records from e.g., La Grande Pile (Woillard, 1978) and Les Echets (de Beaulieu and Reille, 1984). These records, among others, have been used to develop annual, summer and winter temperature reconstructions as well as reconstructions of annual precipitation (Guiot et al, 1989; Klotz et al, 2004; Kühl, et al, 2007). Further examples of biotic proxies used to reconstruct climate change in the last interglacial-glacial cycle include the faunal proxies chironomidae and coleoptera. Both chironomids and coleoptera have both been used to reconstruct summer temperature change on a millennial scale over large sections of the last interglacial-glacial cycle in this region, with coleoptera being used to reconstruct winter temperatures also (Ponel, 1995; Walkling and Coope, 1996; Behre et al, 2005; Engels et al, 2008). Due to the limited temporal coverage of individual records however it may be necessary to utilise multiple

records to produce a complete picture of palaeotemperature development using multiple proxies (e.g. Heiri et al, 2014a). The reconstructions available for the last interglacial-glacial cycle from central Europe display a clear trend towards cooler temperatures following the Eemian and declining to a minimum at the LGM. This long term cooling trend is interrupted by several stadial and interstadial coolings and warmings (Guiot et al, 1989; Ponel, 1995; Kühl, et al, 2007; Heiri et al, 2014a).

Chironomids as a proxy of July air temperature

Chironomids are good indicators of environmental conditions in lakes, and have been recognized as such for over a century (Thienemann, 1921). They are an important biotic proxy for the development of quantitative July air temperature reconstructions from past climatic intervals (Brooks et al, 2007). The Chironomidae are a family of flies in the order Diptera, of which there are ca 10,000 species worldwide (Armitage et al, 2012). The majority of those species lay egg masses in lakes and other aquatic systems. They then live through four larval stages, the first stage being planktonic and stages two through four generally being benthic or epiphytic, followed by a pupal stage before the emergence of the adult fly (Walker, 2001). In lakes, particularly shallow ones, the composition of larval chironomid assemblages is closely related to summer temperature (Eggermont and Heiri, 2012). The chitinous head capsules of chironomid larvae preserve in high abundances in lake sediments, being identifiable to the generic or morphotype level (Brooks et al, 2007). These characteristics make them a suitable biotic proxy for use in palaeoecological and palaeoclimatic interpretations (Brooks et al, 2007) as well as implementation in quantitative July air temperature reconstructions (Langdon et al, 2008; Luoto, 2009a; 2009b; Larocque et al 2001; Heiri et al, 2011). This is an approach that has been used frequently for the Lateglacial interval (e.g., Brooks and Birks, 2000; Heiri and Millet, 2005; Tóth et al, 2012; Bolland et al, 2020) and less often for the older intervals during or prior to the LGM, e.g., in eastern Germany (MIS 3: Engels et al, 2008), northern Italy (LGM: Samartin et al, 2016) and northern Finland (MIS 5d–c, MIS-3; Helmens et al, 2009; 2012; Engels et al, 2010; 2014). These examples, while providing valuable and much needed data describing temperature change for their respective intervals, are often representative of only segments of the last interglacial-glacial cycle/transition and therefore individually their use in assessing long term millennial-scale changes in ecosystem or climatic development is limited.

Thesis Objectives

This thesis has set out to produce new chironomid-based July air temperature reconstructions covering large and previously understudied intervals of the last interglacial-glacial cycle. By using sediments from Burgäschisee, Swiss plateau, and Füramoos, Southern Germany, the project aims to contribute to the development of a continuous "millennial-scale" record that will facilitate better understanding the magnitude, timing and effects of climatic change for last interglacial-glacial cycle in central Europe. In order to achieve this aim, there are three primary objectives set out:

- **Objective 1:** Produce new "millennial- scale" central European chironomid records spanning large sections of the last interglacial- glacial cycle.

- **Objective 2**: Use the new chironomid records to infer lake development and within lake changes in ecology at the two studied sites.

- **Objective 3:** Use the new chironomid records to infer quantitative estimate of July air temperatures.

2. Study sites

The study sites of this thesis are from the Swiss plateau and the German Alpine forelands, both of which are located in central Europe (Figure 1). There is a long tradition of the development of palaeoclimate records from the last glacial to Holocene interval from the Alpine region (Heiri et al, 2014a) and there are several classical studies of the last interglacial-glacial interval in the wider central European region from Germany (e.g. Samerberg: Grüger, 1979; Eurach: Beug, 1979; Jammertal: Müller, 2000 and Füramoos: Müller et al, 2003), France (e.g. La Grande Pile: Woillard, 1978; Les Echtes: de Beaulieu and Reille, 1984) and Switzerland (e.g. Beerenmosli: Wegmüller, 1992; Meikirch II: Welten, 1988).

Both the Burgäschisee and Füramoos sites that are the focus of this thesis are products of glacial processes. For Burgäschisee, situated between the Jura mountains and the Alps (Figure 1), the westward retreat of the Rhone glacier left a deposit of old ice that was subsequently surrounded by and possibly inundated by glacial silts. The melting of this ice left a depression in the landscape that filled with water forming the lake (Guthruf et al, 1999). Conversely, the Füramoos palaeolake has undergone full succession into a modern forest and is situated on the alpine forelands of southern Germany (Figure 1) in a small basin between two glacial moraines that formed during Rissian glacial period (Schreiner, 1992). Subglacial erosion created a depression in which the palaeolake formed and the sediments were subsequently protected from erosion by glacial meltwater by the Moraine ridges (Figure 1; Müller et al, 2001).

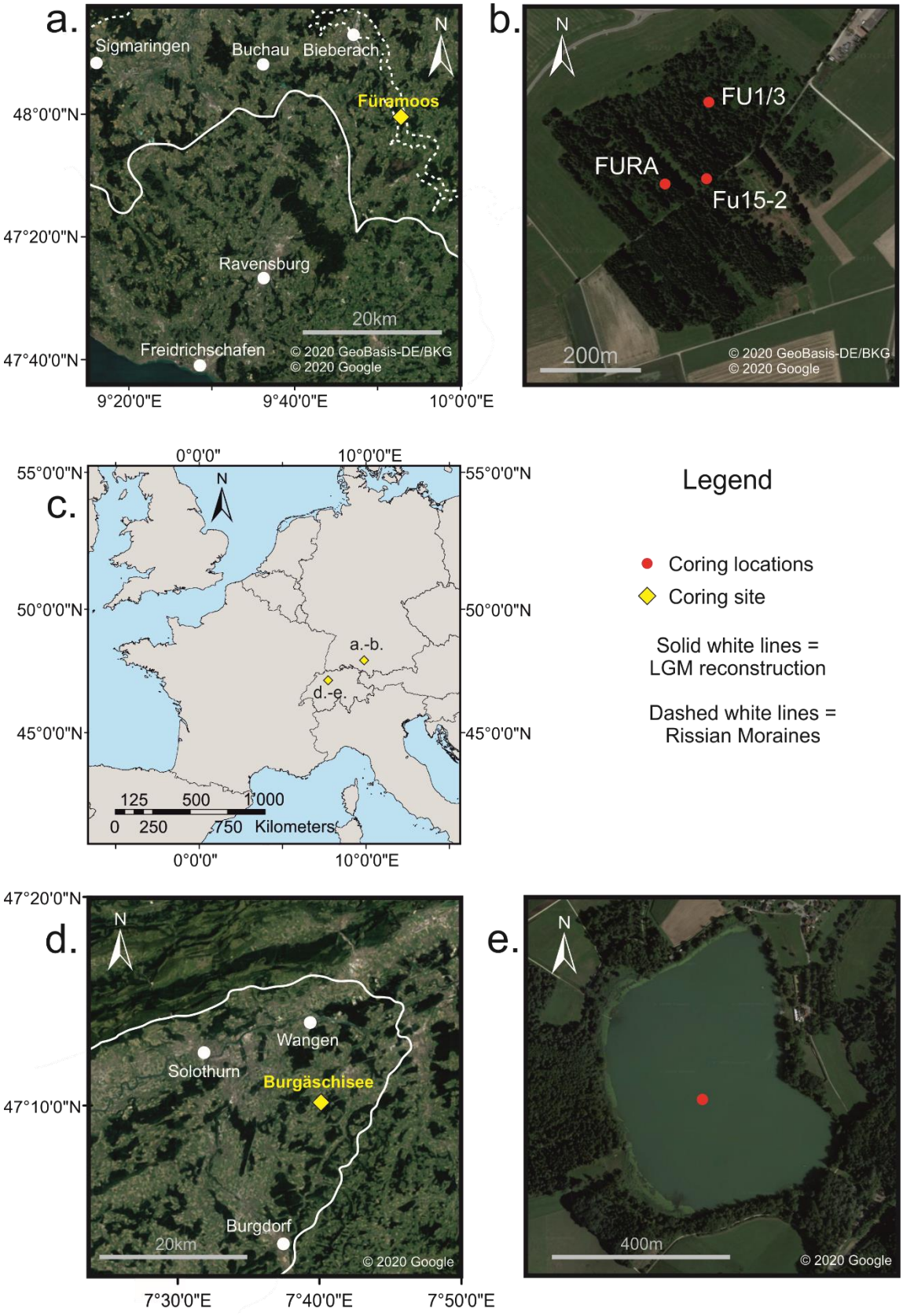

Figure 1: Overview of study locations used in this thesis. a-b. Füramoos; c. Füramoos and Burgäschisee sites in European context and d-e. Burgäschisee. Rissian moraines plotted in a. digitised from Kern et al., (2019) and originally derived from Müller (2001). LGM in a. digitised from Kern et al. (2019) and originally derived from Schreiner (1992). LGM reconstruction in d. digitised from Bini et al., (2009).

3. Methodology

Coring, core correlation and dating

Sediments cores from Burgäschisee were obtained in two coring campaigns on September 2009 and April 2014 by the Paleoecology group from the Institute of Plant Sciences, University of Bern. The cores were taken from the deepest part of the lake using a UWITEC prison corer and reaching a sediment depth of 15 m. Sediment cores Burg A-C were taken in the first campaign and Core I in the second, to fill a gap existing in the cores Burg A-C. Correlation of the Burgäschisee cores was developed by Rey et al., (2017) and the adapted age depth model that we used is described in Paper I (Bolland et al, 2020). This adapted model used a combination of palynostratigraphy and 14C dating in order to date the Lateglacial sections of the Burgäschisee core.

There were a total of three coring locations in the Füramoos site from which chironomid samples were taken, the Fu15-1/2 cores, the FU1/3 cores and the FURA cores (Figure 1). Correlation of the core segments was undertaken by Institute of Earth Science, Heidelberg University (Kern et al, 2019; in progress) who produced a continuous composite core covering the interval from the Rissian Lateglacial to the Bellamont 1, 2, 3 complex, to which the Fu15-1/2 cores were correlated. Paper II outlines how the sediment cores FU1/3 and FURA were correlated to develop the Füramoos composite core for the early to mid-Würmian. The correlation of the Fu15-2 core segment 790-890 cm (analysed in Paper III) to the Füramoos composite core was achieved based on LOI and palynostratigraphy (Appendix 1). As described in Papers II and III, the Füramoos composite core age depth model used in this thesis was determined by the correlation of the composite core to Müller et al., (2003) via palynostratigraphy, and the age constraints provided by this publication were used. These correlations are presented for the entire Füramoos composite core in Appendix 2 alongside the Füramoos composite core age depth model used in this thesis.

Chironomid Analysis

Chironomid samples were taken at variable resolutions from their respective sediment cores, ranging from every 2-12cm based on the available chronological information (Paper I, Bolland et al, 2020; Papers II, III; Appendix Figure 1) in order to achieve a “millennial-scale” resolution. The volume of sediment used ranged from 0.5 to 20cm^3 depending on chironomid concentrations in those samples.

Sediments were sieved in 100 and 200µm mesh sieves in many instances following chemical pre-treatment outlined in the respective papers. All chemical pre-treatments used are variations of the method outlined in Brooks et al., (2007) in which the sediments are deflocculated using 10% KOH solution, using different temperature 10% KOH and time intervals of sample immersion, based on the difficulty of processing the sediments. Following sieving the chironomid samples were picked from a Bogorov tray under stereomicroscope (30 - 50 x magnification) along with other aquatic remains. Samples were air dried and mounted in Euparal mounting medium using a compound microscope at 40 - 100 x magnification. In order to achieve the minimum recommended chironomid head capsule counts of 45 - 50, a minimum of 80 head capsules per cm^3 were aimed for (Heiri and Lotter, 2001; Larocque, 2001; Quinlan and Smol, 2001). Some samples contained less than the minimum recommended counts and so in several instances adjacent samples were joined to achieve the required head capsule counts (see Paper I, Bolland et al, 2020; Papers, II and III). Head capsules with a complete mentum or more than half were counted as one chironomid and head capsules with a half mentum were counted as one half (Appendix Figure 3). Head capsules with less than half a mentum were disregarded. Other invertebrate remains were also counted based on minimum number of individuals present in the sample including *Daphnia*, Sialidae, Ceratopogonidae, oribatid mites, Ephemeroptera, Trichoptera, Plecoptera, Tipulidae, *Triops* and *Plumatella* resting cysts. Characeae Oogonia were also counted. Over the course of this thesis a total of 245 samples were processed for chironomid analysis.

Quantitative temperature reconstructions were developed using a chironomid-temperature inference model based on the Swiss-Norwegian calibration dataset based on modern surface-sediment samples from 274 lakes in Switzerland and Norway (Heiri et al, 2011). The dataset describes the distribution of 154 chironomid taxa and covers a July air temperature gradient of 3.5 to 18.4°C and mean July air temperatures were estimated from the fossil datasets using a two-component weighted averaging partial least squares model (WAPLS; ter Braak and Juggins, 1993; ter Braak et al., 1993). Due to some samples in the new chironomid record being at a different taxonomic resolution to the Swiss-Norwegian calibration dataset some samples needed to be aggregated to a slightly lower taxonomic resolution, both in the fossil data and the calibration dataset (see Paper I, Bolland et al, 2020; Papers, II and III). Furthermore, some few taxa were excluded from the model because they were not present in the calibration dataset. Papers I (Bolland et al, 2020), II and III detail further reconstruction diagnostic statistics that were used to describe and assess the reliability of the temperature reconstructions.

4. Summary in Brief in Relation to the Thesis Objectives

Objective 1: Produce new "millennial- scale" Central European chironomid records spanning large sections of the last interglacial-glacial cycle.

There were a total of 245 chironomid samples analysed in Papers I (Bolland et al, 2020), II and III of which 221 contained high enough concentrations of chironomds to use in further analysis featuring a total of 56 chironomid types in the Burgäschisee sequence and 84 types in the composite Füramoos sequence. Following the joining of samples to increase count numbers and omission of samples with counts that were too low, there were a total of 203 chironomid samples utilised in this thesis. The age depth models indicated that for those intervals covered by the two analysed chironomid records a millennial scale resolution was achieved. Furthermore, large intervals of the chironomid record achieved a "centennial-scale" resolution exceeding the millennial scale resolution outlined in Objective 1. However, large sections of the last interglacial-glacial cycle, are not covered by the new data. Notably the onset of the Eemian and early Eemian are absent from the Fu15-2 core and the late MIS 3 and most of MIS 2 (ca. 18-50 ka) are not covered by the new reconstructions. In the case of the Early Eemian, the absence is a result of an unconformity within the Fu15-2 core, the details of which are explored thoroughly in Paper III. Future analyses on other Füramoos sediment cores may possibly be able to fill this gap in the available temperature reconstruction. For the later section there is an hiatus from ca. 40-18 ka in the Füramoos record resulting from pronounced morphodynamics during the last glacial (Müller et al, 2003) which could not be analysed. The early Lateglacial and the interval between ca. 40-50 ka were present in the Füramoos cores according to pollen data. However, there were no chironomids, presumably because the lake was too unproductive to support diverse and abundant chironomid assemblages.

There were several challenges in the development of the chironomid records and the first of these was sediment processing in large intervals of the Füramoos cores. In many samples the sediments consisted of a highly compacted, very organic material that could not be sieved easily in spite of relatively harsh chemical treatments (Papers II and III). In an ideal sample, all sediment surrounding and within the remains would be sieved away leaving only the chironomid head capsules and other associated remains. However, for the depths 844-813cm corresponding to the Eemian interglacial in the Fu15-2 cores very little to no sediment was removed. Similarly, samples from the following Brörup

interstadial and first part of the Odderade were difficult to process and very little sediment was removed by sieving. This resulted in three problems for these samples. Firstly, the material that was "sieved" or rather, broken into slightly smaller pieces, remained in the sample. As a result, when manually picking chironomids from the Bogorov tray, all of that sedimentary material remaining needed to be sorted through to find the invertebrate remains. This process was incredibly time consuming, in some instances taking two working days to pick an entire sample containing relatively low concentrations of chironomids.

Secondly, when picking chironomids all specimens in a sample should ideally be counted in order to obtain a complete picture of the chironomid assemblage. With such a large volume of sediment to pick through, the number of chironomids missed during this phase was likely to have been higher than had there been no remaining sedimentary matrix, despite all best efforts. Larger chironomids are easier to spot than smaller chironomids when picking and therefore the number missed may have been disproportionate and have had some influence on the resulting temperature reconstruction.

Finally, as a result of the aforementioned highly compacted, very organic material, many chironomids were damaged during the sieving and picking process. The specific issues are discussed in detail within Papers II and III. In summary, the loss of identifying features led to some loss in taxonomic resolutions in raw data (e.g. certain Tanytarsus morphotypes). A similar scenario was also observed in the Burgäschisee core (Paper I, Bolland et al, 2020), although in this instance presumably due to damage due to sieving samples in highly inorganic sediments. In all instances the issue was related to the genus *Tanytarsus* either missing mandibles, antennal pedestals or both. The WAPLS regression model used for all papers in this thesis has been suggested to perform better when the chironomid assemblage data is at the highest possible taxonomic resolution (Heiri and Lotter, 2010). A further study using live chironomid assemblages also suggests that higher taxonomic resolution facilitates inferences of more subtle environmental changes (Greffard et al, 2011). Therefore for some sections of the analyzed records, Tanytarsus specimens without diagnostic features such as antennal pedestals or mandibles were assigned to specific morphotypes based on the proportion of the identified specimens which had these structures.

Objective 2: Use of the new chironomid record to infer lake development and within lake changes in ecology.

Prior to implementing a chironomid-based temperature reconstruction it is important to determine how the lake from which chironomid assemblages were sampled developed over time. Understanding the in-lake changes in ecology is an essential component to the determination of, how variables other than temperature have affected the chironomid assemblage and also whether or not a chironomid-based temperature reconstruction is suitable for the given record. Temperature drives chironomid assemblages both directly, through mediating development, emergence and respiration of individual chironomids and indirectly by forcing in lake changes such as thermal stratification strength and oxygen availability, as well as nutrient availability (Brodersen and Quinlan, 2006; Eggermont et al, 2012; Dickson and Walker, 2015). Any changes in these environmental conditions unrelated to temperature change could possibly lead to a change in reconstructed temperature and therefore a possible bias in the reconstruction when the assemblage data is used in the transfer function model. In all three papers presented here, changes in the chironomid assemblage are interpreted to constrain changes in in-lake environments such as trophic state, oxygen and water table changes, and to assess whether shifts in chironomid assemblage composition actually agree with expected changes due to temperature change. These interpretations are supported by analyses of additional invertebrate remains preserved in the sediment cores such as Sialidae, Ceratopogonidae and oribatid mites, as well as LOI data and pollen assemblages to evaluate any confounding variables that might affect a subsequent temperature reconstruction (Juggins, 2013).

The most prominent example of how essential this step is relates to the occurrence of *Corynocera abmigua* in the analysed records. This species has been observed to occur *en masse* both in modern surface samples (Brodersen and Lindegaard, 1999) as well as dominating fossil assemblages (e.g. Heiri and Millet, 2005; Larocque-Tobler et al, 2010; Paper, II and III). Although occurring within the temperature range of 6.8 to 12.9°C in the Swiss-Norwegian calibration dataset (Heiri et al, 2011) *Corynocera abmigua* does not show a clear relationship with temperature in arctic and subarctic environments (Olander et al, 1999) and has been observed to occur in warm lowland lakes in Denmark (Brodersen and Lindegaard, 1999). High abundances of *Corynocera ambigua* in the Füramoos record, reaching higher than 65% in some samples represent a situation which is difficult to interpret climatologically and temperature values reconstructed from such samples should only be reconstructed with caution. Such samples in the analysed records were also associated with “poor”

goodness of fit with temperature as indicated in both Papers II and III and the implications of this are explored therein.

A further example of how we addressed the issue of confounding variables is presented in Paper I (Bolland et al, 2020) where we explore the possibility of lake nutrients level change influencing the chironomid assemblage. To do this we utilised a dataset of chironomid surface samples from 28 deep stratified European lakes from Lapland to Southern Italy (Verbruggen et al, 2011) to assess changes in the fossil chironomid assemblages that would be typical for variations in Total Phosphorus (TP) concentrations in modern lakes. In brief, a semiquantitative reconstruction of TP was achieved by passively plotting the Burgäschisee chironomid assemblage data in a Detrended Canonical Correspondence Analysis (DCCA) of the training set data using TP as the only constraining variable (Bolland et al, 2020). As the lakes in the modern dataset are deep and stratified the chironomid assemblages are largely decoupled from direct effects of surface water and air temperatures and therefore the changes in the DCCA axis 1 scores are considered to be representative of changes in nutrient conditions. By utilising this method we were able to differentiate indicated changes in the chironomid assemblage composition typical for changes nutrient conditions from those typical for changes in temperature.

Objective 3: Use the new chironomid record to infer a quantitative estimates of July air temperature.

The chironomid-based temperature reconstructions from all three manuscripts is presented in Figure 2. The three sample running average of temperature reconstruction results varies between 7.5 -16 °C over the study intervals with the lowest temperatures associated with the Rissian Lateglacial (7.5 – 8 °C) and the highest temperatures associated with the Early Odderade (16 °C). In general reconstruction diagnostic statistics indicated a “good” goodness of fit to temperature however there are several samples, primarily in Paper II, that have “no good” or “no close” modern analogues. This is not necessarily problematic as one of the strengths of WA-PLS regression, the method used for the temperature reconstructions, is that it performs relatively well in non-analogue situations (Lotter et al, 1999). However, as indicated above, samples with a high proportion of *Corynocera ambigu*a and a poor fit with temperature are difficult to interpret palaeoclimatologically and inferences from such samples should only be interpreted with caution.

A first key finding of this thesis is that forest opening is not necessarily associated with decreasing July air temperatures. Stadials A and B are intervals of forest opening in the Füramoos cores characterized the increase of steppic vegetation types including *Artemisia* and Poaceae (Müller et al, 2003; Helmens et al, 2014 and references therein; Paper II and III). More broadly, Stadial A is correlated to the Herning and Melisey I stadials while Stadial B is correlated to the Rederstall and Melisey II stadials (Helmens et al, 2014). At Füramoos, vegetation changes during Stadial A and Stadial B do not appear to have been driven by decreases in July air temperature. For Stadial A, although its onset is associated with a 1.5 - 2 °C July air temperature decrease, temperature decreases alone do not appear to be sufficient to force forest opening. Temperatures during Stadial A vary between 12 - 13°C and are very similar to the range of reconstructed temperatures of 12 - 13.5°C that prevailed for most of the Late Eemian which was characterised by a boreal forest dominated by *Pinus* and *Picea* (Beck et al, 2016; Caudullo et al, 2016; Durrant et al, 2016). As temperatures during most of the Late Eemian and Stadial A were in the same range, yet are associated with different vegetation types, this suggests that an environmental variable other than temperature was driving the vegetation assemblage. Similarly, reconstructed Stadial B temperatures of 13.5 - 14°C are very close to those of the mid-late Brörup of 14°C. However the Late Brörup forest opens from 90-100% arboreal pollen to 50-75% arboreal pollen in Stadial B (Figure 2). This evidence presented in Papers II and III suggests that forest openings during Stadial intervals A and B were largely independent of July air temperature. In Papers II and III we discuss which climatic variables could have forced forest opening during these intervals and suggest that changes in seasonality, driven by decreases in temperature of the coldest month and/or changes in precipitation were likely responsible.

A second key finding is that major temperature changes in the chironomid-based July air temperature reconstruction are associated with changes in July insolation (Figure 3). This includes all the major centennial- to millennial-scale reconstructed temperature changes that are not associated with or caused by major variations in the abundance of *Corynocera ambigua*, a taxon identified as problematic for temperature reconstruction (see above). Those major July air temperature changes are the decrease from the mid to late Eemian (ca. 125-115 ka; Paper III), the MIS 5a/4 transition (ca. 85-75 ka; Paper II) and the onset of the Bölling interstadial (ca. 16-14 cal. BP; Paper I, Bolland et al, 2020). In the Burgäschisee record July temperature increase to over 10°C is associated with initial afforestation of the Swiss plateau (Paper I, Bolland et al, 2020) while further temperature increase to 15°C is associated with far more prominent forest development and closing. Conversely the temperature decreases associated with the MIS5a/4 transition (Paper II; 15 to 12°C) are associated with forest opening and increase in herbaceous taxa, while the mid-late Eemian transition (Paper 3; 15.5 to 8.5°C) is associated

with the transition from an *Abies*/*Carpinus* to *Pinus*/*Picea* forest. In all three instances, changes in July insolation, changes in the chironomid inferred July air temperature and vegetation assemblage change coincide (Figure 3).

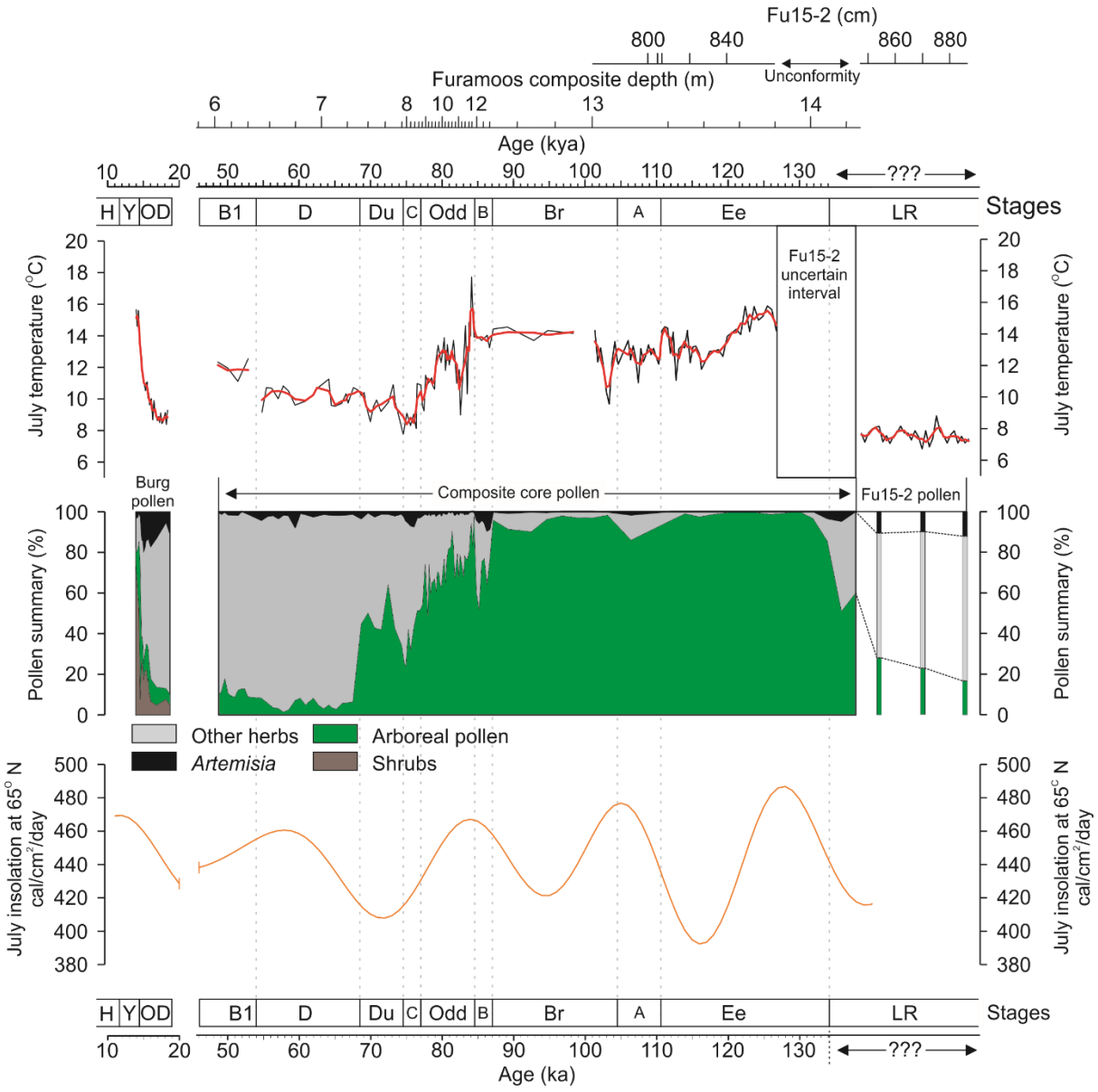

Figure 2: Thesis data summary. a. Chironomid inferred July air temperature reconstructions from Papers I, II and III with the Burgäschisee temperature reconstruction adjusted to the altitude of Füramoos; b. vegetation change summarised as variations in arboreal pollen, shrubs, *Artemisia* and other herbs in the Burgäschisee record (Rey et al, 2017) and in variations in arboreal pollen, *Artemisia* and other herbs in the Füramoos record (pollen data from composite core interval 49 to 99 ka are from Paper II; the remaining 99 ka to Rissian Lateglacial interval from the composite core is from Kern et al., (in progress), and pollen data from Fu15-2 is from Becker et al, 2018); c. July insolation at 65° N (Berger and Loutre, 1991). Stages abbreviations refer to LR; Late Rissian glacial; Ee: Eemian interglacial; A: Stadial A; Br: Brörup; B: Stadial B; Od: Odderade; C: Stadial C; Du: Durnten; D: Stadial D; B1: Bellamont 1; OD: Oldest Dryas; Y, Youngest Dryas and Bölling/Alleröd intervals; H: Holocene.

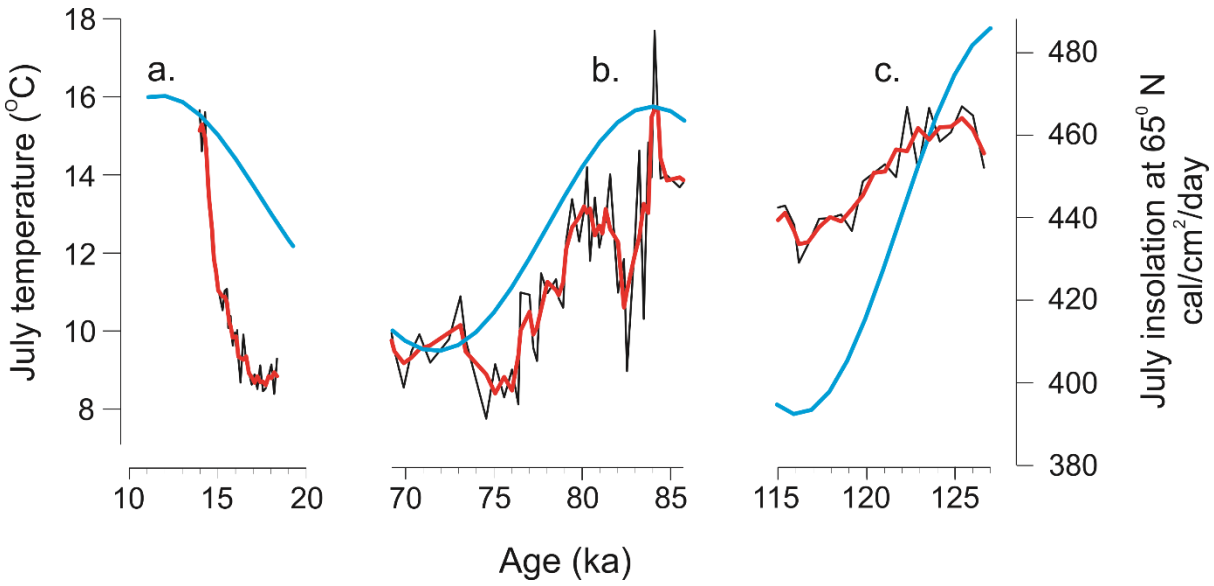

Figure 3: Three largest temperature changes in the chironomid based temperature reconstructions produced in papers I, II and III not driven by changes in *Corynocera ambigua*, a taxon identified as potentially problematic in the temperature reconstruction. Reconstructed temperatures are shown with associated changes in July insolation at 65° N (Berger and Loutre, 1991). a. Onset of the Bölling interstadial (Paper I); b. MIS 5a/ 4 transition (Paper II) and c. transition from the mid to late Eemian (Paper III)

Within Papers I (Bolland et al, 2020), II and III the development of these chironomid records, ecological analysis, temperature reconstructions and implications are discussed in detail. Paper I has been accepted and published with *Quaternary Science reviews*. Paper II had been submitted to *Quaternary Science Reviews*. Paper III is in the final stages of development prior to submission to the journal *Boreas* in the next few months.

Paper I

Quaternary Science Reviews 243 (2020) 106484

Contents lists available at ScienceDirect

Quaternary Science Reviews

journal homepage: www.elsevier.com/locate/quascirev

Summer temperature development 18,000–14,000 cal. BP recorded by a new chironomid record from Burgäschisee, Swiss Plateau

Alexander Bolland [a, *], Fabian Rey [a, b], Erika Gobet [b], Willy Tinner [b], Oliver Heiri [a]

[a] Geoecology, Department of Environmental Sciences, University of Basel, Klingelbergstrasse 27, CH-4056, Basel, Switzerland
[b] Institute of Plant Sciences and Oeschger Centre for Climate Change Research, University of Bern, Altenbergrain 21, CH-3013, Bern, Switzerland

ARTICLE INFO

Article history:
Received 1 April 2020
Received in revised form
3 July 2020
Accepted 10 July 2020
Available online 3 August 2020

Keywords:
Chironomids
Palaeoecology
Palaeolimate
Temperature
Lateglacial
Afforestation

ABSTRACT

The termination of the Last Ice Age after the Last Glacial maximum (LGM) represents a dynamic period in the history of the circum-north Atlantic region. So far, there are few reliably dated climatic reconstructions covering the Lateglacial period prior to 14,700 cal. BP in Central and Northern Europe. We present a new chironomid record for the period 18,000–14,000 cal. BP, from Burgäschisee, Switzerland. Chironomid assemblages immediately following glacier retreat were dominated by taxa indicative of cold, oligotrophic conditions such as *Sergentia coracina* -type and *Micropsectra radialis* -type. A gradual transition to assemblages with moderate abundances of taxa indicative of warmer climatic conditions such as *Dicrotendipes nevosus* -type and *Tanytarsus glabrescens* -type started after ca. 16,100 cal. BP. This initial and gradual chironomid assemblage shift culminated in a more pronounced and rapid inferred temperature change at the Oldest Dryas/Bølling transition at ca. 14,700 cal. BP, where further types indicative of warm conditions such as *Tanytarsus lactescens* -type first occurred and replaced chironomids indicative of colder conditions such as *Paracladius* and *Protanypus*. We estimated past July air temperature changes from the chironomid assemblages by applying to the record a chironomid-temperature transfer function that is based on chironomid distribution data from 274 lakes in Switzerland and Norway. The resulting reconstruction, which features a sample-specific root mean square error of prediction of 1.36–1.46 °C, indicates temperatures around 9 °C at the beginning of the record. An initial gradual warming phase initiating at ca. 16,100 cal. BP is recorded reaching values around 10 °C for the period 16,100–15,500 cal. BP. Temperatures continue to increase reaching values around 12 °C for the period preceding the Bølling warming, when temperatures rose rapidly to values around 15 °C. The early temperature rise to values of 10–12 °C prior to the Bølling warming agrees with widespread vegetation changes recently reported for this region based on palaeobotanical analyses, which indicate a shift from herbaceous tundra to shrub tundra with low density tree birch stands with open canopies. Together, these results suggest an earlier Lateglacial temperature increase in southwest Central Europe than expected based on earlier palaeobotanical reconstructions, although with a less pronounced warming than has been reported for ca. 16,000 cal. BP from south of the Alps. This early Lateglacial warming agrees with glacier reconstructions which suggest several step-wise reductions of glacier extent in this period as well as with evidence from other palaeotemperature reconstructions and suggests that not only Southern Europe but significant parts of Europe north of the Alps may have been characterized by early Lateglacial warming well before the rapid warming at ca. 14,700 cal. BP.

1. Introduction

The end of the last ice age (termination I) represents one of the most dynamic and widespread natural environmental and climatic regime shifts in the past 100 ka. Termination I coincided with increasing northern hemisphere insolation, rising sea levels and massive freshwater inputs into the global oceans following the Last Glacial Maximum (LGM: ca. 26,500 - 19,000 years ago), during which time relative sea level was ca. 130 m lower than it is today (Clark et al., 2009). Between 19,000 and 17,000 years ago increasing temperatures are registered for many parts of the globe, in accordance with rising northern hemisphere insolation values (He et al.,

* Corresponding author.
E-mail address: alexanderwilliam.bolland@unibas.ch (A. Bolland).

https://doi.org/10.1016/j.quascirev.2020.106484

2013). Increases in greenhouse gas concentrations recorded in ice cores during this period are generally interpreted as the result of a complex interplay between changes in overturning circulation in the Southern Ocean and North Atlantic, sea ice extent, atmospheric circulation and biological activity associated with these mechanisms following initial warming (e.g. Petit et al., 1999; Fischer et al., 2008; Marcott et al., 2014). Water isotope records from Antarctic ice cores indicate an increase in southern hemisphere temperatures starting as early as 20,000–18,000 years ago (NAIS Divide Members, 2013).

Evidence for a long-term temperature increase during termination I from the southern hemisphere and at the global scale contrasts to the situation in the northern North Atlantic region where environmental changes were particularly dynamic. Rapid, high volume variations in freshwater input into the North Atlantic have been considered as potential causes for reduced Atlantic Meridional Overturning Circulation (AMOC; Clark et al., 2012; Stern and Lisiecki, 2013) during large parts of this interval, reducing transport of warm waters from southern latitudes northwards (e.g. McManus et al., 2004) and maintaining low North Atlantic (Liu et al., 2009; Mojtahid et al., 2017) sea surface temperatures. As a consequence, it is generally considered that cold conditions prevailed in large sections of the northern North Atlantic region until the abrupt increase in AMOC and associated abrupt warming at the transition to the Lateglacial (Bølling/Allerød) interstadial ca. 14,700 years ago (e.g. Clark et al., 2012; Rasmussen et al., 2014).

The abrupt changes in the North Atlantic Ocean are reflected in vegetation reconstructions that, in the circum-North Atlantic region, are the primary information source for understanding climate dynamics on the continents during termination I. For Southern Europe comprehensive vegetation reconstructions are available for the entirety of the LGM and Termination I, both regionally from marine cores (Fletcher and Goñi, 2008; Fletcher et al., 2010) and more locally in terrestrial records from sites that were never glaciated (e.g. Pons and Reille, 1988; Watts et al., 1996; Allen et al., 2000; Tzedakis et al., 2002; Kaltenrieder et al., 2009). In contrast, most well dated Northern and Central European sites, including sites in France and Northern Spain, have chronological constraints of ca. 14,500–18,000 calibrated radiocarbon years BP (cal. BP) for their lowermost dates (e.g. Magny et al., 2006; Wehrli et al., 2007; Millet et al., 2012). Many of these sites were covered by ice during the LGM and early parts of Termination I (e.g. Hughes et al., 2016) and in large sections of Central and Northwest Europe that were not ice covered a dry climate prevailed (e.g. Hoek and Bohncke, 2002), limiting the number of lakes and therefore also of limnological records. Until now, few Northern and Central European records exist which are reliably dated and describe vegetational assemblages prior to the onset of the Bølling/Allerød interstadial ca. 14,700 cal. BP (Lotter et al., 1999; Duprat-Oualid et al., 2017; Rey et al., 2017; 2020). As a consequence, it remains difficult to constrain when temperatures first started to rise after the LGM on mainland Europe and how far in the European interior the climatic development followed that of the North Atlantic during the early termination.

Based on the available evidence, persistence of a cold tundra and/or steppic environment has been assumed for Central Europe following the LGM until the regional reforestation at the onset of the Bølling (e.g: Lotter et al., 1992; Wehrli et al., 2007). However, new evidence from ^{14}C dated lake sediments from the Northern Swiss lowlands indicates a clear transition from herb tundra into a more diverse herb/shrub tundra as early as 16,000 cal. BP (Rey et al., 2017; 2020). Recent pollen-morphological differentiation of tree and shrub birches allowed to track the expansion of first tree *Betula* stands at around 16,000 cal BP, a vegetational pattern that was unknown before (Rey et al., 2017; 2020). The implication is the possibility of warming ca. 1300 years prior to the rapid warming phase at the onset to the Bølling period around 14,700 cal. BP. Afforestation prior to the Bølling onset has previously been observed in pollen records from the western Mediterranean region (Fletcher et al., 2010) and both pollen- and chironomid-based temperature reconstructions have indicated early warming at Lago di Origlio (Southern Switzerland) chronologically placed at the same time as the new evidence from the Northern Swiss lowlands (Tinner and Vescovi, 2005; Samartin et al., 2012). There are however no well-dated, vegetation-independent terrestrial temperature records from north of the Alps to corroborate this hypothesized early temperature increase. Since vegetation development in a tundra and/or steppe environment is not only determined by temperature, but can potentially also be strongly influenced by moisture changes (Tinner, 2007; Samartin et al., 2017), such independent temperature reconstructions would be crucial for confirming that these vegetation changes really were the direct consequences of warmer temperatures during the Early Lateglacial period.

Chironomid analysis is an excellent tool for reconstructing past summer temperature changes because of the strong relationship between chironomid distribution and July air temperatures (Brooks and Birks, 2001; Heiri and Lotter, 2005; Eggermont and Heiri, 2012). This relationship has allowed the production of modern calibration training sets which can be used to develop quantitative chironomid-based temperature inference models to reconstruct palaeotemperature development from lake sediment records (Brooks et al., 2006). There are many examples of chironomids being used to reconstruct Lateglacial temperature changes in Switzerland (e.g. Heiri and Lotter, 2005; Ilyashuk et al., 2009; Samartin et al., 2012) and other regions of Central, Western and Northern Europe (e.g. Brooks and Birks, 2000; Heiri and Millet, 2005; Heiri et al., 2007a; Watson et al., 2010; Millet et al., 2012; Birks et al., 2014) as well as Southern Europe (Heiri et al., 2007b; Larocque and Finsinger, 2008; Samartin et al., 2017). However, as with the aforementioned pollen analysis, only very few chironomid-based temperature reconstructions from Europe, such as those described by Millet et al. (2012, Western Pyrenees, France) and Samartin et al. (2012, Ticino, Southern Switzerland), cover the crucial time interval before the beginning of the Lateglacial Interstadial ca. 14,700 cal. BP and are supported by independent chronological constraints for this older section of the Lateglacial period. Up to the present, no such chironomid-based temperature reconstructions are available for the Central European lowlands north of the Alps.

Here, we present a new chironomid record from Burgäschisee in the Western Swiss Plateau covering the Early Lateglacial period from ca. 18,300 to 14,000 cal. BP. In-lake environmental changes inferred from the record are discussed in relation to the taxonomic turnover in chironomid assemblages. Furthermore, we develop a new quantitative, chironomid-based summer temperature reconstruction from the record which covers the full Early Lateglacial period since lake formation following local deglaciation. Previous pollen analyses from the same sediment record have revealed evidence for a pre-Bølling vegetation change from steppe to shrub tundra, suggesting increasing temperatures in this region from ca. 16,000 cal. BP onwards (Rey et al., 2017). Therefore, the new temperature record can be directly compared to local vegetation changes to assess whether this independent palaeotemperature evidence really supports that increasing summer temperatures were responsible for local vegetation compositional turnover around 16,000 cal. BP. Finally, we discuss the implications of our results for constraining palaeotemperature development in Switzerland and early Lateglacial temperature development on continental Europe.

2. Material and methods

2.1. Site description

Burgäschisee is a small kettle hole lake, formed following the retreat of the Rhone glacier westwards across the Swiss plateau, situated between the Jura Mountains and the Alps (Fig. 1; 47°10′8.5″N, 7°40′5.9″E) at 465 m a.s.l. (Fig. 1). A section of ice remaining after glacier retreat was subsequently surrounded and possibly covered by sediments after which the ice melted, leaving a depression and forming the lake (Guthruf et al., 1999). Today, Burgäschisee is eutrophic, has a 23 ha surface area, maximum depth of 31 m and a catchment of 319 ha (Guthruf et al., 1999). Four inflows feed the lake from the Southwest and a single outflow drains the lake to the North (Müller-Beck, 2005). The lake level was lowered by 2 m in 1943 in order to drain wetlands for agricultural use (Arn, 1945). The outflow of the lake has been artificially modified to release deep, hypolimnetic waters since 1977 to reduce the nutrient loading of the lake and improve the water quality (Ambühl and Stumm, 1984).

Annual rainfall is ca. 1100 mm (data from Koppigen 1981–2010 climate normals), ca. 6 km from Burgäschisee (MeteoSwiss, 2020), and the wettest months occur May through August with more than 100 mm of precipitation per month. July is the warmest month reaching 18.6 °C on average while the annual average temperature is 9.1 °C.

2.2. Coring

Two field campaigns were carried out at Burgäschisee in 2009 and 2014. Three parallel cores (Burg A-C) were retrieved in 2009 using a UWITEC piston corer with a diameter of 60 mm at the deepest point of the lake reaching a coring depth of 15 m. A further core, Burg I, was retrieved in 2014 to create a master sequence using lithostratigraphic markers for the core correlation (Rey et al., 2017). The core section analysed in the present study consists of silt (1037-846 cm) and fine detritus gyttja which is partially laminated (846-826 cm). A detailed description of the sedimentology is provided in Rey et al. (2017).

2.3. Dating and vegetation history

The Burgäschisee sediment record is dated by a total of 16 radiocarbon dates, 4 of which are used to date the section presented here as described in Rey et al. (2017). ^{14}C samples were analysed at the Laboratory for the Analysis of Radiocarbon at Bern University, the Laboratory of Ion Beam Physics at ETH Zurich, and the Poznan Radiocarbon Laboratory using Accelerator Mass Spectrometry (AMS). Calib 7.1 (Stuiver and Reimer, 1993) was used to calibrate the radiocarbon dates using the IntCal13 calibration curve (Reimer et al., 2013). An age-depth relationship for the entire Burgäschisee sequence is available based on the program clam 2.2 (Blaauw, 2010) as described in Rey et al. (2017).

Lateglacial sections of this age model were characterized by relatively large uncertainties (Fig. 2). For the present study, we

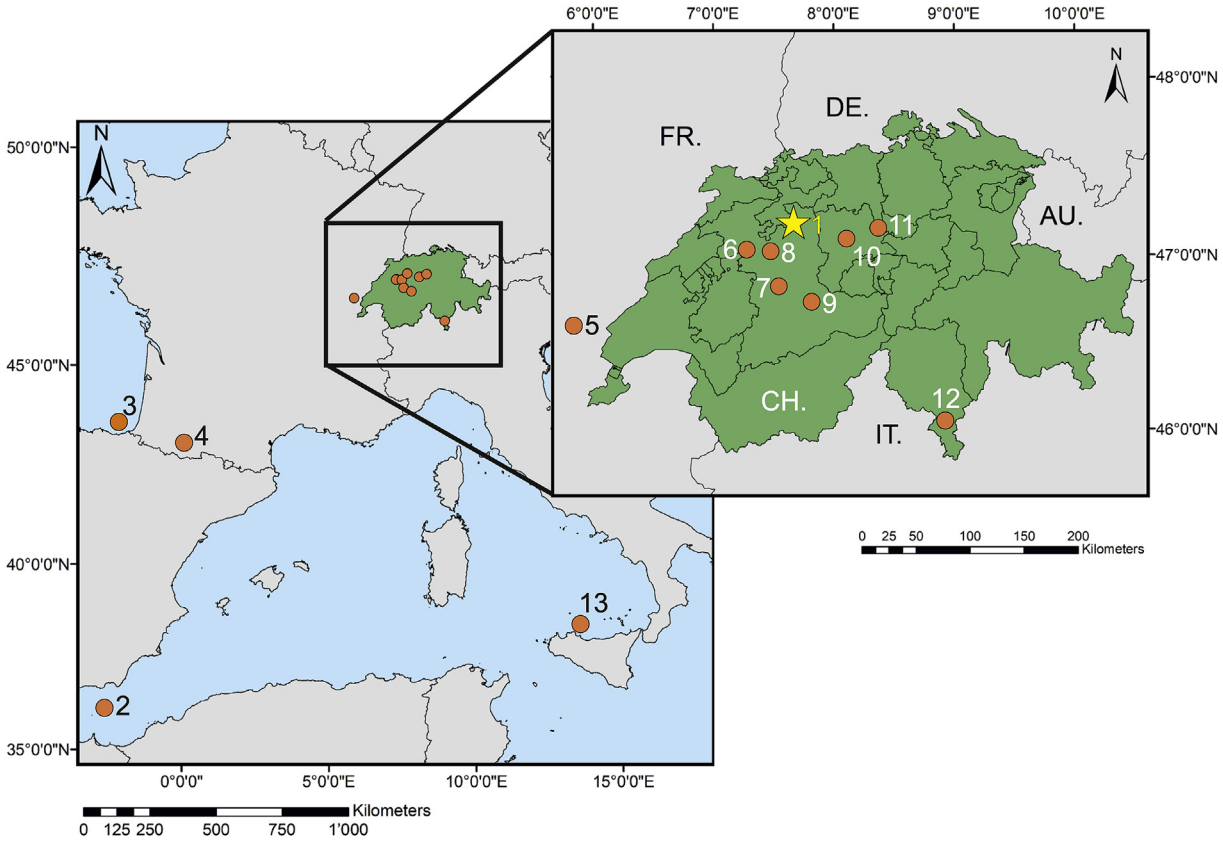

Fig. 1. Location of Burgäschisee in Switzerland (green area) and of other records discussed in text. 1: Burgäschisee (Rey et al., 2017; This study); 2: Core MD95-2043, Alboran Sea (Cacho et al., 2001; Fletcher et al., 2010); 3: Core KS04-16, Bay of Biscay (Martínez-García et al., 2015); 4: Ech Palaeolake (Millet et al., 2012); 5: Lac Lautrey (Heiri and Millet, 2005); 6: Lobsigensee (Elias and Wilkinson, 1983); 7: Gerzensee (Brooks and Heiri, 2013; Lotter et al., 2012; Ammann et al., 2013; van Raden et al., 2013); 8: Moossee (Rey et al., 2020); 9: Sieben Hengste (Luetscher et al., 2015); 10: Soppensee (Lotter, 1999); 11: Rotsee (Lotter and Zbinden, 1989); 12: Lago di Origlio (Samartin et al., 2012) and 13: Core BS79-38, Tyrrhenian Sea (Cacho et al., 2001). (For interpretation of the references to colour in this figure legend, the reader is referred to the Web version of this article.)

therefore also explored an alternative age model using other available age estimates for major vegetation changes on the Swiss Plateau between 13,800 and 14,700 cal. BP. Several studies have shown that major shifts in vegetation such as the reforestation and increase in *Juniperus* at the Oldest Dryas to Bølling transition or the increase in *Pinus* at the Older Dryas cold oscillation happened at the same time as pronounced changes in climatic conditions on the Swiss Plateau as apparent in lake marl $\delta^{18}O$ records, therefore indicating that these vegetation shifts happened synchronously across the Swiss Plateau (Lotter et al., 1992; Eicher and Siegenthaler, 1976), at least at the multidecadal to centennial scale relevant for the present study. The ages of prominent Lateglacial vegetation changes in the Burgäschisee record as dated in other Lateglacial sediment sequences on the Swiss Plateau therefore provide further age constraints for the record.

Three strong palynostratigraphical age markers were identified which correspond to distinct vegetative transitions in the Burgäschisee pollen stratigraphy (Table 1) and were correlated to the well-dated Gerzensee pollen stratigraphy (Ammann et al., 2013), a record that is representative of regional vegetation development across the Western Swiss lowlands for this study period. Ages of these vegetation changes in the Gerzensee record show an excellent agreement with ages as assessed in the ^{14}C dated pollen record from Moossee, 22 km southwest of Burgäschisee, situated at almost identical altitude (512 m asl; Fig. 2). Furthermore, the inferred age of the increase in lake marl $\delta^{18}O$ record of Gerzensee at the beginning of the Bølling at 14,685–14,590 cal. BP, which coincides with the increase in *Juniperus* and reforestation of the Swiss Plateau, shows an excellent agreement with the pronounced increase in precipitation $\delta^{18}O$ inferred for 14,658 ± 40 cal. BP (Luetscher et al., 2015) based on the U/Th dated speleothem from Sieben Hengste (46 km from Burgäschisee, 22 km from Gerzensee), supporting the estimated age for this vegetation change on the Swiss Plateau.

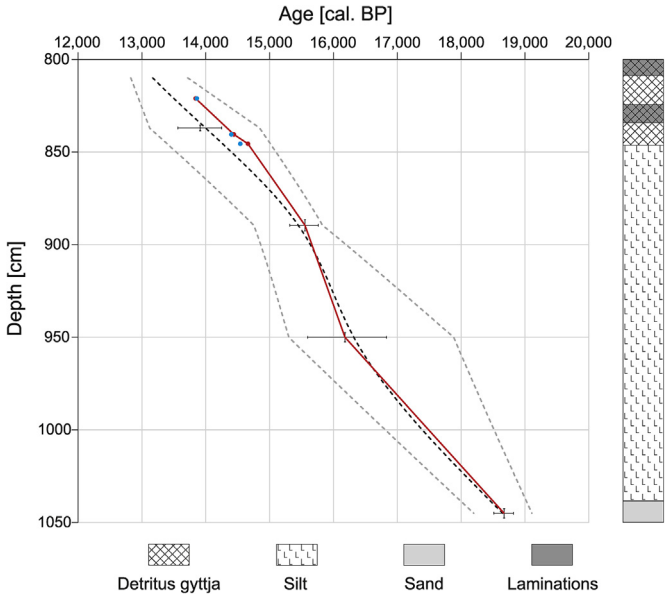

Fig. 2. Lithology and age depth model of the oldest sections of the Burgäschisee record. Black crosses indicate the ^{14}C dates used by Rey et al. (2017, Table 1), dotted black and grey lines the original age-depth relationship described in this study as well as the associated 95% error estimates. Red circles represent the age of palynostratigraphical tie points in the Burgäschisee record as dated in the Gerzensee pollen record (Ammann et al., 2013, Table 1), blue circles age estimates for these tie points as dated in the Moossee pollen record (Rey et al., 2020). Age estimates for Lateglacial section of the Moossee record are based on 6 AMS ^{14}C dates and the Gerzensee record is dated based on the correlation of lake marl $\delta^{18}O$ values with the NGRIP Greenland ice core $\delta^{18}O$ record (age uncertainties for the latter record are estimated as 169–186 years for this interval (maximum counting error); Rasmussen et al., 2006). Moossee and Gerzensee are both situated on the Swiss Plateau in close proximity to Burgäschisee (22 and 39 km distant from the lake, respectively). The red line indicates the revised age model for the Burgäschisee record based on linear interpolation between the radiocarbon dates in the lower part of the record and the palynological tie points in the upper section (see text for details). (For interpretation of the references to colour in this figure legend, the reader is referred to the Web version of this article.)

These pollen-inferred ages suggest that one of the ^{14}C ages (835.5–838.5 cm, 13,997 cal yr BP) is slightly younger than expected based on the pollen based age estimates (Fig. 2). When comparing the Burgäschisee chironomid record with other palaeoclimate records, we therefore use a revised age-depth model based on linear interpolation between median calibrated ^{14}C ages for the older part of the record and the three pollen-inferred ages for the upper part of the sequence between 849 and 823 cm sediment depth (Table 1, Fig. 2). This revised age depth relationship is fully within the chronological error associated with the original age depth model of Rey et al. (2017) (Fig. 2). For information we also provide the figures comparing chironomid-inferred temperatures with other palaeoenvironmental reconstructions discussed in our study (Figs. 5 and 6) on the original age scale presented by Rey et al. (2017) in the online supplementary information.

The main traits of vegetation history at Burgäschisee over the past 18,700 years are presented in Rey et al. (2017). The pollen data suggest open steppe/tundra vegetation (Rey et al., 2020) shortly after deglaciation at ca. 19,200 cal BP (Ivy-Ochs et al., 2004), with the presence of some shrubs including *Betula nana* and *Juniperus*. Herb dominated tundra ecosystems persisted until ca. 16,000 cal BP when there was a marked increase of tree *Betula*, *Betula nana* and other shrubs pointing to the spread of shrub tundra and tree stands (Rey et al., 2017). However, the prevailing presence of herbaceous pollen values (>60% including abundant *Artemisia* and *Helianthemum*) shows that steppic environments persisted and still dominated the vegetation. The Oldest Dryas/Bølling transition was characterized by afforestation within the catchment of Burgäschisee with a short term mass expansion of shrubs (*Juniperus* pollen >60%) during early sections of the Bølling warming period (Ammann et al., 2013) followed by a sharp rise in tree *Betula* pollen which suggests the formation of birch forests. At the same time, the organic content of the sediment rises sharply, showing increased organic productivity in the lake (Rey et al., 2017).

2.4. Sampling and analysis of fossil chironomids and other aquatic invertebrates

Samples were taken every ca. 4–6 cm using 2–20 cm^3 of wet sediment per sample. A total of 36 samples were analysed at absolute sediment depths between 826 and 1032 cm. The samples were left in room temperature in 10% KOH for 6 h and sieved over a 100 μm sieve. Chironomid head capsules as well as other chitinous aquatic invertebrate remains were picked from other sieve residue in a Bogorov tray under a stereomicroscope (30–50× magnification), dried on coverslips and mounted on microscope slides in Euparal before being identified at 40–100× magnification using a compound microscope. A minimum head capsule count of 80 was aimed for to ensure that more than the recommended 50 head capsules were found per sample (Heiri and Lotter, 2001; Quinlan and Smol, 2001). Two samples nevertheless resulted in less than the 50 head capsules (sample depths 836 and 888 cm contained 47 and 42 head capsules, respectively). Head capsules with a complete mentum or greater than half a mentum were counted as one specimen, head capsules with half a mentum were counted as half a specimen and head capsules with less than half a mentum were disregarded.

Taxonomic identification followed Wiederholm (1983), Schmid

Table 1
Radiocarbon dates and calibrated ages from the Burgäschisee record. ^{14}C dates are from Rey et al. (2017). Ages are calibrated with the program Calib 7.1 (Stuiver and Reimer, 1993) and the IntCal13 calibration curve (Reimer et al., 2013). Pollen-inferred ages represent the age of these landscape scale vegetation changes as assessed in the sediments of Gerzensee, 58 km from Burgäschisee (van Raden et al., 2013). Radiocarbon analysis was conducted at Laboratory of Ion Beam Physics, ETH Zurich, Switzerland[a]; Laboratory for the Analysis of Radiocarbon, Bern University, Switzerland[b] and Poznan Radiocarbon Laboratory, Poland[c].

Lab. code	Depth (cm)	Material/age marker	^{14}C age (BP)	Age (cal BP)	Age 2σ range (cal BP)	Age used in age/depth relationship (cal BP)
	818.5–823.5	Palynological stratigraphy (*Betula* phase to Allerød Pine and *Betula* phase)		13,840		13,840
BE-2552.1.1[b]	835.5–838.5	*Betula* fruits, fruit scale	12,050 ± 130	13,997	13,579–14,414	Not used
	838.5–842.5	Palynological stratigraphy (*Juniperus* peak to *Betula* phase)		14,440		14,440
	842.5–848.5	Palynological stratigraphy (Oldest Dryas to *Juniperus* peak)		14,660		14,660
ETH-43949[a]	886.5–892.5	*Betula nana* fruit scales, fruits; periderm deciduous, leaf fragments deciduous, bud scales deciduous, twiglet, bark	13,000 ± 50	15,540	15,316–15,764	15,540
BE-2553.1.1[b]	947.5–952.5	Twiglet	13,440 ± 200	16,140	15,512–16,767	16,140
Poz-60131[c]	1042.5–1047.5	Twiglet	15,400 ± 70	18,665	18,512–18,817	18,665

(1993), Brooks et al. (2007), and Anderson et al. (2013). For graphical and statistical interpretation, specimens that could not be identified to the highest taxonomic resolution (e.g. due to missing mouthparts) were assigned to categories based on the ratio of identified specimens within the sample. For these calculations, taxa which could not be assigned beyond subfamily/tribe level (i.e. unidentified Chironomidae, Chironomini, Tanytarsini, Orthocladiinae) were excluded.

2.5. Zonation and ordination analyses

Zonations were derived using the clustering algorithm CONISS (Grimm, 1987) and zonations were compared with a Broken Stick Model to assess the statistical significance of the zonal boundaries (Bennett, 1996). CONISS was calculated with Rioja (Juggins, 2017) and Vegan (Oksanen et al., 2007) packages using R studio version 1.1.463 (RStudio Team, 2015).

Major changes in chironomid assemblage composition were summarized with a Detrended Correspondence Analysis (DCA) using CANOCO 5.0 (ter Braak and Smilauer, 2018) and square root transformed percentage data. Changes were summarized as DCA axis 1 values expressed in standard deviation (SD) units, the length of DCA axis 1 was 2.5 SD. Changes in in-lake nutrient concentrations and affected variables such as algal productivity or oxygen concentrations in the lake can have a major influence on lacustrine chironomid assemblages (e.g. Brodersen and Quinlan, 2006). We used direct gradient analysis of a dataset representing chironomid assemblage composition in 28 deep and stratified lakes across Europe (41.7–68.4°N; Verbruggen et al., 2011) to explore the extent that changes in fossil chironomid assemblages at Burgäschisee were typical for shifts to more nutrient-rich (eutrophic) or nutrient-poor (oligotrophic) conditions. We analysed the data from these 28 lakes with Detrended Canonical Correspondence Analysis (DCCA) using total phosphorus (TP) concentrations at these sites as only constraining variable. As a consequence, DCCA axis 1 is constrained to represent changes in modern chironomid assemblages related to between-site differences in TP values. Fossil samples from Burgäschisee were entered in this analysis as passive samples, and variations in their DCCA axis 1 values can therefore be interpreted as indicating whether past assemblage changes were towards assemblages more typical for nutrient-rich or nutrient-poor lakes in the calibration dataset. TP values are used for constraining DCCA since phosphorus is typically the limiting element for algal growth in lakes. The applied dataset includes lakes from Lapland to Southern Italy (Verbruggen et al., 2011), and TP values correlate to some extent with both air temperatures and hypolimnetic oxygen availability at these study lakes. All of these lakes are deep (22–370 (mean 100) m water depth), stratified systems, however, in which larval chironomid assemblages are largely decoupled from the direct effects of air and surface water temperatures. Changes in DCCA axis 1 are therefore considered to mainly reflect changes in respect to different nutrient conditions at the studied lakes and not the influence of temperature on chironomid assemblages, in contrast to the shallower lakes that were used to develop the chironomid-temperature transfer function for reconstruction of past summer temperatures from the Burgäschisee chironomid assemblages (see section 2.6 below). DCCA was calculated on square-root transformed percentage data using the program CANOCO 4.5 (Leps and Smilauer, 2003).

2.6. Temperature reconstruction

A chironomid-temperature inference model based on the Swiss-Norwegian calibration dataset (Heiri et al., 2011) was used

to develop quantitative temperature estimates from fossil chironomid assemblages in Burgäschisee. The model is based on samples from 274 lakes throughout Switzerland and Norway, describing distribution data of 154 chironomid taxa and covering a July temperature gradient of 3.5–18.4 °C. In contrast to the dataset used for exploring chironomid assemblage changes typical for changes in nutrient availability (see section 2.5.) this dataset consisted of considerably shallower lakes (mean 10 m, 5–95% percentile range 1.3–26 m, range 0.5–77 m maximum water depth) for which strong relationships between chironomid assemblage composition and summer temperature values have been demonstrated (e.g. Eggermont and Heiri, 2012) and that perform well for development of chironomid-temperature transfer functions.

A two component weighted averaging partial least squares model (WAPLS; ter Braak and Juggins, 1993; ter Braak et al., 1993) was used to produce the temperature reconstruction, percentages were square root transformed before calculations. Of the 64 chironomid morphotypes originally identified in the Burgäschisee record, some had to be amalgamated for the temperature reconstruction resulting in 53 types in total. The resulting inference model featured a cross validated (bootstrapped) root mean square error of prediction of 1.40 °C and a r^2 value of 0.87 between observed mean July air temperature values and those inferred based on chironomid assemblages in the modern calibration data. WA-PLS was calculated using the program C2 version 1.77 (Juggins, 2007).

2.7. Reconstruction error and diagnostic statistics

Sample specific error estimates were calculated for each reconstructed temperature in the Burgäschisee record using bootstrapping (9999 cycles, Birks et al., 1990). Fossil sample were compared with samples in the calibration dataset to identify assemblages with “no good” and “no close” analogues using squared chi-square distance (Birks et al., 1990). The 5th and 2nd percentiles of all distances within the modern calibration data samples were used as thresholds to identify fossil samples without good and close analogues, respectively (Birks, 1990; Toth et al., 2015). Furthermore, goodness-of-fit statistics (Birks et al., 1990, 2010) were used to identify samples with an unusual composition, which might indicate that variables other than temperature were exerting a dominating influence on assemblages. Fossil assemblages were analysed as passive samples in a Canonical Correspondence Analysis (CCA) of the modern calibration dataset with mean July air temperature as only constraining variable. Residual distances to CCA axis 1 were considered to represent “goodness-of-fit” with temperature, and thresholds of the 90th and 95th percentile of residual distances of modern calibration dataset samples to axis 1 were used to identify samples with a “poor” or “very poor” fit with temperature (Birks, 1990; Toth et al., 2015). Finally, for each sample we examined the percentage of identified chironomids that were not represented in the calibration dataset, as well as the percentage of identified chironomids that were rare in the calibration data (represented by a Hill’s N2 lower than 5; Heiri et al., 2003). Analogue statistics were calculated with the program C2 version 1.77 (Juggins, 2007) and CCA with CANOCO 4.5 (Leps and Smilauer, 2003).

3. Results

3.1. The Burgäschisee chironomid record

A total of 56 chironomid taxa were identified from 36 samples. Downcore changes in the Burgäschisee chironomid record mostly showed gradual changes in assemblages with two periods of accelerated turnover which have been identified as statistically significant breaks by CONISS zonation. The zones identified by CONISS (Burg 1 through Burg 3) are used here for describing chironomid assemblage change in the Burgäschisee core.

Within Zone Burg 1 (1032–951 cm) the assemblages were dominated by *Sergentia coracina*-type with *Paratanytarsus austriacus*-type, *Microtendipes pedellus*-type, *Tanytarsus lugens*-type, *Micropsectra radialis*-type and *Procladius* as subdominant taxa (Fig. 3). In zone Burg 2 (951–844.5 cm) a gradual turnover in chironomid assemblages is observed, with types previously absent beginning to occur and the gradual disappearance of types which were dominant in Burg 1 associated with a moderate increase in chironomid concentrations (Fig. 3). While *Sergentia coracina*-type continued to dominate the assemblage, shifts in the sub-dominant taxa such as *Paratanytarsus austriacus*-type, *Tanytarsus lugens*-type, *Micropsectra radialis*-type, *Protanypus* and *Procladius* occurred. These taxa started to decrease at the onset of Zone Burg 2, coinciding with the first occurrence of *Corynocera oliveri*-type and *Tanytarsus mendax*-type in the record. Later on within Burg 2 other types such as *Chironomus plumosus*-type, *Tanytarus glabrescens*-type, *Tanytarsus lactescens*-type and *Pagastiella* occurred. Zone Burg 3 (844.5–8262 cm) is apparently defined not by the presence of new types, but largely by the disappearance of types present in Zones Burg 1 and Burg 2, such as *Paratanytarsus austriacus*-type and *Protanypus.* Other types which were already present in Burg 2 increased in abundance. The only new type of note is *Polypedilum nubeculosum*-type which appears immediately after the onset of Burg 3. The change in chironomid assemblage into Burg 3 is accompanied by the appearance and abundance changes of many other aquatic invertebrates in the record including large increases in Ceratopogonidae, Ephemeroptera and aquatic/semi terrestrial mites as well as a distinct decline in *Daphnia pulex*-type ephippia.

3.2. Ordination

Axis 1 of a DCA of chironomid assemblages in Burgäschisee explains 31.8% of the variance in the assemblage data and displays little to no change within Burg 1 (Fig. 4). At the onset of Burg 2, DCA axis 1 scores begin to gradually shift to lower values and continue to do so throughout the rest of the zone, representing the gradual change in assemblage composition identified in Fig. 3. Burg 3 represents the lowest DCA axis 1 scores, the culmination of an accelerated change in DCA axis 1 values beginning prior to the end of Burg 2, with the largest DCA axis 1 change recorded at the Burg 2/Burg 3 transition. Together, these results suggest little assemblage change in the oldest sections of the record, the beginning of a gradual trend to assemblages typical for the youngest sections around 940–950 cm and then a more rapid shift to the assemblages dominating in the youngest section at about the Burg 2/Burg transition.

When the Burgäschisee fossil chironomid assemblages are added passively into a DCCA of modern chironomid assemblage data, with axis 1 constrained to represent changes in TP between the modern sites, samples from Burg 1 are characterized by DCCA

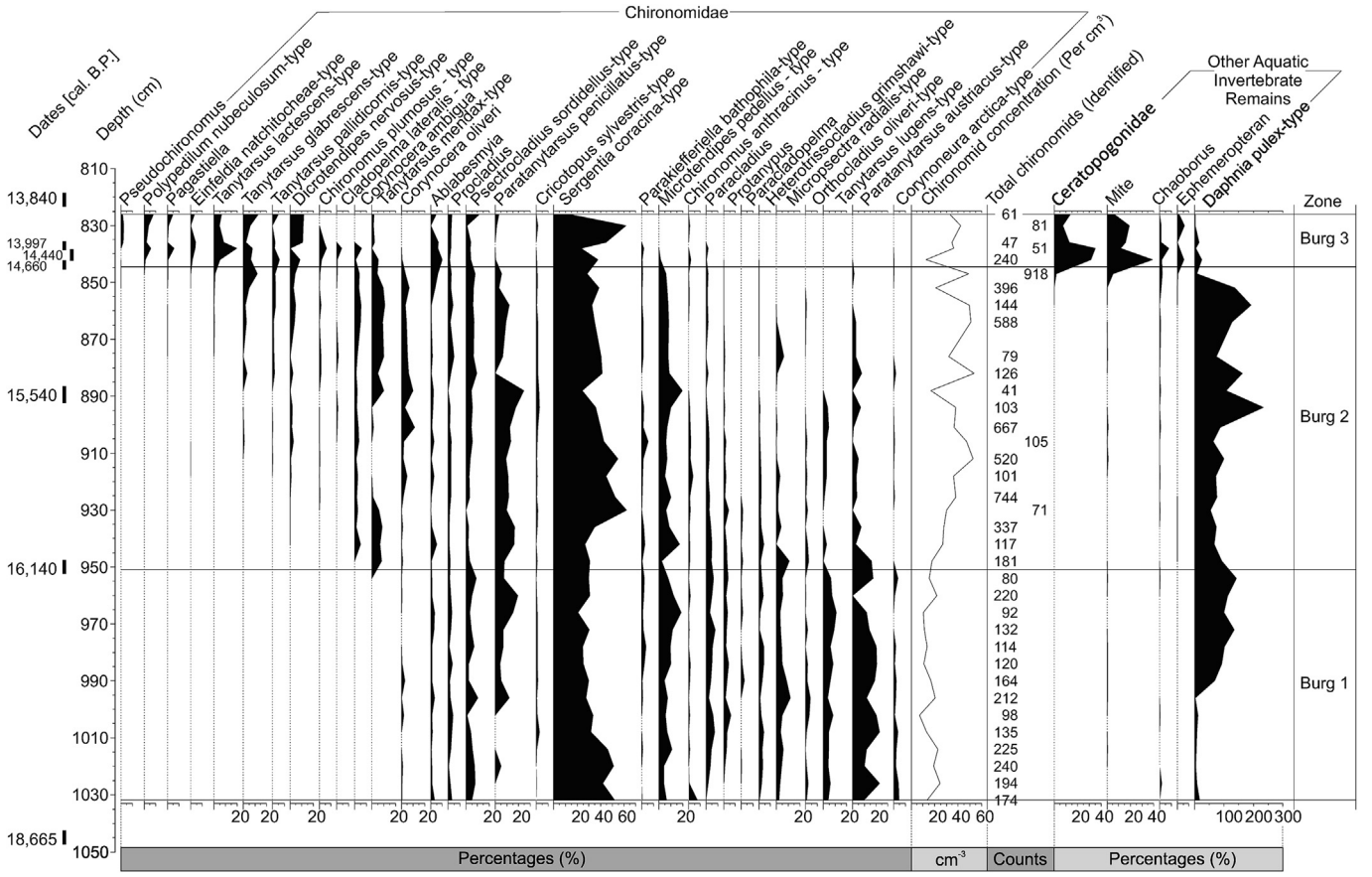

Fig. 3. Fossil chironomid assemblages in the sediments of Burgäschisee. Of the 56 types identified 31 types are shown to document general trends in assemblage turnover. Abundances of chironomid types are shown as a percentage relative to the total number of identified chironomid head capsules whereas other aquatic invertebrate remains are presented as a percentage of the total number of chironomids in a sample including those that were not identified. Ages indicate medians of calibrated age estimates as indicated in Table 1.

axis 1 scores typical for relatively nutrient-poor lakes. DCCA axis 1 scores shift to slightly lower values between ca. 1000 to 900 cm, suggesting that the lake may have experienced a moderate nutrient enrichment in this phase. However, from 900 cm onwards no further shift in DCCA axis 1 scores is apparent, even though major changes in chironomid assemblage composition were registered at Burgäschisee (Figs. 3 and 4).

3.3. Chironomid inferred temperature

Chironomid-inferred mean July air temperatures within Burg 1 show little change and remain ca. 9 °C for most of the zone with some increased variation toward the transition to Burg 2 (Fig. 4). Around the Burg 1/Burg 2 transition, however, inferred temperatures increase to ca. 10 °C and continue to rise gradually to values around 12 °C across zone Burg 2. In contrast, the transition from Burg 2 to Burg 3 is categorised by a rapid increase in temperature from ca. 12 °C–14.5 °C within a relatively short period. In Burg 3 values initially continue to increase, but reach a plateau around ca. 15 °C in the younger part of the zone.

3.4. Reconstruction analogue and performance statistics

Goodness-of-fit statistics indicated that none of the samples in the record have either a “poor fit” or “very poor fit” with temperature (Fig. 4). Analogue statistics showed that only 8 of the samples had no good analogue in the calibration data, whereas most samples (78%) had no close analogue (Fig. 4). *Psectrocladius calcaratus*-type and *Symposiocladius* were the only taxa in the fossil record that were not included in the modern calibration dataset and transfer function. The maximum abundance of these taxa in any sample was 2.0%. Additionally, taxa considered rare (Hill’s N2 < 5) in the training set (*Einfeldia*, *Propsilocerus* and *Paracricotopus*) were present at less than 3% maximum relative abundances in the Burgäschisee record (Fig. 4). Overall the analogue and performance statistics therefore indicate that most taxa in the Burgäschisee record were well represented in the applied transfer function and that, even though close analogues were rare, most fossil samples had a good analogue in the calibration dataset.

4. Discussion

4.1. Chironomid assemblage and lake development

Chironomid assemblages in the early Lateglacial sediments of Burgäschisee are dominated by taxa typically found in cold, oligotrophic lakes in arctic to subarctic environments. For example, *Sergentia coracina*-type, *Micropsectra radialis*-type and *Paratanytarsus austriacus*-type are commonly found in oligotrophic alpine and/or arctic lakes (Brooks and Birks, 2001; Heiri and Lotter, 2010; Heiri et al., 2011). *Sergentia coracina*-type dominates over much of the Burgäschisee sequence. The taxon is eurybathic and typical for lakes that are situated in cold to temperate climates (Brooks et al., 2007; Heiri et al., 2011) and represents oligo-to

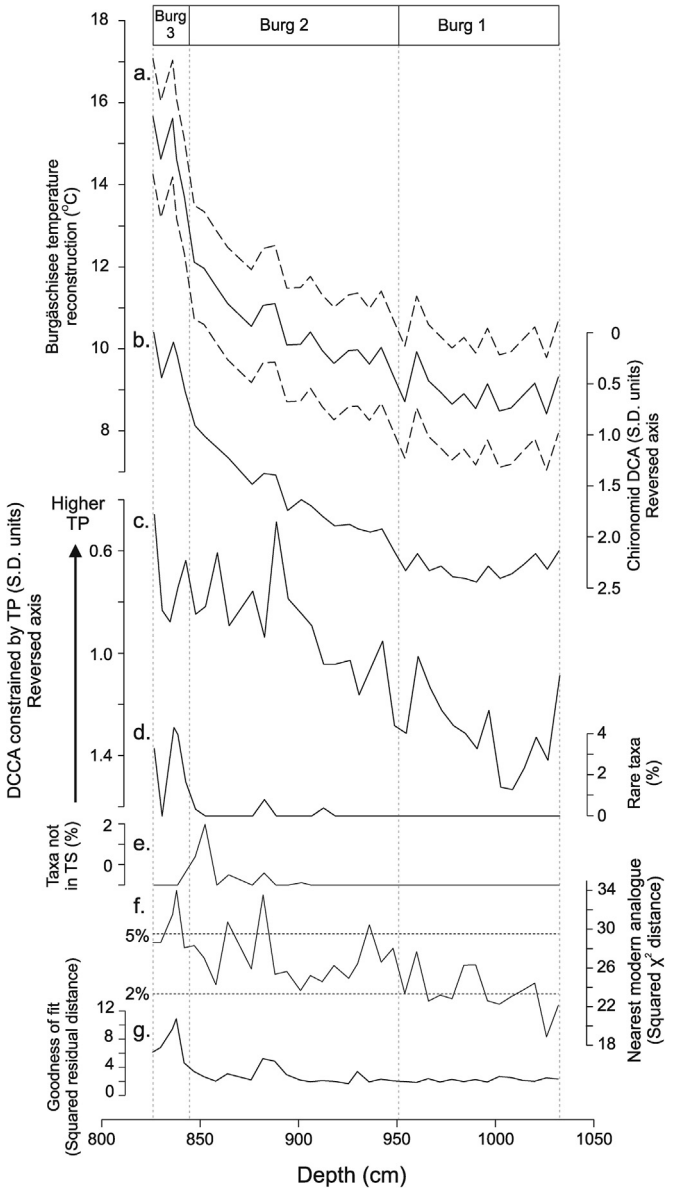

Fig. 4. Chironomid-inferred temperatures from the Burgäschisee record together with ordination results and reconstruction diagnostic statistics. (a) Chironomid-inferred July air temperatures (black solid line) including the sample-specific error of prediction (eSEP; dashed black lines); (b) first axis scores of a DCA of chironomid assemblages in the Burgäschisee record (c) DCCA axis 1 scores for Burgäschisee chironomid samples in DCCA constrained by TP (Verbruggen et al., 2011); see text for details. In this analysis lakes with high TP are characterized by low DCCA axis 1 values as indicated by the arrow; (d) abundance of rare taxa in the Burgäschisee record (N2<5 in the calibration dataset); (e) percentage of taxa in the Burgäschisee record not in the calibration dataset; (f) squared chi-square distance of fossil samples to the nearest modern analogue in the calibration dataset. The horizontal lines indicate thresholds for samples with no close (2%) and no good (5%) analogue in the modern calibration data (following Toth et al., 2015) and (g) goodness of fit statistics. All goodness-of-fit values are well below the thresholds for "poor fit" and "very poor fit" (16.0 and 21.9 respectively) and these threshold values are therefore not indicated.

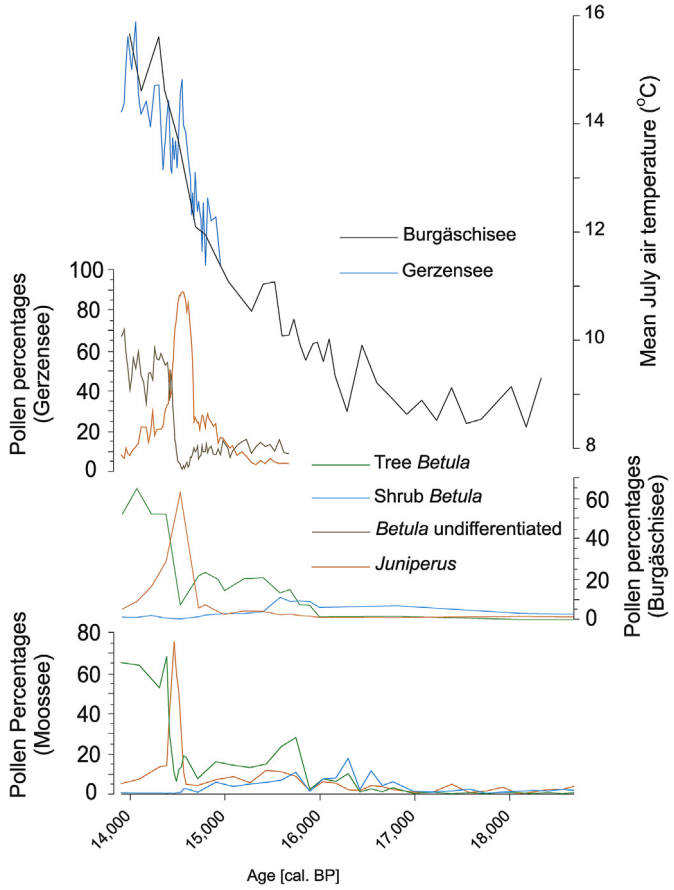

Fig. 5. Chironomid temperature reconstructions from the Northern Swiss Plateau corrected to 465 m a.s.l. (Burgäschisee, this publication; Gerzensee, Lotter et al., 2012) compared with selected pollen types in the Burgäschisee (Rey et al., 2017), Gerzensee (Ammann et al., 2013; shrub *Betula nana* was not separated from tree *Betula* pollen in this study) and Moossee (Rey et al., 2020) records. The Gerzensee record is presented on the age scale of van Raden et al. (2013). For the oldest section we only present samples within 300 years of the Oldest Dryas - Bølling transition, however, since this represents the lowest distinctive age tie point in the Gerzensee record, and lower sections are only very poorly constrained by the available chronological information.

mesotrophic conditions (Brundin, 1956 in Hofmann, 2001). From ca. 16,200 cal. BP (ca. 950 cm) onwards there is a gradual change in chironomid assemblages with taxa typical for warmer climate conditions starting to occur and increasing in abundance, while some taxa that originally dominated in the sequence, such as *Paratanytarsus austriacus*-type and *Micropsectra radialis*-type disappear. For example, the new immigrants *Tanytarsus pallidicornis*-type and *Tanytarsus glabrescens*-type are presently found in subalpine to lowland lakes in the Alps (e.g. Heiri and Lotter, 2010; Heiri et al., 2011). At ca. 14,600 cal. BP (ca. 845 cm), a number of taxa increase which are usually abundant in lowland lakes and temperate climatic conditions, such as *Tanytarsus lactescens*-type and *Polypedilum nubeculosum*-type. At the same time, the abundances of Ceratopogonidae, oribatid mite and chaoborid remains increase. Ceratopogonidae and oribatid mites are common in littoral environments in lakes (e.g. Szadziewski et al., 1997; Solhøy and Solhøy, 2000), particularly in aquatic macrophyte belts, suggesting that the shoreline vegetation may have become more strongly developed and structured in the lake. Chaoborid larvae are common in lakes with seasonal anoxia (Quinlan and Smol, 2010; Ursenbacher et al., 2020). The increase in chaoborids, though not very pronounced, may therefore indicate more stable thermal stratification of the lake and more pronounced anoxia in its deep-water environment.

Overall, the development of chironomid assemblages at Burgäschisee is typical for periods of increasing temperatures, with cold-adapted and oligotrophic taxa dominating the earliest sections of the record and taxa usually found in warmer, more nutrient-rich and oxygen-depleted environments more abundant during the Bølling period (from ca. 14,660 cal. BP/845 cm onwards). The

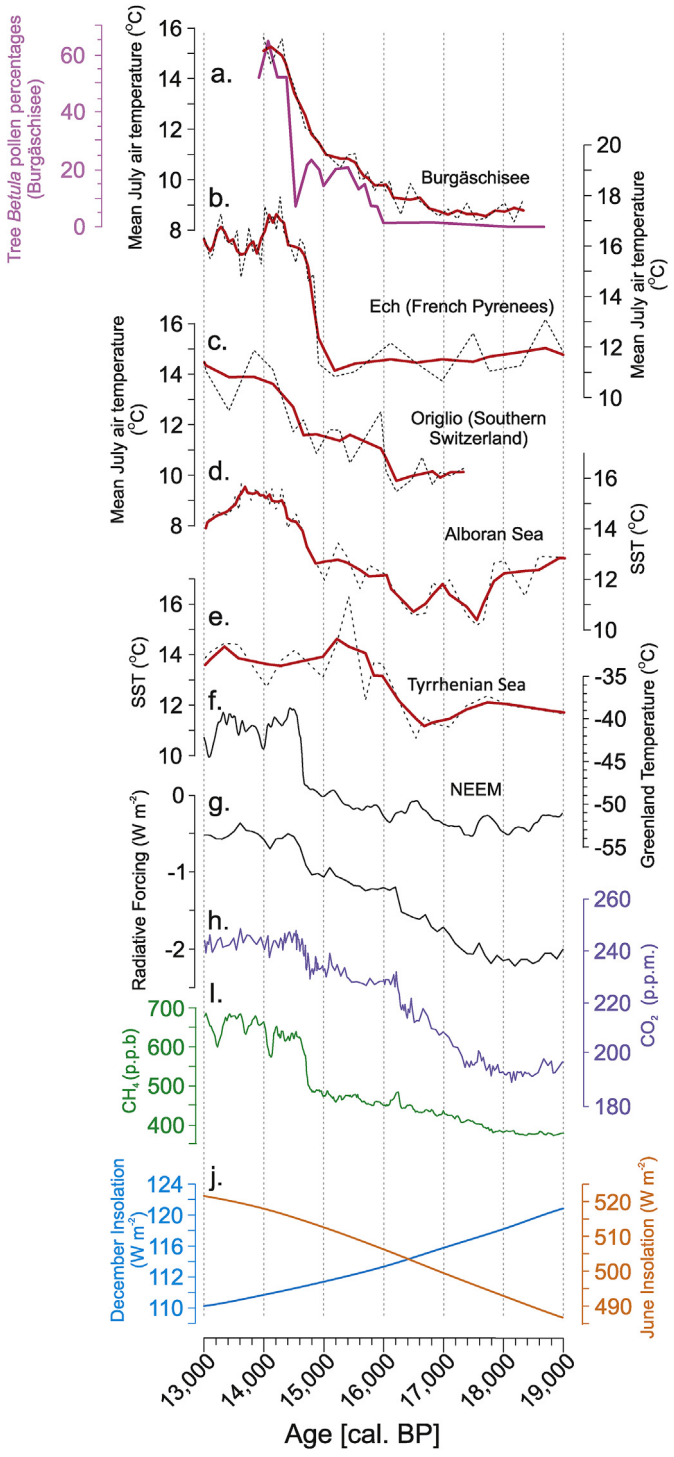

Fig. 6. Palaeotemperature records for the early Late Glacial. For temperature records (plots a. - e.) the dashed black line represents unsmoothed values whereas the solid red line represents a three sample running average. a. Burgäschisee chironomid temperature record from the Swiss lowlands and Burgäschisee tree *Betula* pollen percentages (solid pink line, Rey et al., 2017); b. Ech Palaeolake chironomid-inferred temperature (Data digitized from Millet et al., 2012); c. Lago di Origlio chironomid-inferred temperature (Samartin et al., 2012); d. Alboran sea surface temperature (SST; Cacho et al., 2001); e. Tyrrhenian SST (Cacho et al., 2001); f. NEEM temperature reconstruction (Buizert et al., 2014); g. Total radiative forcing from greenhouse gasses (Schilt et al., 2010; Marcott et al., 2014); h. CO_2 from West Antarctic Ice Sheet Divide ice core (WDC; Marcott et al., 2014); i: CH_4 from WDC (WAIS Divide Project Members, 2013; Marcott et al., 2014) and j. Summer and December insolation curves for 45°N (Berger and Loutre, 1991). (For interpretation of the references to colour in this figure legend, the reader is referred to the Web version of this article.)

strongest shift in assemblage composition occurred at the transition between chironomid zones Burg 2 and 3, which coincides with the Oldest Dryas/Bølling transition, as is clearly indicated by both changes in DCA axis 1 scores (Fig. 4) and the statistically significant zonal boundary identified at this transition by CONISS (Fig. 3). However, the trend in assemblage composition clearly started much earlier with the onset of Burg 2, at ca. 16,200 cal. BP (ca. 950 cm). Temperatures tend to co-vary with nutrient availability, and in consequence often also oxygen availability for deepwater fauna in lakes. This can be observed among modern lakes, e.g. as represented in chironomid-temperature calibration datasets (Brodersen and Anderson, 2002; Heiri and Lotter, 2005). However, similar patterns are apparent in downcore records as well where assemblages of cold-indicating chironomids also tend to be dominated by taxa adapted for oxygen-rich and nutrient-poor conditions (e.g. Hofmann, 2001; Velle et al., 2010), whereas warm-adapted assemblages are often dominated by more eutrophic taxa that are also better able to survive low oxygen conditions (Brodersen and Anderson, 2002; Eggermont and Heiri, 2012). To explore the extent to which chironomid assemblage change in the Burgäschisee record can be explained by changes in nutrient concentrations, rather than temperatures, we compared downcore trajectories in chironomid assemblage composition with modern (subfossil) chironomid assemblages in 28 deep lakes across Europe (Verbruggen et al., 2011) using direct gradient analysis (Fig. 4). Since these lakes are all deep and stratified (max. water depth mostly 30 m and deeper), it can be expected that between-lake variations in chironomid assemblage composition in this dataset are mainly driven by nutrient and oxygen concentrations rather than air or surface water temperatures (Verbruggen et al., 2011). The results of this analysis revealed that there is some co-variation in chironomid assemblage changes toward assemblage states typical for more nutrient-rich lakes (indicated by DCCA axis 1 values, Fig. 4c) and towards assemblages typical for warmer lakes (indicated by chironomid-inferred temperatures, Fig. 4b). However, the trend toward assemblages representative for nutrient-rich, stratified lakes appears to start well before the trend towards assemblages typical for warmer lakes (Fig. 4). Furthermore, after 15,600 cal BP (ca. 894 cm), when chironomid-inferred temperatures were clearly increasing, there is no evidence for shifts in the DCCA towards assemblage states typical for more nutrient-rich lakes. These analyses therefore suggest that, even though there will have been some co-variation between increasing temperatures and increasing nutrient concentrations at Burgäschisee during the Lateglacial, as can be expected based on other Lateglacial chironomid records from Europe (e.g. Brooks and Birks, 2001; Heiri and Millet, 2005), shifts towards assemblages typical for warmer lake ecosystems cannot be easily explained simply by the increasing nutrient concentrations in the lake. Instead, these shifts, particularly from 15,600 cal. BP onwards, seem to be mainly driven by increasing temperature, without a corresponding trajectory towards assemblage composition typical for more nutrient-rich lakes.

S. coracina-type, which dominates throughout the Burgäschisee record, is able to survive in cool arctic to subarctic lakes, but also in temperate lakes where thermal stratification maintains a cool profundal zone (Hofmann, 2001) as long as that the trophic state is oligo-mesotrophic and allows sufficient oxygen below the thermocline (Brundin, 1956 in Hofman, 2001). Based on the modern water depth, and the length of the sediment sequence, Burgäschisee may have been as deep as 39–41 m during the early late glacial. Hypolimnetic oxygen apparently remained high enough to allow the survival of *S. coracina*-type in the deep, cold profundal habitats of the lake even in the temperate climate conditions after the Oldest Dryas – Bølling transition. It could be expected that the persistence of a large, cool profundal compartment, and of those

chironomid types inhabiting it, could influence the temperature reconstruction, leading to a depression in reconstructed temperatures and a more gradual transition of chironomid assemblages than expected for shallower lakes. However, in our record the transition between Burg 2 and 3 coincided perfectly with the transition between the Oldest Dryas and Bølling zones and local reforestation as represented in the Burgäschisee pollen record (Rey et al., 2017), speaking against such a delayed response of chironomid assemblages in the lake. Furthermore, absolute values of the Burgäschisee chironomid-inferred temperature reconstruction agree well with a similar reconstruction from a shallow water (littoral) sediment core from Lake Gerzensee (see 4.2.2, below), suggesting that the depth of the lake did not lead to a significant depression of chironomid-based temperature inferences at Burgäschisee.

4.1.1. Comparison of the new temperature record with regional vegetation development

The Burgäschisee chironomid record has provided the first well dated high-resolution Early Lateglacial temperature reconstruction in the Northern Swiss lowlands that is not based on vegetation proxies. It covers almost the entire period, from landscape stabilisation after glacial termination and retreat, to the Bølling interstadial. Chironomid remains were abundant enough for inferring temperatures immediately after sands are no longer deposited into the lake (ca. 18,300 cal. B.P.). Between ca. 18,300–16,100 cal. BP the temperature reconstruction indicates relatively stable low July air temperatures of ca. 9 °C (Fig. 5), values 9–10 °C cooler than today. This is in agreement with the Burgäschisee pollen record which indicates a tree-less steppe tundra dominated by a diverse array of herb flora as well as thickets of small shrubs, including the dwarf birch *Betula nana* (Rey et al., 2017). Furthermore, this finding agrees with other pollen records from lowland Switzerland which consistently indicate a tundra environment for this time period (e.g. Rey et al., 2020; Beckmann et al., 2004; Lotter et al., 1999; Lotter and Zbinden, 1989). At present, the potential upper, temperature-limited treeline in the Alps coincides with mean July air temperatures around 7.5–9.5 °C (Landolt, 2003), and therefore inferred July air temperatures are consistent with the palaeovegetation data.

At ca. 16,200 cal. BP (broadly correlating with the transition to chironomid assemblage zone Burg 2) chironomid-inferred July air temperatures at Burgäschisee increase from ca. 9 °C to ca. 10 °C (Fig. 5). This increase corresponds with the increase in shrub pollen in the Burgäschisee record, particularly of *Betula nana, Salix,* and *Juniperus*. Furthermore *Betula* trees expanded, likely forming first stands in the tundra (Rey et al., 2017, Fig. 5), even though the vegetation around Burgäschisee remained dominated by herbs. This implies a transition from a herb-dominated steppe tundra to shrub tundra, with tree stands or small woodlands dominated by *Betula* occupying favourable sites. Palaeobotanical data from other pollen records across the northern Swiss lowlands display a similar vegetational reorganisation at other sites (e.g. Lotter, 1999; Beckmann et al., 2004; Rey et al., 2020) prior to afforestation at 14,700 cal. BP. It has been suggested that the early expansion of shrub tundra may have been the consequence of delayed pedogenesis and associated increase in nutrient availability for terrestrial plants (Ammann et al., 1983). However, glaciological evidence suggests that glacier retreat occurred as early as ca. 19,000 cal. BP (±1000 years) (Ivy Ochs et al., 2004) in the study region which is in excellent agreement with the oldest radiocarbon dated lake sediment sequences on the Swiss Plateau which reach back to as early as 19,180 cal. BP at Moossee (Rey et al., 2020). This would imply a 3000-year period in which pedogenesis did not modulate vegetational distributions, followed by a near synchronous vegetational composition shift across the entire northern Swiss lowlands. As Rey et al. (2017; 2020) point out, it seems more likely that after initial pedogenesis and landscape stabilisation a synchronous and regional increase in July temperature above 10 °C enabled shrub and tree taxa to establish and expand in lowland Switzerland. Our new temperature record from Burgäschisee indicates a clear shift towards chironomid assemblages typical for higher temperatures at this transition, and, as consequence an increase in chironomid-inferred temperatures that coincides with this vegetation change. This provides clear support for the hypothesis that an increase in summer temperatures is responsible for this observed, large-scale vegetation change on the Swiss Plateau before afforestation at 14,700 cal. BP.

Chironomid-inferred temperatures in the Burgäschisee record continue to increase throughout zone Burg 2, reaching values as high as 12–12.5 °C while the vegetation composition established after the temperature increase at ca. 16,000 cal. BP does not change significantly. The temperature rise culminates in a rapid temperature increase from ca. 12.0–15 °C at the transition from Burg 2 into Burg 3 (Fig. 5), coinciding with the Oldest Dryas/Bølling transition in the pollen record. In other pollen profiles and palaeotemperature reconstructions from Switzerland the temperature increase associated with the Oldest Dryas/Bølling transition has been estimated to have taken place very rapidly with a duration between 40 and 95 years (van Raden et al., 2013; Luetscher et al., 2015). At Burgäschisee, this transition seems to occur slightly more slowly, but this may be the consequence of a relatively low sampling resolution in the chironomid record during this transition as well as of the dating uncertainty. This transition occurs synchronously with reorganisations of vegetation around Burgäschisee with an initial short-lived increase in *Juniperus* pollen (up to 60%; Fig. 5), typical for Lateglacial afforestation in lowland Switzerland, followed by an increase in *Betula* pollen representative for tree *Betula* species in the pollen record (Rey et al., 2017). This finding agrees well with other climate records from Central Europe which consistently indicate a rapid warming phase at the Oldest Dryas/Bølling transition. For example, oxygen isotope records from speleothem and lake marl sequences indicate a rapid increase in temperature at ca. 14,700 cal. B.P. (Lotter et al., 1992, 2012; van Raden et al., 2013; Luetscher et al., 2015).

4.1.2. Burgäschisee chironomid-inferred temperatures compared with other climate reconstructions

The Burgäschisee record represents one of the few, well-dated palaeoclimate records from Southwestern Central Europe with independent age estimates older than the Oldest Dryas/Bølling transition. In the lowest section between ca. 18,300–16,200 cal. BP, July air temperatures of ca. 9 °C are inferred. These temperatures agree with the vegetation reconstructions for lowland Switzerland at this time interval, which indicate a treeless tundra environment with some shrub elements (see section 4.2.1.). Furthermore, similar July air temperature values 8–10 °C below modern have also been reported for full glacial conditions based on climate model-based estimates for the study region (e.g. Ludwig et al., 2017). During the start of the first warming phase at ca. 16,200–16,000 cal. BP, chironomid-inferred temperatures increase to around 10 °C. This again agrees with the vegetation reconstruction which indicates a change from a largely treeless environment to a tree-shrub tundra at this time, a vegetation transition which at the alpine treeline can presently be observed at July air temperatures around 7.5–9.5 °C (Landolt, 2003). From the latest sections of the Oldest Dryas onwards several other quantitative temperature records are available from Central Europe (Heiri et al., 2014). The second available chironomid-based July air temperature reconstruction from the Swiss Plateau originates from Gerzensee, 58 km from Burgäschisee.

This lake sediment record extends ca. 40 cm below the Oldest Dryas/Bølling transition (Lotter et al., 2012; Brooks and Heiri, 2013). However, since there is no reliable basal age constraint for this sequence it remains unclear how rapid sedimentation rates are in this section of the record which essentially remains undated. In the sediments just preceding the Oldest Dryas/Bølling transition chironomid-inferred temperatures of 12 °C are recorded, values very similar to the reconstructed temperatures at Burgäschisee of ca. 11.5 °C (Fig. 5). At the transition, both the Burgäschisee and Gerzensee chironomid records indicate a rapid increase of July air temperatures from ca. 12 to ca. 15 °C, followed by a more gradual increase during the early Bølling period.

The increase in temperature at the Oldest Dryas/Bølling transition in the Burgäschisee and Gerzensee records is of similar amplitude as the increase by 2–3 °C inferred for this transition in the French Jura mountains (Heiri and Millet, 2005) and Central Switzerland (Larocque et al., 2010) based on chironomids, and for the Swiss Plateau based on mixed aquatic insect taxa (Elias and Wilkinson, 1983). Additionally, both the Burgäschisee record and that of Heiri and Millet (2005) display a gradual temperature increase in the early Bølling which is in agreement with the increasing summer insolation values during the Lateglacial interstadial (Berger and Loutre, 1991), and, e.g., the oxygen isotope-based reconstructions of mean annual air temperature from Ammersee and Gerzensee (von Grafenstein et al., 1999, 2013). In contrast, some other summer temperature reconstructions from Northern Switzerland, for example pollen-based reconstructions (e.g. Lotter et al., 2012) show a more pronounced warming at the Oldest Dryas/Bølling transition and higher early Bølling than late Bølling temperatures. Lotter et al. (2012) discuss that this discrepancy may be due to temperatures during different seasons than summer and/or precipitation influencing vegetation in the Swiss Plateau during this interval.

The temperature development inferred by chironomids at Burgäschisee is also consistent with the inferred glacier retreat after the end of the Last Glacial Maximum in Northern Switzerland. Several phases of glacier retreat suggest warming episodes well before the Oldest Dryas/Bølling transition, including at ca. 16,000 cal. BP (e.g. Ivy-Ochs et al., 2008; Heiri et al., 2014). However, further phases of glacier retreats between 18,000 and 14,700 cal. BP are inferred based on past glacier extent, which are not represented as warming phases in our chironomid record (Ivy-Ochs et al., 2008). This may be because glaciation and glacier extent are not only determined by summer temperatures but also precipitation, local humidity and other factors that influence glacier extent and ice dynamics (Kerschner and Ivy-Ochs, 2008).

Additional chironomid-based reconstructions that encompass the period 16,000–14,700 cal. BP and are reliably dated in this interval are available from south of the Alps, from the Ticino region of Southern Switzerland (Lago di Origlio, Samartin et al., 2012), and from Western France in the Northern Pyrenees (Ech Palaeolake; Millet et al., 2012). These reconstructions agree with the Burgäschisee record in that a distinct increase in July air temperatures is inferred at the Oldest Dryas/Bølling transition, i.e. an abrupt temperature increase in the range of 2–5 °C (Fig. 6). However, as discussed in Samartin et al. (2012) temperatures in the Lago di Origlio record show a stepwise increase for the pre-Bølling, with a distinct increase by ca. 2.5 °C recorded at ca. 16,000 cal. BP followed by a relatively stable period prior to the temperature rise at the transition to the Bølling. This pre-Bølling increase at 16,000 cal. BP coincides with reforestation in Northern Italy and other sections of the northern Mediterranean region (Samartin et al., 2012), with increases in sea-surface temperatures inferred from marine records in the Mediterranean (Cacho et al., 2001), as well as with climatic ameliorations inferred from speleothems for the Eastern Mediterranean region (e.g. Fleitmann et al., 2009). In contrast, the chironomid-inferred record from the Ech palaeolake, situated in the northern Pyrenees only 128 km from the Atlantic coastline, displays no clear trend in temperatures during the pre-Bølling period. It seems therefore that changes in chironomid-inferred temperatures at Burgäschisee can be interpreted as intermediate between the situation at Ech, which during the entire period ca. 19,000 to 14,700 cal. BP was apparently influenced by the prevailing cold conditions over the North Atlantic resulting in the maintenance of low temperatures (Millet et al., 2012; Martínez-García et al., 2015); and Lago di Origlio where the chironomid-based temperature reconstruction displays a stepwise increase with a distinct pre-Bølling warming occurring at 16,000 cal. BP. Lago di Origlio has a climate typical for the Southern Alps, shielded from both Northern and Western air masses by the Alpine arc and presently maintaining an “Insubrian” climate (Brzeziecki et al., 1995) in which temperatures are close to those of more southern regions of the Mediterranean area (Bugmann, 1996). Therefore, it is not surprising that the temperature reconstruction from this site shows a similar temperature development as seen in records from the Mediterranean Sea (Alboran and Tyrrhenian seas; Cacho et al., 2001), which also show a clear increase in temperature from ca. 16,200 cal. BP onwards (Fig. 6). Presently the climate in the region of Burgäschisee is characterized by a strong westerly influence (National Centre for Climate Services, 2014), both during the winter and summer months. Although significant air circulation pattern changes have been suggested for the last deglaciation (e.g. Luetscher et al., 2015; Becker et al., 2016), it can be expected that a significant westerly influence will have prevailed during the entire Lateglacial period. At the same time increasing summer insolation and greenhouse gas concentrations would have promoted increasing summer temperatures, explaining the “mixed” pattern of temperature changes at Burgäschisee intermediate between the situation at Ech and Lago di Origlio.

5. Conclusions

Our new, quantitative summer temperature reconstruction from northern Switzerland, together with recent palynological results demonstrating distinct vegetation changes on the Swiss Plateau around ca. 16,000 (Rey et al., 2017; 2020), indicate that summer temperatures were increasing in this region well before the major Lateglacial warming inferred at the Oldest Dryas/Bølling transition at ca. 14,700 cal. BP. This pattern agrees with temperature variations reported for lower latitude regions of Europe (e.g. Fletcher et al., 2010). It is also consistent with the increasing greenhouse gas concentrations and Northern hemisphere summer insolation values, as these would be expected to lead to progressively warmer summer climate in large sections of the northern hemisphere during this time interval. Our results therefore suggest that even though large parts of Central and Northern Europe were still covered by tundra to steppe vegetation during the period ca. 19,000 to 14,700 cal. BP (Rey et al., 2017; 2020), distinct warming trends may already have influenced summer temperatures at least in the southwestern sector of Central Europe. They also challenge the conventional view that major parts of Central and Northwestern Europe did not show major Lateglacial warming prior to 14,700 cal. BP, an interpretation that is in agreement with $\delta^{18}O$ records from the GRIP and GISP ice core records from Greenland (Johnsen et al., 2001), which also do not show major warming prior to this date. In this context it is interesting to note that temperature reconstructions from the Greenland ice cores which take into account additional information next to the $\delta^{18}O$ record, such as combined reconstructions based on borehole temperature and $\delta^{18}O$ (GRIP ice core, Johnsen et al., 2001) or $\delta^{15}N\text{-}N_2$ (Neem ice core,

Buizert et al., 2014) show evidence for a similar early Lateglacial warming as recorded in our new Burgäschsee record (Fig. 6). This suggests that also Greenland and possibly other parts of the northern circum-Atlantic region may have been affected by such an early pre-Bøllling Lateglacial warming.

Author statement

Alexander Bolland and Oliver Heiri: Conceptualization, Methodology, Validation, Formal Analysis, Writing - Original Draft and Project administration. Alexander Bolland, Erika Gobet, Fabian Rey: Investigation. Alexander Bolland: Data curation and Visualization. Oliver Heiri, Fabian Rey, Erika Gobet, Willy Tinner: Supervision. Oliver Heiri: Funding acquisition. Alexander Bolland, Oliver Heiri, Erika Gobet, Willy Tinner and Fabian Rey: Resources and Writing - Review & Editing.

Data availability

Chironomid data associated with this study as well as the chironomid-inferred temperature data have been deposited at the Dryad online data repository: https://doi.org/10.5061/dryad.08kprr509 (www.datadryad.org/).

Declaration of competing interest

The authors declare that they have no known competing financial interests or personal relationships that could have appeared to influence the work reported in this paper.

Acknowledgments

We thank all members of the field work team: Willi Tanner, Richard Niederreiter, André F. Lotter, Claire Rambeau, Marianne Steffen, Camilla Calò, Stéphanie Samartin, Elisa Vescovi, Stefanie Wirth, Stewart Bishop, Martin Tschanz and Florencia Oberli. We also thank both reviewers for helpful suggestions that have improved our manuscript. This research has been supported by the Swiss National Science Foundation (SNSF grant 200021_165494).

Appendix A. Supplementary data

Supplementary data to this article can be found online at https://doi.org/10.1016/j.quascirev.2020.106484.

References

Allen, J.R., Watts, W.A., Huntley, B., 2000. Weichselian palynostratigraphy, palaeovegetation and palaeoenvironment; the record from Lago Grande di Monticchio, southern Italy. Quat. Int. 73, 91–110.
Ambühl, H., Stumm, W., 1984. Bericht über die Auswirkungen der Tiefenwasserableitung im Burgäschisee. EAWAG.
Ammann, B., Chaix, L., Eicher, U., Elias, S.A., Gaillard, M.J., Hofmann, W., Siegenthaler, U., Tobolski, K., Wilkinson, B., 1983. Vegetation, insects, molluscs and stable isotopes from late Würm deposits at Lobsigensee (Swiss Plateau). Studies in the late Quaternary of Lobsigensee 7. Rev. Paleobiol. 2, 221–227.
Ammann, B., van Leeuwen, J.F., van der Knaap, W.O., Lischke, H., Heiri, O., Tinner, W., 2013. Vegetation responses to rapid warming and to minor climatic fluctuations during the Late-Glacial Interstadial (GI-1) at Gerzensee (Switzerland). Palaeogeogr. Palaeoclimatol. Palaeoecol. 391, 40–59.
Andersen, T., Cranston, P.S., Epler, J.H. (Eds.), 2013. Chironomidae of the Holarctic Region: Keys and Diagnoses: Larvae. Scandinavian Society of Entomology.
Arn, H., 1945. Die Melioration des Gebietes um den Burgäschisee und die See-Absenkung. Verlag nicht ermittelbar.
Becker, P., Seguinot, J., Jouvet, G., Funk, M., 2016. Last Glacial Maximum precipitation pattern in the Alps inferred from glacier modelling. Geograph. Helv. 71 (3), 173–187.
Beckmann, M., 2004. Pollenanalytische Untersuchung der Zeit der Jäger und Sammler und der ersten Bauern an zwei Lokalitäten des Zentralen Schweizer Mittellandes. Diss. Bot. 390, 1–223.
Bennett, K.D., 1996. Determination of the number of zones in a biostratigraphical sequence. New Phytol. 132 (1), 155–170.
Berger, A., Loutre, M.F., 1991. Insolation values for the climate of the last 10 million years. Quat. Sci. Rev. 10 (4), 297–317.
Birks, H.J.B., Braak, C.T., Line, J.M., Juggins, S., Stevenson, A.C., 1990. Diatoms and pH reconstruction. Philos. Trans. Roy. Soc. B 327 (1240), 263–278.
Birks, H.J.B., Heiri, O., Seppä, H., Bjune, A.E., 2010. Strengths and weaknesses of quantitative climate reconstructions based on Late-Quaternary. Open Ecol. J. 3 (1), 68–110.
Birks, H.H., Aarnes, I., Bjune, A.E., Brooks, S.J., Bakke, J., Kühl, N., Birks, H.J.B., 2014. Lateglacial and early-Holocene climate variability reconstructed from multi-proxy records on Andøya, northern Norway. Quat. Sci. Rev. 89, 108–122.
Blaauw, M., 2010. Methods and code for 'classical'age-modelling of radiocarbon sequences. Quat. Geochronol. 5 (5), 512–518.
Bugmann, H.K., 1996. A simplified forest model to study species composition along climate gradients. Ecology 77 (7), 2055–2074.
ter Braak, C.J., Juggins, S., 1993. Weighted averaging partial least squares regression (WA-PLS): an improved method for reconstructing environmental variables from species assemblages. In: Twelfth International Diatom Symposium. Springer, Dordrecht, pp. 485–502.
ter Braak, C.J.F., Juggins, S., Birks, H.J.B., Van der Voet, H., 1993. Weighted averaging partial least squares regression (WA-PLS): definition and comparison with other methods for species-environment calibration. In: Multivariate Environmental Statistics, vol. 6. Elsevier, pp. 525–560.
ter Braak, J.F., Smilauer, P., 2018. Canoco Reference Manuel and User's Guide: Software for Ordination (Version 5.10). Microcomputer Power, Ithaca, NY, USA), p. 536.
Brodersen, K.P., Anderson, N.J., 2002. Distribution of chironomids (Diptera) in low arctic West Greenland lakes: trophic conditions, temperature and environmental reconstruction. Freshw. Biol. 47 (6), 1137–1157.
Brodersen, K.P., Quinlan, R., 2006. Midges as palaeoindicators of lake productivity, eutrophication and hypolimnetic oxygen. Quat. Sci. Rev. 25 (15–16), 1995–2012.
Brooks, S.J., 2006. Fossil midges (Diptera: Chironomidae) as palaeoclimatic indicators for the Eurasian region. Quat. Sci. Rev. 25 (15–16), 1894–1910.
Brooks, S.J., Birks, H.J.B., 2000. Chironomid-inferred Late-glacial air temperatures at Whitrig Bog, southeast Scotland. J. Quat. Sci. 15 (8), 759–764.
Brooks, S.J., Birks, H.J.B., 2001. Chironomid-inferred air temperatures from Late-glacial and Holocene sites in north-west Europe: progress and problems. Quat. Sci. Rev. 20 (16–17), 1723–1741.
Brooks, S.J., Heiri, O., 2013. Response of chironomid assemblages to environmental change during the early Late-glacial at Gerzensee, Switzerland. Palaeogeogr. Palaeoclimatol. Palaeoecol. 391, 90–98.
Brooks, S.J., Langdon, P.G., Heiri, O., 2007. The Identification and Use of Palaeartic Chironomidae Larvae in Palaeoecology. QRA Technical guide No10. Quaternary Research Association, London UK, p. 276.
Brundin, L., 1956. Die bodenfaunistischen Seetypen und ihre Anwendbarkeit auf die Südhalbkugel. Zugleich eine Theorie der produktionsbiologischen Bedeutung der glazialen Erosion. Inst. Freshw. Res. Drottningholm Rep. 37, 186–235.
Brzeziecki, B., Kienast, F., Wildi, O., 1995. Modelling potential impacts of climate change on the spatial distribution of zonal forest communities in Switzerland. J. Veg. Sci. 6 (2), 257–268.
Buizert, C., Gkinis, V., Severinghaus, J.P., He, F., Lecavalier, B.S., Kindler, P., Leuenberger, M., Carlson, A.E., Vinther, B., Masson-Delmotte, V., White, J.W., 2014. Greenland temperature response to climate forcing during the last deglaciation. Science 345 (6201), 1177–1180.
Cacho, I., Grimalt, J.O., Canals, M., Sbaffi, L., Shackleton, N.J., Schönfeld, J., Zahn, R., 2001. Variability of the western Mediterranean Sea surface temperature during the last 25,000 years and its connection with the Northern Hemisphere climatic changes. Paleoceanography 16 (1), 40–52.
Clark, P.U., Dyke, A.S., Shakun, J.D., Carlson, A.E., Clark, J., Wohlfarth, B., Mitrovica, J.X., Hostetler, S.W., McCabe, A.M., 2009. The last glacial maximum. Science 325 (5941), 710–714.
Clark, P.U., Shakun, J.D., Baker, P.A., Bartlein, P.J., Brewer, S., Brook, E., Carlson, A.E., Cheng, H., Kaufman, D.S., Liu, Z., Marchitto, T.M., 2012. Global climate evolution during the last deglaciation. Proc. Natl. Acad. Sci. Unit. States Am. 109 (19), 1134–1142.
Duprat-Oualid, F., Rius, D., Bégeot, C., Magny, M., Millet, L., Wulf, S., Appelt, O., 2017. Vegetation response to abrupt climate changes in Western Europe from 45 to 14.7 k cal a BP: the Bergsee lacustrine record (Black Forest, Germany). J. Quat. Sci. 32 (7), 1008–1021.
Eggermont, H., Heiri, O., 2012. The chironomid-temperature relationship: expression in nature and palaeoenvironmental implications. Biol. Rev. 87 (2), 430–456.
Eicher, U., Siegenthaler, U., 1976. Palynological and oxygen isotope investigations on Late-Glacial sediment cores from Swiss lakes. Boreas 5 (2), 109–117.
Elias, S.A., Wilkinson, B., 1983. Lateglacial insect fossil assemblages from Lobsigensee (Swiss plateau). Studies in the late quaternary of Lobsigensee 3. Rev. Paleobiol. 2 (2), 189–204.
Fischer, H., Behrens, M., Bock, M., Richter, U., Schmitt, J., Loulergue, L., Chappellaz, J., Spahni, R., Blunier, T., Leuenberger, M., Stocker, T.F., 2008. Changing boreal methane sources and constant biomass burning during the last termination. Nature 452 (7189), 864–867.
Fleitmann, D., Cheng, H., Badertscher, S., Edwards, R.L., Mudelsee, M., Göktürk, O.M., Fankhauser, A., Pickering, R., Raible, C.C., Matter, A., Kramers, J., 2009. Timing

and climatic impact of Greenland interstadials recorded in stalagmites from northern Turkey. Geophys. Res. Lett. 36 (19) https://doi.org/10.1029/2009GL040050.
Fletcher, W.J., Goñi, M.F.S., 2008. Orbital-and sub-orbital-scale climate impacts on vegetation of the western Mediterranean basin over the last 48,000 yr. Quat. Res. 70 (3), 451–464.
Fletcher, W.J., Goñi, M.S., Peyron, O., Dormoy, I., 2010. Abrupt climate changes of the last deglaciation detected in a Western Mediterranean forest record. Clim. Past 6, 245–264.
von Grafenstein, U., Erlenkeuser, H., Brauer, A., Jouzel, J., Johnsen, S.J., 1999. A mid-European decadal isotope-climate record from 15,500 to 5000 years BP. Science 284 (5420), 1654–1657.
von Grafenstein, U., Belmecheri, S., Eicher, U., van Raden, U.J., Erlenkeuser, H., Andersen, N., Ammann, B., 2013. The oxygen and carbon isotopic signatures of biogenic carbonates in Gerzensee, Switzerland, during the rapid warming around 14,685 years BP and the following interstadial. Palaeogeogr. Palaeoclimatol. Palaeoecol. 391, 25–32.
Grimm, E.C., 1987. CONISS: a FORTRAN 77 program for stratigraphically constrained cluster analysis by the method of incremental sum of squares. Comput. Geosci. 13 (1), 13–35. https://doi.org/10.1016/0098-3004(87)90022-7.
Guthruf, J., Zeh, M., Guthruf-Seiler, K., 1999. Kleinseen im Kanton Bern. Amt für Gewässerschutz und Abfallwirtschaft des Kantons Bern. Gewässer-und Bodenschutzlabor, pp. 32–34.
He, F., Shakun, J.D., Clark, P.U., Carlson, A.E., Liu, Z., Otto-Bliesner, B.L., Kutzbach, J.E., 2013. Northern Hemisphere forcing of Southern Hemisphere climate during the last deglaciation. Nature 494 (7435), 81–85.
Heiri, O., Lotter, A.F., 2001. Effect of low count sums on quantitative environmental reconstructions: an example using subfossil chironomids. J. Paleolimnol. 26 (3), 343–350.
Heiri, O., Lotter, A.F., Hausmann, S., Kienast, F., 2003. A chironomid-based Holocene summer air temperature reconstruction from the Swiss Alps. Holocene 13 (4), 477–484.
Heiri, O., Lotter, A.F., 2005. Holocene and Lateglacial summer temperature reconstruction in the Swiss Alps based on fossil assemblages of aquatic organisms: a review. Boreas 34 (4), 506–516.
Heiri, O., Millet, L., 2005. Reconstruction of late glacial summer temperatures from chironomid assemblages in lac Lautrey (Jura, France). J. Quat. Sci. 20 (1), 33–44.
Heiri, O., Cremer, H., Engels, S., Hoek, W.Z., Peeters, W., Lotter, A.F., 2007a. Late-glacial summer temperatures in the Northwest European lowlands: a chironomid record from Hijkermeer, The Netherlands. Quat. Sci. Rev. 26 (19–21), 2420–2437.
Heiri, O., Filippi, M.L., Lotter, A.F., 2007b. Lateglacial summer temperature in the Trentino area (Northern Italy) as reconstructed by fossil chironomid assemblages in Lago di Lavarone (1100 m asl). Studi Trentini Sci. Nat. Acta Geol. 82, 299–308.
Heiri, O., Lotter, A.F., 2010. How does taxonomic resolution affect chironomid-based temperature reconstruction? J. Paleolimnol. 44 (2), 589–601.
Heiri, O., Brooks, S.J., Birks, H.J.B., Lotter, A.F., 2011. A 274-lake calibration data-set and inference model for chironomid-based summer air temperature reconstruction in Europe. Quat. Sci. Rev. 30 (23–24), 3445–3456.
Heiri, O., Koinig, K.A., Spotl, C., Barrett, S., Brauer, A., Drescher-Schneider, R., Gaar, D., Ivy-Ochs, S., Kerschner, H., Luetscher, M., Moran, A., Nicolussi, K., Preusser, F., Schmidt, R., Schoeneich, P., Schworer, C., Sprafke, T., Terhorst, B., Tinner, W., 2014. Palaeoclimate records 60-8 ka in the Austrian and Swiss Alps and their forelands. Quat. Sci. Rev. 106, 186–205. https://doi.org/10.1016/j.quascirev.2014.05.021.
Hughes, A.L., Gyllencreutz, R., Lohne, Ø.S., Mangerud, J., Svendsen, J.I., 2016. The last Eurasian ice sheets–a chronological database and time-slice reconstruction, DATED-1. Boreas 45 (1), 1–45.
Hoek, W.Z., Bohncke, S.J.P., 2002. Climatic and environmental events over the Last Termination, as recorded in The Netherlands: a review. Neth. J. Geosci. 81 (1), 123–137.
Hofmann, W., 2001. Late-Glacial/Holocene succession of the chironomid and cladoceran fauna of the Soppensee (Central Switzerland). J. Paleolimnol. 25 (4), 411–420.
Ilyashuk, B., Gobet, E., Heiri, O., Lotter, A.F., van Leeuwen, J.F., van der Knaap, W.O., Ilyashuk, E., Oberli, F., Ammann, B., 2009. Lateglacial environmental and climatic changes at the Maloja Pass, Central Swiss Alps, as recorded by chironomids and pollen. Quat. Sci. Rev. 28 (13–14), 1340–1353.
Ivy-Ochs, S., Schäfer, J., Kubik, P.W., Synal, H.A., Schlüchter, C., 2004. Timing of deglaciation on the northern Alpine foreland (Switzerland). Eclogae Geol. Helv. 97 (1), 47–55.
Ivy-Ochs, S., Kerschner, H., Reuther, A., Preusser, F., Heine, K., Maisch, M., Kubik, P.W., Schlüchter, C., 2008. Chronology of the last glacial cycle in the European Alps. Quat. Sci. Rev. 23, 559–573.
Johnsen, S.J., Dahl-Jensen, D., Gundestrup, N., Steffensen, J.P., Clausen, H.B., Miller, H., Masson-Delmotte, V., Sveinbjörnsdottir, A.E., White, J., 2001. Oxygen isotope and palaeotemperature records from six Greenland ice-core stations: Camp Century, Dye-3, GRIP, GISP2, Renland and NorthGRIP. Quat. Sci. Rev. 16 (4), 299–307.
Juggins, S., 2007. C2: Software for Ecological and Palaeoecological Data Analysis and Visualisation (User Guide Version 1.5). Newcastle University, Newcastle upon Tyne, p. 77.
Juggins, S., 2017. Rioja: Analysis of Quaternary Science Data. R package version (0.9-21). http://cran.r-project.org/package=rioja.
Kaltenrieder, P., Belis, C.A., Hofstetter, S., Ammann, B., Ravazzi, C., Tinner, W., 2009. Environmental and climatic conditions at a potential Glacial refugial site of tree species near the Southern Alpine glaciers. New insights from multiproxy sedimentary studies at Lago della Costa (Euganean Hills, Northeastern Italy). Quat. Sci. Rev. 28 (25–26), 2647–2662.
Kerschner, H., Ivy-Ochs, S., 2008. Palaeoclimate from glaciers: examples from the eastern Alps during the alpine lateglacial and early Holocene. Global Planet. Change 60, 58–71.
Landolt, E., 2003. Unsere Alpenflora. Gustav Fisher, Stuttgart, Germany.
Larocque, I., Finsinger, W., 2008. Late-glacial chironomid-based temperature reconstructions for Lago Piccolo di Avigliana in the southwestern Alps (Italy). Palaeogeogr. Palaeoclimatol. Palaeoecol. 257 (1–2), 207–223.
Larocque-Tobler, I., 2010. Reconstructing temperature at Egelsee, Switzerland, using North American and Swedish chironomid transfer functions: potential and pitfalls. J. Paleolimnol. 44 (1), 243–251.
Lepš, J., Šmilauer, P., 2003. Multivariate Analysis of Ecological Data Using CANOCO. Cambridge university press.
Liu, Z., Otto-Bliesner, B.L., He, F., Brady, E.C., Tomas, R., Clark, P.U., Carlson, A.E., Lynch-Stieglitz, J., Curry, W., Brook, E., Erickson, D., 2009. Transient simulation of last deglaciation with a new mechanism for Bølling-Allerød warming. Science 325 (5938), 310–314.
Lotter, A.F., Eicher, U., Siegenthaler, U., Birks, H.J.B., 1992. Late-glacial climatic oscillations as recorded in Swiss lake sediments. J. Quat. Sci. 7 (3), 187–204.
Lotter, A.F., 1999. Late-glacial and Holocene vegetation history and dynamics as shown by pollen and plant macrofossil analyses in annually laminated sediments from Soppensee, central Switzerland. Veg. Hist. Archaeobotany 8 (3), 165–184.
Lotter, A.F., Zbinden, H., 1989. Late-Glacial pollen analysis, oxygen-isotope record, and radiocarbon stratigraphy from Rotsee (Lucerne), Central Swiss Plateau. Eclogae Geol. Helv. 82 (1), 191–202.
Lotter, A.F., Heiri, O., Brooks, S., van Leeuwen, J.F., Eicher, U., Ammann, B., 2012. Rapid summer temperature changes during Termination 1a: high-resolution multi-proxy climate reconstructions from Gerzensee (Switzerland). Quat. Sci. Rev. 36, 103–113.
Luetscher, M., Boch, R., Sodemann, H., Spötl, C., Cheng, H., Edwards, R.L., Frisia, S., Hof, F., Müller, W., 2015. north Atlantic storm track changes during the last glacial maximum recorded by alpine speleothems. Nat. Commun. 6, 6344.
Ludwig, P., Pinto, J.G., Raible, C.C., Shao, Y., 2017. Impacts of surface boundary conditions on regional climate model simulations of European climate during the Last Glacial Maximum. Geophys. Res. Lett. 44 (10), 5086–5095.
Magny, M., Aalbersberg, G., Bégeot, C., Benoit-Ruffaldi, P., Bossuet, G., Disnar, J.R., Heiri, O., Laggoun-Defarge, F., Mazier, F., Millet, L., Peyron, O., 2006. Environmental and climatic changes in the Jura mountains (eastern France) during the Lateglacial–Holocene transition: a multi-proxy record from Lake Lautrey. Quat. Sci. Rev. 25 (5–6), 414–445.
Marcott, S.A., Bauska, T.K., Buizert, C., Steig, E.J., Rosen, J.L., Cuffey, K.M., Fudge, T.J., Severinghaus, J.P., Ahn, J., Kalk, M.L., McConnell, J.R., 2014. Centennial-scale changes in the global carbon cycle during the last deglaciation. Nature 514 (7524), 616–619.
Martínez-García, B., Rodríguez-Lázaro, J., Pascual, A., Mendicoa, J., 2015. The "Northern guests" and other palaeoclimatic ostracod proxies in the late Quaternary of the Basque Basin (S Bay of Biscay). Palaeogeogr. Palaeoclimatol. Palaeoecol. 419, 100–114.
McManus, J.F., Francois, R., Gherardi, J.M., Keigwin, L.D., Brown-Leger, S., 2004. Collapse and rapid resumption of Atlantic meridional circulation linked to deglacial climate changes. Nature 428 (6985), 834–837.
MeteoSwiss, 2020. Klimadiagramme und Normwerte pro Station. Federal Office of Meteorology and Climatology MeteoSwiss, Zurich-Airport, Switzerland.
Millet, L., Rius, D., Galop, D., Heiri, O., Brooks, S.J., 2012. Chironomid-based reconstruction of Lateglacial summer temperatures from the Ech palaeolake record (French western Pyrenees). Palaeogeogr. Palaeoclimatol. Palaeoecol. 315, 86–99.
Mojtahid, M., Toucanne, S., Fentimen, R., Barras, C., Le Houedec, S., Soulet, G., Bourillet, J.F., Michel, E., 2017. Changes in northeast Atlantic hydrology during Termination 1: insights from Celtic margin's benthic foraminifera. Quat. Sci. Rev. 175, 45–59.
Müller-Beck, H., 2005. Seeberg, Burgäschisee-Süd: Bauten und Siedlungsgeschichte. Acta Bernensia II, Teil 2. Stämpfli, Bern.
NAIS Divide Members, 2013. Onset of deglacial warming in West Antarctica driven by local orbital forcing. Nature 500 (7463), 440–444.
National Centre for Climate Services, 2018. In: CH2018 - Klimaszenarien für die Schweiz. National Centre for Climate Services, Zürich, 24 S.
Oksanen, J., Kindt, R., Legendre, P., O'Hara, B., Stevens, M.H.H., Oksanen, M.J., Suggests, M.A.S.S., 2007. The vegan package. Community Ecol. Package 10, 631–637.
Petit, J.R., Jouzel, J., Raynaud, D., Barkov, N.I., Barnola, J.M., Basile, I., Bender, M., Chappellaz, J., Davis, M., Delaygue, G., Delmotte, M., 1999. Climate and atmospheric history of the past 420,000 years from the Vostok ice core, Antarctica. Nature 399 (6735), 429–436.
Pons, A., Reille, M., 1988. The Holocene-and upper Pleistocene pollen record from Padul (Granada, Spain): a new study. Palaeogeogr. Palaeoclimatol. Palaeoecol. 66 (3–4), 243–263.
Quinlan, R., Smol, J.P., 2001. Setting minimum head capsule abundance and taxa deletion criteria in chironomid-based inference models. J. Paleolimnol. 26 (3), 327–342.

Quinlan, R., Smol, J.P., 2010. Use of subfossil Chaoborus mandibles in models for inferring past hypolimnetic oxygen. J. Paleolimnol. 44 (1), 43–50.
RStudio Team, 2015. RStudio. Integrated Development for R. RStudio, Inc., Boston, MA. http://www.rstudio.com/.
van Raden, U.J., Colombaroli, D., Gilli, A., Schwander, J., Bernasconi, S.M., van Leeuwen, J., Leuenberger, M., Eicher, U., 2013. High-resolution late-glacial chronology for the Gerzensee lake record (Switzerland): δ18O correlation between a Gerzensee-stack and NGRIP. Palaeogeogr. Palaeoclimatol. Palaeoecol. 391, 13–24.
Rasmussen, S.O., Andersen, K.K., Svensson, A.M., Steffensen, J.P., Vinther, B.M., Clausen, H.B., Siggaard-Andersen, M.L., Johnsen, S.J., Larsen, L.B., Dahl-Jensen, D., Bigler, M., 2006. A new Greenland ice core chronology for the last glacial termination. J. Geophys. Res. Atmos. 111 (D6).
Rasmussen, S.O., Bigler, M., Blockley, S.P., Blunier, T., Buchardt, S.L., Clausen, H.B., Cvijanovic, I., Dahl-Jensen, D., Johnsen, S.J., Fischer, H., Gkinis, V., 2014. A stratigraphic framework for abrupt climatic changes during the Last Glacial period based on three synchronized Greenland ice-core records: refining and extending the INTIMATE event stratigraphy. Quat. Sci. Rev. 106, 14–28.
Rey, F., Gobet, E., van Leeuwen, J.F., Gilli, A., van Raden, U.J., Hafner, A., Wey, O., Rhiner, J., Schmocker, D., Zünd, J., Tinner, W., 2017. Vegetational and agricultural dynamics at Burgäschisee (Swiss Plateau) recorded for 18,700 years by multi-proxy evidence from partly varved sediments. Veg. Hist. Archaeobotany 26 (6), 571–586.
Rey, F., Gobet, E., Schwörer, C., Hafner, A., Szidat, S., Tinner, W., 2020. Climate impacts on vegetation and fire dynamics since the last deglaciation at Moossee (Switzerland). Clim. Past. 16, 1347–1367. https://doi.org/10.5194/cp-16-1347-2020.
Reimer, P.J., Bard, E., Bayliss, A., Beck, J.W., Blackwell, P.G., Bronk Ramsey, C., Buck, C.E., Cheng, H., Edwards, R.L., Friedrich, M., Grootes, P.M., Guilderson, T.P., Haflidason, H., Hajdas, I., Hatté, C., Heaton, T.J., Hoffmann, D.L., Hogg, A.G., Hughen, K.A., Kaiser, K.F., Kromer, B., Manning, S.W., Niu, M., Reimer, R.W., Richards, D.A., Scott, E.M., Southon, J.R., Staff, R.A., Turney, C.S.M., van der Plicht, J., 2013. IntCal13 and Marine13 radiocarbon age calibration curves 0–50,000 years cal BP. Radiocarbon 55, 87–1869. https://doi.org/10.2458/azu_js_rc.55.16947.
Samartin, S., Heiri, O., Lotter, A.F., Tinner, W., 2012. Climate warming and vegetation response after Heinrich event 1 (16 700–16 000 cal yr BP) in Europe south of the Alps. Clim. Past 8 (6), 1913–1927.
Samartin, S., Heiri, O., Joos, F., Renssen, H., Franke, J., Brönnimann, S., Tinner, W., 2017. Warm Mediterranean mid-Holocene summers inferred from fossil midge assemblages. Nat. Geosci. 10 (3), 207–212.
Schilt, A., Baumgartner, M., Schwander, J., Buiron, D., Capron, E., Chappellaz, J., Loulergue, L., Schüpbach, S., Spahni, R., Fischer, H., Stocker, T.F., 2010. Atmospheric nitrous oxide during the last 140,000 years. Earth Planet Sci. Lett. 300 (1–2), 33–43.
Schmid, P.E., 1993. A key to the Larval Chironomidae and their instars from Austrian Danube region streams and rivers: with particular reference to a numerical taxonomic approach. 1. Diamesinae, Prodiamesinae and Orthocladiinae. Selbstverl.
Solhøy, I.W., Solhøy, T., 2000. The fossil oribatid mite fauna (Acari: Oribatida) in late-glacial and early-Holocene sediments in Kråkenes Lake, western Norway. J. Paleolimnol. 23 (1), 35–47.
Stern, J.V., Lisiecki, L.E., 2013. North Atlantic circulation and reservoir age changes over the past 41,000 years. Geophys. Res. Lett. 40 (14), 3693–3697.
Stuiver, M., Reimer, P.J., 1993. Extended 14 C data base and revised CALIB 3.0 14 C age calibration program. Radiocarbon 35 (1), 215–230.
Szadziewski, R., Krzywinski, J., Gilka, W., 1997. Diptera Ceratopogonidae, Biting Midges, 2, pp. 243–263. The aquatic insects of North Europe.
Tinner, W., 2007. Plant Macrofossil Methods and Studies/Treeline Studies.
Tinner, W., Vescovi, E., 2005. Ecologia e oscillazioni del limite degli alberi nelle Alpi dal Pleniglaciale al presente. In: Frisia, Silvia, Filippi, Maria Letizia, Borsato, Andrea (Eds.), Cambiamenti climatici e ambientali in Trentino: dal passato prospettive per il futuro. Studi Trent. Sci. Nat., Acta. Geol., vol. 82, pp. 7–14.
Tóth, M., Magyari, E.K., Buczkó, K., Braun, M., Panagiotopoulos, K., Heiri, O., 2015. Chironomid-inferred Holocene temperature changes in the south Carpathians (Romania). Holocene 25 (4), 569–582.
Tzedakis, P.C., Lawson, I.T., Frogley, M.R., Hewitt, G.M., Preece, R.C., 2002. Buffered tree population changes in a Quaternary refugium: evolutionary implications. Science 297 (5589), 2044–2047.
Ursenbacher, S., Stötter, T., Heiri, O., 2020. Chitinous aquatic invertebrate assemblages in Quaternary lake sediments as indicators of past deep-water oxygen concentration. Quat. Sci. Rev. S0277-3791(19)30950-30953.
Velle, G., Brodersen, K.P., Birks, H.J.B., Willassen, E., 2010. Midges as quantitative temperature indicator species: lessons for palaeoecology. Holocene 20 (6), 989–1002.
Verbruggen, F., Heiri, O., Meriläinen, J.J., Lotter, A.F., 2011. Subfossil chironomid assemblages in deep, stratified European lakes: relationships with temperature, trophic state and oxygen. Freshw. Biol. 56 (3), 407–423.
WAIS Divide Project Members, 2013. Onset of deglacial warming in West Antarctica driven by local orbital forcing. Nature 500 (7463), 440–444.
Watson, J.E., Brooks, S.J., Whitehouse, N.J., Reimer, P.J., Birks, H.J.B., Turney, C., 2010. Chironomid-inferred late-glacial summer air temperatures from Lough Nadourcan, Co. Donegal, Ireland. J. Quat. Sci. 25 (8), 1200–1210.
Watts, W.A., Allen, J.R.M., Huntley, B., 1996. Vegetation history and palaeoclimate of the last glacial period at Lago Grande di Monticchio, southern Italy. Quat. Sci. Rev. 15 (2–3), 133–153.
Wehrli, M., Tinner, W., Ammann, B., 2007. 16 000 years of vegetation and settlement history from Egelsee (Menzingen, central Switzerland). Holocene 17 (6), 747–761.
Chironomidae of the Holarctic region: keys and diagnoses: larvae. In: Wiederholm (Ed.), Scandinavian Soc. Entomol.

Supplementary material

Supplementary Figures 1 and 2 show Figures 5 and 6 with the chironomid based temperature reconstruction and pollen record from Burgäschisee on the original age scale described in Rey et al. (2017) rather than the revised age scale shown in Figure 2 of our article. However, biostratigraphical evidence (cited in the main manuscript text) indicates that vegetation and climatic changes at the Oldest Dryas to Bølling transition (ca. 14,600 cal. BP) happened synchronously across the Swiss Plateau. We therefore consider the revised chronology of Figure 2 (used for the Figures of the main manuscript) more reliable for lateglacial sections of the Burgäschisee record.

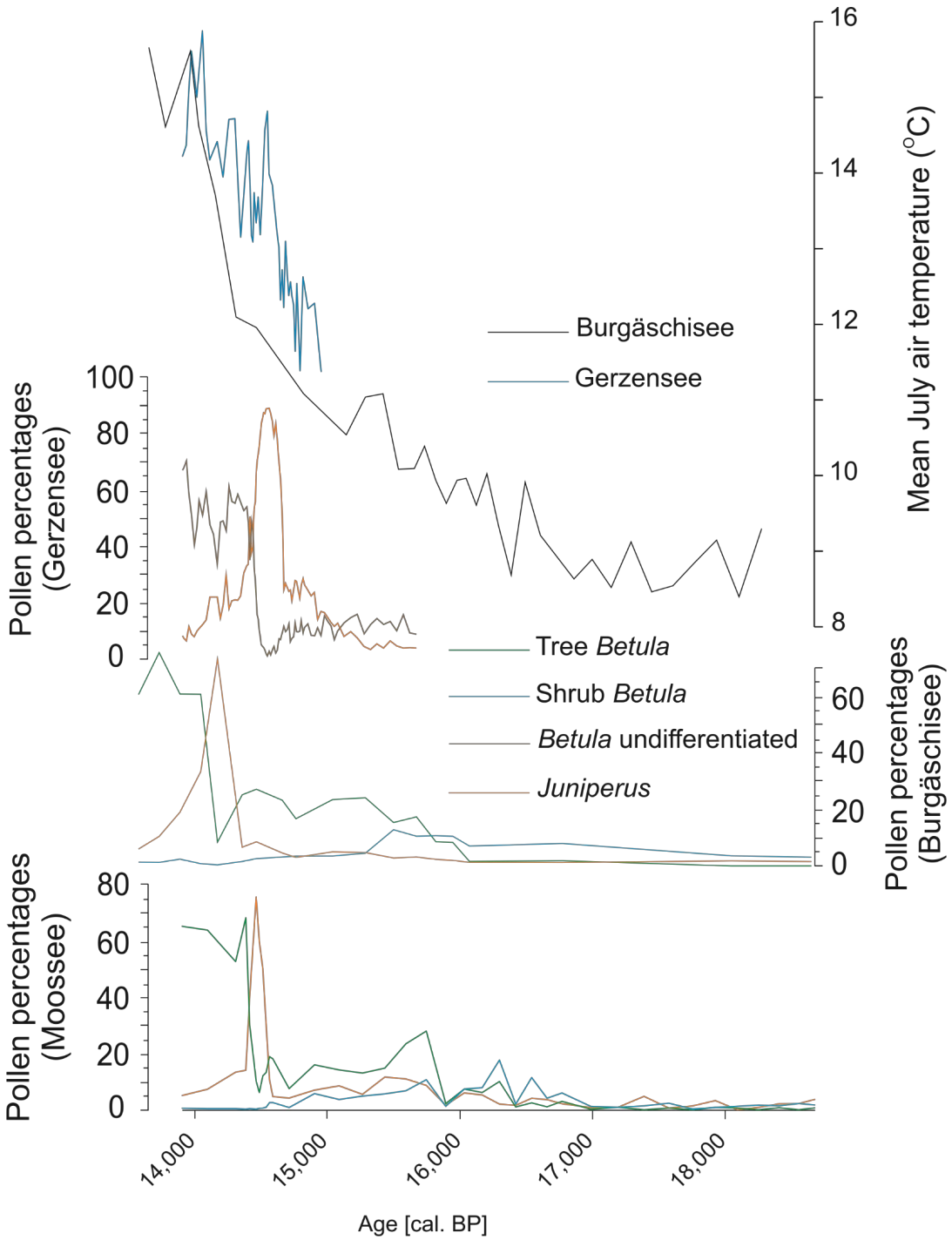

Supplementary Figure 1: Chironomid temperature reconstructions from the Northern Swiss Plateau corrected to 465 m a.s.l. (Burgäschisee, this publication; Gerzensee, Lotter et al, 2012) compared with selected pollen types in the Burgäschisee (Rey et al, 2017), Gerzensee (Ammann et al, 2013; shrub *Betula nana* was not separated from tree *Betula* pollen in this study) and Moossee (Rey et al, 2020) records. In this supplementary plot all data from Burgäschisee is shown on the age depth model of Rey et al. (2017). The Gerzensee record is presented on the age scale of van Raden et al. (2013). For the oldest section we only present samples within 300 years of the Oldest Dryas - Bølling transition, however, since this represents the lowest distinctive age tie point in the Gerzensee record, and lower sections are only very poorly constrained by the available chronological information.

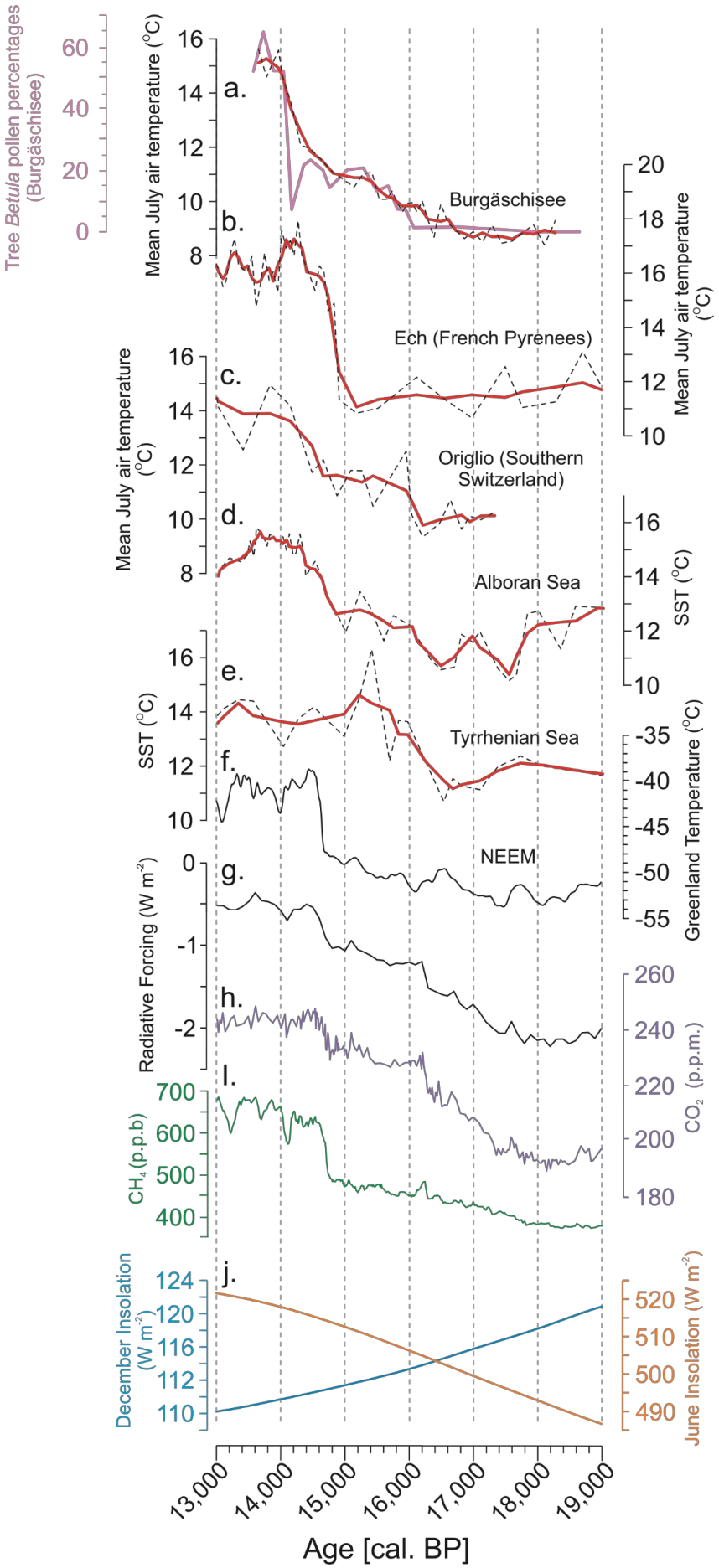
Tree Betula pollen percentages (Burgäschisee)
Mean July air temperature (°C)
a.
b.
Burgäschisee
Ech (French Pyrenees)
c.
Origlio (Southern Switzerland)
d.
Alboran Sea
e.
Tyrrhenian Sea
SST (°C)
f.
NEEM
Greenland Temperature (°C)
Radiative Forcing (W m-2)
g.
h.
CO2 (p.p.m.)
I.
CH4 (p.p.b)
j.
December Insolation (W m-2)
June Insolation (W m-2)
13,000
14,000
15,000
16,000
17,000
18,000
19,000
Age [cal. BP]

Supplementary Figure 2: Palaeotemperature records for the early Late Glacial. For temperature records (plots a. - e.) the dashed black line represents unsmoothed values whereas the solid red line represents a three sample running average. a. Burgäschisee chironomid temperature record from the Swiss lowlands and Burgäschisee tree *Betula* pollen percentages (solid pink line, Rey et al, 2017). In this supplementary plot all data from Burgäschisee is shown on the age depth model of Rey et al. (2017); b. Ech Palaeolake chironomid-inferred temperature (Data digitized from Millet et al, 2012); c. Lago di Origlio chironomid-inferred temperature (Samartin et al, 2012); d. Alboran sea surface temperature (SST; Cacho et al, 2001); e. Tyrrhenian SST (Cacho et al, 2001); f. NEEM temperature reconstruction (Buizert et al, 2014); g. Total radiative forcing from greenhouse gasses (Schilt et al, 2010; Marcott et al, 2014); h. CO_2 from West Antarctic Ice Sheet Divide ice core (WDC; Marcott et al, 2014); i: CH_4 from WDC (WAIS Divide Project Members, 2013; Marcott et al, 2014) and j. Summer and December insolation curves for 45°N (Berger and Loutre, 1991).

Paper II

Summer temperatures during the Last Glaciation (MIS 5c to MIS 3) inferred from a 50,000-year chironomid record from Füramoos, southern Germany

Alexander Bolland[1], Oliver A. Kern[2], Frederik J. Allstädt[2], Dorothy Peteet[3], Andreas Koutsodendris[2], Jörg Pross[2], and Oliver Heiri[1]

[1]Geoecology, Department of Environmental Sciences, University of Basel, Klingelbergstrasse 27, CH-4056 Basel, Switzerland

[2]Paleoenvironmental Dynamics Group, Institute of Earth Sciences, Heidelberg University, Im Neuenheimer Feld 234, D-69120 Heidelberg, Germany

[3]Lamont-Doherty Earth Observatory, Palisades, New York, USA

Corresponding author:

Alexander Bolland

Geoecology, Department of Environmental Sciences, University of Basel, Klingelbergstrasse 27, CH-4056 Basel, Switzerland

E-mail: alexanderwilliam.bolland@unibas.ch

Abstract

There is a sparsity of long, continuous palaeotemperature records for the last glacial period in central Europe, particularly for the interval corresponding to Marine Isotope Stages (MIS) 4 and 3. Here we present a new, ca. 50-ka-long chironomid record from Füramoos, southern Germany, covering the interval from MIS 5a to MIS 3 that we use it to examine lake development and then to quantitatively reconstruct mean July air temperatures. Chironomid assemblages with high abundances of taxa such as *Polypedilum nubeculosu*m-type, *Microtendipes pedellus*-type, *Cladopelma lateralis*-type and *Dicrotendipes nervosus*-type imply a shallow-lake setting for the majority of the examined interval, which is corroborated by other aquatic remains such as oribatid mites, Sialidae and Ceratopogonidae. The sections of the sequence corresponding to the Brörup interstadial (ca. 99 to 87 ka), Stadial B (ca. 87 to 84.5 ka) and the early Odderade (ca. 84.5 to 80 ka) contain chironomid assemblages comprised of *Tanytarsus glabrescens*-type and *Tanytarsus mendax*-type and indicate relatively warm temperatures. Assemblages from the late Odderade (ca. 80–77 ka), Stadial C (ca. 77–74.5 ka), Dürnten (ca. 74.5–68.5 ka) and Stadial D (ca. 68.5–54 ka) are dominated by taxa such as *Sergentia coracina*-type and *Tanytarsus lugens*-type and are typical for cooler conditions. Reconstructed July temperatures for the early Würmian (Brörup to early Odderade; ca. 99–80 ka) are 13–14 °C. Values decline to <10 °C during the late Odderade and Stadial C (ca. 80–77 ka) around the MIS 5a/4 transition. This decrease is coeval with a pronounced decrease in northern Hemisphere summer insolation. Values stay in the range of 9–11°C during the Dürnten and Stadial D (ca. 54–74.5 ka) and increase again to 12.5 °C during the Bellamont 1 interstadial (ca. 54–46 ka). Reconstructed July temperatures track changes in arboreal pollen percentages at Füramoos and agree with a summer-temperature decrease during the early to mid-Würmian as reported by other palaeotemperature records from Europe and the North Atlantic. Our chironomid record from Füramoos provides valuable new insights into Würmian climate dynamics in Central Europe, and corroborates other temperature reconstructions from the early to mid-Würmian glacial period.

Introduction

The last glacial period (in southern Central Europe referred to as the Würmian Glaciation) is dated to ca. 115–15 thousand years (ka) ago based on marine isotope stratigraphy (Imbrie et al, 1984; Shackleton et al, 2003) and terrestrial vegetation change (Sánchez Goñi et al, 2008), covering Marine Isotope Stages (MIS) 5d to 2. It was characterized by major glaciation on the continents (Hughes et al, 2013; Hughes and Gibbard, 2018), an associated decrease in sea level (Waelbroeck et al, 2002; Spratt and Lisiecki, 2016), a general trend to increased continentality (Caspers and Freund, 2001; Helmens, 2014), and distinct centennial- to millennial-scale changes in terrestrial ecosystems, notably vegetation (Behre and Lade, 1986; Woillard, 1978; Müller et al, 2003; Fletcher et al, 2010). Over large parts of Europe, vegetation changed from the forested conditions of the last interglacial to tundra or steppe vegetation during the coldest phases of the last glaciation (Behre and Lade, 1986; Woillard, 1978; Müller et al, 2003; Fletcher et al, 2010). During the last glacial period, climate in the North Atlantic region was also associated with a number of rapid, centennial-scale cooling and warming events (stadials and interstadials). In Greenland ice core $\delta^{18}O$ records, 26 stadials and 25 interstadials are documented between the current and the last interglacial (Dansgaard et al, 1993; Rasmussen et al, 2014). Several of these events have been detected in stable-isotope data from speleothems in Europe particularly for the early/mid-Würmian ca. 115–60 ka (Boch et al, 2011; Moseley et al, 2020) and have been correlated to distinct vegetation changes on the European continent (e.g., Woillard, 1978; Müller et al, 2003; Fletcher et al, 2010 and references therein). Importantly, however, not all Greenland interstadials appear to be associated with corresponding vegetation changes possibly due to plant-migration lags (Müller et al, 2003; Fletcher et al., 2010; Helmens, 2014).

Quantitative palaeotemperature records play an important role for understanding climatic and environmental changes during the last glaciation. They can be used to assess the performance of climate models (e.g., Renssen and Isarin, 2001; Heiri et al, 2014) and are also necessary for assessing, and in some cases modelling the impact of past climatic changes on vegetation, landscape and glacier dynamics (Hubbard et al, 2006; Lischke et al, 2013; Seguinot et al, 2018). However, continuous centennial to millennial scale palaeotemperature reconstructions that cover long continuous time intervals of the last glaciation are rare for Europe north of the Alps. Vegetation-based reconstructions are available for the long pollen records of Samerberg, Jammertal, Füramoos, Les Echets (Klotz et al, 2004) and Gröbern (Kühl et al, 2007), usually providing information on summer temperature, winter temperature and/or changes in humidity. Beetle-based reconstructions of the mean temperatures of the coldest and warmest months have been derived from La Grande Pile (Ponel, 1995) in eastern

France as well as Gröbern (Walkling and Coope, 1996) and Oerel (Behre et al, 2005) in northern Germany.

Important quantitative information on past climatic conditions has also become available through the analysis of chironomids, a group of aquatic insects whose larval remains preserve well in lake sediments and can be identified to the generic or morphological type level (Brooks et al, 2007). The distribution of chironomid assemblages in lakes is closely related with summer temperatures (Eggermont and Heiri, 2012), and fossil chironomid analysis has been used to develop quantitative summer-temperature reconstructions (Langdon et al, 2008; Luoto, 2009a; 2009b; Larocque et al 2001; Heiri et al, 2011). This approach has been followed to reconstruct past summer changes during the Lateglacial (e.g., Brooks and Birks, 2000; Heiri and Millet, 2005; Tóth et al, 2012; Bolland et al, 2020). However, only very few records, usually representing only sections of the last glacial period are available for earlier parts of the Würmian glaciation. Notable examples come from eastern Germany (MIS 3: Engels et al, 2008), northern Italy (Last Glacial Maximum: Samartin et al, 2012), Austria (Ilyashuk et al, 2020) and Northern Finland (MIS 5d–c, MIS 3; Helmens et al, 2009; 2012; Engels et al, 2010; 2014). While these records provide valuable information for the examined time intervals, they represent fragmented intervals of the last glacial period. Thus, they do not allow the assessment of long-term, multi-millennial-scale changes in ecosystem or climatic development.

Here we provide the first millennial- to centennial-scale resolution chironomid-based temperature reconstruction covering a ca. 50,000-years-long, continuous interval of the last glacial period from the classical site of Füramoos, southern Germany. Our new record covers the interval from the Brörup interstadial to the Bellamont 1 interstadial (MIS 5c–3; ca. 98–49 ka), an interval for which there is widespread evidence of increasing continentality connected to climatic cooling across Central and Northern Europe (Caspers and Freund, 2001; Helmens, 2014). As such, it contributes to better understanding the magnitude, timing and effects of climate change during the last glacial period in Central Europe.

2. Methodology

2.1 Site description and coring

Füramoos Ried is a peat bog covered by a modern forest in southern Germany's alpine foreland with a modern mean July air temperature of 16.6°C (climate-data.org). The bog is formed in a 1100 m long and 600 m wide basin, and situated at 662 meters above sea level between two Rissian glacial moraines (Schreiner, 1996; Busschers et al, 2008) preserving a near-continuous record of environmental change from the end of the Rissian glaciation to the onset of the Holocene (Schreiner, 1981; Müller et al, 2003; Winterholler, 2004; Kern et al, 2019). Our study is based on three sediment cores termed FU1, FU3, and FURA that cover different portions of the limnotelmatic succession deposited in the Füramoos Ried. The cores FU1 and FU3 were taken at 47°59'32.474" N, 9°53'13.905" E within a horizontal distance of 1.5 m using a Wacker Neuson BH-65 drill hammer (inner core diameter: 5 cm) (Kern et al, 2019). The FURA core was collected in 2001 at 47°59'26.9" N 9°53'10.1" E using a mobile drilling rig and has an inner diameter of 10 cm.

The cores FU1 and FU3 were correlated based on X-ray fluorescence (XRF) core scanning data (Ca normalized to total counts). The correlated FU1/3 core sequence was correlated to the FURA core based on XRF data (Ti:Al ratio) and supported by Loss on Ignition (LOI) data.

2.2. Pollen analysis

For palynological analyses, a sediment volume of 1–3 cm^3 was used per sample. *Lycopodium* tablets were added before chemical treatment for estimation of pollen concentrations (Stockmarr, 1971). Sample processing followed Eisele et al., (1994) and comprised the treatment with 10% HCl, 10% NaOH and 40-45% HF, followed by acetolysis. Samples with high concentrations of clastic material were subjected to density separation using sodium polytungstate. Residues were embedded in "Kaiser's glycerine jelly", fixed on microscope slides and analysed with a Carl Zeiss Axio Scope A1® microscope (400-1000x magnification) at the Institute of Earth Science, Heidelberg University. *Ranunculus aquatilis* (Müller et al, 2003) is included in *Ranunculus acris*-type, following Beug (2004). The pollen results are used here to confirm the correlation of the sediment cores and ensure a reliable correlation of the study results to the sequence described by Müller et al., (2003) and will be described in detail elsewhere.

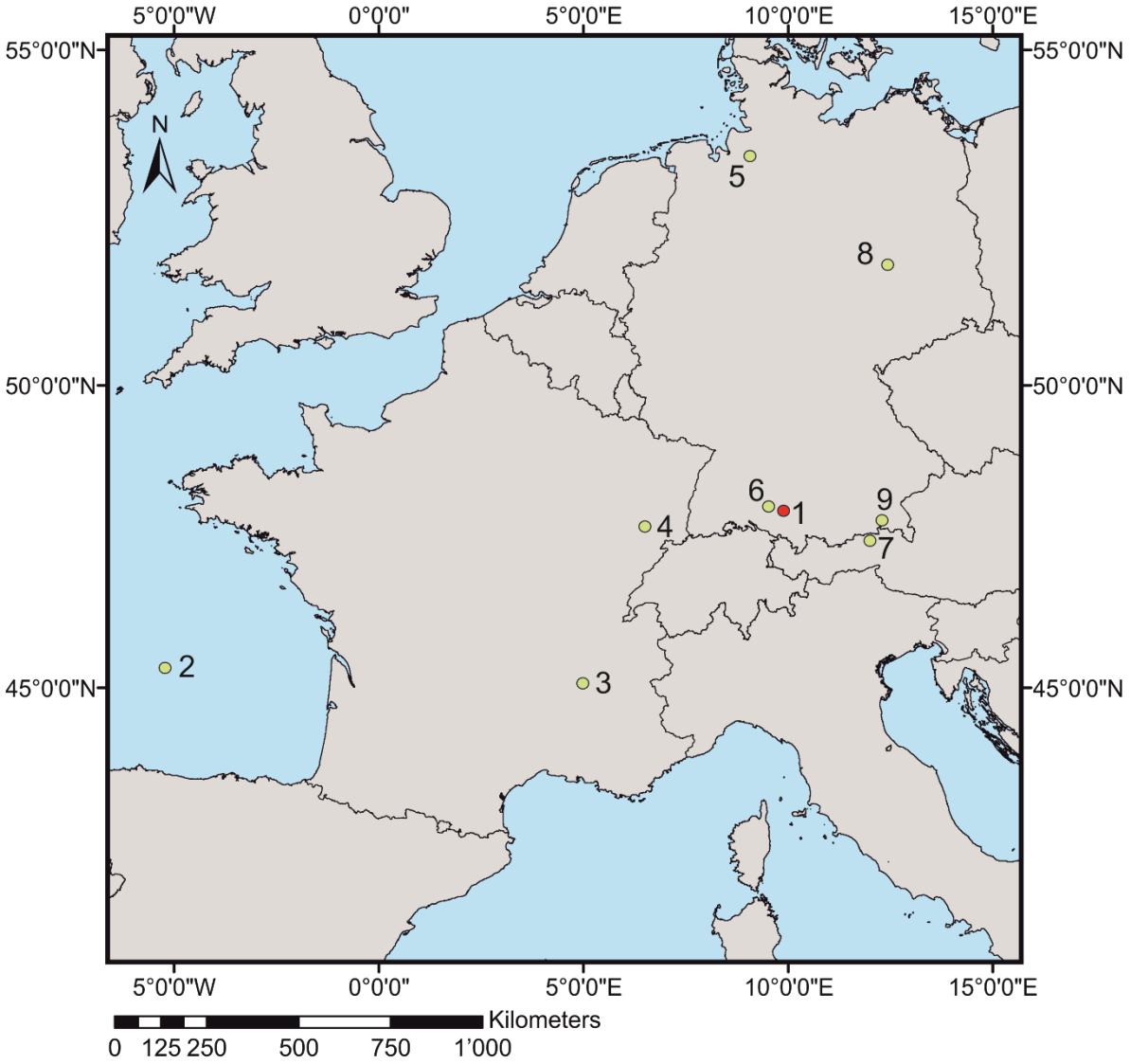

Figure 1: Locations of the records that have been used to produce temperature reconstructions referred to in the text: 1. Füramoos (red circle; Müller et al, 2003; this study); 2. Cores MD95-2042, SU81-18 (Sánchez Goñi et al, 2008; 2013), MD01-2444 (Martrat et al, 2007); 3. MD99-2331 and MD03-2697 (Sánchez Goñi et al, 2008; 2013); 4. Core MD04-2845 (Sánchez Goñi et al, 2008; 2013); 5. Les Echets (de Beaulieu and Reille, 1984; 1989); 6. La Grande Pile (Woillard, 1978); 7. Oerel (Behre and Lade, 1986; Behre, 1989; Behre and van der Plicht, 1992; Behre et al, 2005); 8. Jammertal (Müller, 2000); 9. Unterangerberg (Ilyashuk et al, 2020); 10. Gröbern (Litt, 1994; Walkling and Coope, 1996); 11. Samerberg (Grüger, 1979).

2.3. X-ray fluorescence core scanning and LOI

X-ray fluorescence core scanning was performed on all cores at the Institute of Earth Sciences, Heidelberg University using an Avaatech (GEN-4) XRF core scanner. In this study we use normalized Ca and the ratio of Ti/Al to correlate the FU1, FU3 and FURA sediment cores. A 10 kV Rh anode X-ray tube without a filter was used with a spatial resolution of 5 mm, a counting time of 10 s, a 150 mA

current, and a slit size of 10 mm crosscore and 5mm downcore. A 4-µm-thick Ultralene® foil was placed over the core halves after they were smoothed for analysis to avoid core desiccation and contamination of the detector window. The bAxilBatch software (Version 1.4, July 2016; www.brightspec.be) was used to process the X-ray spectra.

Sedimentary organic matter content measurements were taken every 4 cm in both the FURA and FU1/3 cores using LOI at 550°C (Heiri et al, 2001). Analysis was conducted the Institute of Earth Science, Heidelberg University.

2.4. Lithology and dating

Based on the lithology, coring depth and palynological information, the cores FU1 and FU3 mainly cover the late early Würmian to middle Würmian, and the FURA core covers the interval from the Rissian Lateglacial to the middle Würmian (sensu Chaline and Jerz, 1984 in Preusser, 2003). The analysis in this study focuses on the younger section from 4.67 – 12.90m from the Brörup interstadial onwards.

Müller et al., (2003) developed an age-depth model for their core from Füramoos by aligning the pollen record from that core with palaeoclimate records from the North Atlantic (McManus et al, 1994) and Greenland (Dansgaard et al, 1993). This allowed the placement the pollen record within the marine isotope stratigraphy (Martinson et al, 1987). Our new Füramoos composite record was correlated to the record of Müller et al., (2003) based on pollen assemblages, tied at the onset of each of the following time intervals: Brörup, Stadial B, Odderade, Stadial C, Dürnten, Stadial D, Bellamont 1 and Stadial E (Figure 2). The ages of the onset of each of these intervals as reported in Müller et al., (2003) were used to provide an age assessment of our Füramoos composite core. According to this correlation, the sediment sections of the present study cover the time interval from Greenland interstadial (GIS) 23, correlated to the middle of the Brörup interstadial, to Greenland interstadials (GIS) 13 and 14, correlated with the Bellamont 1 interstadial (Müller et al, 2003). Thus, they represent the time interval from the later part of MIS 5 to early MIS 3.

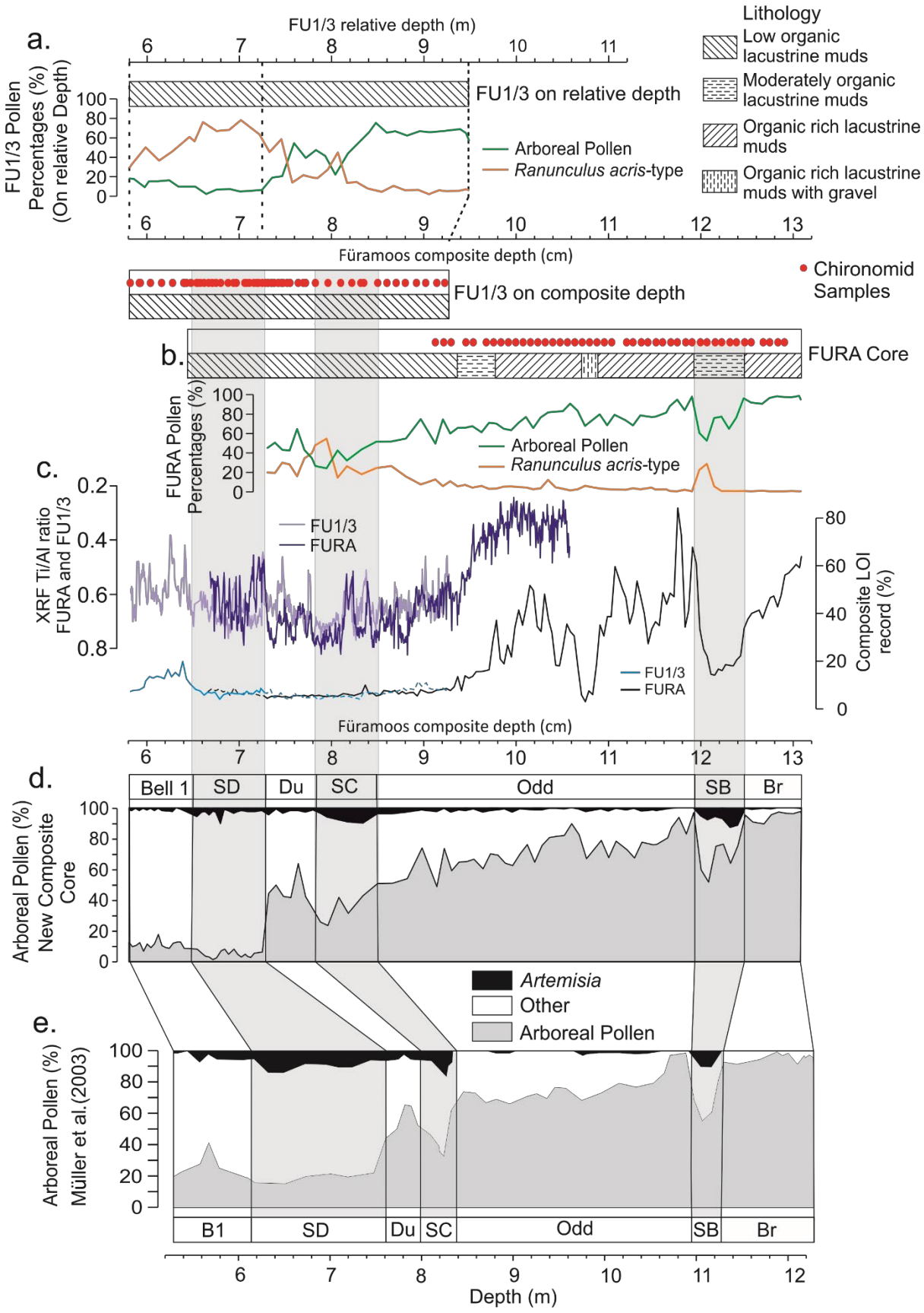
a.
FU1/3 relative depth (m)
FU1/3 Pollen Percentages (%) (On relative Depth)
FU1/3 on relative depth
Arboreal Pollen
Ranunculus acris-type
Lithology
Low organic lacustrine muds
Moderately organic lacustrine muds
Organic rich lacustrine muds
Organic rich lacustrine muds with gravel
Füramoos composite depth (cm)
FU1/3 on composite depth
Chironomid Samples
b.
FURA Core
FURA Pollen Percentages (%)
Arboreal Pollen
Ranunculus acris-type
c.
XRF Ti/Al ratio FURA and FU1/3
FU1/3
FURA
Composite LOI record (%)
Füramoos composite depth (cm)
d.
Bell 1
SD
Du
SC
Odd
SB
Br
Arboreal Pollen (%) New Composite Core
Artemisia
Other
Arboreal Pollen
e.
Arboreal Pollen (%) Müller et al.(2003)
B1
SD
Du
SC
Odd
SB
Br
Depth (m)

Figure 2: Correlation diagram illustrating how the composite core was produced from the FU1/FU3 and FURA cores, and how the composite core was correlated to the pollen record of Müller et al., (2003). Selected data are displayed for presentation purposes. a. Lithology, % arboreal pollen and % *Ranunculus acris*-type as well as position of chironomid samples in the FU1/FU3 cores plotted both on relative coring depth and composite coring depth. b. Lithology, % arboreal pollen and % *Ranunculus acris*-type as well as position of chironomid samples in the FURA core plotted on composite depth. c. Ti/Al ratio based on XRF analyses as well as Loss on Ignition (LOI) data from FU1/FU3 and FURA cores plotted against composite depth. d. Arboreal pollen and *Artemisia* pollen percentages for new composite record plotted on composite depth as well as position of stadials and interstadials in the new record identified based on stratigraphic data (FURA pollen data from 7.32 to 14.28 m composite depth and FU1/3 pollen data from 4.66 to 7.27 m). e. Pollen data and position of stadials and interstadials in the record of Müller et al., (2003) plotted on original depth scale of this record. Br: Brörup, SB: Stadial B, Odd: Odderade, SC: Stadial C, Du: Dürnten, SD: Stadial D, B1: Bellamont 1.

2.5. Chironomid sample preparation and analysis

Forty-six samples were selected for chironomid analysis from the FURA cores (9.14–12.91 m composite depth) and 71 samples from the FU1/FU3 cores (4.67–9.24 m composite depth; Figure 2). The incorporation of the FURA core into the composite core and subsequent re-evaluation of the chronology has resulted in an uneven sampling distribution of chironomid samples, ranging from one sample every 2 cm to every 12 cm with some exceptions. Sediment volume ranged between 0.5 – 10.3 cm^3 per sample depending on chironomid concentrations. Samples above 9.6 m required no chemical pre-treatment. Samples below 9.60 m were heated in 10% KOH for 15 minutes at 85°C due to sediment compaction and difficulty sieving the compact organic sediments. Samples were sieved with 100 µm mesh-size, and chironomid head capsules as well as other chitinous aquatic invertebrate remains were picked from a Bogorov tray under stereomicroscope (30–50 x magnification). Samples were then dried and mounted in Euparal before identification at 40–100 x magnification using a compound microscope. A minimum head capsule count of 80 was aimed for to produce more than the recommended 50 head capsules per sample (Heiri and Lotter, 2001). Head capsules with a complete mentum or greater than half a mentum were counted as one specimen, head capsules with half a mentum were counted as half a specimen and head capsules with less than half a mentum were disregarded. Next to chironomids the remains of Sialidae, Ceratopogonidae, *Daphnia*, Ephemeroptera, oribatid mites, Trichoptera, Plecoptera, Sciaridae and Tipulidae as well as Characeae oogonia and *Plumatella* statoblasts were mounted and identified.

2.6. Chironomid identification

Taxonomic identification followed Wiederholm (1983), Schmid (1993), Brooks et al., (2007), and Anderson et al., (2013). Specimens not identified to a sufficient taxonomic level (e.g. unidentified Chironomini) were excluded from further analysis. Some sections of the record contained a relatively large number of damaged *Tanytarsus*-type head capsules with broken antennal pedestals, presumably due to the difficulty separating them from the amorphous organic matter in the samples. For presentation and numerical analysis of the results these specimens were assigned to the morphotypes *Tanytarsus mendx*-type and *Tanytarus pallidicornis*-type, the only *Tanytarsus* morphotypes in the relevant sediment sections, based on the ratio of identified head capsules with diagnostic features on the antennal pedestals. Remains of Sialidae, Ceratopogonidae, Ephemeroptera, Trichoptera, Plecoptera, Sciaridae and Tipulidae were identified to this taxonomic level based on a photo collection of mounted modern specimens at Geoecology, University of Basel (Courtney-Mustaphi et al., in preparation), oribatid mites based on descriptions in Solhøy (2001) and Characeae oogonia based on Haas (1994). *Daphnia* and *Plumatella* were identified to morphological types based on Vandekerkhove et al., (2004) and Francis (2001).

2.7. Zonation and ordination analysis

The clustering algorithm CONISS (Grimm, 1987) was used to determine zonations in the chironomid record that were subsequently tested for statistical significance using a Broken Stick Model (Bennett, 1996). R studio version 1.1.463 (RStudio Team, 2015) was used to calculate CONISS using *rioja* (Juggins, 2017) and *vegan* (Oksanen et al, 2019) packages. A Detrended Correspondence Analysis (DCA) was used to summarize major changes in the chironomid assemblage using CANOCO 5 (Šmilauer and Leps, 2014). These numerical analyses were based on square root transformed percentage data.

2.8. Temperature reconstruction

A chironomid-based temperature reconstruction was produced using a chironomid-temperature calibration dataset and temperature inference model based on surface-sediment samples from 274 Swiss and Norwegian lakes (Heiri et al, 2011). A two-component weighted averaging partial least squares model (WAPLS; ter Braak and Juggins, 1993; ter Braak et al, 1993) was used to estimate mean July air temperatures from fossil assemblages. The model featured a root mean square error of prediction of 1.42 °C and an r^2 of 0.90 between predicted and observed temperatures when assessed using bootstrapping within the calibration dataset. In the Füramoos record some samples were

aggregated with their adjacent samples to achieve higher numbers of chironomids per sample (minimum: 40 head capsules), resulting in a total of 77 chironomid samples of the original 93 samples where chironomids were present. Of the original 76 types identified, some had to be aggregated, and one type, i.e., *Constempellina – Thienemanniola*, was excluded since it was not represented in the calibration data, resulting in 67 types used in total. Percentages were square root transformed prior to the calculations.

Squared chi-square distance was used to identify assemblages with either "no close" or "no good" modern analogues (Birks et al, 1990) in the modern calibration set, with thresholds for identifying such samples set as the 2nd and 5th percentiles of all distances within the modern calibration data samples, respectively (Birks et al, 1990; Tóth et al, 2015). A Canonical Correspondence Analysis (CCA) of the calibration dataset was produced with the fossil data analysed as passive samples and the only constraining variable set as mean July air temperature. The 90th and 95th percentile of residual distances of the modern calibration dataset samples to axis 1 were used to determine samples in the fossil record with a "poor" and "very poor" "goodness of fit" to temperature respectively (Birks, 1990; Tóth et al, 2015). Furthermore, sample specific estimated standard errors of prediction were calculated by using bootstrapping (9999 cycles, Birks et al, 1990) and the percentage of taxa absent from the training set as well as the number of rare taxa (N2<5 in the calibration dataset; Heiri et al, 2003) in the samples was calculated. C2 Version 1.7.7 was used to calculate analogue statistics (Juggins, 2007) and CANOCO 5 was used to produce the CCA (ter Braak and Smilauer, 2018). Analyses were based on square root transformed percentages.

3. Results

3.1. Würmian chironomid record

The new chironomid record consists of 92 chironomid samples that contained large enough chirnomid counts to use in analysis following omission of samples with no chironomids and the joining of samples with fewer than 40 headcapsules (Figure 3). CONISS zonation identified four statistically significant breaks in the chironomid record, resulting in five chironomid zones: Chironomid Zone Füramoos (CZF) 1 through 5. From the 116 samples originally processed for chironomid analysis 24 samples did not contain enough chironomid remains to be used.

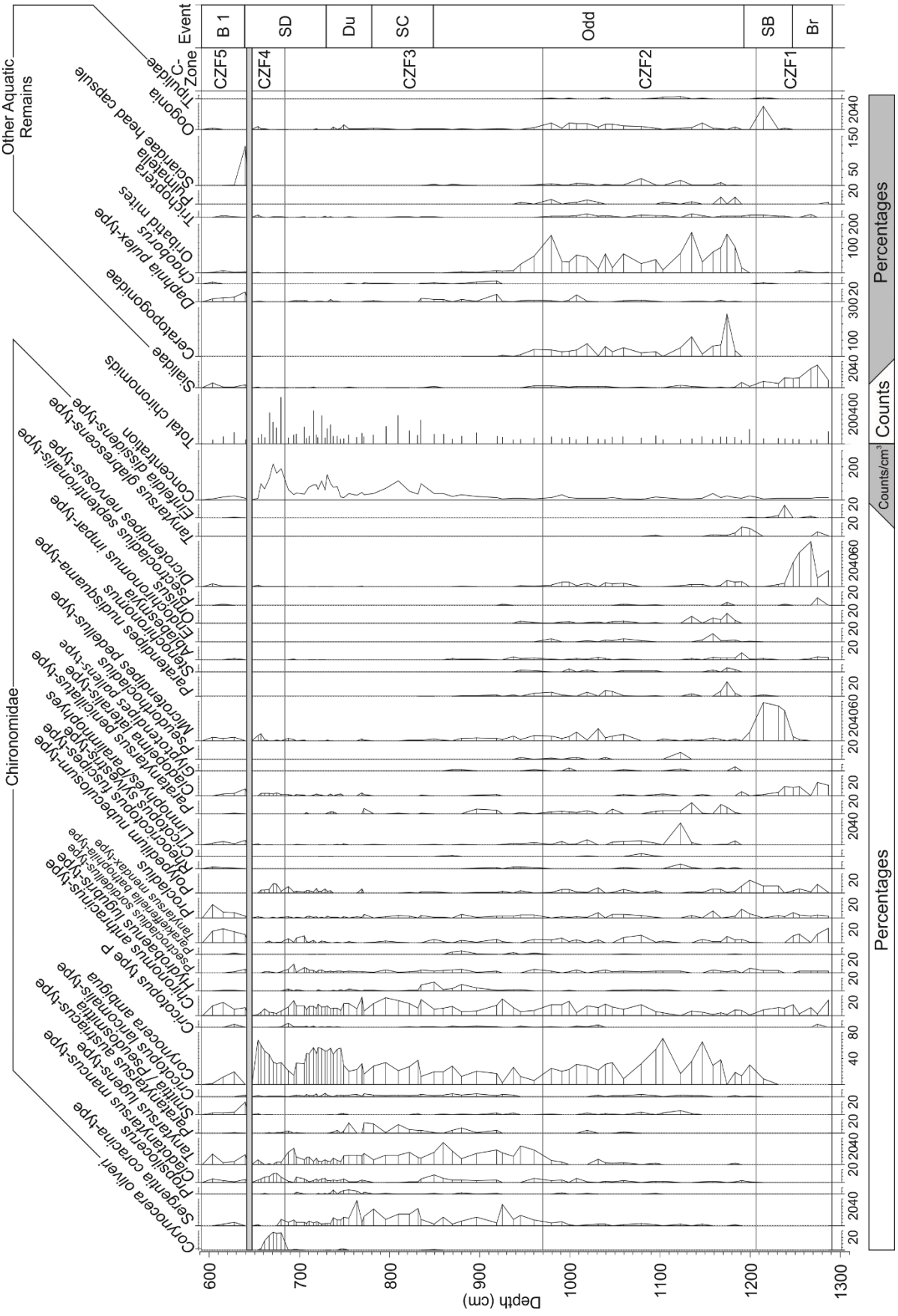

Figure 3: Distribution of chironomids in the Füramoos composite record plotted against composite depth. Chironomid remains are displayed as a percentage of total identified chironomids. C-zone is

Chironomid Zone determined by CONISS zonation. Other aquatic remains are displayed as a percentage relative to total chironomids including those that were not identified at higher taxonomic resolution. Chironomid types below 5 % in the record are not shown (41 types). Chironomid types are ordered according to abundance weighted average depth of occurrence, with types more abundant at the top of the core displayed on the left and those more abundant at the bottom displayed on the right. The grey horizontal bar indicates a sediment section without chironomids (see text for details). Br: Brörup, SB: Stadial B, Odd: Odderade, SC: Stadial C, Du: Dürnten, SD: Stadial D, B1: Bellamont 1.

CZF 1 (12.07–12.91 m) contains two intervals in which *Dicrotendipes nervosus*-type and *Microtendipes pedellus*-type dominate, respectively. *Chironomus anthracinus*-type and *Polypedilum nubeculosum*-type are subdominant in this section. Sialidae and *Cladopelma lateralis*-type are at their highest abundances in the entire record in CZF 1, but decline in abundance throughout the zone. CZF 2 (9.70–12.07 m) is dominated by *Corynocera ambigua* and, to a lesser extent, by *Chironomus anthracinus*-type throughout the zone. A subtle shift in chironomid assemblages is observed in this zone with types such as *Tanytarsus glabrescens*-type only occurring in the first part and then disappearing while other types, such as *Tanytarsus lugens*-type and *Sergentia coracina*-type occur intermittently before increasing in abundance towards the end. High abundances of Ceratopogonidae and oribatid mites are a prominent feature of CZF 2, and Sialidae remain present in this zone, but are less abundant relative to CZF 1. Within CZF 3 (6.84–9.70 m), *Chironomus anthracinus*-type and *Corynocera ambigua* remain in relatively high abundance, but are joined by increasing abundances of *Tanytarsus lugens*-type and *Sergentia coracina*-type, all four types becoming co-dominant. Many of the remains that were present in CZF 2 persist into the earliest section of CZF 3, such as *Paratendipes nudisquama*-type, oribatid mites and Ceratopogonidae, but decline and disappear shortly after the transition. The main distinguishing feature of CZF 4 (6.54–6.84 m) is the dominance of *Corynocera oliveri*. *Sergentia coracin*a-type disappears and *Tanytarsus lugens*-type decreases in abundance, whereas *Corynocera ambigua* persists at high abundances. The highest concentration of chironomids are found in CZF 4. CZF 4 and CZF 5 are separated by an interval in which no chironomids and only a single Sciaridae head capsule were found. The beginning of CZF 5 (6.04–6.4 m) coincides with an increase in chironomid concentrations to usable levels with initial high abundances of *Smittia/Pseudosmittia* as well as Sciaridae. *Tanytarsus pallidicornis*-type, *Corynocera ambigua*, *Chironomus anthracinus*-type, *Procladius* and *Tanytarsus mendax*-type dominate in this zone, and *Daphnia ephippia* is also abundant.

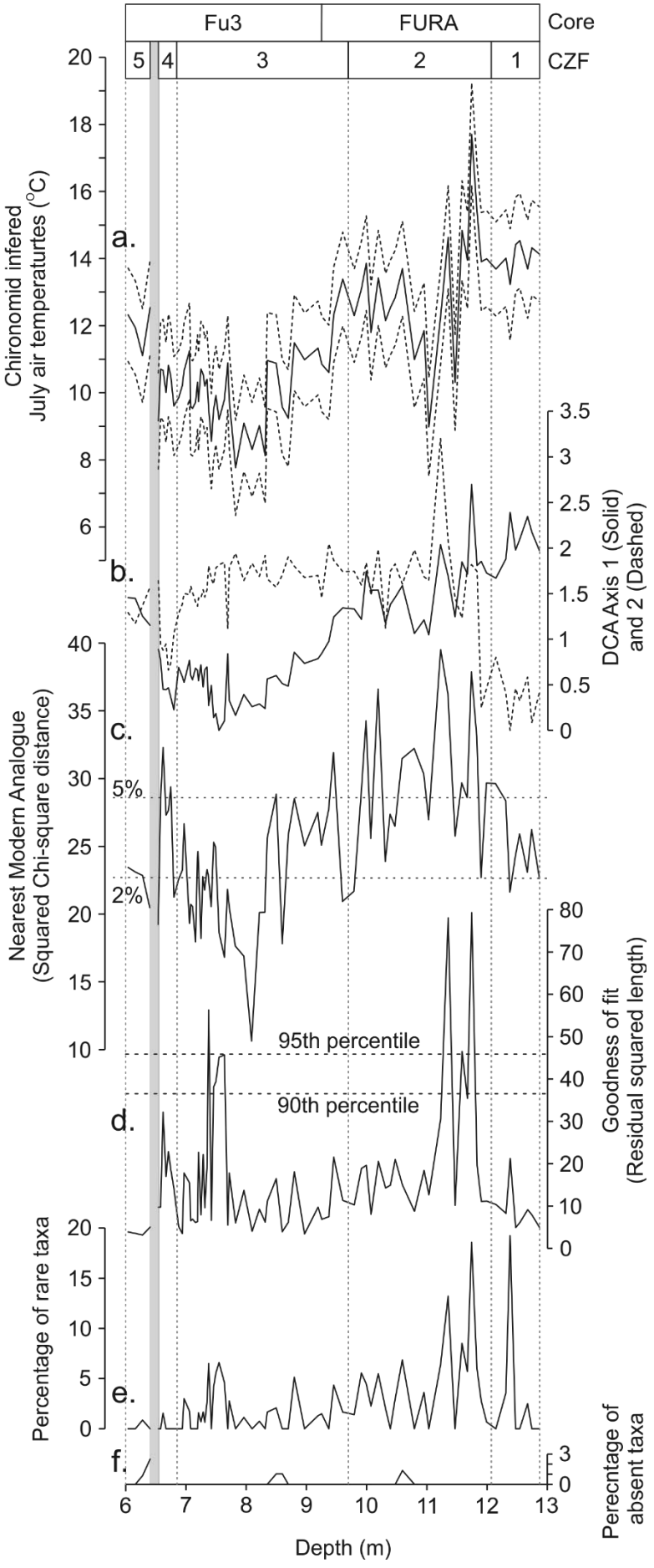
Fu3
FURA
Core
5
4
3
2
1
CZF
a.
b.
c.
d.
e.
f.
Chironomid infered July air temperaturtes (°C)
DCA Axis 1 (Solid) and 2 (Dashed)
Nearest Modern Analogue (Squared Chi-square distance)
5%
2%
95th percentile
90th percentile
Goodness of fit (Residual squared length)
Percentage of rare taxa
Perecntage of absent taxa
Depth (m)

Figure 4: Chironomid-inferred July air temperatures together with ordination results and associated diagnostic statistics from the Füramoos composite record. a. Chironomid-inferred July air temperatures (solid line) and associated error estimates (dashed lines); b. DCA Axis 1 (solid line) and Axis 2 (dashed line); c. squared chi-square distance of fossil samples to the nearest modern analogue in the calibration dataset. Samples with no close (2 %) and no good (5 %) analogues in the modern calibration data are indicated by dashed horizontal lines (following Tóth et al, 2015); d. goodness of fit statistics. Samples with a "poor fit" or "very poor fit" at the 90th and 95th percentiles of all residual distances of the modern calibration dataset samples are indicated by the dashed horizontal lines, respectively; e. percentage of taxa in the Füramoos samples that are rare in the Swiss-Norwegian training set; f. percentage of taxa in the Füramoos samples that are absent from the Swiss-Norwegian training set. Grey bar lines indicate a short section between CZF 4 and 5 without chironomids.

3.3. Chironomid-inferred temperature and ordination results

Chironomid-inferred July air temperatures within CZF 1 are relatively stable around 14°C (Figure 4). Within CZF 2 temperatures decrease to values around 12–13°C, although this trend is interrupted by major short-term variations, including a single sample positive excursion to 18°C (11.74m) and two negative excursions consisting of one and three samples, respectively, to ca. 10.5°C (11.47m) and ca. 9–12°C (10.79 to 11.03 m) in the middle of the zone. Within CZF 3, chironomid-inferred July air temperatures decrease in a stepwise fashion to 11°C between 9.40 and 8.30 m, and then to 8.5°C between 8.40 and 7.80 m before increasing and fluctuating between 9–11°C for the rest of the zone. For CZF 4, temperatures are ca. 10.5°C although the value for the final sample prior to the zone with no chironomids decreased to 9°C. The final zone CZF 5 shows a temperature increase to 11–12°C.

DCA Axis 1 and 2 explain 10.83 % and 7.96 % of the variance in the assemblage data, with axis lengths of 2.7 and 3.2 S.D., respectively (Figure 4). There is a general shift for DCA Axis 1 to lower values along the record, from initial values of 2.25 to 0.5 S.D. after 7.50 m depth. In the youngest section values increase again to reach 1.5 S.D. at 6.04 m composite depth. Overall DCA Axis 1 appears to represent changes in chironomid-inferred temperature in the Füramoos composite core. DCA Axis 2 displays more marked changes than DCA Axis 1, increasing from 0.5 to 3.25 S.D. at the beginning of CZF 2 before decreasing to 2.0 S.D. and remaining at stable until CZF 4 where S.D. units fall to 1. Following the chironomid-free zone, S.D. units increase again to 1.5 S.D.

Modern-analogue statistics indicate that overall most samples in the record have a good analogue in the calibration data (Figure 4), although samples with close analogues are mainly restricted to CZF 3. However, within most zones, with the exception of CFZ 5, individual samples have no good analogues. Most samples have a good fit with temperature. However, there are two sections in the record (11.23–11.83 m and 7.35–7.69 m) where many samples have a poor or very poor fit with temperature. Taxa not represented in the training set were below 3 % for the entire record.

Abundances of rare taxa were generally below 8 %, but some samples contained as many as 19 % of rare taxa.

4. Discussion

4.1. Chironomid assemblage and lake development

Several chironomid taxa typical for lacustrine conditions persist over large sections of the studied interval and generally indicate conditions typical for a relatively shallow lake environment. For example, *Polypedilum nubeculosum*-type, *Microtendipes pedellus*-type, *Cladopelma lateralis*-type and *Dicrotendipes nervosus*-type can all be abundant in shallow-water environments (e.g., Beattie, 1982; Walker et al, 1991; Lods-Crozet and Lachavanne, 1994; Millet et al, 2007; Korhola et al, 2000; Nazarova et al, 2017; Tóth et al, 2019) and occur in temperate lowland to subarctic/subalpine lakes (e.g., Walker et al, 1991; Heiri et al, 2011, Brooks and Birks, 2000). Several common chironomids (e.g., *Tanytarsus mendax*-type, *Tanytarsus lugens*-type, *Chironomus anthracinus*-type, *Procladius*, *Sergentia coracina*-type) can also be found in deepwater environments beneath a thermally stratified water column; type specific oxygen requirements permitting (e.g., Saether, 1979). However, these taxa also colonize shallower sections of lake basins under suitable conditions (e.g., Porinchu and Cwynar, 2000; Hofmann, 2001; Nazarova et al, 2017; Tóth et al, 2019). For example, for *Tanytarsus lugens*-type and *Sergentia coracina*-type this is only possible in cool conditions (e.g., Brundin, 1949, Heiri et al, 2011). *Corynocera ambigua*, an abundant and in some sections dominating chironomid, is common in shallow-water settings, but also occurs in deep-water habitats in some stratified lakes (e.g., Heiri, 2004). The species has been reported to dominate in lakes with abundant characeans (e.g., Fjellberg, 1972; Brodersen and Lindegaard, 1999), but has also been considered a cold-indicator (Luoto, 2009a) common in sediments from the last glaciation (e.g., Hofmann, 1983a; 1983b; Gandouin et al, 2016). However, more recent evidence suggests that it may have a wider thermal tolerance and temperature range (Brodersen and Lindegaard, 1999). Shifts between these dominating chironomid morphotypes as well as variations in less abundant taxa and non-chironomid invertebrates suggest several changes in lake conditions at Füramoos.

CZF 1 (12.07–12.91 m; ca. 85–99 ka) corresponds with the later part of the Brörup interstadial (12.47–12.91 m; ca. 87–99 ka) and the first sections of the following Stadial B (12.07–12.47 m; ca. 84.5–87 ka), intervals associated with MIS 5b and c, respectively (Müller et al, 2003), and consists of two lithologically distinct units. Sediments associated with the Brörup interstadial are highly organic lacustrine muds whereas sediments associated with Stadial B are only moderately organic, with a

higher inorganic content (Figure 2). Those samples associated with the late Brörup interstadial (ca. 87–99 ka) were difficult to process as the compressed highly organic material expanded beyond the initial sample volume once soaked and sieved, a feature also identified by Behre et al., (2005) from similar sediments at Oerel. Within CZF 1 there is a distinct chironomid assemblage change at ca. 87 ka associated with the transition from the late Brörup interstadial (*Dicrotendipes nervosus*-type dominance) to Stadial B (*Microtendipes pedellus*-type dominance). McGarrigle, (1980) showed that *Microtendipes pedellus*-type prefers lower sedimentary organic-matter content while *Dicrotendipes* seems to prefer sediments with decaying plant matter and/or detrital leaves (Pope et al, 1999), suggesting that sediment composition may have influenced the assemblage. Furthermore, the removal of *Tanytarsus mendax*-type at this transition may indicate a cooling (Heiri et al, 2011). A shallow-water environment is supported by the persistent presence of Sialidae larvae, benthic predators indicative of littoral conditions and muddy lake bottoms (Lemdahl, 2000). Overall CZF 1 indicates a shallow and relatively productive lake that cooled and became less productive at the Brörup/Stadial B transition.

CZF 2 (9.70–12.07 m; ca. 70.5–85 ka), corresponding to the final part of Stadial B and the majority of the Odderade interstadial, is dominated by the taxon *Corynocera ambigua,* which has a wide ecological tolerance (Brodersen and Lindegaard, 1999). At the onset of CZF 2 the subdominant taxa are *Polypedilum nubeculosum*-type, *Tanytarus glabrescens*-type and *Microtendipes pedellus*-type, all of which imply a warm mesotrophic environment (Beattie, 1982; Heiri and Lotter, 2005; Langdon et al, 2006; Brooks et al, 2007). The invertebrate assemblage is characterised by a higher influence of remains originating from shallower sections of lakes that may suggest a shallower environment, a more structured or productive littoral zone or enhanced transport from the lake margins towards the center. This is typified by the high abundances of oribatid mites, which can be representative of both shallow aquatic and terrestrial environment in and around lakes (Riva-Caballero et al, 2010; Heggen et al, 2012), and Ceratopogonidae, which indicate relatively warm and shallow aquatic environments (Walker and MacDonald, 1995; Ilyashuk et al, 2005). *Limnophyes/Paralimnophyes,* often associated with shallow-water and sometimes semi-terrestrial conditions (Porinchu and Cwynar, 2000; Massaferro and Brooks, 2002; Millet et al, 2007; Nazarova et al, 2017), is also recorded. Larvae of Sciaridae, remains of which can be found regularly in this zone, are terrestrial (Heiri and Lotter, 2007) and suggest some inwash of terrestrial invertebrate remains. Therefore, it appears that for a large part of CZF 2 relatively low lake levels prevailed at the FURA coring location, although most encountered chironomid taxa are aquatic, indicating that site was well within the lake. Towards the end of CZF 2, the abundances of oribatid mites and Ceratopogonidae decline indicating a reduced influence of the

shallow littoral environment, while occurrences of *Sergentia coracina*-type and *Tanytarus lugens*-type increase, indicating relatively cool temperatures (Brooks et al, 2007; Frey, 1988; Heiri et al, 2011; Nazarova et al, 2017). Overall, CZF 2 indicates an initial warm period with a potential expansion of the littoral zone and subsequent gradual cooling.

CZF 3 (6.84–9.70 m; ca. 73.5–79.5 ka) corresponds to the end of the Odderade interstadial (8.49–9.70 m; ca. 79.5–77 ka), Stadial C (7.81–8.49 m; ca. 74.5–77 ka), the Dürnten interstadial (7.30–7.81 m; ca. 68.5–74.5 ka) and the first half of Stadial D (6.84–7.30 m; ca. 68.5–73.5 ka), therefore covering the MIS 5/4 transition (Müller et al, 2003). The initial increases of *Sergentia coracina*-type and *Tanytarsus lugens*-type that began in CZF 2 continue, which in shallow water environment imply continued cooling (Frey, 1988; Brundin, 1949; Brooks et al, 2007; Heiri et al, 2011). *Paratanytarsus austriacus*-type also appears, lending further evidence to a cooling (Boggero et al, 2006; Brooks et al, 2007; Heiri et al, 2011). Littoral non-chironomid remains including oribatid mites and Sialidae decrease, possibly indicating a somewhat higher lake level. Towards the end of the zone during the Dürnten interstadial beginning at ca. 71 ka, increasing abundance of *Corynocera ambigua* with associated decreases in *Sergentia coracina*-type and *Tanytarsus lugens*-type and the removal of *Paratanytarsus austriacus* type possibly imply warming.

CZF 4 (6.54–6.84 m; ca. 55–73.5 ka) represents the later part of Stadial D and is characterized by a large increase of *Corynocera oliveri*, a cold stenotherm taxon typical of cold arctic environments (Brooks and Birks, 2000), at the onset. *Sergentia coracina*-type and *Tanytarsus lugens*-type have been shown to dominate the chironomid assemblage under cold climatic conditions in shallow-water environments (Brooks et al, 2007; Frey, 1988; Heiri et al, 2011; Nazarova et al, 2017). Following CZF 4 there is a short interval (6.40–6.54 m; ca. 53–55 ka) in which chironomid head capsules and other aquatic invertebrate fossils decrease in abundance or were absent, suggesting lake productivity was too low to maintain abundant and diverse chironomid assemblages.

CZF 5 (6.04–6.40 m; ca. 49–53 ka), corresponding to the Bellamont 1 interstadial (within MIS 3; Müller et al. 2003) consists of four samples. The lowermost sample features high abundances of *Smittia/Pseudosmittia*, two semi-terrestrial taxa, suggesting a very low water depth at the beginning of this zone. This is confirmed by high abundances of Sciaridae larvae. This zone also displays relatively high abundances of *Tanytarsus pallidicornis*-type, a chironomid morphotype typical of littoral

conditions and relatively warm temperatures (Heiri and Lotter, 2010; Nazarova et al, 2017), whereas many chironomids that were already dominant in the previous zones return at low abundances, confirming lacustrine conditions. Above 6.04 m core depth, the sediment contained <1 chironomid per cm^3, suggesting that the lake was not productive enough to support abundant and diverse chironomid assemblages.

In summary, chironomid assemblages in the Füramoos record indicate relatively shallow, near-shore environments over the entire analysed sediment section, which spans from ca. 49 to 99 ka. Overall there is an increase along the sequence of chironomid taxa that are, in shallow-water environments, indicative of relatively cool climate conditions. Several relatively minor changes in chironomid assemblages and other invertebrate remains suggest moderate changes in lake level and lake depth at both FU1/FU3 and FURA coring sites. The absence of Chironomidae in high enough abundance and diversity to analyse between CZF 4 and CZF 5, as well as after CZF5, is attributed to low lake productivity.

4.2 Chironomid-inferred temperature and coeval Füramoos pollen data

Pollen evidence from Würmian sediments at Füramoos describes a series of stadial and interstadial conditions which can be seen as phases of forest opening and forest reestablishment and/or closing respectively (Figure 2; Müller et al, 2003). The new chironomid record represents four interstadials, i.e., the late Brörup, Odderade, Dürnten and Bellamont 1, associated with increased arboreal pollen percentages relative to the adjacent stadials preceding and/or following them. The stadials (named Stadials B, C and D) have been correlated with climatic changes in the North Atlantic by Müller et al., (2003). In general, the arboreal taxa present at Füramoos over the study interval are *Pinus*, *Picea* and *Betula.* In addition, there are a series of thermophilous tree taxa for the earliest Würmian, and the stadials are associated with increased percentages of herbs such as Poaceae and *Artemisia* (Müller et al, 2003).

Chironomid-inferred temperatures ranged from 7.8 to 17.7°C in the studied sediment section between ca. 49 and 99 ka. Many of the encountered chironomid assemblages have no close modern analogues in the modern calibration data (Figure 4) and, in some parts of the section (beginning of Odderade and Dürnten) assemblages have a poor or very poor fit with temperature. However, WA-PLS regression usually performs relatively well in non-analogue situations (Lotter et al, 1999). The

moderate lake-level changes suggested by the ecological analyses of the chironomid and other invertebrate assemblages (see Section 4.1.) may have had some influence on the temperature reconstruction. However, lakes with a wide depth range are incorporated in the applied calibration dataset and transfer function (0.9–85 m water depth; Heiri and Lotter, 2010; Heiri et al, 2011), and the influence of water depth on the reconstruction is therefore incorporated in the prediction error of the model and the sample-specific estimated standard errors of prediction, which ranged from 1.4 to 1.7°C. The strongest influence of past lake-level changes can be expected within the Bellamont 1 interstadial for a single sample, where very high abundances of semi-terrestrial chironomids (*Smittia/Pseudosmitta*) and terrestrial midge remains (Sciaridae) suggest very low water depth. This sample immediately follows the interval 6.40–6.54m in which there were no chironomids found. XRF analysis in the section 6.39–6.41m indicates an increase of S and Ca which could indicate an increase in evaporative minerals such as gypsum and calcite. This seems to corroborate the inference of decreasing lake level inferred by high abundances of *Smittia/Pseudosmitta*. However as there is a persistent presence of the alga *Pediastrum* throughout the 6.40–6.54m interval, the possibility that the lake completely dried out seems less likely. Based on earlier studies of chironomid assemblages from lake surface sediments, such shallow water conditions may have led to an overestimation of July temperatures (Heiri et al. 2003). However, inferred temperatures from this sample are not noticeably different from other Bellamont 1 interstadial samples.

The most pronounced short-term (centennial-scale) temperature variations are recorded for the Odderade interstadial (8.49–11.93 m; ca. 77–84.5 ka). Short-term (single-sample) maxima and minima are inferred in this section. However, the amplitude of these short-term variations exceeds expected variations in mean July temperature during the early Würmian. A more pronounced (3-sample average) centennial-scale temperature decrease of ca. 8.5°C is also apparent in the early part of the Odderade interstadial between 10.95–11.47 m (ca. 82–83 ka) that does not agree with reported stadials from Central Europe. These minimum temperatures are associated with >65 % abundance of *Corynocera ambigua*, a species originally described as a cold indicator (Luoto, 2009a) and found to dominate relatively cool samples of the applied transfer function and calibration dataset (Heiri et al, 2011). However, several studies have shown that in some situations *C. ambigua* can occur in relatively warm climatic conditions, such as eutrophic lowland lakes in Denmark (Brodersen and Lindegaard, 1999) or relatively warm lakes in Russia (Nazarova et al, 2015). Hence, the temperature preference of this species is not clearly constrained by presently available ecological studies. Short-term temperature excursions in this part of the record should therefore be interpreted with caution unless

further independent evidence becomes available for a centennial-scale temperature variation within the Odderade Interstadial.

4.2.1. Brörup interstadial (Br)

Sediments attributed to the Brörup interstadial (ca. 87–99 ka) are associated with chironomid-inferred July air temperatures of ca. 13.5–14.5°C. Müller et al., (2003) indicate dominance of arboreal pollen representing cool temperate to boreal forests consisting primarily of *Pinus, Betula* and *Picea* for the same interval and therefore the new temperature reconstruction is in agreement with the pollen assemblage. During peak interstadial conditions, climate was favourable for the growth of thermophilous tree taxa such as *Carpinus*, *Quercus* and *Corylus*, which reached up to 15 % (Müller et al, 2003). Although our new chironomid record does not cover the Brörup climatic optimum, it describes the late Brörup interval and transition into Stadial B, thereby providing a basis from which to analyse the climatic development of Stadial B.

4.2.2. Stadial B (SB)

Average chironomid-inferred July air temperatures during Stadial B (ca. 84.5–87 ka) at Füramoos were 13.7°C, values slightly lower (<1°C) than during the Brörup interstadial. The new pollen data show high *Artemisia* and low arboreal pollen in this interval (Figure 2) supporting previous work by Müller et al., (2003). This suggests a forest opening during the Stadial B interval. The organic-matter content in the sediments also decreases, and higher *Artemisia* percentages document an increase in steppe conditions and a dryer climate (Müller et al, 2003). The absence of major chironomid-inferred temperature change during Stadial B suggests that summer-temperature changes are unlikely to have resulted in the observed vegetation turnover and forest opening. Previous work by Lotter et al., (2012) suggests that chironomids and vegetation respond differently to seasonal temperature and humidity changes, with chironomids being more influenced by summer temperature and vegetation being more influenced by winter temperature and precipitation. Therefore, it appears that either changes in winter temperature, continentality or moisture availability drove forest opening during Stadial B.

4.2.3. Odderade (Odd)

The early part of the Odderade interstadial (ca. 77–84.5 ka) is characterised by an increase in chironomid-inferred July air temperatures from 14°C to slightly higher values, with a single-sample

peak of 17.7°C. Pollen assemblages in this part of the record almost reach 100 % arboreal pollen (Figure 2) and Müller et al., (2003) show that different thermophilous tree taxa such as *Quercus*, *Corylus* and *Carpinus* were abundant at the very beginning of the Odderade, present at pollen abundances >20%. Chironomid-inferred temperatures from Füramoos are very variable in this part of the record, and as discussed above, short-term inferred cooling in this section of the record (ca. 82–83 ka) should be interpreted with caution. Furthermore, most of the early Odderade represents a "no-good" modern-analogue situation and contains samples with a "poor" goodness of fit to temperature (Figure 4), coincident with low reconstructed temperatures in the early Odderade. Importantly, the later cooling into Stadial C is associated with "good" fit to temperature statistics and samples that have closer modern analogues than those indicating the earlier Odderade cooling (Figure 4). Overall, we observe a general, long-term decrease in chironomid-inferred temperatures from the onset to the end of the Odderade, falling from initial temperatures of ca. 15°C to as low as 11°C. This cooling is associated with a decline in tree-pollen percentages over the Odderade interstadial interval (Figure 5).

4.2.4. Stadial C (SC)

July temperature reconstructions for Stadial C (ca. 74.5–77 ka) range from 7.8 to 11°C (Figure 4), with a sustained interval of ca. 9°C. These temperatures are typical for treeline or low-tundra environments in Central Europe (Landolt, 2003). In accordance, tree-pollen percentages abruptly decrease at Füramoos during Stadial C (Figure 2), with an almost complete disappearance of both *Pinus* and *Picea* pollen at the onset of Stadial C, *Betula* contributing the majority of the arboreal pollen and *Artemisia* increasing in the pollen record (Müller et al, 2003). Tree *Betula* has not been differentiated from the shrub birch *Betula nana* in this interval so it is possible that either tree *Betula* survived in isolated stands during Stadial C or that summer temperatures became too cool to sustain tree growth.

4.2.5. Dürnten (Du)

Sediments correlated to the Dürnten interstadial (ca. 68.5–74.5 ka) are associated with a chironomid-inferred temperature increase to 10°C (Figure 4). During this interval the local pollen assemblage shows a decrease in *Artemisia* percentages and an increase in arboreal pollen indicating forest expansion at Füramoos (Figure 2). As trees require summer temperatures exceeding 8.5–10°C to grow depending on the species (Landolt, 2003), this finding is in agreement with the chironomid-based temperature record.

4.2.6. Stadial D (SD)

Chironomid-inferred temperatures during Stadial D remain at 9.5-10.5°C (three sample running average; Figure 5), while arboreal pollen is reduced to 20 % and *Artemisia* expands, suggesting the development of an arctic tundra or steppe environment. Previously, Müller et al., (2003) suggested that the cooling associated with the beginning of Stadial D eliminated local refugia and prevented remigration of tree taxa through the Stadial D interval. Based on size measurements of pollen grains, these authors showed that *Betula* largely originated from the dwarf shrub *Betula nana*, leading them to conclude that most areas north of the Alps were completely treeless during this interval. Our new chironomid-inferred temperatures support this hypothesis. Fluctuating around 10 °C summer temperature, they are at upper limit of the reported minimum temperature requirement for tree growth in Central Europe (Landholt et al, 2003).

4.2.7. Bellamont 1 (B1)

For Bellamont 1, chironomid-inferred July temperatures show an increase from 9.5–10.5°C to ca. 12°C based on three sample running averages (Figure 5). Earlier pollen analyses at Füramoos showed that this interval was characterized by the immigration of plants typical for a slightly warmer climate than during Stadial D, such as *Juniperus*, *Hippophaë* and *Selaginella*, and analyses of *Betula* pollen suggest the remigration of the tree birch *Betula alba* (Müller et al, 2003). The increase in tree-pollen percentages is corroborated by our own pollen data (Figure 5) leading us to conclude that that more favourable summer temperatures above 10°C (Landholt et al, 2003) facilitated tree remigration to the Füramoos site.

4.3 Comparison with other quantitative summer temperature estimates from Europe

There are few quantitative palaeotemperature records from central and western Europe that cover large parts of the examined interval and can be directly compared with our chironomid-based temperature reconstruction, mainly based on pollen and beetle (coleopteran) records. In the following discussion we use the correlations between previously published European temperature records and our Füramoos dataset as outlined in Supplementary Information 1. For the earliest part of our record, absolute July air temperature values reconstructed based on other approaches generally agree with our new chironomid-based temperature reconstruction. For example, Brörup July temperature ranges produced from our new chironomid record (13.5–14.5°C) fall within the temperature ranges yielded by beetle assemblages at Gröbern (range of reconstructed temperature ranges of 12–17°C; Walkling

and Coope, 1996), Oerel (11–19°C; Behre et al, 2005) and La Grande Pile (9–26°C; Ponel, 1995) as well as the available pollen reconstructions from Füramoos, Jammertal, Les Echets, Samerberg (Klotz et al, 2004) and Gröbern (Kühl et al, 2007; range of reconstructed means: 9.5–20°C; Supplementary Table 1). Interestingly, neither the temperature ranges presented from these records nor our new chironomid-based record suggest major summer-temperature cooling during Stadial B, with only the lowermost estimated temperature range of the Gröbern beetle record (9–16°C for Stadial B; Walkling and Coope, 1996) falling below 10°C. This may suggest that summer temperature did not play a major role in forest opening during this interval. For the interval from Stadial D to the Bellamont 1 interstadial, the only summer-temperature records available for comparison are from La Grande Pile (Ponel, 1995) and Oerel (Behre et al, 2005), both of which are based on beetle remains. All three available temperature records (i.e., Füramoos – this study; Oerel – Behre et al, 2005; La Grande Pile – Ponel, 1995) suggest that MIS 3 interstadial summer temperatures were colder than during MIS 5c and MIS 5a, with the exception of the upper temperature range reconstructed from La Grande Pile following the Pile complex (21°C; see Supplementary Table 1). This range of 9.5–13.5°C suggests that summer temperatures during the MIS 3 interstadials were cool, but still warm enough in the interstadial sections to support the growth of trees that can survive at the transition zone from tundra to forest in Central Europe. This scenario is corroborated by the Füramoos pollen record, which shows an increase in the percentages of arboreal pollen primarily the pioneer *Betula,* in the Bellamont 1 interglacial (Müller et al, 2003).

4.4 Comparison with Atlantic and European palaeoclimate records

Our chironomid-based temperature record indicates a pronounced, long-term decrease in July temperatures in Central Europe, from values around 14°C in the Brörup interstadial to values around 8.5°C in Stadial C (Figure 5), with minimum temperatures in this stadial. The mean temperature of the warmest month as inferred through beetle-based reconstructions from La Grande Pile, France (Ponel, 1995; Guiter et al, 2003), also shows a transition to cooler temperatures across this interval, as do pollen-based reconstructions of mean annual temperature at Les Echets and La Grande Pile (Guiot et al, 1993). Conspicuous declines in tree pollen abundances are observed across the interval at Füramoos (Müller et al, 2003) and many other terrestrial European sites (e.g. Jammertal: Müller, 2000; Samerberg: Grüger, 1979; La Grande Pile: Woillard, 1978; Oerel: Behre and Lade, 1986). Similar vegetational transitions are documented in pollen records from the Iberian margin and the North Atlantic, with more thermophilic assemblages transitioning to less thermophilic assemblages (Sánchez Goñi et al, 2008). Furthermore, there is a general increase in the cold-indicating planktonic foraminifer

N. pachyderma (s) at these locations, although the long-term trend is strongly influenced by short-term variations on the centennial-scale for this species within the examined sediment records (Sánchez Goñi et al, 2008). Our new chironomid record from Füramoos agrees with these reconstructed trends towards cooler temperatures, although the decrease in chironomid-inferred temperatures appears to happen earlier (ca. 85-75 ka) than in the Iberian and North Atlantic records (ca. 80-70 ka). This millennial-scale temperature decrease in the Füramoos chironomid record occurs together with a pronounced decrease in Northern Hemisphere summer insolation (Berger and Loutre, 1991; Figure 5), indicating that summer temperatures in this interval may have been strongly affected by insolation changes. It also suggests that the transition of vegetation types reconstructed for Füramoos based on pollen (Müller et al, 2003) may have been driven to a considerable extent by decreasing summer temperatures, particularly for younger sections of this interval (Figure 5). Whereas July air temperatures around 14°C as recorded for earlier parts of the record may sustain a wide range of European tree taxa and forest types, temperatures around 8.5–11 °C as inferred for the youngest sections (Stadial C to Stadial D) can only be tolerated by boreal and subalpine trees such as *Betula*, *Picea* or *Pinus*. These temperature values are typical for the transition between forest and tundra in Central Europe (Landholt et al, 2003).

Temperature change in Europe during the Würmian glaciation has been shown to be closely associated with centennial-scale variations in North Atlantic climate and ocean circulation. Greenland ice core $\delta^{18}O$ records indicate a series of stadials and interstadials also observed in variations in speleothem $\delta^{18}O$ records from Central Europe (Boch et al, 2011). There were also centennial-scale decreases in polar foraminifera in the North Atlantic (McManus et al, 1994; Sánchez Goñi et al, 2008) and, for interstadials during the early Würmian, there were expansions of more thermophilous tree taxa in continental Europe (Müller et al, 2000, 2003; Sánchez Goñi et al, 2008; Wulf et al, 2018; Figure 5). Pollen records from the Iberian margin suggest variable, but decreasing temperatures in the interval covered by our record (Sánchez Goni et al, 2008; Fletcher et al, 2010). As indicated above, the most pronounced millennial-scale cooling as recorded by pollen assemblages in the Bay of Biscay appeared to have been between ca. 70–80 ka. However, this longer term trend was interrupted by shorter term, pollen inferred intervals of warmer climate that have been correlated with GIS 21-19 (Sánchez Goñi et al, 2008). Similarly, vegetation changes associated with the Odderade and Dürnten interstadials, that have been correlated with GIS 20 and 21, have been observed in the pollen record of Füramoos (Müller et al, 2003; Figure 5). The new chironomid-based July air temperature reconstruction shows some evidence of minor temperature increases at the onset of the Odderade and Dürnten interstadials (Müller et al, 2003). However, overall centennial-scale temperature

variations that could be related to stadial-interstadial transitions are not very pronounced and less prominent than the multi-millennial-scale temperature trends in the data.

During Stadial D, regions north of the Alps are considered to have been largely treeless, with most local tree refugia eradicated (Müller et al, 2003). Based on the correlation of the Füramoos record with the Greenland isotope records by Müller et al., (2003), GIS stages 17, 18 and 19 occurred during the Stadial D interval. However, short term variations in pollen assemblages during Stadial D that could represent vegetation change during GIS 17-19 are not detected in the Füramoos record (Müller et al, 2003, Figure 5). Since particularly GIS 18-19 were relatively short-lived events (Figure 5), it is possible that this is a matter of sample resolution. However, there are other examples of pollen records from Europe in which one or more of the GIS stages 17, 18 and 19 are absent (Fletcher et al, 2010). Chironomid inferred July air temperatures for Stadial D vary between 9–10.5°C and also present no clear indication of GIS stages 17, 18 and 19. Overall our results suggest that July air temperature appears to have played an important role in driving vegetation change during some sections of the Füramoos record, particularly during the inferred temperature decrease and temperature minimum during the Odderade and Stadial C (Figure 5). However, in other intervals summer temperature was apparently not limiting tree growth or driving vegetation change. For example, the chironomid inferred July air temperatures for Stadial D are typical for treeline or low-tundra environments in Central Europe (Landolt, 2003). If local arboreal refugia would have been present, increases in arboreal pollen associated with temperatures above 10°C would have been expected assuming the other taxa specific demands for tree growth had been met, however no such arboreal pollen increase is observed. Similarly, during Stadial B, arboreal pollen decreases from 95 to 50%, while reconstructed July air temperature decreases only 0.5°C, remaining at similar values as during parts of the Brörup. This implies that summer temperature change was not the driver of this forest opening in the Füramoos region. The latter observation agrees with the review of Helmens (2014) who reports very little summer temperature change in Europe during MIS 5b relative to MIS5c and MIS5a, the intervals corresponding to the Brörup-Stadial B-Odderade transitions.

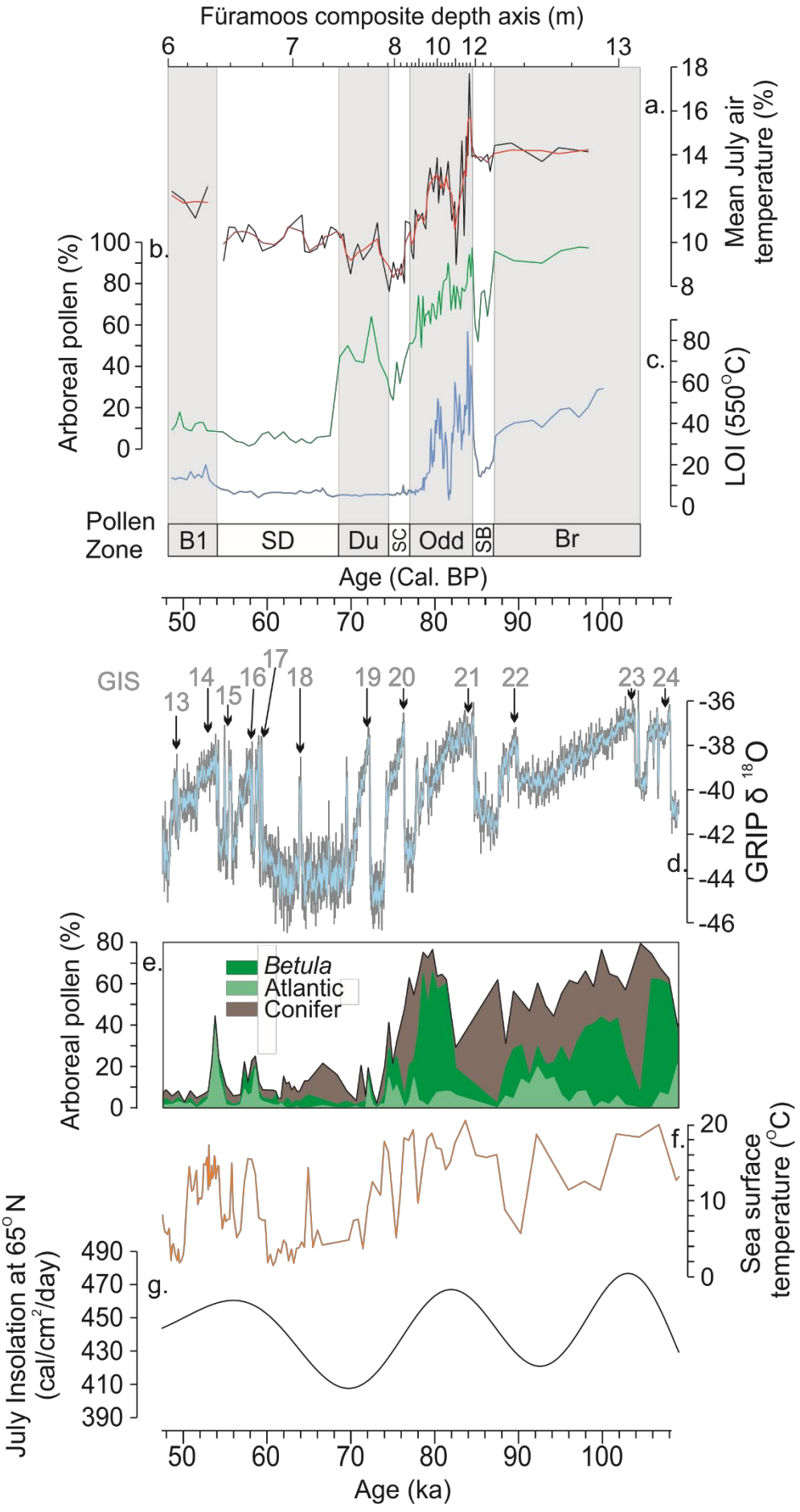
Füramoos composite depth axis (m)
6
7
8
10
12
13
a.
Mean July air temperature (%)
18
16
14
12
10
8
b.
Arboreal pollen (%)
100
80
60
40
20
0
c.
LOI (550°C)
80
60
40
20
0
Pollen Zone
B1
SD
Du
SC
Odd
SB
Br
Age (Cal. BP)
50
60
70
80
90
100
GIS
13
14
15
16
17
18
19
20
21
22
23
24
-36
-38
-40
-42
-44
-46
d.
GRIP δ18O
e.
Arboreal pollen (%)
80
60
40
20
0
Betula
Atlantic
Conifer
f.
Sea surface temperature (°C)
20
10
0
g.
July Insolation at 65° N (cal/cm²/day)
490
470
450
430
410
390
50
60
70
80
90
100
Age (ka)

Figure 5: a. Chironomid-inferred July air temperature reconstruction (black) and three sample running average (red); b. Füramoos composite core arboreal pollen percentages; c. Füramoos composite core LOI at 550°C; d. NGRIP $\delta^{18}O$ record, Greenland (North Greenland Ice Core Project members 2004). Greenland Isotope Stages (GIS) are indicated (Rasmussen et al, 2014); e: Bay of Biscay (core MD04-2845) pollen record. Atlantic forest pollen includes *Corylus, Carpinus, Fagus,* deciduous *Quercus* and *Betula* (*Betula* presented separately; Sánchez Goñi et al, 2008; 2013); f. June, July, August sea-surface temperatures from the Bay of Biscay (core MD04-2845) (Sánchez Goñi et al, 2008); g. Summer insolation at 65°N (Berger and Loutre, 1991). MD04-2845 data presented on ACER project members (2017) chronology.

5. Conclusions

We present the longest chironomid-based, quantitative temperature reconstruction from the Würmian glacial period to date, covering the interval from the Brörup (MIS 5c; ca. 99 ka) to the Bellamont 1 interstadials (MIS 3; ca. 49 ka) at centennial to millennial resolution. Chironomid assemblages suggest that the study site at Füramoos was a relatively shallow lake during this interval, with assemblages indicating warmer conditions (dominated, e.g., by *Cladopelma lateralis*-type and *Tanytarsus mendax*-type) over the course of the record giving way to assemblages indicating cooler conditions (dominated, e.g., by *Tanytarsus lugens*-type and *Sergentia coracina*-type). Both the chironomid assemblages and associated non-chironomid remains imply a decrease in lake productivity at ca. 55–53 ka, with the consequence that after ca. 49 ka the lake did not support abundant and diverse invertebrate assemblages.

The chironomid-based July temperature reconstruction shows decreasing temperatures of ca. 14°C in the Brörup, ca. 14°C during Stadial B, 10–16°C during the Odderade and 10–11°C during Stadial D, and an increase to 12°C during the Bellamont 1 interstadial. Overall, our results support other palaeotemperature records from Europe in indicating a distinct cooling during the early to middle Würmian. The strongest summer temperature decrease is registered in our record during the Odderade interstadial, synchronous with a major decrease in summer insolation and prior to forest opening and development of a steppic tundra associated with MIS 4. The inferred summer-temperature decrease during Stadial B was relatively minor, and inferred temperatures during Stadial D were cool but variable. The lowest summer temperatures in the examined interval prevailed during Stadial C, with initial July air temperature decreases beginning during the Odderade interstadial when cool summers may have contributed to the elimination of forests at Füramoos and wider Central Europe.

Acknowledgements

The contributions of Bertil Mächtle and Gerd Schukraft (†) to the FU1/FU3 coring campaign, and of George Kukla (†), Ulrich Müller and Guy Seret to the FURA coring campaign are gratefully acknowledged. We also thank Nichole Anest for core handling at the Lamont-Doherty Core Repository. This research has been supported by the Swiss National Science Foundation (SNSF grant 200021_165494).

Supplementary Material

1. Correlating lacustrine sequences from the Würmian Glacial period

Correlations between lacustrine sequences in Europe are generally well constrained for the early Würmian complex with St. Germain I and II correlated to the Brörup and the Odderade (Helmens, 2014). However, in the later Würmian stratigraphic correlation becomes more difficult. At Füramoos, the Odderade interstadial represents a forested interval with an initial phase of closed forest containing up to 20% thermophilic tree that develops into a more open forest (80% arboreal pollen) containing *Picea, Pinus* and *Betula* (Müller et al, 2003). Subsequently, Stadial C is characterised by an initial arboreal pollen decrease to 35% and associated with increases of *Artemisia* and *Ranunculus acris*-type to 10 and 55% respectively. Subsequent afforestation in the Dürnten interstadial is indicated by arboreal pollen increase to 65% that opens again at the onset of Stadial D, indicated by arboreal pollen abundances of 10%. For the Füramoos pollen record, stadials and interstadials have been correlated to GIS and GS stages by Müller et al., (2003), the interstadials Odderade and Dürnten being correlated to GIS 21 and the first part of GIS 20, respectively. Some studies have not separated GIS 20 and 21 into discrete events, rather GIS 20 and 21 are aggregated with GIS 20 and GS 21 into the Odderade (e.g., Ilyashuk et al, 2020). For presentation in Supplementary Table 1 we follow Müller et al., (2003) and treat the Dürnten and Stadial C (GIS 20 and GS 21) as distinct intervals.

1. Our correlations to the Füramoos chironomid record

For the early Würmian complex St. Germain I and II are widely agreed to correlate to the Brörup and the Odderade, and more broadly with MIS 5c and MIS 5a (Helmens et al, 2014). Beginning with Stadial C we correlate pollen assemblage zones between European lake sediment records based on GIS stages. We rely on correlations between pollen records and GIS stages that have been made available in the literature for those records we wish to correlate. In the list below, we outline exactly how we derived those correlations.

(1) The Oerel and Glinde interstadials and the Ebersdorf stadial represent the Moershoofd complex from the Oerel record (Behre et al, 2005). The Oerel and Glinde interstadials were correlated to GIS 14, 15, 16 and 17 by Dansgaard et al., (1993). We use the GIS stages 14, 15, 16 and 17 to correlate the Moershoofd complex to the Füramoos record in Supplementary Table 1.

(2) The Pile complex at La Grande Pile (Woillard, 1978) is correlated to the Moershoofd complex (Helmens, 2014). We therefore use the GIS stages 14, 15, 16 and 17 to correlate the Pile and Goulotte complex to the Füramoos record in Supplementary Table 1.
    a. We use samples 26, 27 and 29 from Ponel (1995) to represent the Pile complex.
    b. Ognon 1 (correlated to the Dürnten interstadial by Guiter et al, 2003) is not represented in the beetle-based reconstructions of Ponel (1995) due to a missing sample.

(3) For Gröbern (Walkling and Coope, 1996; Kuhl et al, 2007) it is not clear if the Odderade has been correlated with GIS 21 only or if it has been correlated with GIS 20, 21 and GS 21 (therefore including the Dürnten and Stadial C). Here we correlate the Odderade from Gröbern with the Odderade from Füramoos, representing GIS 21 only, in Supplementary Table 1 below.

(4) The Odderade samples from Unterangerberg are from intervals corresponding to GIS 21 and 20 (Ilyashuk et al, 2020). We therefore split the samples into Odderade (GIS 21) and Dürnten (GIS 20) samples based on their correlations to GIS stages. There were no samples from the intervening Stadial C (GS 21).

(5) From Klotz et al., (2004) we present the modern analogue vegetation types method reconstruction.

A comparison of quantitative palaeotemperature estimates from different studies correlated with the Füramoos record as outlined above is provided in Supplementary Table 1.

Supplementary Table 1: Ranges of mean January and July temperatures inferred from Germany, Austria and France (Figure 1) presented in respective stratigraphical zones correlated to the Füramoos record. Stage names and associated GIS and MIS stages from the original publication are displayed for transparency. Diachroneities between terrestrial stratigraphy and marine stages are not considered for presentation purposes. July temperatures are in orange and January temperatures are in blue. MTW: Mean temperature of the warmest month, MTC: mean temperature of the coldest month, temp: temperature. All temperature ranges are expressed in °C.

Author	Site										
		MIS	3			4	5a			5b	5c
		GIS	13	14 15	16 17	18, 19	20		21		22, 23, 24
		GS	14	15	16 17	18, 19, 20		21		22	23, 24
This Study	Füramoos (Chironmids)	Stage	Bellamont 1		Stadial D		Dürnten	Stadial C	Odderade	Stadial B	Brörup
		July temp	11 to 12.5		9 to 11		8.5 to 11	7.5 to 11	9 to 17	13 to 14	13.5 to 14.5
Klotz et al (2004)	Klotz et al. (2004) Füramoos correlations	MIS					3	4	5a	5b	5c
		GIS					14, 15 , 16, 17	18, 19, 20	21		22, 23, 24
		GS					14, 15, 16	17, 18, 19, 20		21	
		Stage					Interstadial	Stadial	St. Germain II	Melisey II	St. Germain I
	Füramoos (Pollen)	MTW					14 to 16.5	13 to 16.5	13.5 to 18	13 to 16.5	11.5 to 18
		MTC					-14.5 to -9	-11 to -9	-14.5 to -2	-18 to -11	-15.5 to -5.5
	Klotz et al. (2004) Jammertal, les Echtes and Samerberg correlations	MIS				4			5a	5b	5c
		GIS				18, 19, 20			21		22, 23, 24
		GS				17, 18, 19, 20				21	
		Stage				Stadial			St. Germain II	Melisey II	St. Germain I
	Jammertal (Pollen)	MTW				11 to 18			14.5 to 18	11 to 18	9.5 to 18
		MTC				-17 to -8			-17 to -3	-19 to -4	-14.5 to -5
	Les Echets (Pollen)	MTW				4.5 to 20.5			16 to 20	10.5 to 17	15 to 20
		MTC				-16 to 2			-15 to 3	-20 to 2	-5 to 2.5
	Samerberg (Pollen)	MTW				12.5 to 17			14 to 17	14 to 17.5	15 to 17
		MTC				-15 to -5.5			-13.5 to -5.5	-15.5 to -9.5	-12.5 to -6
Behre et al (2005)	Oerel (Beetles)	Stage		Moershoofd Complex					Odderade		Brörup
		MTW		9.5 to 11					7.5 to 19		11 to 19
		MTC		-17.5 to -5					-22 to 4		-14.5 to - 7.5
Ponel (1995)	La Grande Pile (Beetles)	Stage		Pile Complex					St. Germain II	Melisey II	St. Germain I
		MTW	7 to 21	10 to 13.5		10 to 18			16 to 20	13.5 to 23	9 to 26
		MTC	-39 to -2.5	-17.5 to 0		-17.5 to 8.5			-18 to 15	14.5 to 8.5	-17 to 12.5
Walking and Coope (1996)	Gröbern (Beetles)	Stage						???	Odderade	Rederstall	Late Brörup
		MTW						11 to 11.5	11.5 to 17	9 to 16	12 to 17
Kühl et al (2007)	Gröbern (Pollen)	July temp							17 to 17.5	12.5 to 16.5	16.5 to 17.5
		January temp							-12.5 to -8.5	-19 to -10.5	-15.5 to -8.5
Ilyashuk et al (2020)	Unterangerberg (Chironomds)	Stage					MIS 5a				
		July temp					14		13 to 18		

References

ACER project members. 2017. CLAM age model and biomes of sediment core MD04-2845. PANGAEA, https://doi.org/10.1594/PANGAEA.872808

Andersen, T., Cranston, P.S. and Epler, J.H. eds., 2013. Chironomidae of the Holarctic Region: Keys and Diagnoses: Larvae. Scandinavian Society of Entomology.

Beattie, D.M., 1982. Distribution and production of the larval chironomid populations in Tjeukemeer. *Hydrobiologia*, *95*(1), pp. 287-306.

de Beaulieu, J.L.D. and Reille, M., 1984. A long upper Pleistocene pollen record from Les Echets, near Lyon, France. Boreas, 13(2), pp. 111-132.

de Beaulieu, J.L. and Reille, M., 1989. The transition from temperate phases to stadials in the long Upper Pleistocene sequence from Les Echets (France). *Palaeogeography, Palaeoclimatology, Palaeoecology*, *72*, pp. 147-159.

Behre, K.E., 1989. Biostratigraphy of the last glacial period in Europe. *Quaternary Science Reviews*, *8*(1), pp. 25-44.

Behre, K.E. and Lade, U., 1986. Eine Folge von Eem und 4 Weichsel-Interstadialen in Oerel/Niedersachsen und ihr Vegetationsablauf. *E&G Quaternary Science Journal*, *36*(1), pp. 11-36.

Behre, K.E. and van der Plicht, J., 1992. Towards an absolute chronology for the last glacial period in Europe: radiocarbon dates from Oerel, northern Germany. *Vegetation History and Archaeobotany*, *1*(2), pp. 111-117.

Behre, K.E., Hölzer, A. and Lemdahl, G., 2005. Botanical macro-remains and insects from the Eemian and Weichselian site of Oerel (northwest Germany) and their evidence for the history of climate. *Vegetation History and Archaeobotany*, *14*(1), pp. 31-53.

Bennett, K.D., 1996. Determination of the number of zones in a biostratigraphical sequence. *New Phytologist.* 132(1), pp. 155-170.

Berger, A. and Loutre, M.F., 1991. Insolation values for the climate of the last 10 million years. *Quaternary Science Reviews*, *10*(4), pp. 297-317.

Beug, H, J., 2004. *Leitfaden der Pollenbestimmung für Mitteleuropa und angrenzende Gebiete*. Dr. Friedrich Pfeil: München.

Birks, H.J.B., Braak, C.T., Line, J.M., Juggins, S. and Stevenson, A.C., 1990. Diatoms and pH reconstruction. *Philosophical Transactions of the Royal Society of London. B, Biological Sciences*, 327(1240), pp. 263-278.

Boch, R., Cheng, H., Spötl, C., Edwards, R. L., Wang, X., & Häuselmann, Ph. (2011). NALPS: a precisely dated European climate record 120–60 ka. *Climate of the Past*, 7(4), pp. 1247-1259.

Boggero, A., Füreder, L., Lencioni, V., Simcic, T., Thaler, B., Ferrarese, U., Lotter, A.F. and Ettinger, R., 2006. Littoral chironomid communities of Alpine lakes in relation to environmental factors. *Hydrobiologia*, 562(1), pp. 145-165.

Bolland, A., Rey, F., Gobet, E., Tinner, W. and Heiri, O., 2020. Summer temperature development 18,000–14,000 cal. BP recorded by a new chironomid record from Burgäschisee, Swiss Plateau. *Quaternary Science Reviews*, *243*, pp. 106-484.

ter Braak, C.J. and Juggins, S., 1993. Weighted averaging partial least squares regression (WA-PLS): an improved method for reconstructing environmental variables from species assemblages. In *Twelfth International Diatom Symposium* (pp. 485-502). Springer, Dordrecht.

ter Braak, C. J. F., Juggins, S., Birks, H. J. B. and van der Voet, H, Weighted averaging partial least squares regression (WA-PLS): definition and comparison with other methods for species-environment calibration. Chapter 25 in G. P. Patil, and C. R. Rao (Eds.), Multivariate Environmental Statistics. Amsterdam: Elsevier Science Publishers B.V. (1993), pp. 525-560.

ter Braak, C.J. and Šmilauer, P., 2018. Canoco reference manual and user's guide: software for ordination (version 5.10). Biometris, Wageningen University & Research.

Brodersen, K.P. and Lindegaard, C., 1999. Mass occurance and sporadic distribution of Corynocera ambigua Zetterstedt (Diptera, Chironomidae) in Danish lakes. Neo-and palaeolimnological records. *Journal of Paleolimnology*, *22*(1), pp. 41-52.

Brooks, S.J. and Birks, H.J.B., 2000. Chironomid-inferred late-glacial and early-Holocene mean July air temperatures for Kråkenes Lake, western Norway. *Journal of Paleolimnology*, *23*(1), pp. 77-89.

Brooks, S.J., Langdon, P.G. and Heiri, O., 2007. *The identification and use of Palaearctic Chironomidae larvae in palaeoecology*. *Quaternary Research Association Technical Guide*, (10).

Brundin, L., 1949. Chironomiden und ander Bodentiere de sudschwedischen Urgebirgseen. Ein Beitrag zur Kenntnis der bodenfaunistischen Charakterzuge shwedischer oligotropher Seen. *Report of the Insitute of Freshwater Research, Drottningholm*, *30*, pp. 1-914.

Busschers, F.S., Van Balen, R.T., Cohen, K.M., Kasse, C., Weerts, H.J., Wallinga, J. and Bunnik, F.P., 2008. Response of the Rhine–Meuse fluvial system to Saalian ice-sheet dynamics. *Boreas*, *37*(3), pp. 377-398.

Caspers, G. and Freund, H., 2001. Vegetation and climate in the Early-and Pleni-Weichselian in northern Central Europe. *Journal of Quaternary Science: Published for the Quaternary Research Association*, *16*(1), pp. 31-48.

Chaline, J. and Jerz, H., 1984. Arbeitsergebnisse der Subkommission für Europäische Quartärstratigraphie. Stratotypen des Würm-Glazials. *Eiszeitalter und Gegenwart*, *35*, pp. 185-206.

Dansgaard, W., Johnsen, S.J., Clausen, H.B., Dahl-Jensen, D., Gundestrup, N.S., Hammer, C.U., Hvidberg, C.S., Steffensen, J.P., Sveinbjörnsdottir, A.E., Jouzel, J. and Bond, G., 1993. Evidence for general instability of past climate from a 250-kyr ice-core record. *Nature*, *364*(6434), pp. 218-220.

Eggermont, H. and Heiri, O., 2012. The chironomid-temperature relationship: expression in nature and palaeoenvironmental implications. *Biological Reviews*, *87*(2), pp. 430-456.

Eisele, G., Haas, K., and Liner, S., 1994, Methode zur Aufbereitung fossilen Pollens aus

minerogenen Sedimenten, in Frenzel, B., (Ed.), Über Probleme der holozänen Vegetationsgeschichte Osttibets, v. 95: Göttingen, Göttinger Geographische Abhandlungen, pp. 165– 166.

Engels, S., Bohncke, S.J., Heiri, O., Schaber, K. and Sirocko, F., 2008. The lacustrine sediment record of Oberwinkler Maar (Eifel, Germany): Chironomid and macro-remain-based inferences of environmental changes during Oxygen Isotope Stage 3. *Boreas*, *37*(3), pp. 414-425.

Engels, S., Helmens, K.F., Väliranta, M., Brooks, S.J. and Birks, H.J.B., 2010. Early Weichselian (MIS 5d and 5c) temperatures and environmental changes in northern Fennoscandia as recorded by chironomids and macroremains at Sokli, northeast Finland. *Boreas*, *39*(4), pp. 689-704.

Engels, S., Self, A.E., Luoto, T.P., Brooks, S.J. and Helmens, K.F., 2014. A comparison of three Eurasian chironomid–climate calibration datasets on a W–E continentality gradient and the implications for quantitative temperature reconstructions. *Journal of Paleolimnology*, *51*(4), pp. 529-547.

Fletcher, W.J., Goni, M.F.S., Allen, J.R., Cheddadi, R., Combourieu-Nebout, N., Huntley, B., Lawson, I., Londeix, L., Magri, D., Margari, V. and Müller, U.C., 2010. Millennial-scale variability during the last glacial in vegetation records from Europe. *Quaternary Science Reviews*, *29*(21-22), pp. 2839-2864.

Fjellberg, A., 1972. Present and Late Weichselian occurrence of Corynocera ambigua Zett. (Diptera, Chironomidae) in Norway. *Norwegian Journal of Entomology*. 19 (1972), pp. 59-61.

Francis, D. R., 2001. Bryozoan statoblasts. In Smol, J. P., H. J. B. Birks & W. M. Last (eds) Tracking Environmental Change Using Lake Sediments Volume 4 Zoological Indicators. vol 4. Kluwer Academic Publishers, Dordrecht, 105-123.

Frey, D.G., 1988. Littoral and offshore communities of diatoms, cladocerans and dipterous larvae, and their interpretation in paleolimnology. *Journal of Paleolimnology*, *1*(3), pp. 179-191.

Gandouin, E., Rioual, P., Pailles, C., Brooks, S.J., Ponel, P., Guiter, F., Djamali, M., Andrieu-Ponel, V., Birks, H.J.B., Leydet, M. and Belkacem, D., 2016. Environmental and climate reconstruction of the late-glacial-Holocene transition from a lake sediment sequence in Aubrac, French Massif Central: Chironomid and diatom evidence. *Palaeogeography, Palaeoclimatology, Palaeoecology*, *461*, pp. 292-309.

Grimm, E, C., 1987. CONISS: A Fortran 77 program for stratigraphically constrained cluster analysis by the method of incremental sum of squares. *Computers & Geosciences.* 13(1), pp. 13-35.

Grüger, E., 1979. Spätriss, Riss/Würm und Frühwürm am Samerberg in Oberbayern—ein vegetationsgeschichtlicher Beitrag zur Gliederung des Jungpleistozäns. *Geologica bavarica*, *80*, pp. 5-64.

Guiot, J., De Beaulieu, J.L., Cheddadi, R., David, F., Ponel, P. and Reille, M., 1993. The climate in Western Europe during the last Glacial/Interglacial cycle derived from pollen and insect remains. *Palaeogeography, Palaeoclimatology, Palaeoecology*, *103*(1), pp. 73-93.

Guiter, F., Andrieu-Ponel, V., de Beaulieu, J.L., Cheddadi, R., Calvez, M., Ponel, P., Reille, M., Keller, T. and Goeury, C., 2003. The last climatic cycles in Western Europe: a comparison between long continuous lacustrine sequences from France and other terrestrial records. *Quaternary International*, *111*(1), pp. 59-74.

Haas, J.N., 1994. First identification key for charophyte oospores from central Europe. *European Journal of Phycology*, *29*(4), pp. 227-235.

Heggen, M.P., Birks, H.H., Heiri, O., Grytnes, J.A. and Birks, H.J.B., 2012. Are fossil assemblages in a single sediment core from a small lake representative of total deposition of mite, chironomid, and plant macrofossil remains?. *Journal of Paleolimnology*, *48*(4), pp. 669-691.

Heiri, O., 2004. Within-lake variability of subfossil chironomid assemblages in shallow Norwegian lakes. *Journal of Paleolimnology*, *32*(1), pp. 67-84.

Heiri, O. and Lotter, A.F., 2001. Effect of low count sums on quantitative environmental reconstructions: an example using subfossil chironomids. *Journal of Paleolimnology* 26(3), pp. 343-350.

Heiri, O. and Lotter, A.F., 2005. Holocene and Lateglacial summer temperature reconstruction in the Swiss Alps based on fossil assemblages of aquatic organisms: a review. *Boreas*, *34*(4), pp. 506-516.

Heiri, O. and Lotter, A.F., 2007. Sciaridae in lake sediments: indicators of catchment and stream contribution to fossil insect assemblages. *Journal of Paleolimnology*, 38(2), pp. 183-189.

Heiri, O. and Lotter, A.F., 2010. How does taxonomic resolution affect chironomid-based temperature reconstruction? *Journal of Paleolimnology*, 44(2), pp. 589-601.

Heiri, O. and Millet, L., 2005. Reconstruction of Late Glacial summer temperatures from chironomid assemblages in Lac Lautrey (Jura, France). *Journal of Quaternary Science*, *20*(1), pp. 33-44.

Heiri, O., Lotter, A.F. and Lemcke, G., 2001. Loss on ignition as a method for estimating organic and carbonate content in sediments: reproducibility and comparability of results. Journal of paleolimnology, 25(1), pp.101-110.

Heiri, O., Birks, H.J.B., Brooks, S.J., Velle, G. and Willassen, E., 2003. Effects of within-lake variability of fossil assemblages on quantitative chironomid-inferred temperature reconstruction. *Palaeogeography, Palaeoclimatology, Palaeoecology*, *199*(1-2), pp. 95-106.

Heiri, O., Lotter, A.F., Hausmann, S. and Kienast, F., 2003. A chironomid-based Holocene summer air temperature reconstruction from the Swiss Alps. *Holocene,* 13(4), pp. 477-484.

Heiri, O., Brooks, S.J., Birks, H.J.B. and Lotter, A.F., 2011. A 274-lake calibration data-set and inference model for chironomid-based summer air temperature reconstruction in Europe. *Quaternary Science Reviews*, *30*(23-24), pp. 3445-3456.

Heiri, O., Brooks, S.J., Renssen, H., Bedford, A., Hazekamp, M., Ilyashuk, B., Jeffers, E.S., Lang, B., Kirilova, E., Kuiper, S. and Millet, L., 2014. Validation of climate model-inferred regional temperature change for late-glacial Europe. *Nature communications*, *5*(1), pp. 1-7.

Heiri, O., Brooks, S.J., Birks, H.J.B. and Lotter, A.F., 2011. A 274-lake calibration data-set and inference model for chironomid-based summer air temperature reconstruction in Europe. *Quaternary Science Reviews,* 30(23-24), pp. 3445-3456.

Helmens, K.F., Risberg, J., Jansson, K.N., Weckström, J., Berntsson, A., Tillman, P.K., Johansson, P.W. and Wastegård, S., 2009. Early MIS 3 glacial lake evolution, ice-marginal retreat pattern and climate at Sokli (northeastern Fennoscandia). *Quaternary Science Reviews*, *28*(19-20), pp. 1880-1894.

Helmens, K.F., Väliranta, M., Engels, S. and Shala, S., 2012. Large shifts in vegetation and climate during the Early Weichselian (MIS 5d-c) inferred from multi-proxy evidence at Sokli (northern Finland). *Quaternary Science Reviews*, *41*, pp. 22-38.

Helmens, K.F., 2014. The Last Interglacial–Glacial cycle (MIS 5–2) re-examined based on long proxy records from central and northern Europe. *Quaternary Science Reviews*, *86*, pp. 115-143.

Hofmann, W., 1983a. Stratigraphy of subfossil Chironomidae and Ceratopogonidae (Insecta: Diptera) in late glacial littoral sediments from Lobsigensee (Swiss Plateau). Studies in the late Quaternary of Lobsigensee 4. *Revue de Paléobiologie*, *2*(2), pp. 205-209.

Hofmann, W., 1983b. Stratigraphy of Cladocera and Chironomidae in a core from a shallow North German lake. *Hydrobiologia*, *103*(1), pp. 235-239.

Hofmann, W., 2001. Late-Glacial/Holocene succession of the chironomid and cladoceran fauna of the Soppensee (Central Switzerland). *Journal of Paleolimnology*, 25(4), pp. 411-420.

Hubbard, A., Sugden, D., Dugmore, A., Norddahl, H. and Pétursson, H.G., 2006. A modelling insight into the Icelandic Last Glacial Maximum ice sheet. *Quaternary Science Reviews*, *25*(17-18), pp. 2283-2296.

Hughes, P.D., Gibbard, P.L. and Ehlers, J., 2013. Timing of glaciation during the last glacial cycle: evaluating the concept of a global 'Last Glacial Maximum' (LGM). *Earth-Science Reviews*, *125*, pp. 171-198.

Hughes, P.D. and Gibbard, P.L., 2018. Global glacier dynamics during 100 ka Pleistocene glacial cycles. *Quaternary Research*, *90*(1), pp. 222-243.

Ilyashuk, E.A., Ilyashuk, B.P., Hammarlund, D. and Larocque, I., 2005. Holocene climatic and environmental changes inferred from midge records (Diptera: Chironomidae, Chaoboridae, Ceratopogonidae) at Lake Berkut, southern Kola Peninsula, Russia. *The Holocene*, *15*(6), pp. 897-914.

Ilyashuk, E.A., Ilyashuk, B.P., Heiri, O. and Spötl, C., 2020. Summer temperatures and lake development during the MIS 5a interstadial: New data from the Unterangerberg palaeolake in the Eastern Alps, Austria. *Palaeogeography, Palaeoclimatology, Palaeoecology*, 560, 110020.

Imbrie, J., Hays, J.D., Martinson, D.G., McIntyre, A., Mix, A.C., Morley, J.J., Pisias, N.G., Prell, W.L. and Shackleton, N.J., 1984. "The orbital theory of Pleistocene climate: Support from a revised chronology of the marine d18O record" in Milankovitch and Climate Part 1, A. L. Berger, Ed. et al. (D. Reidel, 1984), pp. 269–305.

Juggins, S., 2007. C2: Software for ecological and palaeoecological data analysis and visualisation (user guide version 1.5). Newcastle upon Tyne: Newcastle University, 77.

Juggins, S., 2017. rioja: Analysis of Quaternary Science Data, R package version (0.9-21). (http://cran.r-project.org/package=rioja).

Kern, O.A., Koutsodendris, A., Mächtle, B., Christanis, K., Schukraft, G., Scholz, C., Kotthoff, U. and Pross, J., 2019. XRF core scanning yields reliable semiquantitative data on the elemental composition of highly organic-rich sediments: Evidence from the Füramoos peat bog (Southern Germany). *Science of The Total Environment*, *697*, 134110.

Klotz, S., Müller, U., Mosbrugger, V., de Beaulieu, J.L. and Reille, M., 2004. Eemian to early Würmian climate dynamics: history and pattern of changes in Central Europe. *Palaeogeography, Palaeoclimatology, Palaeoecology*, *211*(1-2), pp. 107-126.

Korhola, A., Olander, H. and Blom, T., 2000. Cladoceran and chironomid assemblages as qualitative indicators of water depth in subarctic Fennoscandian lakes. *Journal of Paleolimnology*, *24*(1), pp. 43-54.

Kühl, N., Litt, T., Schölzel, C. and Hense, A., 2007. Eemian and Early Weichselian temperature and precipitation variability in northern Germany. *Quaternary Science Reviews*, *26*(25-28), pp. 3311-3317.

Landolt E. 2003. Unsere Alpenflora. Stuttgart, Germany: Gustav Fisher

Langdon, P.G., Ruiz, Z.O.E., Brodersen, K.P. and Foster, I.D., 2006. Assessing lake eutrophication using chironomids: understanding the nature of community response in different lake types. *Freshwater Biology*, *51*(3), pp. 562-577.

Langdon, P.G., Holmes, N. and Caseldine, C.J., 2008. Environmental controls on modern chironomid faunas from NW Iceland and implications for reconstructing climate change. *Journal of Paleolimnology*, *40*(1), pp. 273-293.

Larocque, I., Hall, R.I. and Grahn, E., 2001. Chironomids as indicators of climate change: a 100-lake training set from a subarctic region of northern Sweden (Lapland). *Journal of Paleolimnology*, *26*(3), pp. 307-322.

Lemdahl, G., 2000. Lateglacial and Early Holocene insect assemblages from sites at different altitudes in the Swiss Alps—implications on climate and environment. *Palaeogeography, Palaeoclimatology, Palaeoecology*, *159*(3-4), pp. 293-312.

Lischke, H., von Grafenstein, U. and Ammann, B., 2013. Forest dynamics during the transition from the Oldest Dryas to the Bølling–Allerød at Gerzensee—a simulation study. *Palaeogeography, Palaeoclimatology, Palaeoecology*, *391*, pp. 60-73.

Litt, T., 1994. Paläoökologie, Paläobotanik und Stratigraphie des-Jungquartärs im nordmitteleuropäischen Tiefland: unter besonderer Berucksichtigung des Elbe-Saale-Gebietes. J. Cramer (Berlin-Stuttgart): 185 pp.

Lods-Crozet, B. and Lachavanne, J.B., 1994. Changes in the chironomid communities in Lake Geneva in relation with eutrophication, over a period of 60 years. *Archiv für Hydrobiologie*, *130*(4), pp. 453-471.

Lotter, A.F., Walker, I.R., Brooks, S.J. and Hofmann, W., 1999. An intercontinental comparison of chironomid palaeotemperature inference models: Europe vs North America. *Quaternary Science Reviews*, *18*(6), pp. 717-735.

Lotter, A.F., Heiri, O., Brooks, S., van Leeuwen, J.F., Eicher, U. and Ammann, B., 2012. Rapid summer temperature changes during Termination 1a: high-resolution multi-proxy climate reconstructions from Gerzensee (Switzerland). *Quaternary Science Reviews*, *36*, pp. 103-113.

Luoto, T.P., 2009a. Subfossil Chironomidae (Insecta: Diptera) along a latitudinal gradient in Finland: development of a new temperature inference model. *Journal of Quaternary Science*, *24*(2), pp. 150-158.

Luoto, T.P., 2009b. A Finnish chironomid-and chaoborid-based inference model for reconstructing past lake levels. *Quaternary Science Reviews*, *28*(15-16), pp. 1481-1489.

Martinson, D.G., Pisias, N.G., Hays, J.D., Imbrie, J., Moore, T.C. and Shackleton, N.J., 1987. Age dating and the orbital theory of the ice ages: Development of a high-resolution 0 to 300,000-year chronostratigraphy 1. *Quaternary Research*, *27*(1), pp. 1-29.

Martrat, B., Grimalt, J.O., Shackleton, N.J., de Abreu, L., Hutterli, M.A. and Stocker, T.F., 2007. Four climate cycles of recurring deep and surface water destabilizations on the Iberian margin. *Science*, *317*(5837), pp. 502-507.

Massaferro, J. and Brooks, S.J., 2002. Response of chironomids to Late Quaternary environmental change in the Taitao Peninsula, southern Chile. *Journal of Quaternary Science: Published for the Quaternary Research Association*, *17*(2), pp. 101-111.

McGarrigle, M.L., 1980. The distribution of chironomid communities and controlling sediment parameters in L. Derravaragh, Ireland. In *Chironomidae* (pp. 275-282). Pergamon.

McManus, J.F., Bond, G.C., Broecker, W.S., Johnsen, S., Labeyrie, L. and Higgins, S., 1994. High-resolution climate records from the North Atlantic during the last interglacial. *Nature*, *371*(6495), pp. 326-329.

Millet, L., Vannière, B., Verneaux, V., Magny, M., Disnar, J.R., Laggoun-Défarge, F., Walter-Simonnet, A.V., Bossuet, G., Ortu, E. and de Beaulieu, J.L., 2007. Response of littoral chironomid communities and organic matter to late glacial lake—level, vegetation and climate changes at Lago dell'Accesa (Tuscany, Italy). *Journal of Paleolimnology*, *38*(4), pp. 525-539.

Moseley, G.E., Spötl, C., Brandstätter, S., Erhardt, T., Luetscher, M. and Edwards, R.L., 2020. NALPS19: sub-orbital-scale climate variability recorded in northern Alpine speleothems during the last glacial period. *Climate of the Past*, *16*(1), pp. 29-50.

Müller, U.C., 2000. A Late-Pleistocene pollen sequence from the Jammertal, south-western Germany with particular reference to location and altitude as factors determining Eemian forest composition. *Vegetation History and Archaeobotany*, *9*(2), pp. 125-131.

Müller, U.C., Pross, J. and Bibus, E., 2003. Vegetation response to rapid climate change in Central Europe during the past 140,000 yr based on evidence from the Füramoos pollen record. *Quaternary Research*, *59*(2), pp. 235-245.

Nazarova, L., Self, A.E., Brooks, S.J., van Hardenbroek, M., Herzschuh, U. and Diekmann, B., 2015. Northern Russian chironomid-based modern summer temperature data set and inference models. *Global and Planetary Change*, *134*, pp. 10-25.

Nazarova, L., Bleibtreu, A., Hoff, U., Dirksen, V. and Diekmann, B., 2017. Changes in temperature and water depth of a small mountain lake during the past 3000 years in Central Kamchatka reflected by a chironomid record. *Quaternary International*, *447*, pp. 46-58.

North Greenland Ice Core Project members 2004. High-resolution record of the Northern Hemisphere climate extending into the last interglacial period. *Nature*, *431*, pp. 147-151.

Oksanen, J., Guillaume Blanchet, F., Friendly, M., Kindt, R., Legendre, P., McGlinn, D., Minchin, P.R., O'Hara, R. B., Simpson, G, L., Solymos, P., Henry, M., Stevens, H., Szoecs, E and Wagner. H. 2019. vegan: Community Ecology Package. R package version 2.5-5.

Ponel, P., 1995. Rissian, Eemian and Würmian Coleoptera assemblages from La Grande Pile (Vosges, France). *Palaeogeography, Palaeoclimatology, Palaeoecology*, *114*(1), pp. 1-41.

Pope, R.J., Gordon, A.M. and Kaushik, N.K., 1999. Leaf litter colonization by invertebrates in the littoral zone of a small oligotrophic lake. *Hydrobiologia*, *392*(2), pp. 99-112.

Porinchu, D.F. and Cwynar, L.C., 2000. The Distribution of Freshwater Chironomidae (Insecto: Diptera) across Treeline near the Lower Lena River, Northeast Siberia, Russia. *Arctic, Antarctic, and Alpine Research*, *32*(4), pp. 429-437.

Preusser, F., Geyh, M.A. and Schlüchter, C., 2003. Timing of Late Pleistocene climate change in lowland Switzerland. *Quaternary Science Reviews*, *22*(14), pp. 1435-1445.

Rasmussen, S.O., Bigler, M., Blockley, S.P., Blunier, T., Buchardt, S.L., Clausen, H.B., Cvijanovic, I., Dahl-Jensen, D., Johnsen, S.J., Fischer, H. Gkinis, V, Guillevic, M, Hoek, WZ, Lowe, J, Pedro, J, Popp, T, Seierstad, I, Steffensen, J, Svensson, A, Winstrup, M., 2014. A stratigraphic framework for abrupt climatic changes during the Last Glacial period based on three synchronized Greenland ice-core records: refining and extending the INTIMATE event stratigraphy. *Quaternary Science Reviews*, *106*, pp. 14-28.

Renssen, H. and Isarin, R.F.B., 2001. The two major warming phases of the last deglaciation at∼ 14.7 and∼ 11.5 ka cal BP in Europe: climate reconstructions and AGCM experiments. *Global and Planetary Change*, *30*(1-2), pp. 117-153.

de la Riva-Caballero, A., Birks, H.J.B., Bjune, A.E., Birks, H.H. and Solhøy, T., 2010. Oribatid mite assemblages across the tree-line in western Norway and their representation in lake sediments. *Journal of Paleolimnology*, *44*(1), pp. 361-374.

RStudio Team (2015). RStudio: Integrated Development for R. RStudio, Inc., Boston, MA URL http://www.rstudio.com/.

Saether, O.A., 1979. Chironomid communities as water quality indicators. *Ecography*, *2*(2), pp. 65-74.

Samartin, S., Heiri, O., Vescovi, E., Brooks, S.J. and Tinner, W., 2012. Lateglacial and early Holocene summer temperatures in the southern Swiss Alps reconstructed using fossil chironomids. *Journal of Quaternary Science*, *27*(3), pp. 279-289.

Sánchez Goñi, M.F.S., Landais, A., Fletcher, W.J., Naughton, F., Desprat, S. and Duprat, J., 2008. Contrasting impacts of Dansgaard–Oeschger events over a western European latitudinal transect modulated by orbital parameters. *Quaternary Science Reviews*, *27*(11-12), pp. 1136-1151.

Sánchez Goñi, M.F.S., Bard, E., Landais, A., Rossignol, L. and d'Errico, F., 2013. Air–sea temperature decoupling in western Europe during the last interglacial–glacial transition. *Nature Geoscience*, *6*(10), pp. 837-841.

Schmid, P.E., 1993. A key to the larval Chironomidae and their instars from Austrian Danube region streams and rivers: with particular reference to a numerical taxonomic approach. 1. Diamesinae, Prodiamesinae and Orthocladiinae. Selbstverl.

Schreiner, A. 1981. Quartärgeologische Untersuchungen in der Umgebung von Interglazialvorkommen im östlichen Rheingletschergebiet (Baden-Württemberg).

Schreiner, A. 1996. Erläuterungen zu 8025 Bad Wurzach: Geologische Karte von Baden-Württemberg 1:25 000 (1st ed.), Landesvermessungsamt Baden-Württemberg, Freiburg

Seguinot, J., Ivy-Ochs, S., Jouvet, G., Huss, M., Funk, M. and Preusser, F., 2018. Modelling last glacial cycle ice dynamics in the Alps. *The Cryosphere*, *12*(10), pp. 3265-3285.

Shackleton, N.J., Sánchez-Goñi, M.F., Pailler, D. and Lancelot, Y., 2003. Marine isotope substage 5e and the Eemian interglacial. *Global and Planetary change*, *36*(3), pp. 151-155.

Šmilauer, P. and Lepš, J., 2014. Multivariate analysis of ecological data using CANOCO 5. Cambridge University Press.

Solhøy, T., 2001. Oribatid mites. In Smol, J. P., H. J. B. Birks & W. M. Last (eds) Tracking Environmental Change Using Lake Sediments Volume 4 Zoological Indicators. vol 4. Kluwer Academic Publishers, Dordrecht, pp. 81-104.

Spratt, R.M. and Lisiecki, L.E., 2016. A Late Pleistocene sea level stack. *Climate of the Past*, *12*(4), pp. 1079-1092.

Stockmarr, J.A., 1971. Tablets with spores used in absolute pollen analysis. *Pollen et Spores*, *13*, pp. 615-621.

Tóth, M., Magyari, E.K., Brooks, S.J., Braun, M., Buczkó, K., Bálint, M. and Heiri, O., 2012. A chironomid-based reconstruction of late glacial summer temperatures in the southern Carpathians (Romania). *Quaternary Research*, *77*(1), pp. 122-131.

Tóth, M., Magyari, E.K., Buczkó, K., Braun, M., Panagiotopoulos, K. and Heiri, O., 2015. Chironomid-inferred Holocene temperature changes in the South Carpathians (Romania). *Holocene*. 25(4), pp. 569-582.

Tóth, M., van Hardenbroek, M., Bleicher, N. and Heiri, O., 2019. Pronounced early human impact on lakeshore environments documented by aquatic invertebrate remains in waterlogged Neolithic settlement deposits. *Quaternary Science Reviews*, *205*, pp. 126-142.

Vandekerkhove, J., Declerck, S., Vanhove, M., Brendonck, L., Jeppesen, E., Conde Porcuna, J.M. and De Meester, L., 2004. Use of ephippial morphology to assess richness of anomopods: potentials and pitfalls. *Journal of Limnology*, *63*(1s), pp. 75-84.

Waelbroeck, C., Labeyrie, L., Michel, E., Duplessy, J.C., McManus, J.F., Lambeck, K., Balbon, E. and Labracherie, M., 2002. Sea-level and deep water temperature changes derived from benthic foraminifera isotopic records. *Quaternary Science Reviews*, *21*(1-3), pp. 295-305.

Walker I.R. and MacDonald G.M., 1995. Distributions of Chironomidae (Insecta: Diptera) and other freshwater midges with respect to treeline, Northwest Territories, Canada. *Arctic* and Alpine *Research, 27,* 258-263.

Walker, I.R., Smol, J.P., Engstrom, D.R. and Birks, H.J.B., 1991. An assessment of Chironomidae as quantitative indicators of past climatic change. *Canadian Journal of Fisheries and Aquatic Sciences*, *48*(6), pp. 975-987.

Walkling, A.P. and Coope, G.R., 1996. Climatic reconstructions from the Eemian/Early Weichselian transition in Central Europe based on the coleopteran record from Gröbern, Germany. *Boreas*, *25*(3), pp. 145-159.

Wiederholm, T. 1983. Chironomidae of the Holarctic region. Keys and diagnoses. Part 1. Larvae. 67. *Entomologica Scandinavica 457*, pp.

Winterholler, K., 2004. Zur jungpleistozänen Landschaftsentwicklung am Füramooser Ried (Oberschwaben). Beiträge zur Geomorphologie, Bodengeographie und Quartärforschung., Geographischen Institut der Universität Tübingen, pp. 155-180.

Woillard, G.M., 1978. Grande Pile peat bog: a continuous pollen record for the last 140,000 years. *Quaternary Research*, 9(1), pp. 1-21.

Wulf, S., Hardiman, M.J., Staff, R.A., Koutsodendris, A., Appelt, O., Blockley, S.P., Lowe, J.J., Manning, C.J., Ottolini, L., Schmitt, A.K., Smith, V.C., Tomlinson, E.l., Vakhrameeva, P., Knipping, M., Kotthoff, U., Milner, A.M., Christanis. K., Kalaitzidis, S., Tzedakis, P.C., Schmiedl, G., and Pross, J. 2018. The marine isotope stage 1–5 cryptotephra record of Tenaghi Philippon, Greece: towards a detailed tephrostratigraphic framework for the Eastern Mediterranean region. *Quaternary Science Reviews*, *186*, pp. 236-262.

Paper III

Summer-temperature development during the Eemian interglacial and earliest Würmian glacial at Füramoos, southern Germany

Alexander Bolland[1], Oliver A. Kern[2], Andreas Koutsodendris[2], Jörg Pross[2], and Oliver Heiri[1]

[1]Geoecology, Department of Environmental Sciences, University of Basel, Klingelbergstrasse 27, CH-4056 Basel, Switzerland

[2]Paleoenvironmental Dynamics Group, Institute of Earth Sciences, Heidelberg University, Im Neuenheimer Feld 234, D-69120 Heidelberg, Germany

Corresponding author:

Alexander Bolland

Geoecology, Department of Environmental Sciences, University of Basel, Klingelbergstrasse 27, CH-4056 Basel, Switzerland

E-mail: alexanderwilliam.bolland@unibas.ch

Abstract

Eemian pollen records from central Europe describe a transition from thermophilous tree taxa in the early Eemian to boreal tree taxa in the late Eemian with forest opening in the subsequent stadial. The available summer temperature reconstructions covering the mid- to late Eemian transition show decreasing values during that time, although depending on the proxy type and locality absolute values vary considerably. Here we present a new chironomid record from the classical site of Füramoos, southern Germany, that covers the mid-Eemian to the end of the first Würmian stadial (ca. 125–104.5 ka). This record allows us (i) to describe lake development in the former Füramoos paleolake and (ii) to quantitatively reconstruct July air temperature during that time. This record is augmented by chronologically less well constrained results from the same site for the late Rissian glaciation as well as the early Brörup interstadial of the early Würmian glaciation. The late Rissian sediments are dominated by two chironomid taxa, *Sergentia coracina*-type and *Micropsectra radialis*-type, indicating very cold, oligotrophic conditions. The sediment core analysed contains an unconformity at the late Rissian/Eemian transition and analysis continues in the mid-Eemian. Mid Eemian sediments contained *Tantyatsus glabrescens*-type as well as Tanytarsus mendax-type suggesting that temperatures were relatively high. During the late Eemian, typically thermophilic taxa such as *Tantyatsus glabrescens*-type disappear, suggesting decreasing temperatures. The onset of Stadial A is associated with increases in *Microtendipes pedellus*-type and *Tanytarsus lugens*-type, which suggests cooling and fewer available nutrients in the Füramoos palaeolake. Early Brörup sediments contain *Tanytarsus glabrescens*-type and *Psectrocladius sordidellus*-type, suggesting an increase in nutrient availability again as well as a slight increase in July air temperature. Reconstructed July air temperatures show a decline from 16 to 12°C during the mid Eemian associated with decreasing northern hemisphere July insolation, the transition to the late Eemian coinciding with the 12°C July air temperatures. Late Eemian temperatures vary between 12 and 14°C and remain in the range of 12–13.5°C in Stadial A.

1. Introduction

During the last interglacial interval, the Eemian, global temperatures were 1–2°C higher than pre-industrial values (Masson-Delmotte et al, 2013; Otto-Bliesner et al, 2013; Turney and Jones, 2010) and as a result of large-scale deglaciation sea level was 6–9 m higher than today (Dutton et al, 2015). The Eemian is broadly correlated to Marine Isotope Stage (MIS) 5e (Dansgaard et al, 1993) but there is a ca. 6000 year lag between the onset of MIS 5e and afforestation in some terrestrial records from central Europe (Shackleton et al, 2003). Transition from the penultimate (i.e., Rissian) glacial to the Eemian was characterised by greenhouse gas concentrations rising on a global scale (Lüthi et al, 2008; Schilt et al, 2010) and increasing northern hemisphere summer insolation (Berger and Loutre, 1991).

Terrestrial records from central Europe identify the Eemian as a heavily forested interval chronologically in between the open landscapes of the previous glacial and the first phase of forest opening in the following glacial complex (Turner and West, 1968). Over large parts of Europe, steppic tundras associated with the penultimate glaciation transitioned into forest biomes at the onset of the Eemian (e.g., Litt, 1994). Eemian vegetation reconstructions for central Europe indicate a characteristic succession of arboreal taxa, with the pioneers *Pinus* and *Betula* giving way to thermophilic taxa including, but not limited to *Quercus, Corylus, Taxus, Abies* and *Carpinus*, and a late Eemian transition to coniferous forests dominated by *Pinus* and *Picea* along with *Betula* (e.g. Müller, 2000). The end of the Eemian in central Europe is characterized by a strong increase in the percentages of herbs, and particularly Poaceae, at the expense of tree-pollen percentages that marks the onset of the last glacial period (e.g., Woillard et al, 1978; Müller et al, 2003).

For terrestrial environments in Europe, quantitative proxy-based temperature reconstructions for the Eemian interglacial and Würmian glacial periods have been produced from pollen (e.g., Kühl and Litt, 2003; Kühl et al, 2007), beetle (Ponel, 1995; Walkling and Coope, 1996; Behre et al, 2005) and chironomid assemblages (Engels et al, 2008; 2010; 2014; Plikk et al, 2019; Ilyashuk et al, 2020; Bolland et al, 2020). The use of multiple proxies for temperature estimation is vital for understanding continental temperature development because different proxies can respond differently to environmental forcing factors (Lotter et al et al, 2012). Hence, by utilising multiple proxies it is possible to develop an integrated picture of past climatic change, ideally identifying different seasonal variables such as summer temperature, winter temperature and continentality.

The fossil remains of chironomid larvae are an excellent proxy for reconstructing environmental change, being ubiquitous, diverse, nearly eurytopic as a family and remaining well preserved in lacustrine sediments (Brooks et al, 2007). They allow the assessment of in-lake environmental change through time and, because of their close relationship with summer air temperatures, can be used to quantitatively reconstruct mean July air temperature by numerically comparing the fossil assemblages to modern assemblages (Brooks, 2006; Eggermont and Heiri, 2012). Here we present a new chironomid record covering the late Rissian, Eemian and early Würmian from Füramoos, southern Germany, to infer environmental change in the Füramoos palaeolake and produce a chironomid-based July air temperature reconstruction. Our new record yields a stratigraphically well constrained, centennial-scale temperature reconstruction from the mid-Eemian (ca. 125 ka) to the end of Stadial A (ca. 104.5 ka), thus covering the transition from the mid-Eemian to the late Eemian and the subsequent Stadial A. Our record also provides insights into July air temperatures during the Late Rissian glaciation, prior to the onset of the Eemian and the early Brörup interstadial that follows Stadial A.

2. Methods

2.1 Site description and coring

The Füramoos Ried peat bog was formed in a basin between two Rissian glacial moraines on the German alpine foreland (Schreiner, 1996; Busschers et al, 2008) situated at 662 meters above sea level. Its sediments represent a nearly continuous archive of environmental change from the end of the Rissian glaciation to the Holocene (Schreiner, 1981; Müller et al, 2003; Winterholler, 2004; Kern et al, 2019). The modern mean July air temperature is 16.6°C for the interval 1982 to 2012 (climate-data.org). The study is based on two parallel sediment cores (Fu15-1 and Fu15-2) that were retrieved from Füramoos at 47°59’26.149” N, 9°53’13.318” E in 2015 using a mobile drilling rig within a horizontal distance of 1.5 m from each other.

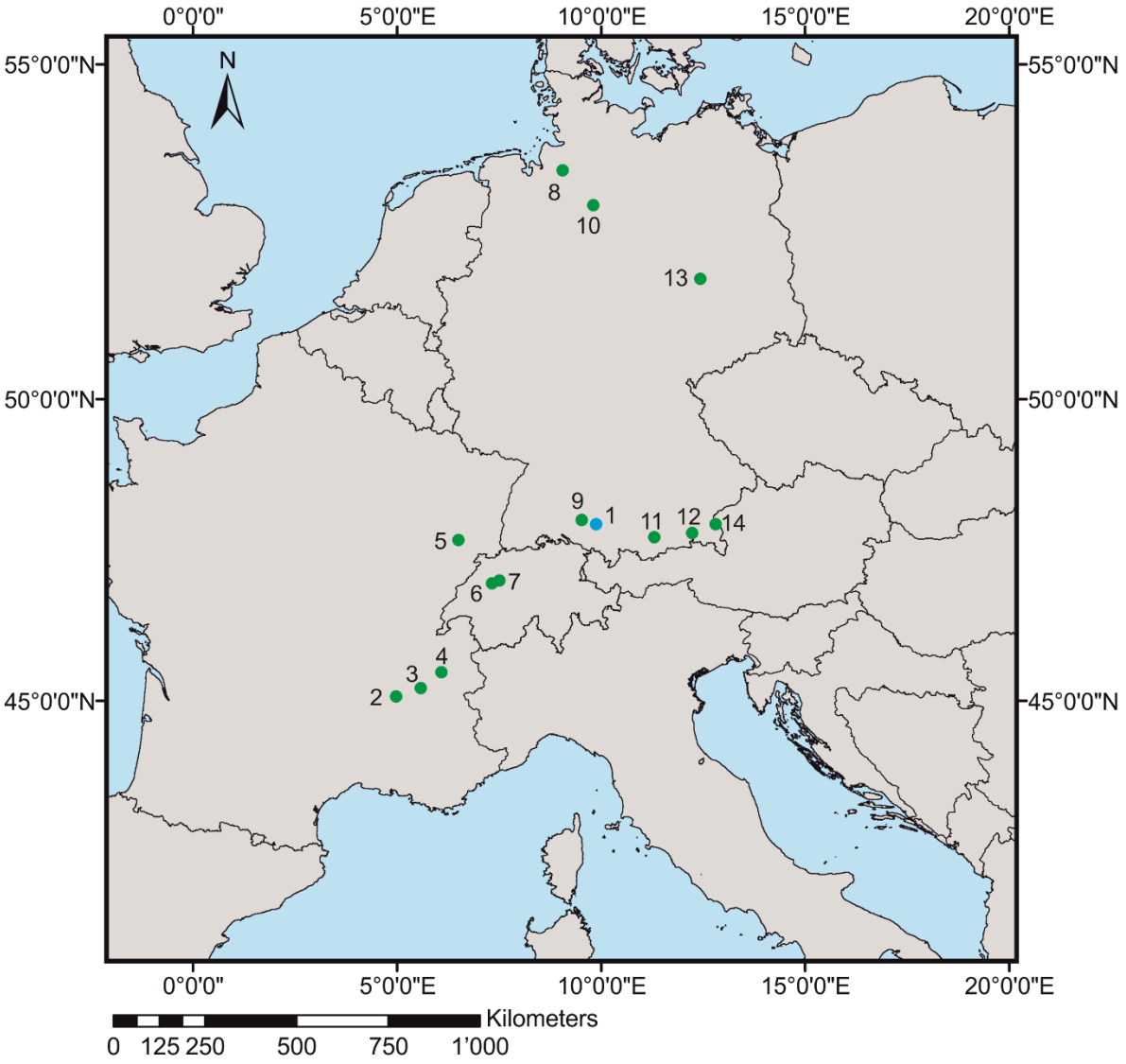

Figure 1: Site locations of temperature reconstructions referred to in the text for the interval from the Rissian glacial interval to the Brörup interstadial : 1. Füramoos (blue circle; Müller et al, 2003; Klotz et al, 2003; 2004; this study); 2. Les Echets (Klotz et al, 2004); 3. La Flachère (Klotz et al, 2003); 4. Lathulie (Klotz et al, 2003); 5. La Grande Pile (Woillard, 1978; Ponel, 1995; Kühl and Litt, 2003; Klotz et al, 2004); 6. Meikirch II (Klotz et al, 2003); 7. Beerenmösli (Klotz et al, 2003); 8. Oerel (Behre et al, 2005); 9. Jammertal (Müller, 2000; Klotz et al, 2003; 2004; Müller et al, 2005); 10. Bispingen (Kühl and Litt, 2003); 11. Eurach (Klotz et al, 2003); 12, Samerberg (Grüger, 1979; Klotz et al, 2003; 2004); 13. Gröbern (Litt, 1994; Walkling and Coope, 1996; Kühl and Litt, 2003; 2007); 14. Ziefen (Klotz et al, 2003).

2.2 Lithology

In this study we describe the results from a single sediment core segment Fu15-2 790–890 cm (hereafter referred to as "Fu15-2 core") that contains sediments from the Rissian glaciation, Eemian interglacial, Stadial A and early Brörup interstadial (Figure 2). The sediments have previously been

correlated to Müller et al., (2003), also from Füramoos (Becker, 2018; Kern et al, 2019). These correlations indicate that sediment depths between 890–857 cm are from the Rissian glacial that are primarily grey glacial clays with some fine sand grains. Sediment depths 857–819 cm are from the Eemian interglacial. The Eemian sediments are divided into two sections, one composed of fen peat between 855–837 cm and one composed of moderately organic lacustrine muds between 837–819 cm. Under the microscope Eemian sediments are largely homogenous, and due to the high degree of humification individual plant remains cannot be identified (Kern et al, 2019). Sediments from depths 819–803 cm are low organic lacustrine muds that correspond to Stadial A and Sediments from depths 803–790cm is fen peat corresponding to the Brörup interglacial. Macroscopically, sediment layers from the Brörup appear to form plates of organic-rich, highly humified sediments that can be easily separated from one another in layers but remain difficult to bend or break individually.

2.3. Pollen sample preparation and analysis

For the present study, eight pollen samples were processed across the transition interval from Rissian glacial sediments to Eemian fen peat (851–857 cm) in order to complement the previously available, low-resolution (12 cm) palynological dataset for the examined core segment of Becker (2018). For palynological processing, 1cm^3 was used per sample, and *Lycopodium* tablets were added for estimation of pollen concentrations prior to chemical treatment (Stockmarr, 1971). Sediments were processed in 10% NaOH following Eisele et al., (1994). Residues were embedded in glycerine jelly, mounted on microscope slides and analysed with a Carl Zeiss Axio Scope A1® microscope (400–1000 x magnification) at the Institute of Earth Sciences, Heidelberg University.

2.4. Loss on Ignition (LOI) analysis

The organic-matter content of the sediment was measured in 89 samples between 794 and 897 cm core depth using 0.5–2g of sediment per sample. The percentage of organic matter in each sample was determined following Loss on Ignition (LOI) at 550°C following Heiri et al., (2001). LOI was conducted at Research Group Geoecology, Basel University.

2.5. Chironomid sample preparation and analysis

94 chironomid samples were taken every 1 cm along the sediment core between absolute sediment depths of 794 and 888 cm. The volume of sediment used ranged between 1 and 6 cm3. For samples

taken below and including 857 cm there was no chemical pre-treatment, since the sediments could be sieved easily using water only. However, samples 858 cm and above were heated in 10% KOH for 15 minutes at 85°C due to processing difficulties (see Discussion). All samples were sieved at 100 and 200 µm, and chironomid head capsules as well as other chitinous aquatic invertebrate remains were picked from a Bogorov tray under stereomicroscope (30–50 x magnification). Samples were dried and mounted in Euparal before identification at 40–100 x magnification using a compound microscope. A minimum head count of 80 was aimed for to ensure that more than the recommended 50 head capsules were found per sample (Heiri and Lotter, 2001). Head capsules with a complete mentum or greater than half a mentum were counted as one specimen, head capsules with half a mentum were counted as half a specimen and head capsules with less than half a mentum were disregarded. Furthermore, other invertebrate remains including *Daphnia*, Sialidae, Ceratopogonidae, mites, Ephemeroptera, Trichoptera, Plecoptera in addition to *Plumatella* resting cysts were mounted and identified. Characeae oogonia were also enumerated.

2.6. Chironomid identification

Chironomid identification followed Wiederholm (1983), Schmid (1993), Brooks et al., (2007), and Anderson et al., (2013). Specimens that could only be identified to low taxonomic resolution were excluded from further analysis. Samples consisting of peat were difficult to process (see Discussion) and resulted in a relatively large number of mounted *Tanytarsus* specimens with damaged or missing antennal pedestals. In these sections head capsules belonging to specimens identified as *Tanytarsus* were assigned to the category of *Tanytarsus mendax*-type, since this was the only abundant *Tanytarsus* morphotype present in these samples (see Discussion). The descriptions of Solhøy (2001) and Haas (1994) were used to identify oribatid mites and Characeae oogonia, respectively. *Plumatella* statoblasts and *Daphnia* ephippia were identified based on Francis (2001) and Vandekerkhove et al., (2004). A photo collection of mounted modern specimens at Geoecology, University of Basel (Courtney-Mustaphi et al. in preparation) was used to identify larval mandibles and head capsules of Sialidae, Ceratopogonidae, Ephemeroptera, Trichoptera, and Plecoptera.

2.7. Chironomid-based temperature reconstruction

The Swiss-Norwegian calibration dataset and inference model from Heiri et al., (2011) was used to develop quantitative temperature estimates based on fossil chironomid assemblages. The dataset

describes the distribution data of 154 chironomid taxa from 274 lakes in Switzerland and Norway across a temperature gradient of 3.5 to 18.4 °C. A temperature reconstruction was produced using a two-component weighted averaging partial least squares model (WAPLS; ter Braak and Juggins, 1993; ter Braak et al., 1993). To produce the reconstruction some Füramoos samples needed to be combined to achieve higher chironomid counts (see results section 3.1. and Supplementary material 2). The model used in this study had a root mean square error of prediction of 1.41 and an r^2 of 0.90 between predicted and observed temperatures (estimates based on 9999 bootstrapping cycles). The chironomid samples in the record were identified to a higher resolution than the Swiss-Norwegian training set (Heiri et al, 2011) and therefore some of the original 42 types identified some types were aggregated to match the training set resolution. These were (training set resolution: Fu15-2 core resolution) *Einfeldia*: *E. dissidens*-type, and *E. natchitocheae*-type; *Dicrotendipes: Dicrotendipes nervosus*-type and *Dicrotendipes-notatus* type; *Cricotopus* 292: *Cricotopus laricomalis*-type and *Cricotopus intersectus*-type. Furthermore, one type, i.e., *Psectrocladius calcaratus*-type, was not included in the calibration dataset, resulting in 38 types that formed the basis for chironomid-inferred temperature estimates.

Samples were compared with the modern calibration data using squared chi-square distance to assess whether “close” or “good” analogues existed for fossil samples in the calibration dataset. The 2nd and 5th percentiles of all distances in the modern calibration data samples were set as thresholds for identifying such “close” or “good” modern analogues respectively (Birks et al. 1990; Tóth et al, 2015). Goodness of fit statistics were calculated following Birks et al., (1990) by first producing a Canonical Correspondence Analysis (CCA) of the Swiss-Norwegian training set data with mean July air temperature set as the only constraining variable. The fossil data were analysed as passive samples. Samples with a “poor” or “very poor” fit with temperature were identified by using the 90th and 95th percentile of residual distances of the modern calibration dataset samples to axis 1 respectively (Birks et al, 1990; Tóth et al, 2015). Bootstrapping with 9999 cycles was used to calculate sample specific estimated standard errors of prediction for reconstructed temperatures (Birks et al., 1990). Rare taxa (N2<5 in the calibration dataset; Heiri et al, 2003) and taxa absent from the training set were also calculated. The CCA was produced using CANOCO 5 (ter Braak and Smilauer, 2018) and analogue statistics were calculated using the programme C2 Version 1.7.7 (Juggins, 2007). All analyses were based on square root transformed percentages.

2.8. Zonation and ordination analysis

Zones in the chironomid record were determined using the clustering algorithm CONISS (Grimm, 1987) and a Broken Stick Model (Bennett, 1996) was used to test them for statistical significance. These analyses were calculated using the *Rioja* (Juggins, 2017) and *Vegan* (Oksanen et al, 2019) packages on R studio version 1.1.463 (RStudio Team, 2015). A Detrended Correspondence Analysis (DCA) was calculated in CANOCO 5.1 (Smilauer and Leps, 2014) to summarize major changes in the chironomid assemblage using square root transformed percentage data. Both analyses were conducted following sample aggregation (see Section 2.5.) and were calculated based on square root transformed percentages.

3. Results

3.1. LOI and organic matter content

The organic-matter content of Rissian sediments in the Fu15 core (887–857 cm) ranges between 0.8 and 5.7 % (Figure 2). Between 857 and 850 cm, there is an abrupt increase in organic-matter content from 0.8–5.7 to 71 % (Figure 2). The organic-matter content remains very high (between 53 and 74 %) for the interval from 850 to 853 cm before declining to 28–44 % in the interval 835–820 cm. Low LOI values (12.5–19.5 %) characterize the interval 818–804 cm. Further upcore, LOI values increase sharply to 43–69 % in the interval from 803 to 794cm.

3.2 Pollen Analysis

The eight new samples between 851 and 857 cm core depth show an abrupt transition from non-arboreal pollen (NAP) dominance to *Corylus* dominance when sampled at a continuous 1cm resolution (Figure 2; Supplementary Figure 1). Together with the information from the previously available samples of Becker (2018) from the same core section, the samples show steppe tundra in the Rissian glacial interval (890–857 cm) identified by high non-arboreal pollen (NAP) percentages of 65–80 % associated with *Artemisia* abundances of 10–15 %. There is an abrupt transition at the onset of the Eemian at 857cm with arboreal pollen percentages rising to 90% of which *Corylus* comprises 70% and *Quercus* 15% of the abundance. At 851.5 cm *Corylus* and *Quercus* are replaced by *Abies* and *Carpinus*

that increase to values of 50 and 27 %. At 826 cm *Abies* declines to 5 % abundance and *Carpinus* disappeares from the record with *Pinus* abundances increasing to 70%. During Stadial A, at 814 cm there is an increase in NAP to 18 % coinciding with a decrease in *Pinus* from 70% in the Eemian to 36%. *Pinus* abundances decline further to 10 % in the Brörup interstadial coinciding with maximum abundances of *Betula* of 67%.

The pollen analysis indicates an unconformity at the transition from the Rissian glacial to the Eemian interstadial. There is well documented evidence from central European sites documenting past vegetation changes at the transition of the Rissian glacial to the Eemian interglacial. For example Kühl and Litt., (2003) display a correlation of six sites from France, the Netherlands, and Germany showing that the Eemian began with a pollen Zone dominated by *Betula* that is followed by pollen Zones characterised by *Pinus* then *Quercus* and *Corylus*. Continuous sampling at 1cm resolution of the Rissian / Eemian transition in the Fu15-2 core (851–857 cm) describes neither the *Betula* nor *Pinus* dominated zones, rather an immediate transition from NAP dominated Rissian sediments to a *Corylus* dominated Eemian. It remains possible that the results are caused by very low sedimentation rates and extreme post depositional sediment compaction, however this seems unlikely.

3.3. Correlations to earlier Füramoos records

The results of the LOI and pollen analyses allow correlation of the Fu15-2 core to the earlier total organic carbon and pollen records of Müller et al., (2003). The percentages of total organic carbon from Müller et al., (2003) are consistently lower than LOI as the latter measures total organic matter percentages. Two tie points were used to correlate the Fu15-2 core with the record of Müller et al., (2003) shown in Figure 2 (*1 and *4). Tie point *1 represents the beginning of the Brörup interglacial and is based on increasing LOI values following the low values during Stadial A. Tie point *4 uses palynostratigraphy to tie the transition of the *Corylus*-dominated to *Abies/Carpinus*-dominated pollen assemblages in the Fu15-2 core to the record of Müller et al., (2003). Tie points *2 and *3 are marked by LOI and total organic carbon decreases that are evident in both the Fu15-2 core and the core of Müller et al., (2003). *2 and *3 have not been used in correlation or dating, but support our alignment of the two records. The age estimates for tie points *1 (ca. 104.5 ka) and *4 (ca. 125 ka) in Müller et al., (2003) were used to create an age depth model. A linear interpolation was used between the points to derive age estimates for the interval from the mid Eemian to end of Stadial A. The Rissian sediments below the unconformity (857–897 cm) remain temporally less well constrained, although

their Rissian age is unequivocal (Müller et al, 2003). The ages of the sediments above tie point *1 (794–803 cm core depth) are also poorly constrained but unequivocally from the Brörup interstadial.

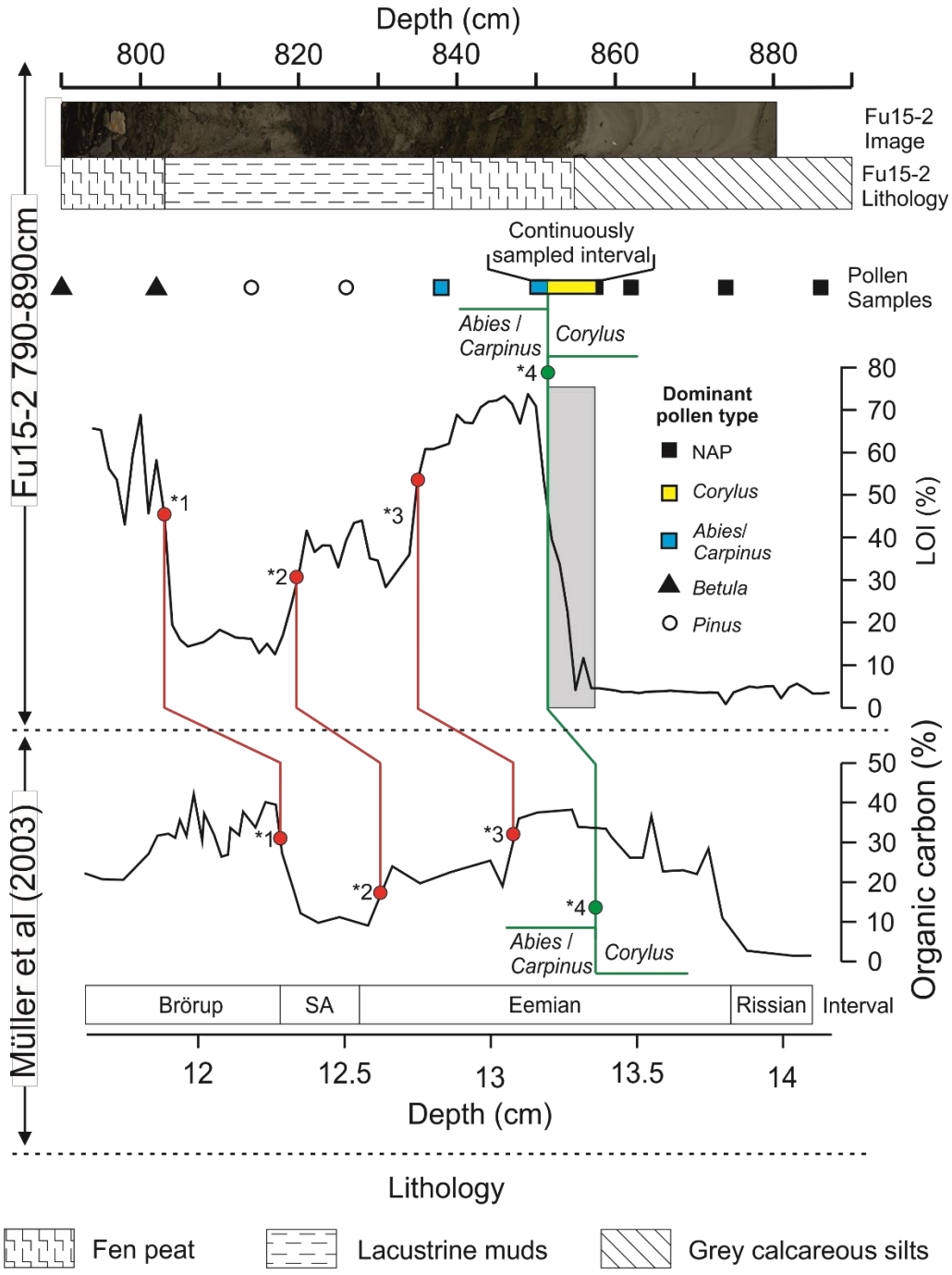

Figure 2: Correlations between the Fu15-2 core and the published data of Müller et al. (2003). The red lines labelled *1, *2 and *3 are correlations based on changes in the LOI (this study) and total organic carbon % (Müller et al, 2003). The green line labelled *4 is a correlation based on the palynostratigraphical transition from *Corylus*-dominated to *Abies*/*Carpinus*-dominated pollen assemblages. *1 and *4 indicate the positions of tie points used to anchor the Fu15-2 core within the chronology of Müller et al., (2003) as developed for a nearby core. The grey bar indicates the suggested unconformity (851–857 cm core depth) that cannot be reliably correlated with Müller et al., (2003). NAP: Non-Arboreal Pollen; SA: Stadial A. See Supplementary Figure 1 for a more detailed description of this core correlation.

3.4. The Füramoos chironomid record

Chironomid counts range from 26 to 193 head capsules per sample. Samples were aggregated based on chironomid head capsule counts; >30; >40 and >45 head capsules, 45 being the minimum number recommended for statistical analysis of fossil chironomid assemblages (Heiri and Lotter, 2001). This produced three records with a total of 92, 84 and 82 samples per record, respectively. These records were then used to perform temperature reconstructions for sensitivity testing, and the qualitative difference between the temperature reconstructions was minimal between reconstructions (Supplementary material 2). We therefore continued this study using a minimum head capsule count of 30 and a total of 92 chironomid samples for all further analysis and presentation. CONISS zonation of the chironomid record identified five statistically significant breaks in the chironomid assemblage, resulting in six chironomid Zones, i.e., Füramoos chironomid Zone (FCZ) 1 through 6.

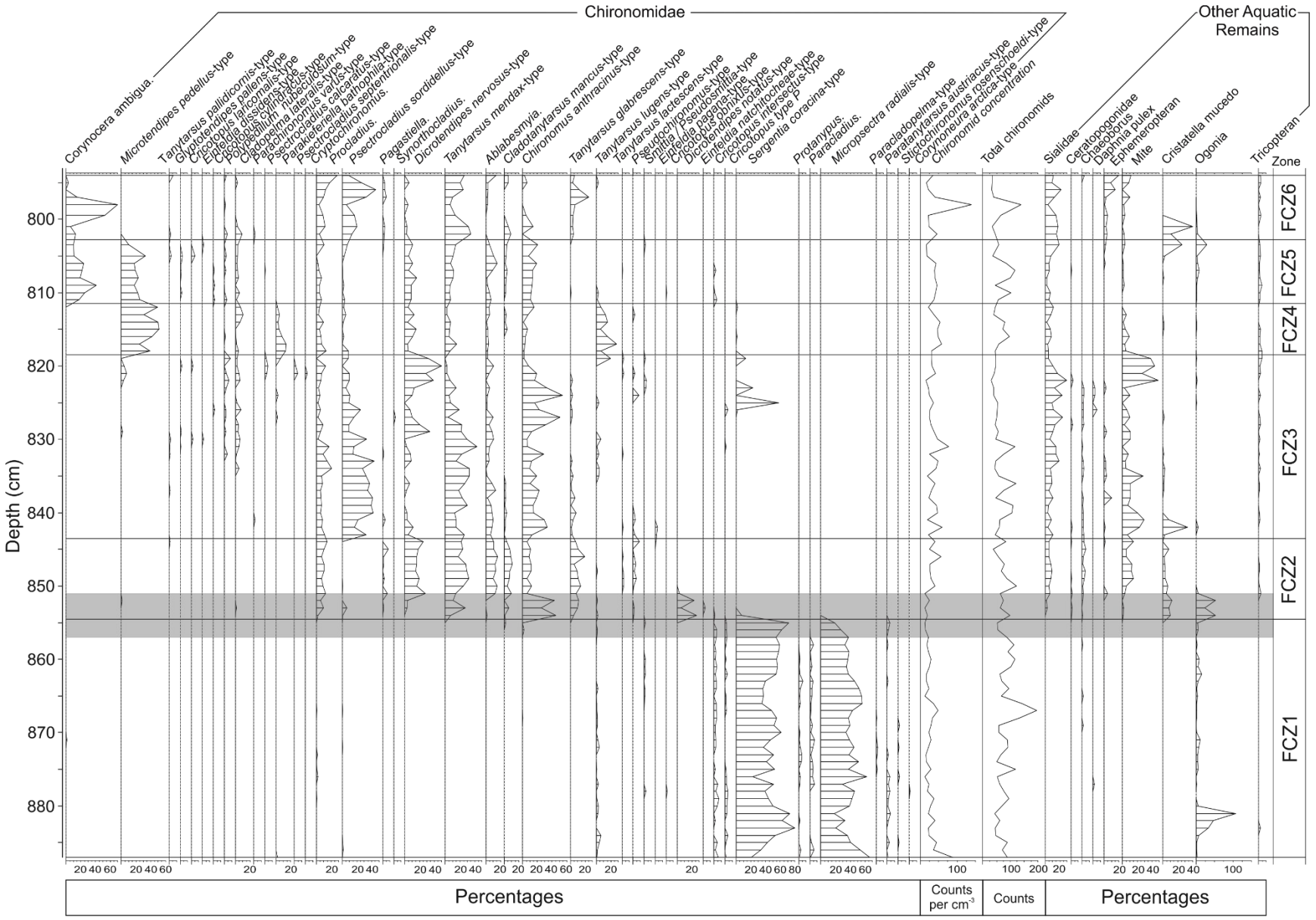
Chironomidae
Other Aquatic Remains
Corynocera ambigua.
Microtendipes pedellus-type
Tanytarsus pallidicornis-type
Glyptotendipes pallens-type
Cricotopus laricomalis-type
Einfeldia dissidens-type
Cricotopus cylindraceus-type
Polypedilum tuberculatum-type
Cladopelma lateralis-type
Parachironomus varus-type
Psectrocladius calcaratus-type
Parakiefferiella bathophila-type
Psectrocladius septentrionalis-type
Cryptochironomus.
Procladius.
Psectrocladius sordidellus-type
Pagastiella.
Synorthocladius.
Dicrotendipes nervosus-type
Tanytarsus mendax-type
Ablabesmyia.
Cladotanytarsus mancus-type
Chironomus anthracinus-type
Tanytarsus glabrescens-type
Tanytarsus lugens-type
Tanytarsus lactescens-type
Pseudochironomus-type
Smittia / Pseudosmittia
Einfeldia pagana-type
Cricotopus obnixus-type
Dicrotendipes notatus-type
Einfeldia natchitochee-type
Cricotopus intersectus-type
Sergentia coracina-type
Protanypus.
Paracladius.
Micropsectra radialis-type
Paracladopelma-type
Paratanytarsus austriacus-type
Stictochironomus rosenschoeldi-type
Corynoneura arctica-type
Chironomid concentration
Total chironomids
Sialidae
Ceratopogonidae
Chaoborus
Daphnia pulex
Ephemeropteran
Mite
Cristatella mucedo
Ogonia
Tricopteran
Zone
Depth (cm)
800
810
820
830
840
850
860
870
880
FCZ6
FCZ5
FCZ4
FCZ3
FCZ2
FCZ1
20 40 60
20 40 60
20
20
20
20 40
20 40
20 40
20
20
20 40 60
20
20
20
20 40 60 80
20 40 60
100
100
200
20
20
20 40
20 40
100
Percentages
Counts per cm-3
Counts
Percentages

Figure 3: Distribution of chironomids in the Fu15-2 790–890 cm core segment of the Füramoos record. Chironomid remains are displayed as percentages of total identified chironomids. Other aquatic remains are displayed as percentages of total chironomids including those that were not identified at higher taxonomic resolution. "Zone" represents the chironomid zones determined by CONISS zonation. Chironomid types are ordered according to abundance weighted average depth of occurrence, with types more abundant at the top of the core displayed on the left and those more abundant at the bottom displayed on the right. All identified chironomid taxa from the core segment are shown The unconformity is displayed as a grey horizontal bar between 851 and 857cm.

Zone FCZ1 (887–854.5 cm) is dominated by *Micropsectra radialis*-type and *Sergentia coracina*-type. Subdominant taxa include *Paracladius*, *Cricotopus* type P, *Cricotopus intersectus*-type, *Paratanytarsus austriacus*-type, *Tanytarsus lugens*-type and *Protanypus*. Zone FCZ2 (854.5–843.5 cm) begins with a drastic change in chironomid assemblages, *Micropsectra radialis*-type and *Sergentia coracina*-type disappear, and there is an increase in chironomid-type diversity. *Tanytarsus glabrescens*-type, *Tanytarsus mendax*-type and *Procladius* dominate throughout the Zone, although there are distinct changes in chironomid types within it. *Chironomus anthracinus*-type and *Dicrotendipes notatus*-type dominate initially before being replaced by *Cladotantarsus mancus*-type, *Dicrotendipes nervosus*-type and *Ablabesmyia*. Within Zone FCZ3 (843.5–818.5 cm) *Dicrotendipes nervosus*-type is replaced by *Psectrocladius sordidellus*-type. *Cladotanytarsus mancus*-type and *Tanytarsus glabrescens*-type initially decrease in abundance at the onset of FCZ3, and disappear later in the Zone, while other taxa that were dominant in FCZ2 persist into FCZ3 and continue to dominate, including *T. mendax*-type, *C. anthracinus*-type*, Ablabesmyia* and *Procladius*. Zone FCZ4 (818.5–811.5 cm) begins with an increase in *Microtendipes pedellus*-type as well as *T. lugens*-type and *Parakieferiella*. The abundance of oribatid mites also decreases markedly from a maximum late in FCZ3. In Zone FCZ5 (811.5–802.5 cm), *T. lugens*-type and *P. bathophila*-type disappear and are replaced with *Corynocera ambigua*, while *M. pedellus*-type decreases in abundance. In Zone FCZ6 (802.5–794 cm), *M. pedellus*-type disappears, and there is a strong increase in *Procladius*, *Psectrocladius sordidellus*-type, and *T. mendax*-type. *T. glabrescens*-type also returns. There is a short, distinct increase in *C. ambigua* percentages within Zone FCZ6, with this type dominating the assemblages with abundances between 70 and 77 %.

3.5. Chironomid-inferred July air temperature and ordination results

Chironomid-inferred temperatures show very little change within Zone FCZ1 fluctuating around 8°C within a range of 7–9 °C (Figure 3). The onset of Zone FCZ-2 displays a marked and abrupt increase in temperature reaching 14°C and increasing to 15–16°C mid-way through the Zone. Later, within FCZ 3, there are distinct fluctuations in temperature but inferred temperatures display a general cooling trend across the Zone with peak temperatures of 14°C and minima of 12°C. After the final cooling in

FCZ 3, temperatures remain at ca. 12.5°C (range: 11–13 °C) within Zone FCZ 4 and 5. FCZ 6 is characterized by a temperature decrease to ca. 10.5°C and finally an increase to ca. 13 °C at the end of the Zone.

DCA Axis 1 and 2 explain 29.7 and 7.5 % of the variance in the chironomid record with axis lengths of 4.2 and 1.9 S.D., respectively. Neither Axis 1 nor 2 vary within FCZ1 but both change markedly at the interface between FCZ1 and 2, DCA axis 1 decreasing from 4 to 0 S.D. and Axis 2 increasing from 0.5 to 1.9 S.D. Axis 1 values remain low in FCZ2 and Axis 2 values decrease slightly after the initial peak. Axis 1 values exhibits signs of gradual increase beginning in FCZ3 culminating in a fluctuating interval resulting from the re-emergence of *Sergentia coracina*-type at the end the Zone, while axis 2 increases during the same interval. Axis 1 decreases into FCZ4, while Axis 2 remains low after the decrease at the end of FCZ3. DCA Axis 1 decreases throughout FCZ 5 and remains at ca. 0.2–0.4 S.D. Axis 2 values decrease from FCZ 4 into FCZ5 and generally increase in FCZ6.

Modern-analogue statistics suggest that no samples in the record have “no good” modern analogue and only some samples, mainly between 820–826 cm and 798–808 cm have “no close” modern analogue (Figure 4). Most samples also have a good fit with temperature (Figure 4) although the interval 796–798 cm is a notable exception with a “very poor” fit with temperature. Taxa that were rare in the training set never exceed 3.5 %, and only two samples contain types (*Psectrocladius calcaratus*-type) not included in the training set reaching a maximum of 4.8 %.

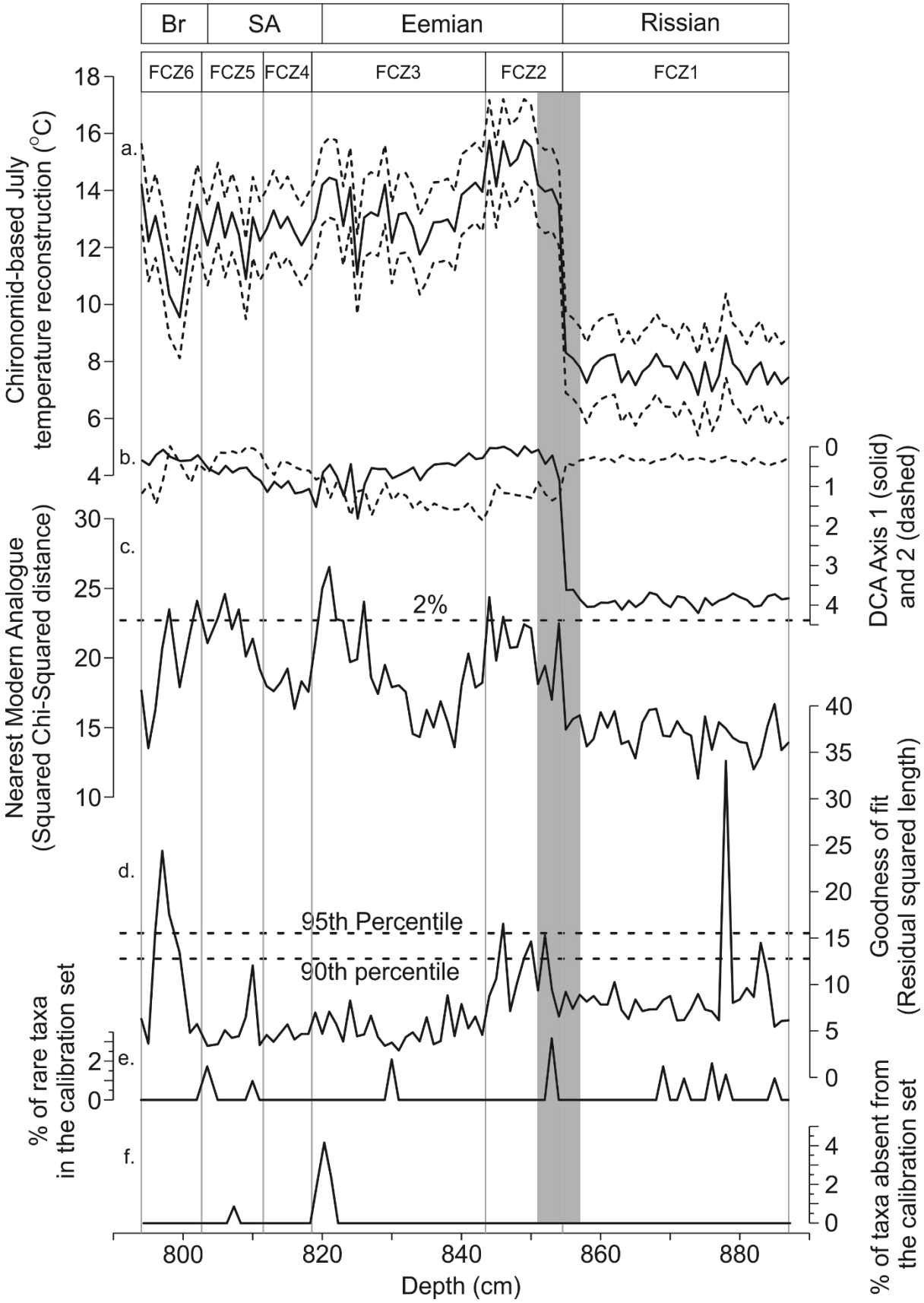
Br
SA
Eemian
Rissian
FCZ6
FCZ5
FCZ4
FCZ3
FCZ2
FCZ1
a.
b.
c.
d.
e.
f.
Chironomid-based July temperature reconstruction (°C)
DCA Axis 1 (solid) and 2 (dashed)
Nearest Modern Analogue (Squared Chi-Squared distance)
2%
95th Percentile
90th percentile
Goodness of fit (Residual squared length)
% of rare taxa in the calibration set
% of taxa absent from the calibration set
Depth (cm)

Figure 4: Chironomid-inferred July air temperatures, ordination results and reconstruction diagnostic statistics based on the Fu15-2 chironomid record. a. Chironomid-inferred July air temperatures (solid line) three sample running mean (red line) and associated error estimates (dashed lines); b. DCA Axis 1 (solid line) and Axis 2 (dashed line) on reversed axis; c. Distance to nearest modern analogue in the calibration dataset (squared chi squared distance). The threshold for identifying no close (2 %) analogue is indicated by the dashed horizontal lines following Tóth et al., (2015) whereas all distances are below the threshold for identifying samples with good analogue situations (28.6); d. goodness of fit statistics with thresholds for "poor fit" or "very poor fit" identified as the 90^{th} and 95^{th} percentiles respectively (dashed lines); e. percentage of fossil taxa that are rare in the Swiss/Norwegian training set and f. percentage of fossil that are absent from the Swiss-Norwegian training set. The grey bar represents the proposed unconformity in the record.

4. Discussion

4.1. Processing and analysis of strongly compacted samples

Fu15-2 core sections 854–818 cm and 803–794 cm consist of strongly compacted sediment with moderate to high organic-matter contents, and extracting chironomid head capsules from them was challenging and very time consuming. The sediments in these sections were very hard, appearing homogenous in the section 854–818 cm, and having a hard structure consisting of platelets of organic matter that were remarkably resistant to bending or breaking in section 803–794 cm. A month of submersion in 4°C water yielded no changes to the consistency of sediments from either section. Breaking the samples into smaller pieces and then immersing them in 10 % KOH at 85°C for 15 minutes (Brooks et al, 2007) loosened the sediment matrix and allowed the material to be more readily separated. Immersing a single large sediment sample , >ca. 2 cm^3, into the 10 % KOH solution only softened the material on the exterior while the internal sediments were unaffected. Sieving the treated sediments removed very little material, only breaking the sediment into smaller pieces and expanding the sediment volume as it became less compact, similarly to what was observed by Behre et al., (2005) in a beetle assemblage reconstruction from peat sediments from Oerel, northern Germany. Most chironomid specimens in samples from sections 854–818 cm and 803–794 cm were trapped in organic material >200 µm in size and needed to be manually pulled out of the sediment matrix for mounting (examples in Figure 5). Many of the specimens from sections 854–818 cm and 803–794 cm were damaged as a result of sediment processing e.g., torn in two with parts critical for identification missing. No further or harsher pretreatments were used as these would likely have resulted in further damage to the remains

Within the sediment sections 854–818 cm and 803–794 cm, many Tanytarsini were missing antennal pedestals and mandibles as they were torn off during mounting. Both the antennal pedestals and mandibles are important identification features for the Tanytarsini, needed to achieve identification at a higher taxonomic resolution (Brooks et al, 2007). For sections 854–818 cm and 803–794 cm, three *Tanytarsus* types were identified that could not be reliably identified to type resolution without the antennal pedestals / mandibles: *Tanytarsus mendax*-type, *Tanytarsus pallidicornis*-type and *Tanytarsus lactescens*-type. In this study, for the entire core, *Tanytarsus mendax*-type were consistently in far higher abundance than both the *Tanytarsus pallidicornis*-type and *Tanytarsus lactescens*-type head capsules. Furthermore, identified *Tanytarsus mendax*-type specimens were present in every sample in the 854–818 cm and 803–794 cm intervals where *Tanytarsus pallidicornis*-type and *Tanytarsus lactescens*-type only occurred intermittently. Therefore, for further analysis all unidentified *Tanytarsus* were reclassified as *Tanytarsus mendax*-type in these sections. Tanytarsini that could not be clearly associated with Tanytarsus were not taken into account for further analysis.

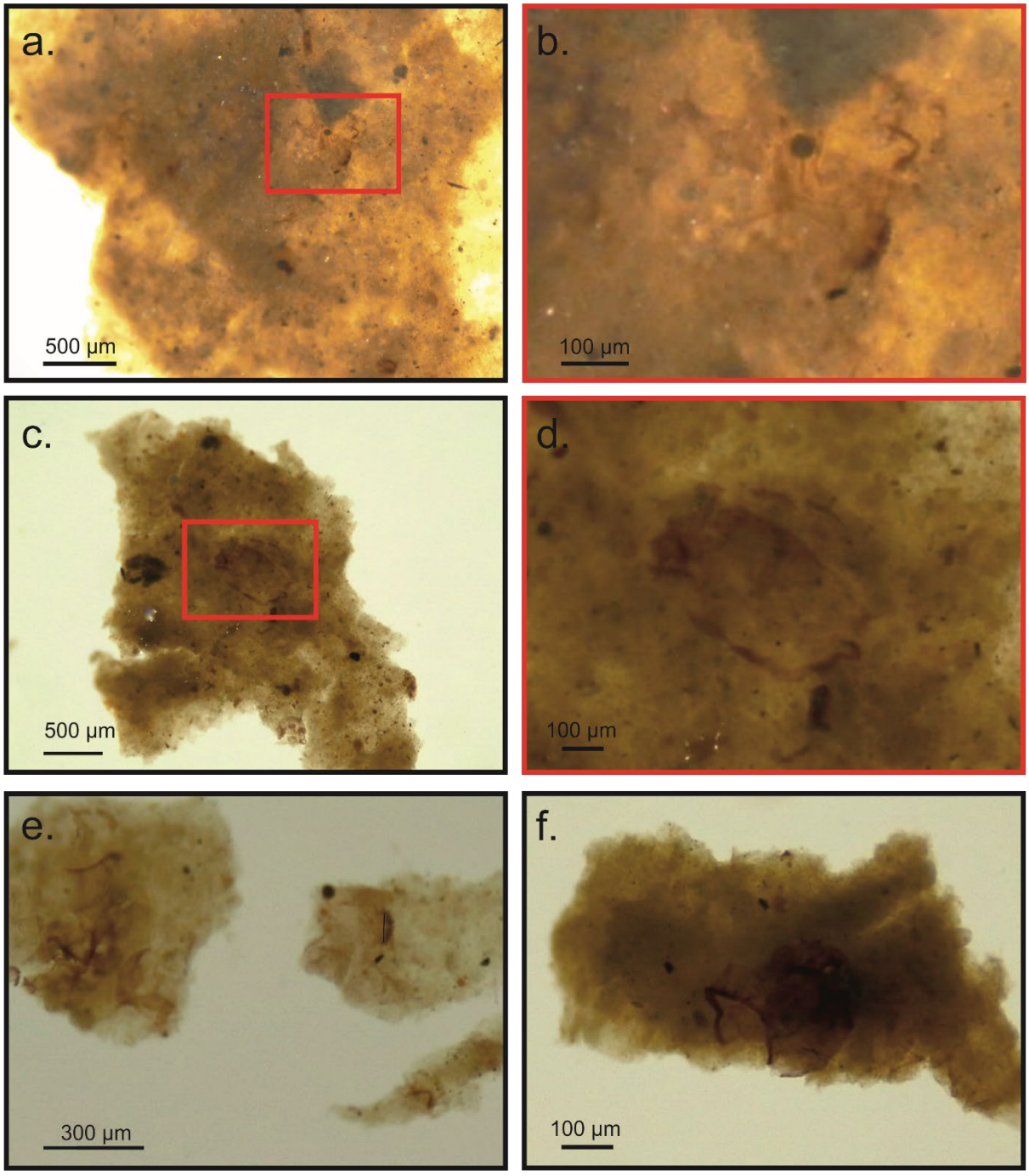

Figure 5: Examples of chironomids embedded in highly compacted fine organic material under stereomicroscope. a-b (796 cm core depth): overview (a) and detailed view (b) of a pair of chironomids trapped in a large piece of organic matter where (b) represents the area encompassed by the red box in (a); c-d (800cm core depth): overview (c) and detailed view (d) of a single chironomid trapped in a large piece of organic matter where (d) represents square area marked in c); e-f (core depths 796 cm and 795 cm respectively): Chironomids "extracted" from the compacted organic material and in need of cleaning. Note that the two chironomids on the right hand side of e. are the same specimens as displayed in a-b. All samples are from peaty sediments.

4.2. Ecological interpretation by assemblage Zone

Chironomid assemblages from Zone FCZ1 indicate prevailing cold temperatures. *Micropsectra radialis*-type and *Sergentia coracina*-type are typical for cold, oligotrophic lakes in subarctic to arctic and subalpine to alpine environments (Heiri et al, 2011). The dominance of *Micropsectra radialis*-type (Figure 2) also indicates highly oxygenated water (Brodersen et al, 2004) and an ultraoligo-/oligotrophic lake environment (Saether, 1979; Brodersen and Anderson, 2002; Brooks et al, 2007) with low productivity. Overall FCZ 1 is cold and oligotrophic.

Many of the taxa present within the first part of Zone FCZ2, such as *Dicrotendipes notatus*-type, *C. anthracinus*-type and *Procladius* have wide thermal tolerances (Brooks et al, 2007; Luoto et al, 2019). *Dicrotendipes notatus*-type, *Chironomus anthracinus*-type and *Tanytarsus glabrescens*-type are dominant at the beginning of FCZ2 suggesting relatively warm conditions (Brooks et al, 2007; Heiri et al, 2011) suggesting warm lake environment. At 851 cm core depth, *Dicrotendipes notatus*-type is replaced by *Dicrotendipes nervosus*-type and the abundance of *Chironomus anthracinus*-type is reduced, at the same time as oribatid mites increase in the record. These changes are associated with abundance increases of *Cladotanytarsus mancus*-type, *Tanytarsus mendax*-type and *Tanytarsus glabrescens*-type, all of which are typical for temperate to warm lakes (Brundin, 1949; Saether et al, 1979; Brodin et al, 1986; Brooks et al, 2007; Heiri et al, 2011). The presence of Sialidae throughout the Zone suggests the presence of a shallow water environment near the coring site (Lemdahl, 2000). Similarly, many of the chironomids in this Zone (e.g. *Dicrotendipes nervosus*-type and *Dicrotendipes notatus*-type) are typical for littoral to sublittoral habitats (Walker et al, 1991; Millet et al, 2007). Overall FCZ 2 is considered representative of a warm, productive lake.

The onset of Zone FCZ3 is defined by a pronounced increase of *Psectrocladius sordidellus*-type and associated decrease of *Dicrotendipes nervosus*-type. Both *Psectrocladius sordidellus*-type and *Dicrotendipes nervosus*-type are associated with littoral to sublittoral habitats in temperate lakes (Brooks et al, 2007; Nazarova et al, 2017) and can occur in lakes across a wide temperature range although the thermal optimum of *Psectrocladius sordidellus*-type is slightly lower than *Dicrotendipes nervosus*-type (Heiri et al, 2011). Less pronounced changes include the decrease and almost complete removal of *Tanytarsus glabrescens*-type and *Cladotanytarsus mancus*-type which supports a decrease in temperature as, while they are both able to occur in cool lakes, these taxa are generally considered to be thermophilic (Brundin 1949; Saether et al, 1979; Brodin et al, 1986; Brooks et al, 2007). In the upper section of FCZ3 there is an oscillation in the chironomid assemblage (between 818.5 and 829.5

cm) where *Tanytarsus mendax*-type and *Psectrocladius sordidellus*-type are replaced by *Dictotendipes nervosus*-type, then by *Chironomus anthracinus*-type and finally, *Sergentia coracina*-type followed by a reversal to *Chironomus anthracinus*-type and *Dicrotendipes nervosus*-type. In a shallow lake environment this change in chironomid assemblages suggests cooling to a temperature minimum at 810 cm with maximum abundances of *Sergentia coracina*-type, which has a preference for cold water (Brooks and Birks, 2000; Heiri and Lotter, 2010; Heiri et al, 2011) followed by a warming. Alternatively, this change could suggest a deepening of the lake reaching a maximum depth at 810 cm followed by a subsequent shallowing. This is because while *Sergentia coracina*-type is a cold stenotherm (Brooks et al, 2007), it is able to persist in temperate lakes in the cool waters beneath a thermocline where there is sufficient oxygen (Hofmann et al, 2001; Bolland et al, 2020). The lake level change scenario is supported by the increasing abundance of oribatid mites following the *Sergentia coracina*-type peak at 826 cm which can indicate shallow littoral environments (de la Riva-Caballero et al, 2010; Heggen et al, 2012). Overall, FCZ3 appears to represent a cooler and less productive lake than FCZ2 that culminates in either a temperature or lake level oscillation.

There is a pronounced change at the onset of Zone FCZ4 with *Microtendipes pedellus*-type replacing *Dicrotendipes nervosus-type*, as well an increase in *Tanytarsus lugens*-type and *Parakieferiella bathophila*-type. *Microtendipes pedellus*-type and *Tanytarsus lugens*-type are typical for cooler lakes (Heiri et al, 2011) with *Tanytarsus lugens*-type also indicating a well oxygenated and more oligotrophic system (Frey, 1988). The low organic matter content in FCZ4 (<20 %) supports the interpretation of a less productive environment and may have promoted the dominance of *Microtendipes pedellus*-type (McGarrigle, 1980; Millet et al, 2007), a taxon that has a preference for sediments with low organic content and a coarse grain size (McGarrigle, 1980). Overall FCZ4 indicates a cool and relatively unproductive lake.

In Zone FCZ5 there is an increase in *Corynocera ambigua* and *Chironomus anthracinus*-type and associated decline in *Microtendipes pedellus*-type and the disappearance of *Tanyatrsus lugens*-type. *Chironomus anthracinus*-type can occur over a broad temperature range of 8 to 16°C (Heiri et al, 2011) and the most telling indication of temperature change in FCZ5 is the disappearance of the cold stenotherm *Tanytarsus lugens*-type, which implies climatic warming relative to FCZ4 (Heiri et al, 2011). Overall the chironomid assemblage from FCZ5 indicates a cool lake with low productivity that may have been warmer than in FCZ4.

The onset of Zone FCZ6 is characterized by a disappearance of *Microtendipes pedellus*-type which, in this record, is restricted to sediments with low organic-matter contents. This may indicate that the decline was a response to increasing LOI associated with FCZ6 as *Microtendipes pedellus*-type has a preference for sediment with low organic content and coarse grain size (McGarrigle, 1980). The increase in LOI suggests a strong increase in productivity and the reoccurrence of *Tanytarsus glabrescens*-type, which reaches up to 25 % in FCZ6, supports an increase in temperatures as it is generally considered to be thermophilic (Brooks et al, 2007; Heiri et al, 2011). Furthermore it is likely that there was a large littoral to sublittoral area in the lake indicated by the high abundances of *Psectrocladius sordidellus*-type (Brooks et al, 2007; Nazarova et al, 2017). Overall, the chironomid assemblage indicates a response to increasing temperatures and increasing productivity in the lake.

4.3. Temperature reconstruction, local vegetation and organic-matter content

In the late Rissian glacial period (887–857 cm) the chironomid-based temperature reconstruction indicates mean July air temperatures of 7–9°C. The landscape around the lake was an open tundra environment as indicated both by the correlation of our record to the sediment core of Müller et al., (2003) and by the pollen samples available for this sediment section (Fig. 2). The lower July air temperature limit for tree growth is presently around 8.5–9.5°C in Central Europe (Landolt, 2003), and therefore the reconstructed temperatures agree with the persistence of open tundra. Similarly, the low organic-matter content of these sediments agrees with the interpretation of a lake situated in cold climate conditions with low in-lake productivity. The exact age of these late Rissian sediments is difficult to constrain based on the available stratigraphical data.

Following the abrupt increase in organic-matter content that suggests an unconformity, the high abundances of *Corylus* in the pollen assemblage identify the sediments from 851 to 835cm as being of mid Eemian origin, based on a comparison with Müller et al., (2003) who present a palynostratigraphical record from the same site. The inferred chironomid-based July air temperatures within this section decrease from 15–15.5 to 12–12.5°C and are associated with the presence of the thermophilic tree species *Corylus* and *Carpinus* which are a common feature of Eemian pollen records in central Europe, e.g., at La Grande Pile; (east France; Woillard, 1978; de Beaulieu and Reille, 1992), Les Echets (east France; de Beaulieu and Reille, 1984; Reille and de Beaulieu, 1990), Jammertal (south Germany; Müller, 2000; Müller et al, 2005) and Gröbern (northeast Germany, Litt, 1994). The productivity of the Füramoos palaeolake, as recorded in the Fu15-2 core, was likely highest in this interval as it is associated with maximum organic-matter contents of 75 %.

The pollen evidence from the Fu15-2 core documents the transition from the mid-Eemian into the late Eemian at 819 cm lasting until 835 cm. The mid to late Eemian transition, identified as the transition from an *Abie*s and *Carpinus* dominated pollen assemblage to a *Pinus* pollen dominated assemblage coincides with chironomid inferred July air temperature decreasing to 12°C (Figure 5). This evidence implies that decreasing July air temperatures may have contributed to the transition from *Abie*s and *Carpinus* forests to *Pinus* and *Picea* forests in the late Eemian, as *Pinus* and *Picea* are typical for cool temperate to boreal forests (Beck et al, 2016; Caudullo et al, 2016; Durrant et al, 2016). Furthermore organic matter content decreases from 60–75 % in the mid-Eemian to 28–45 % in the late Eemian (Figure 2) suggesting that the lake became less productive. Late Eemian temperatures vary between 12–14 °C, temperatures in which *Abie*s and *Carpinus* dominated pollen assemblages persisted in the mid Eemian, however neither the Fu15-2 pollen record or the Müller et al., (2003) Füramoos pollen record indicate subsequent increases in *Abie*s and *Carpinus* in the Late Eemian. Therefore it is possible that other environmental or climatic variables prevented the reestablishment of more thermophilic tree taxa during the late Eemian.

Stadial A occurs in the interval 802.5 and 819 cm in the Fu15-2 core and is associated with low organic matter content decreasing from ca. 40% in the late Eemian to <20 %. *Pinus* dominated forests open, indicated by an initial reduction in arboreal pollen to 90 % that declines further to 65 % in the later part of Stadial A (Müller et al, 2003; Figure 6). The onset of Stadial A is associated with a decrease in chironomid inferred July air temperature from 14 to 12.5 °C, suggesting that initial forest opening could have been driven in part by July air temperature. Chironomid inferred July air temperatures remain between 12 and 13.5 °C within Stadial A, with the exception of a single negative excursion to 11°C associated with >40 % *Corynocera ambigua* abundance. Temperatures in Stadial A are comparable those of the late Eemian and despite the overlapping temperature ranges, the vegetation assemblage as recorded in the Stadial A pollen percentages indicates forest opening as arboreal pollen falls to 65% and herbs such as *Artemisia* increase to 5% and Poaceae increase to 18% (Müller et al, 2003; Figure 6). This implies that while initial forest opening coincides with decreasing July air temperature, July air temperature does not appear to be the variable that prevented forest closing for the remaining Stadial A.

Sediment depths 794–803 cm were deposited during the Brörup interstadial and are categorised by an increase in organic-matter content from <20 % to a range of 45–70%. At the onset of the Brörup interstadial July air temperatures remain in the range of 12–14 °C, similar to the temperature range

described by the chironomid inferred temperature reconstruction for Stadial A. There is an initial increase of *Betula* pollen abundance at the onset of the Brörup to 58% followed by an increase in *Pinus* pollen to 70% indicating forest closing following Stadial A (Müller et al, 2003). As the reforestation during the Brörup is not associated with a July air temperature increase in our record it is likely at a climatic variable other than July air temperature was limiting afforestation during the Stadial A interval, and that variable was no longer limiting in the Brörup. There is a clear temperature decrease to 9.5–10 °C associated with sediment depths 797–799 cm in the Brörup sediments characterized by very high (>50 %) abundances of *Corynocera ambigua*. This taxon was originally described as an indicator of cold temperatures (Luoto, 2009) and has been shown to dominate in the cooler samples of the calibration dataset used in the transfer function (Heiri et al, 2011). However, it has also been reported in lakes with relatively warm temperatures including eutrophied lowland lakes in Denmark (Brodersen and Lindegaard, 1999) and warmer lakes in Russia (Nazarova et al, 2015), thus apparently having a wider thermal tolerance than originally thought (Brodersen and Lindegaard, 1999). Furthermore, the reconstruction diagnostic statistics (Figure 4) show that the 797–799 cm section has an exceptionally poor fit with temperature and thus the inference of cold temperatures in the (797–799 cm) interval should be treated with caution.

4.4. Comparison of summer temperature reconstructions from central Europe based on biotic-proxies

4.4.1. Rissian glaciation

Our new chironomid-based temperature reconstruction from Füramoos yields late Rissian July air temperatures of 7–9°C. These temperatures are consistent with the relatively narrow temperature range produced by beetle-based mean temperature of the warmest month reconstructions from La Grande Pile (8–12°C; Ponel, 1995). Zagwjin (1996) used 31 pollen records from across northwestern and central Europe to produce a pollen-based mean temperature of the warmest month estimate which suggests low temperatures of 10 °C prior to Eemian onset. Kühl and Litt, (2003) indicate warmer Rissian temperatures of 13 °C at Gröbern, Germany using pollen-based probable mean July temperatures, as do Müller et al., (2005) who estimate summer temperatures between 11–13.5°C from Jammertal, southern Germany. The pollen-based reconstructions of Klotz et al., (2003) from sites across eastern France, the Swiss plateau and Germany generally indicate higher Rissian temperature of the warmest month ranges between 10 and 22.5 °C with the exception of Beerenmösli, Switzerland, that has a Rissian temperature range of 5–17.5 °C. Furthermore the warmest temperature range presented by Klotz et al., (2003) for the late Rissian is from Füramoos, where a temperature range of

14–22.5 °C is presented in stark contrast to the 7–9°C resulting from new the chironomid-based reconstruction.

The discrepancy between some of the late Rissian temperature reconstructions (Table 1) could be a result of how the different biotic proxies, that are used to develop the summer temperature reconstructions, respond to climatic changes. Chironomid assemblages in shallow lakes are closely related to summer temperature (Eggermont and Heiri, 2012), but also protected from extreme winter temperature and precipitation changes so long as lake they are in does not completely freeze or dry out (Lotter et al, 2012; Samartin et al, 2017). In contrast the vegetation surrounding a lake is exposed to extreme winter temperatures and is more susceptible to changes in precipitation, and Cheddadi et al., (1998) have shown that pollen can be more reliable for reconstructing January temperatures and precipitation than for July air temperature. Discrepancies in the July air temperature estimations from parallel chironomid- and pollen-based reconstructions have been identified by Lotter et al., (2012) in a study from Gerzensee, Switzerland during the Würmian Lateglacial. The disparities between the reconstructions were attributed to vegetation assemblages responding more strongly to changes in seasonality and precipitation and chironomid assemblages responding more strongly to summer temperature change.

Discrepancies such as the difference between the new chironomid-based July air temperature reconstruction from Füramoos of 7–9 °C and the pollen-based temperature reconstruction of Klotz et al., (2003) of 14–22.5 °C, can also be evaluated by ecologically assessing the assemblages from which the reconstructions were developed. The chironomid assemblage in the Rissian Lateglacial was dominated by two chironomid types, *Micropsecrea radialis*-type and *Sergentia coracina*-type which, as discussed above in section 4.2., indicate a cold, oligotrophic lake, in line with the 7–9°C July temperature range produced by the transfer function in this study. In contrast the pollen assemblage used to produce the 14–22.5 °C mean temperature of the warmest month estimate for the Rissian Lateglacial (Klotz et al, 2003) was dominated by NAP with an abundance of 80 % in the pollen record that included an *Artemisia* abundance of 11 % and Poaceae abundance of 32 %, indicative of a cold steppic tundra. This example highlights the necessity of comparing a temperature reconstruction, or any other quantitative biotic proxy-based reconstruction, against the assemblage from which it was developed, and determining if it makes sense ecologically.

4.4.2 Mid and late Eemian

Summer temperature reconstructions for the mid Eemian from central Europe are very similar despite the different biotic-proxies used in analysis. The chironomid record from Füramoos yields a July air temperature range of 12–16°C for the mid-Eemian (ca. 118–125 ka; Figure 5). This temperature range is similar to the lower range of the estimates for mean temperature of the warmest month using beetle assemblages for La Grande Pile of 13–26°C (Ponel, 1995; Table 1) as well as pollen-based temperature reconstructions that produce temperature estimates from across central Europe indicating a summer temperature range of 14 to 19.5°C (e.g. Kühl and Litt, 2003; Kühl et al, 2007; Table 1). Summer temperature reconstructions for the late Eemian are also similar for central European records produced with biotic-proxies. The new chironomid-based July air temperature reconstructions from Füramoos indicate a temperature range of 12–14 °C for the late Eemian that is in good agreement with the lower range of summer temperature estimates for both beetle-based reconstructions that range from 11–25°C (e.g. Ponel, 1995) and pollen-based temperature reconstructions that range from 10–21.5°C (e.g. Kühl and Litt, 2003; Klotz et al, 2004; Table 1).

In general the proxy-based summer temperature reconstructions presented in Table 1 describe a decrease in temperature from the mid Eemian to the late Eemian and Field et al., (1994) suggest a reduction in growing degree days (calculated relative to 5 °C) from the Eemian thermal optimum to the late Eemian in Bispingen (north Germany) based on pollen data. While overall there is a clear decrease in the lower range of summer temperature estimates in all proxies, many of the upper limits of estimation from the pollen-based summer temperature reconstructions remain relatively warm, indicating thermal conditions uncharacteristic for boreal conifer forests (Kühl and Litt, 2003; Klotz et al, 2004). Beetle-based temperature reconstructions produced with the Mutual Climatic Range method containing many eurythermic species produce very broad estimates of temperature also. Behre et al., (2005) use a calibration method that narrows the temperature range produced from beetle-based mutual climatic range reconstructions of mean temperature of the warmest month from 11–24°C to 16–19°C from Oerel, north Germany, for the Late Eemian (Table 1) but regard the calibrated temperatures as being “rather high”. Nevertheless, many of the estimated summer temperature ranges presented in Table 1 show an overlap with the chironomid-based temperatures, even more so when the error of the chironomid-based temperature reconstruction (± 1.3–1.4 °C) is taken into account.

4.4.3. Stadial A

The chironomid-based July air temperature reconstruction for Füramoos during Stadial A (804.5–111 ka) of 12–13 °C are similar to the reconstructed late Eemian temperatures of 12–14 °C. These results are comparable with the beetle based reconstruction of Walkling and Coope, (1996) who indicate a calibrated temperature range of 8.5–15 °C for the Herning stadial (correlated to Stadial A). Overall the summer temperature ranges produced by the pollen-based reconstructions remain rather broad displaying temperatures of 10–21.5 °C, the lower limits of which are in good agreement with the 12–13 °C chironomid-based July air temperature reconstruction while the upper ranges of the pollen based summer temperature reconstructions are rather high.

4.4.3 Brörup

The Füramoos chironomid record describes a temperature range of 9.5–14 °C for the Brörup interval however the cooling at 797–799 cm is not currently considered representative (see Section 4.3.; Figure 4) and without those two samples the temperature range is 12–14 °C. Comparisons in for the Brörup interstadial should be treated with some caution as the new chironomid record does not cover the entire interval and neither do all of the pollen-based temperature reconstructions (e.g. Müller et al, 2005). However, chironomid-based July air temperature reconstruction ranges produced are within the estimated summer temperature ranges of both the beetle- and pollen-based summer temperature reconstructions (Table 1).

Table 1: Summer temperature reconstructions from central Europe for the Rissian glacial, mid Eemian, late Eemian, Stadial A and the Brörup based on biotic-proxies. July temp: July temperature; MTW: mean temperature of the warmest month; TMAX: mean temperature of the warmest month; TMAXcal calibrated mean values of the mean temperature of the warmest month; Summer temp: summer temperature. We do not compare early Eemian temperatures in this study.

Author	Proxy	Site	MIS Stage	MIS 5C	MIS 5d	MIS 5e	MIS 5e	MIS 5e	MIS 6
			Stage Name	Brörup	Stadial A	Late Eemian	Mid Eemian	Early Eemian	Rissian
This Study	Chironomids	Füramoos (Chironmids)	July temp	9.5 to 14	12 to 13	12 to 14	12 to 16	Unconformity	7 to 8.5
Ponel (1995)	Beetles	La Grande Pile	MTW	12 to 25		11 to 25	13 to 26		8 to 12
Behre et al (2005)	Beetles	Oerel	TMAX	9 to 26		11 to 24			
			TMAXcal	11 to 19		16 to 19			
Walkling and Coope (1996)	Beetles	Gröbern	TMAXcal	11.5 to 17	8.5 to 15	13.5 to 15			
Kühl and Litt (2003)	Pollen	La Grande Pile	July Temp			15 to 18	18 to 19.5		
		Bispingen	July Temp			14.5 to 17.5	16.5 to 17.5		
		Gröbern	July Temp			15	16.5 to 17		13
Klotz et al (2004)	Pollen	Jammertal	MTW	9.5 to 20.5	10 to 18.5	15.5 to 17.5	15.5 to 18.5		
		Les Echtes	MTW	13.5 to 20.5	13.5 to 20.5	14.5 to 17	16 to 18.5		
		Füramoos	MTW	11.5 to 19	11 to 16	10 to 17	16 to 17	Not Compared	
		Samerberg	MTW	10.5 to 19	11 to 21.5	10.5 to 21.5	16 to 19.5		
Kühl et al (2007)	Pollen	Gröbern	MTW	16.5 to 17.5	12.5 to 18	14.5 to 17.5	17 to 18		
Müller et al (2005)	Pollen	Jammertal	Summer temp	11.5 to 19.5	11.5 to 21	17 to 18	18.5		11 to 13.5
Klotz et al (2003)	Pollen	La Flachère	MTW	8 to 18	10 to 22	10 to 19	16.5 to 19		
		Lathuile	MTW	12 to 18	12 to 18	15 to 17	14 to 18.5		16 to 18.5
		Meikirch II	MTW			12 to 20	15.5 to 18		11.5 to 17.5
		Beerenmösli	MTW	12 to 17	10 to 18.5	10 to 18.5	14 to 18.5		5 to 17.5
		Jammertal	MTW	11 to 20	11 to 17.5	12 to 17	16 to 18		13 to 21.5
		Füramoos	MTW	11 to 19.5	11.5 to 15.5	13.5 to 17	15 to 19		14 to 22.5
		Eurach	MTW			13.5 to 18	15 to 18		10 to 19
		Samerberg	MTW	11.5 to 18	11 to 18.5	15 to 18.5	14 to 19		11 to 16.5
		Ziefen	MTW				15 to 18		11 to 20.5
Zagwijn (1996)	Pollen and Macrofossils	31 European sites	Summer temp			13.5	17		10

4.5. Synoptic temperature and climatic development for the Eemian, Stadial A and Brörup

Our new chironomid-based temperature reconstruction shows long term variations in reconstructed temperatures including the cold temperatures inferred for the late Rissian, relatively high temperatures reconstructed for the mid Eemain and lower temperatures inferred for the late Eemain and earliest Würmian sections of the record. This agrees with expected temperature changes for these time periods based on other palaeoclimatic evidence (e.g. Ponel, 1995; Kühl and Litt, 2003; Kühl et al, 2007). The most pronounced reconstructed temperature decrease within the Eemian in the chironomid inferred July air temperature reconstruction, from 16 to 12 °C, is at the transition from the mid to late Eemian and is associated with decreasing northern hemisphere summer insolation (Figure 6; Berger and Loutre, 1991). This suggests that decreasing July temperatures from the mid- to late Eemian may have been driven or reinforced by decreasing July insolation across this interval. Above we suggest that July air temperature change could influenced the vegetational transition from mid to late Eemian by driving the pollen assemblage from *Carpinus* and *Abies* dominance to *Pinus* and *Picea* dominance. Bolland et al., (2020; submitted) also show two examples of large chironomid inferred July air temperature changes in the last glacial interval from Burgäschisee, Swiss plateau and Füramoos, that associated both with changes in northern hemisphere July insolation (Berger and Loutre, 1991) and pollen evidence of major vegetation change. However, Brewer et al., (2008) indicate an increase in seasonality based on an analysis of 17 European terrestrial pollen records, including the one from Füramoos, and indicate that this increased seasonality was driven by decreases in mean temperature of the coldest month. The transition from *Carpinus* and *Abies* forests to *Pinus* and *Picea* forests at Füramoos could therefore have been influenced by decreasing July air temperatures , increasing seasonality or both.

Greenland stadial (GS) and interstadial (GIS) events are recognised as decadal- to centennial-scale shifts in δ18O in the Greenland ice core records covering the Würmian glaciation and the very youngest sections of the Eemian (Rasmussen et al, 2014), many of which are observed in speleothem records such as the NAPLS record from central Europe (Boch et al, 2011; Mosely et al, 2020). Several of these stages have been correlated to stadial and interstadial intervals from central European pollen records also (e.g. Dansgaard et al, 1993; Müller et al, 2003). There are possibly three GS stages that could coincide with decreases in chironomid-inferred temperature in the Fu15-2 core, GS 26, 25 and 24 (Figure 6). GS 26 has a similar age as the transition from the mid to late Eemian and the largest temperature decrease in the chironomid inferred July air temperature reconstruction from 16 to 12 °C (Discussed above). Although changes in the NAPLS speleothem record are very minor during GS26,

this event may possibly have reinforced the cooling trend during the mid Eemian recorded at Füramoos. GS 25 is recorded as a short-lived decrease in d18O in the NALPS speleothem record and may possibly be associated with a very minor reconstructed temperature decrease at the beginning of Stadial A from 14 to 12.5 °C, although temperatures in Stadial A are almost entirely within the reconstructed error margins of the late Eemian temperature reconstructions. Finally, earlier research has linked GS 24 to the Montaigu event (Woillard, 1978; Müller et al, 2003), a well-documented stadial interval in central European pollen records in the Brörup interstadial. The decrease observed in the chironomid-based July air temperature reconstruction between 797–799cm could possibly be representative of the Montaigu event however as discussed above in section 4.3., this decrease is considered uncertain and the Brörup section of the core remains temporally unconstrained.

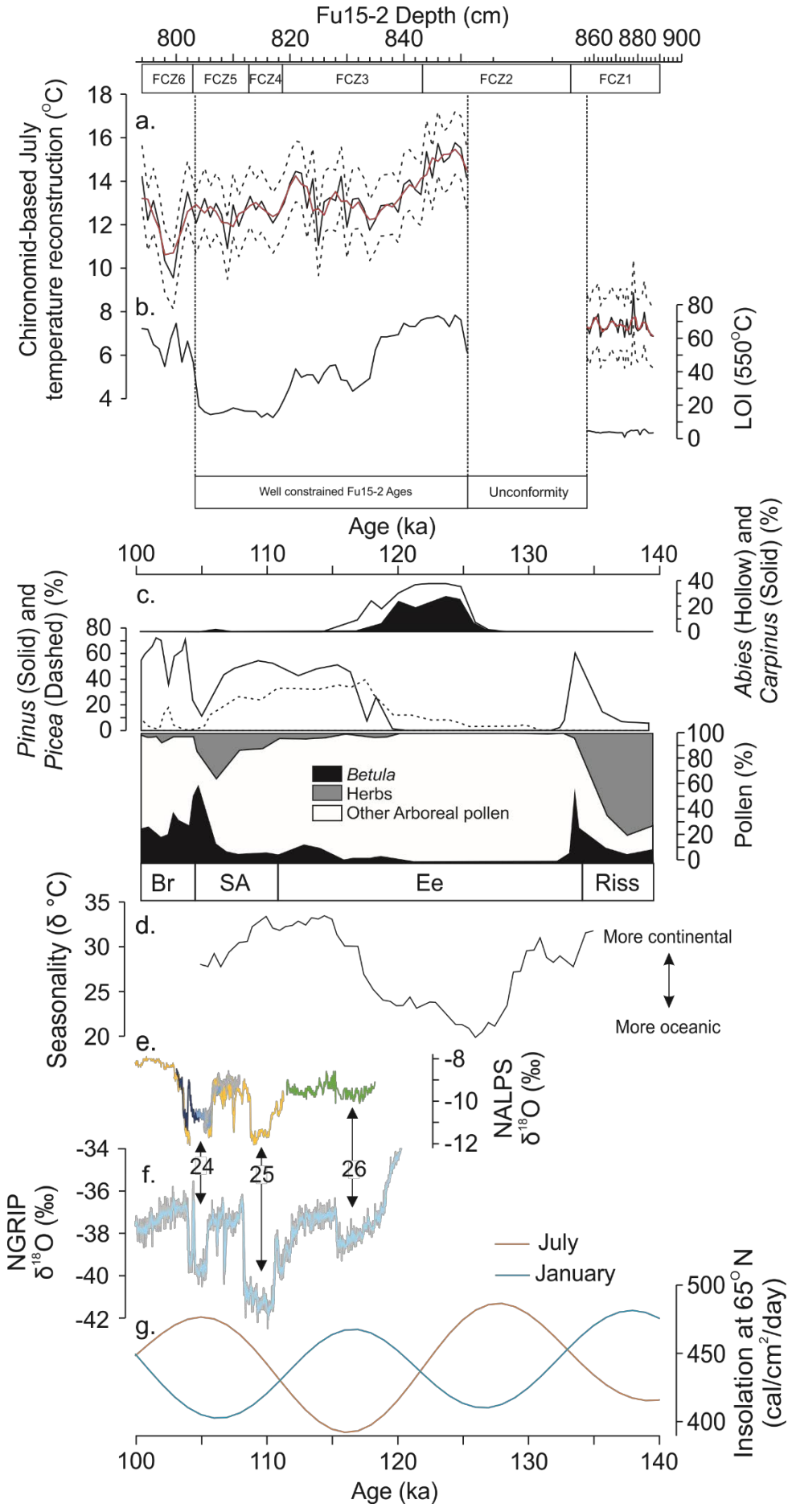
Fu15-2 Depth (cm)
800
820
840
860 880 900
FCZ6
FCZ5
FCZ4
FCZ3
FCZ2
FCZ1
Chironomid-based July temperature reconstruction (°C)
a.
b.
LOI (550°C)
Well constrained Fu15-2 Ages
Unconformity
Age (ka)
Pinus (Solid) and Picea (Dashed) (%)
c.
Abies (Hollow) and Carpinus (Solid) (%)
Betula
Herbs
Other Arboreal pollen
Pollen (%)
Br
SA
Ee
Riss
Seasonality (δ °C)
d.
More continental
More oceanic
e.
NALPS δ18O (‰)
f.
24
25
26
NGRIP δ18O (‰)
July
January
g.
Insolation at 65°N (cal/cm2/day)
Age (ka)

Figure 6: a. Chironomid-inferred July air temperature reconstruction for Füramoos (black line) and associated error estimates (dashed black line) and three sample running average (red line); b. LOI %; c. selected pollen data from the Füramoos pollen record (Müller et al, 2003). *Abies* and *Carpinus* as well as *Pinus* and *Picea* are superimposed, and the summary graph of *Betula*, herbs and other arboreal pollen is stacked; d. Seasonality reconstructed based on 17 European pollen records, higher values indicate more continental climate (Brewer et al, 2008); e. NALPS $\delta^{18}O$ record (Boch et al, 2011; Mosely et al, 2020); f. GRIP $\delta^{18}O$ record on NGRIP chronology (Johnsen et al, 1997; Rasmussen et al, 2014); and g. January and July insolation at 65^{O} (Berger and Loutre, 1991). Numbered arrows indicate GS stages in the NALPS and GRIP records.

5. Conclusions

We present a new chironomid-based July air temperature reconstruction from Füramoos, southern Germany, yielding temperature estimates from the Rissian Lateglacial, the Eemian interglacial, Stadial A, and the Brörup interstadial. Our chironomid-based reconstructions are augmented by palynological information from the same core. The Rissian part of the examined core is characterized by cold summer temperatures of 7–9°C associated with open tundras. Mid Eemian July air temperatures decrease from 16 to 12 °C at the transition to the Late Eemian which is reconstructed to have July air temperatures of 12–14 °C. July air temperatures were at 12–13 °C in Stadial A and remained at 12–14 °C in the Brörup interstadial.

In general, the summer temperature decrease associated with the transition from the mid-Eemian to the late Eemian is in agreement with previously available central European temperature reconstructions. However overall pollen-based reconstruction methods tend to infer higher temperatures than observed in the chironomid record. As discussed, offsets between chironomid-based and pollen based estimates may be to some extent due to a stronger influence of extreme winter temperatures and precipitation changes on vegetation than on chironomid assemblages. Previous studies have conducted parallel pollen-based and chironomid-based temperature reconstructions to assess how the different proxies reconstruct July air temperature (Lotter et al, 2012) and implementing a similar analysis of parallel samples from the Füramoos sediment core in future research would allow a similar comparison for the Eemian and Würmian intervals. Furthermore, proxy-based temperature reconstructions from the late Rissian glacial interval immediately prior to the Eemian interglacial are few and more are required to develop understanding how Eemian climate developed in central Europe.

In the new chironomid-based July air temperature reconstruction we observe the most pronounced decrease in July air temperature within the Eemian associated with decreasing July insolation and the

transition from a thermophilic mid-Eemian forest to a coniferous late Eemian forest at Füramoos. This is similar to previous studies in central Europe from the last glacial period that show large decreases in chironomid inferred July air temperature associated with changes in northern hemisphere July insolation (Bolland et al, 2020; submitted). The new chironomid-based temperature reconstruction provides valuable corroboration and new quantification of temperature development from the Rissian Lateglacial as well as the interval from the mid Eemian to the early Brörup interstadial in the alpine foreland of southern Germany

Acknowledgements

We thank all members of the field work team including Tobias Fischer, Ulrich Kotthoff and Bertil Mächtle who helped retrieving the Fu15-1 and 2 cores from Füramoos. We also thank Susanne Liner for technical support. The generosity and support of Franz Fischer (Füramoos) in providing access to the coring site is gratefully acknowledged. This research has been supported by the Swiss National Science Foundation (SNF grant 200021_165494).

Supplementary material

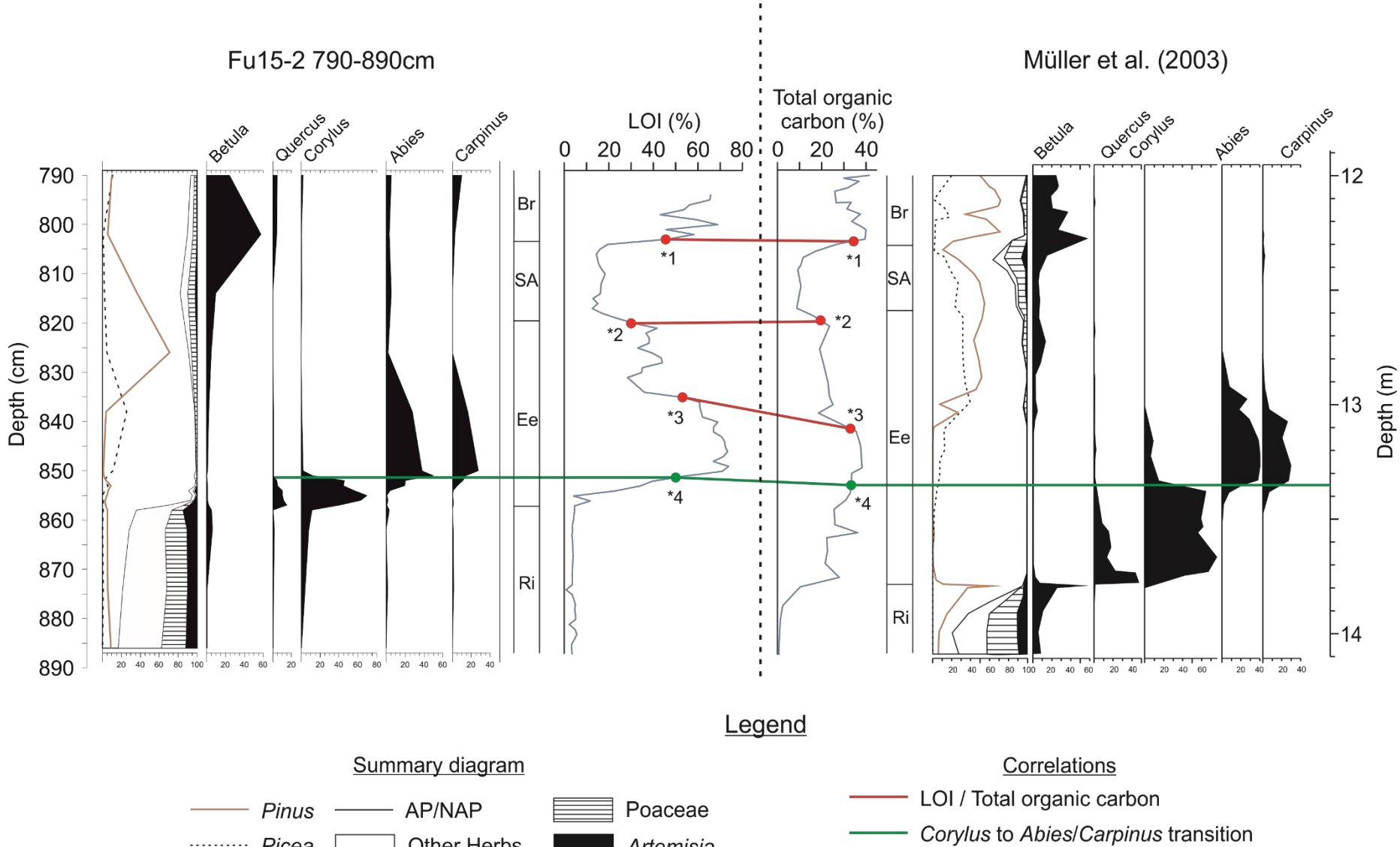
Fu15-2 790-890cm
Müller et al. (2003)
Depth (cm)
Depth (m)
Betula
Quercus
Corylus
Abies
Carpinus
LOI (%)
Total organic carbon (%)
Br
SA
Ee
Ri
*1
*2
*3
*4
Legend
Summary diagram
Pinus
Picea
AP/NAP
Other Herbs
Poaceae
Artemisia
Correlations
LOI / Total organic carbon
Corylus to Abies/Carpinus transition

Supplementary Figure 1: Füramoos site core correlations. *1 and *4 indicate tie points used to derive age estimates for the Fu15-2 core from the Müller et al. (2003) chronology.*1, *2 and*3 indicate correlation points between changes in LOI (%; this study) and organic matter (%; Müller et al, 2003) *4 indicates correlation point for the transition from *Corylus*-dominated to *Abies*/*Carpinus*-dominated pollen assemblages. Ri: Rissian; Ee: Eemian; SA: Stadial A and Br: Brörup.

To determine if it was possible to use a lower head capsule count in the chironomid-based transfer function (see Methods) the chironomid samples were aggregated to three resolutions, >30, >40 and >45 head capsules. The samples were not aggregated further as the minimum number of head capsules recommended is not 50, but recommendations range from 45 to 50 (see e.g., Heiri and Lotter, 2001; Larocque, 2001; Quinlan and Smol, 2001). The three resolutions of chironomid assemblage were used in separate reconstructions as a sensitivity analysis and are presented in Figure 3. There are only very minor differences in the reconstructions based on different resolutions and therefore the highest resolution including samples with head capsule abundances as low as 30 was used.

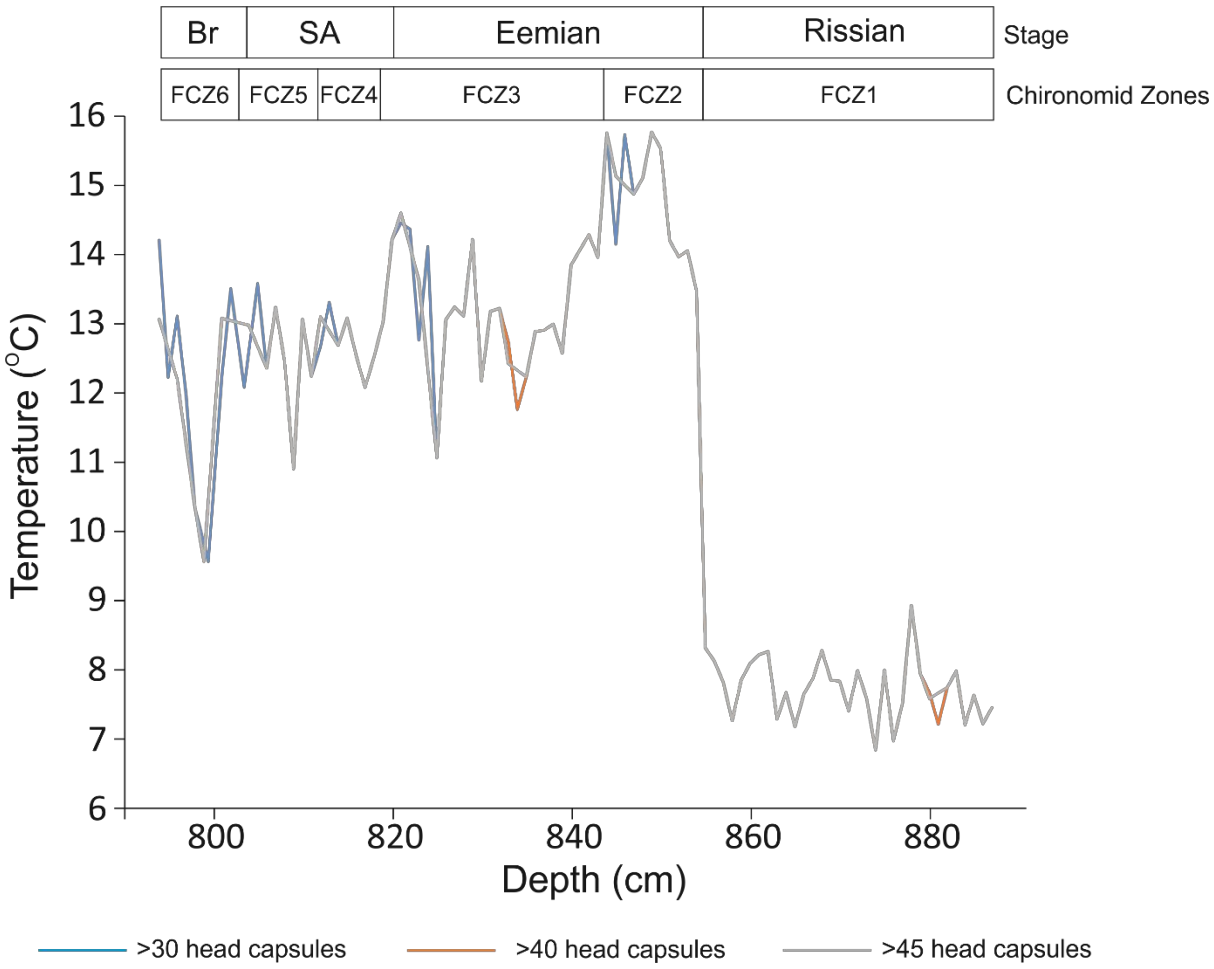

Supplementary Figure 2: Testing sensitivity of the reconstruction in relation to number of chironomid head counts using minimum head count criteria of >30, >40 and >45 head capsules per sample. SA: Stadial A; BR: Brörup.

References

Andersen, T., Cranston, P.S. and Epler, J.H. eds., 2013. Chironomidae of the Holarctic Region: Keys and Diagnoses: Larvae. Scandinavian Society of Entomology.

de Beaulieu, J.L. and Reille, M., 1984. A long upper Pleistocene pollen record from Les Echets, near Lyon, France. *Boreas*, 13(2), pp. 111-132.

de Beaulieu, J.L. and Reille, M., 1992. The last climatic cycle at La Grande Pile (Vosges, France) a new pollen profile. *Quaternary Science Reviews*, 11(4), pp. 431-438.

Beck. P., G. Caudullo, D. de Rigo, W. Tinner, *Betula pendula, Betula pubescens and other birches in Europe: distribution, habitat, usage and threats*. In J. San-Miguel-Ayanz, D. de Rigo, G. Caudullo, T. Houston Durrant, A. Mauri (Eds. 2016), European Atlas of Forest Tree Species. Publication Office of the European Union, pp. 70-73.

Becker, C., 2018. Vegetations-und Klimaentwicklung in Süddeutschland während des Letzten Interglazial-Komplexes anhand neuer Bohrkerne aus Füramoos (Oberschwaben), MSc Thesis, Heidelberg University, Heidelberg.

Behre, K.E., Hölzer, A. and Lemdahl, G., 2005. Botanical macro-remains and insects from the Eemian and Weichselian site of Oerel (northwest Germany) and their evidence for the history of climate. *Vegetation History and Archaeobotany*, 14(1), pp. 31-53.

Bennett, K.D., 1996. Determination of the number of zones in a biostratigraphical sequence. *New Phytologist*. 132(1), pp. 155-170.

Berger, A. and Loutre, M.F., 1991. Insolation values for the climate of the last 10 million years. *Quaternary Science Reviews*, 10(4), pp. 297-317.

Birks, H.J.B., Braak, C.T., Line, J.M., Juggins, S. and Stevenson, A.C., 1990. Diatoms and pH reconstruction. *Philosophical Transactions of The Royal Society B Biological Sciences*. 327(1240), pp. 263-278.

Boch, R., Cheng, H., Spötl, C., Edwards, R.L., Wang, X. and Häuselmann, P., 2011. NALPS: a precisely dated European climate record 120–60 ka. *Climate of the past*, 7, pp. 1247-1259.

Bolland, A., Rey, F., Gobet, E., Tinner, W. and Heiri, O., 2020. Summer temperature development 18,000–14,000 cal. BP recorded by a new chironomid record from Burgäschisee, Swiss Plateau. *Quaternary Science Reviews*, 243, 106484.

ter Braak, C.J. and Juggins, S., 1993. Weighted averaging partial least squares regression (WA-PLS): an improved method for reconstructing environmental variables from species assemblages. In Twelfth International Diatom Symposium (pp. 485-502). Springer, Dordrecht.

ter Braak, C.J.F., Juggins, S., Birks, H.J.B. and Van der Voet, H., 1993. Weighted averaging partial least squares regression (WA-PLS): definition and comparison with other methods for species-environment calibration. In Multivariate environmental statistics (No. 6, pp. 525-560). Elsevier.

ter Braak, J. F., and Smilauer, P., 2018. Canoco reference manuel and user's guide: Software for Ordination (version 5.10). Microcomputer Power (Ithaca, NY, USA), pp. 536.

Brewer, S., Guiot, J., Sánchez-Goñi, M.F. and Klotz, S., 2008. The climate in Europe during the Eemian: a multi-method approach using pollen data. *Quaternary Science Reviews*, 27(25-26), pp. 2303-2315.

Brodersen, K.P. and Anderson, N.J., 2002. Distribution of chironomids (Diptera) in low arctic West Greenland lakes: trophic conditions, temperature and environmental reconstruction. *Freshwater Biology*, 47(6), pp. 1137-1157.

Brodersen, K.P. and Lindegaard, C., 1999. Mass occurance and sporadic distribution of Corynocera ambigua Zetterstedt (Diptera, Chironomidae) in Danish lakes. Neo-and palaeolimnological records. *Journal of Paleolimnology*, 22(1), pp. 41-52.

Brodersen, K.P., Pedersen, O., Lindegaard, C. and Hamburger, K., 2004. Chironomids (Diptera) and oxy-regulatory capacity: an experimental approach to paleolimnological interpretation. *Limnology and Oceanography* 49(5), pp. 1549-1559.

Brodin, Y.W., 1986. The postglacial history of Lake Flarken, southern Sweden, interpreted from subfossil insect remains. *Internationale Revue der gesamten Hydrobiologie und Hydrographie*, 71(3), pp. 371-432.

Brooks, S.J., 2006. Fossil midges (Diptera: Chironomidae) as palaeoclimatic indicators for the Eurasian region. *Quaternary Science Reviews*, 25(15-16), pp. 1894-1910.

Brooks, S.J., Langdon, P.G. and Heiri, O., 2007. The identification and use of Palaearctic Chironomidae larvae in palaeoecology. Quaternary Research Association.

Brooks, S.J. and Birks, H.J.B., 2000. Chironomid-inferred late-glacial and early-Holocene mean July air temperatures for Kråkenes Lake, northwestern Norway. *Journal of Paleolimnology*, 23(1), pp. 77-89.

Brundin, L., 1949. Chironomiden und andere Bodentiere der südschwedischen Urgebirgseen. Ein Beitrag zur Kenntnis der bodenfaunistischen Charakterzüge schwedischer oligotropher Seen. *Report of the Insitute of Freshwater Research, Drottningholm*, *30*, pp. 1-914.

Busschers, F.S., Van Balen, R.T., Cohen, K.M., Kasse, C., Weerts, H.J., Wallinga, J. and Bunnik, F.P., 2008. Response of the Rhine–Meuse fluvial system to Saalian ice-sheet dynamics. *Boreas*, 37(3), pp. 377-398.

Caudullo, G., Tinner, W., & de Rigo, D., . Picea abies in Europe: distribution, habitat, usage and threats. European Atlas of Forest Tree Species. Publ. Off. EU, Luxembourg, San-Miguel-Ayanz, J., de Rigo, D., Caudullo, G., Houston Durrant, T., Mauri, A. (Eds. 2016)

Cheddadi, R., Mamakowa, K., Guiot, J., De Beaulieu, J.L., Reille, M., Andrieu, V., Granoszewski, W. and Peyron, O., 1998. Was the climate of the Eemian stable? A quantitative climate reconstruction from seven European pollen records. *Palaeogeography, Palaeoclimatology, Palaeoecology*, *143*(1-3), pp. 73-85.

Dansgaard, W., Johnsen, S.J., Clausen, H.B., Dahl-Jensen, D., Gundestrup, N.S., Hammer, C.U., Hvidberg, C.S., Steffensen, J.P., Sveinbjörnsdottir, A.E., Jouzel, J. and Bond, G., 1993. Evidence for general instability of past climate from a 250-kyr ice-core record. *Nature*, 364(6434), pp. 218-220.

Dutton, A., Carlson, A.E., Long, A., Milne, G.A., Clark, P.U., DeConto, R., Horton, B.P., Rahmstorf, S. and Raymo, M.E., 2015. Sea-level rise due to polar ice-sheet mass loss during past warm periods. *Science*, *349* (6244).

Durrant T. H., de Rigo D, Caudullo. G., 2016. Pinus sylvestris in Europe: Distribution, habitat, usage and threats. In: European Atlas of Forest Tree Species, Publication Office of the European Union, Luxembourg. Publ. Off. EU Luxembourg, pp. 132–133.

Eggermont, H. and Heiri, O., 2012. The chironomid-temperature relationship: expression in nature and palaeoenvironmental implications. *Biological Reviews*, 87(2), pp. 430-456.

Eisele, G., Haas, K., and Liner, S., 1994, Methode zur Aufbereitung fossilen Pollens aus minerogenen Sedimenten, in Frenzel, B., ed., Über Probleme der holozänen vegetationsgeschichte Osttibets, v. 95: Göttingen, Göttinger Geographische Abhandlungen, p. 165-166.

Engels, S., Bohncke, S.J.P., Bos, J.A.A., Brooks, S.J., Heiri, O. and Helmens, K.F., 2008. Chironomid-based palaeotemperature estimates for northeast Finland during Oxygen Isotope Stage 3. *Journal of Paleolimnology*, 40(1), pp. 49-61.

Engels, S., Helmens, K.F., Väliranta, M., Brooks, S.J. and Birks, H.J.B., 2010. Early Weichselian (MIS 5d and 5c) temperatures and environmental changes in northern Fennoscandia as recorded by chironomids and macroremains at Sokli, northeast Finland. *Boreas*, 39(4), pp. 689-704.

Engels, S., Self, A.E., Luoto, T.P., Brooks, S.J. and Helmens, K.F., 2014. A comparison of three Eurasian chironomid–climate calibration datasets on a W–E continentality gradient and the implications for quantitative temperature reconstructions. *Journal of Paleolimnology*, 51(4), pp. 529-547.

Field, M.H., Huntley, B. and Müller, H., 1994. Eemian climate fluctuations observed in a European pollen record. *Nature*, 371(6500), pp. 779-783.

Francis, D. R., 2001. Bryozoan statoblasts. In Smol, J. P., H. J. B. Birks & W. M. Last (eds) Tracking Environmental Change Using Lake Sediments Volume 4 Zoological Indicators. vol 4. Kluwer Academic Publishers, Dordrecht, pp. 105-123.

Frey, D.G., 1988. Littoral and offshore communities of diatoms, cladocerans and dipterous larvae, and their interpretation in paleolimnology. *Journal of Paleolimnology*, 1(3), pp. 179-191.

Grimm, E, C., 1987. CONISS: A Fortran 77 program for stratigraphically constrained cluster analysis by the method of incremental sum of squares. *Computers & Geosciences*, 13(1), pp. 13-35.

Grüger, E., 1979. Spätriss, Riss/Würm und Frühwürm am Samerberg in Oberbayern—ein vegetationsgeschichtlicher Beitrag zur Gliederung des Jungpleistozäns. *Geologica Bavarica*, 80, pp. 5-64.

Haas, J.N., 1994. First identification key for charophyte oospores from central Europe. European *Journal of Phycology*, 29(4), pp. 227-235.

Heiri, O., Lotter, A.F. and Lemcke, G., 2001. Loss on ignition as a method for estimating organic and carbonate content in sediments: reproducibility and comparability of results. *Journal of Paleolimnology*, 25(1), pp. 101-110.

Heiri, O. and Lotter, A.F., 2001. Effect of low count sums on quantitative environmental reconstructions: an example using subfossil chironomids. *Journal of Paleolimnology*, 26(3), pp. 343-350.

Heiri, O., Birks, H.J.B., Brooks, S.J., Velle, G. and Willassen, E., 2003. Effects of within-lake variability of fossil assemblages on quantitative chironomid-inferred temperature reconstruction. *Palaeogeography, Palaeoclimatology, Palaeoecology,* 199(1-2), pp. 95-106.

Heiri, O. and Lotter, A.F., 2010. How does taxonomic resolution affect chironomid-based temperature reconstruction?. *Journal of Paleolimnology*,. 44(2), pp. 589-601.

Heiri, O., Brooks, S.J., Birks, H.J.B. and Lotter, A.F., 2011. A 274-lake calibration data-set and inference model for chironomid-based summer air temperature reconstruction in Europe. *Quaternary Science Reviews*, 30(23-24), pp. 3445-3456.

Heggen, M.P., Birks, H.H., Heiri, O., Grytnes, J.A. and Birks, H.J.B., 2012. Are fossil assemblages in a single sediment core from a small lake representative of total deposition of mite, chironomid, and plant macrofossil remains?. *Journal of Paleolimnology*, 48(4), pp. 669-691.

Hofmann, W., 2001. Late-Glacial/Holocene succession of the chironomid and cladoceran fauna of the Soppensee (Central Switzerland). *Journal of Paleolimnology*, 25(4), pp. 411-420.

Ilyashuk, E.A., Ilyashuk, B.P., Heiri, O. and Spötl, C., 2020. Summer temperatures and lake development during the MIS 5a interstadial: New data from the Unterangerberg palaeolake in the Eastern Alps, Austria. *Palaeogeography, Palaeoclimatology, Palaeoecology,* 560, 110020.

Johnsen, S.J., Clausen, H.B., Dansgaard, W., Gundestrup, N.S., Hammer, C.U., Andersen, U., Andersen, K.K., Hvidberg, C.S., Dahl-Jensen, D., Steffensen, J.P. and Shoji, H., 1997. The δ18O record along the Greenland Ice Core Project deep ice core and the problem of possible Eemian climatic instability. *Journal of Geophysical Research: Oceans*, 102(C12), pp. 26397-26410.

Juggins, S., 2007. C2: Software for ecological and palaeoecological data analysis and visualisation (user guide version 1.5). Newcastle upon Tyne: Newcastle University, 77.

Juggins, S., 2017. rioja: Analysis of Quaternary Science Data, R package version (0.9-21). (http://cran.r-project.org/package=rioja).

Kern, O.A., Koutsodendris, A., Mächtle, B., Christanis, K., Schukraft, G., Scholz, C., Kotthoff, U. and Pross, J., 2019. XRF core scanning yields reliable semiquantitative data on the elemental composition of highly organic-rich sediments: Evidence from the Füramoos peat bog (Southern Germany). *Science of The Total Environment*, 697, 134110.

Klotz, S., Guiot, J. and Mosbrugger, V., 2003. Continental European Eemian and early Würmian climate evolution: comparing signals using different quantitative reconstruction approaches based on pollen. *Global and Planetary Change*, 36(4), pp. 277-294.

Klotz, S., Müller, U., Mosbrugger, V., de Beaulieu, J.L. and Reille, M., 2004. Eemian to early Würmian climate dynamics: history and pattern of changes in Central Europe. *Palaeogeography, Palaeoclimatology, Palaeoecology,* 211(1-2), pp. 107-126.

Kühl, N. and Litt, T., 2003. Quantitative time series reconstruction of Eemian temperature at three European sites using pollen data. *Vegetation History and Archaeobotany*, 12(4), pp. 205-214.

Kühl, N., Litt, T., Schölzel, C. and Hense, A., 2007. Eemian and Early Weichselian temperature and precipitation variability in northern Germany. *Quaternary Science Reviews*, 26(25-28), pp. 3311-3317.

Landolt E. 2003. Unsere Alpenflora. Stuttgart, Germany: Gustav Fischer.

Larocque, I., 2001. How many chironomid head capsules are enough? A statistical approach to determine sample size for palaeoclimatic reconstructions. *Palaeogeography, Palaeoclimatology, Palaeoecology*, 172(1-2), pp. 133-142.

Lemdahl, G., 2000. Lateglacial and Early Holocene insect assemblages from sites at different altitudes in the Swiss Alps—implications on climate and environment. *Palaeogeography, Palaeoclimatology, Palaeoecology*, 159(3-4), pp. 293-312.

Litt, T., 1994. Paläoökologie, Paläobotanik und Stratigraphie des Jungquartärs im nordmitteleuropäischen Tiefland. Dissertationes Botanicae 227, Cramer, Berlin, Stuttgart, 185pp.

Lotter, A.F., Heiri, O., Brooks, S., van Leeuwen, J.F., Eicher, U. and Ammann, B., 2012. Rapid summer temperature changes during Termination 1a: high-resolution multi-proxy climate reconstructions from Gerzensee (Switzerland). *Quaternary Science Reviews*, 36, pp. 103-113.

Lüthi, D., Le Floch, M., Bereiter, B., Blunier, T., Barnola, J.M., Siegenthaler, U., Raynaud, D., Jouzel, J., Fischer, H., Kawamura, K. and Stocker, T.F., 2008. High-resolution carbon dioxide concentration record 650,000–800,000 years before present. *Nature*, 453(7193), pp. 379-382.

Luoto, T.P., 2009. Subfossil Chironomidae (Insecta: Diptera) along a latitudinal gradient in Finland: development of a new temperature inference model. *Journal of Quaternary Science*, 24(2), pp. 150-158.

Luoto, T.P., Kotrys, B. and Płóciennik, M., 2019. East European chironomid-based calibration model for past summer temperature reconstructions. *Climate Research*, 77(1), pp. 63-76.

Masson-Delmotte, V., M. Schulz, A. Abe-Ouchi, J. Beer, A. Ganopolski, J.F. González Rouco, E. Jansen, K. Lambeck, J. Luterbacher, T. Naish, T. Osborn, B. Otto-Bliesner, T. Quinn, R. Ramesh, M. Rojas, X. Shao and A. Timmermann, 2013: Information from Paleoclimate Archives. In: Climate Change 2013: The Physical Science Basis. Contribution of Working Group I to the Fifth Assessment Report of the Intergovernmental Panel on Climate Change [Stocker, T.F., D. Qin, G.-K. Plattner, M. Tignor, S.K. Allen, J. Boschung, A. Nauels, Y. Xia, V. Bex and P.M. Midgley (eds.)]. Cambridge University Press, Cambridge, United Kingdom and New York, NY, USA.

McGarrigle, M.L., 1980. The distribution of chironomid communities and controlling sediment parameters in L. Derravaragh, Ireland. In Chironomidae (pp. 275-282). Pergamon.

Millet, L., Vannière, B., Verneaux, V., Magny, M., Disnar, J.R., Laggoun-Défarge, F., Walter-Simonnet, A.V., Bossuet, G., Ortu, E. and de Beaulieu, J.L., 2007. Response of littoral chironomid communities and organic matter to late glacial lake—level, vegetation and climate changes at Lago dell'Accesa (Tuscany, Italy). *Journal of Paleolimnology*, 38(4), pp. 525-539.

Moseley, G.E., Spötl, C., Brandstätter, S., Erhardt, T., Luetscher, M. and Edwards, R.L., 2020. NALPS19: sub-orbital-scale climate variability recorded in northern Alpine speleothems during the last glacial period. *Climate of the Past*, 16(1), pp. 29-50.

Müller, U.C., 2000. A Late-Pleistocene pollen sequence from the Jammertal, south-western Germany with particular reference to location and altitude as factors determining Eemian forest composition. *Vegetation History and Archaeobotany*, 9(2), pp. 125-131.

Müller, U.C., Pross, J. and Bibus, E., 2003. Vegetation response to rapid climate change in Central Europe during the past 140,000 yr based on evidence from the Füramoos pollen record. *Quaternary Research*, 59(2), pp. 235-245.

Müller, U.C., Klotz, S., Geyh, M.A., Pross, J. and Bond, G.C., 2005. Cyclic climate fluctuations during the last interglacial in central Europe. *Geology*, *33*(6), pp. 449-452.

Nazarova, L., Self, A.E., Brooks, S.J., van Hardenbroek, M., Herzschuh, U. and Diekmann, B., 2015. Northern Russian chironomid-based modern summer temperature data set and inference models. *Global and Planetary Change*, 134, pp. 10-25.

Nazarova, L., Bleibtreu, A., Hoff, U., Dirksen, V. and Diekmann, B., 2017. Changes in temperature and water depth of a small mountain lake during the past 3000 years in Central Kamchatka reflected by a chironomid record. *Quaternary International*, 447, pp. 46-58.

Oksanen, J.,Guillaume Blanchet, F., Friendly, M., Kindt, R., Legendre, P., McGlinn, D., Minchin, P.R., O'Hara, R. B., Simpson, G, L., Solymos, P., Henry, M., Stevens, H., Szoecs, E and Wagner. H., 2019. vegan: Community Ecology Package. R package version 2.5-5.

Otto-Bliesner, B.L., Rosenbloom, N., Stone, E.J., McKay, N.P., Lunt, D.J., Brady, E.C. and Overpeck, J.T., 2013. How warm was the last interglacial? New model–data comparisons. *Philosophical Transactions of the Royal Society A: Mathematical, Physical and Engineering Sciences*, 371(2001), 20130097.

Plikk, A., Engels, S., Luoto, T.P., Nazarova, L., Salonen, J.S. and Helmens, K.F., 2019. Chironomid-based temperature reconstruction for the Eemian Interglacial (MIS 5e) at Sokli, northeast Finland. *Journal of Paleolimnology*, 61(3), pp. 355-371.

Ponel, P., 1995. Rissian, Eemian and Würmian Coleoptera assemblages from La Grande Pile (Vosges, France). *Palaeogeography, Palaeoclimatology, Palaeoecology*, 114(1), pp. 1-41.

Quinlan, R. and Smol, J.P., 2001. Setting minimum head capsule abundance and taxa deletion criteria in chironomid-based inference models*. Journal of Paleolimnology*, 26(3), pp. 327-342.

R Studio Team (2015). RStudio: Integrated Development for R. RStudio, Inc., Boston, MA URL http://www.rstudio.com/.

Rasmussen, S.O., Bigler, M., Blockley, S.P., Blunier, T., Buchardt, S.L., Clausen, H.B., Cvijanovic, I., Dahl-Jensen, D., Johnsen, S.J., Fischer, H. and Gkinis, V., 2014. A stratigraphic framework for abrupt climatic changes during the Last Glacial period based on three synchronized Greenland ice-core records: refining and extending the INTIMATE event stratigraphy. *Quaternary Science Reviews*, 106, pp. 14-28.

Reille, M. and De Beaulieu, J.L., 1990. Pollen analysis of a long upper Pleistocene continental sequence in a Velay maar (Massif Central, France). *Palaeogeography, Palaeoclimatology, Palaeoecology*, 80(1), pp. 35-48.

de la Riva-Caballero, A., Birks, H.J.B., Bjune, A.E., Birks, H.H. and Solhøy, T., 2010. Oribatid mite assemblages across the tree-line in western Norway and their representation in lake sediments. *Journal of Paleolimnology*, 44(1), pp. 361-374.

Saether, O.A., 1979. Chironomid communities as water quality indicators. *Ecography*, 2(2), pp. 65-74.

Samartin, S., Heiri, O., Joos, F., Renssen, H., Franke, J., Brönnimann, S. and Tinner, W., 2017. Warm Mediterranean mid-Holocene summers inferred from fossil midge assemblages. *Nature Geoscience*, 10(3), pp. 207-212.

Schilt, A., Baumgartner, M., Schwander, J., Buiron, D., Capron, E., Chappellaz, J., Loulergue, L., Schüpbach, S., Spahni, R., Fischer, H. and Stocker, T.F., 2010. Atmospheric nitrous oxide during the last 140,000 years. *Earth and Planetary Science Letters*, 300 (1-2), pp. 33-43.

Schreiner, A., 1981. Quartärgeologische Untersuchungen in der Umgebung von Interglazialvorkommen im östlichen Rheingletschergebiet (Baden-Württemberg).

Schreiner, A., 1996. Erläuterungen zu 8025 Bad Wurzach: Geologische Karte von BadenWürttemberg 1:25 000. 1st ed. Landesvermessungsamt Baden-Württemberg, Freiburg.

Schmid, P.E., 1993. A key to the larval Chironomidae and their instars from Austrian Danube region streams and rivers: with particular reference to a numerical taxonomic approach. 1. Diamesinae, Prodiamesinae and Orthocladiinae. Selbstverlag

Shackleton, N.J., Sánchez-Goñi, M.F., Pailler, D. and Lancelot, Y., 2003. Marine isotope substage 5e and the Eemian interglacial. *Global and Planetary change*, 36(3), pp. 151-155.

Šmilauer, P. and Lepš, J., 2014. Multivariate analysis of ecological data using CANOCO 5. Cambridge university press.

Solhøy, T., 2001. Oribatid mites. In Smol, J. P., H. J. B. Birks & W. M. Last (eds) Tracking Environmental Change Using Lake Sediments Volume 4 Zoological Indicators. vol 4. Kluwer Academic Publishers, Dordrecht, pp. 81-104.

Stockmarr, J.A., 1971. Tabletes with spores used in absolute pollen analysis. Pollen spores, 13, pp. 615-621.

Tóth, M., Magyari, E.K., Buczkó, K., Braun, M., Panagiotopoulos, K. and Heiri, O., 2015. Chironomid-inferred Holocene temperature changes in the South Carpathians (Romania). *Holocene*. 25(4), pp. 569-582.

Turner, C. and West, R.G., 1968. The subdivision and zonation of interglacial periods. *Eiszeitalter und Gegenwart,* 19(93), p .101.

Turney, C.S. and Jones, R.T., 2010. Does the Agulhas Current amplify global temperatures during super-interglacials?. *Journal of Quaternary Science*, 25(6), pp. 839-843.

Vandekerkhove, J., Declerck, S., Vanhove, M., Brendonck, L., Jeppesen, E., Conde Porcuna, J.M. and De Meester, L., 2004. Use of ephippial morphology to assess richness of anomopods: potentials and pitfalls. *Journal of Limnology*, 63(1s), pp. 75-84.

Walker, I.R., Smol, J.P., Engstrom, D.R. and Birks, H.J.B., 1991. An assessment of Chironomidae as quantitative indicators of past climatic change. *Canadian Journal of Fisheries and Aquatic Sciences*, 48(6), pp. 975-987.

Walkling, A.P. and Coope, G.R., 1996. Climatic reconstructions from the Eemian/Early Weichselian transition in Central Europe based on the coleopteran record from Gröbern, Germany. *Boreas*, 25(3), pp. 145-159.

Wiederholm. ed., 1983. Chironomidae of the Holarctic Region: Keys and Diagnoses: Larvae. Scandinavian Society of Entomology.

Winterholler, K., 2004. Zur jungpleistozänen Landschaftsentwicklung am Füramooser Ried (Oberschwaben). Beiträge zur Geomorphologie, Bodengeographie und Quartärforschung., D. Geographisches Inst. der Univ. Tübingen, pp. 155–180.

Woillard, G.M., 1978. Grande Pile peat bog: a continuous pollen record for the last 140,000 years. *Quaternary Research*, 9(1), pp. 1-21.

Zagwijn, W.H., 1996. An analysis of Eemian climate in western and central Europe. *Quaternary Science Reviews*, 15(5-6), pp. 451-469.

8. Conclusions

In introducing this thesis three overarching **Objectives** were identified. In regards to **Objective 1** the project was able to produce new chironomid records covering large sections of the last interglacial-glacial cycle. However, results from the Rissian Lateglacial to Early Eemian transition and the Early Eemian are missing the a result of a sedimentary unconformity, but for those sections that were present many intervals were resolved on a centennial-scale resolution exceeding the millennial scale specification identified in **Objective 1.** Furthermore, Paper II and Paper III in particular, document the extraction of chironomids from non-standard sediments that were difficult to process, providing a basis with which to advance the method. Papers I, II and III were then used to reconstruct environmental change within the respective lake systems fulfilling **Objective 2.** The assemblages primarily described changes in temperature, nutrient state and organic content, and to a lesser extent changes in lake level. Using the chironomid assemblage to qualitatively assess changes in the environment within Burgäschisee and Füramoos was an essential step towards developing a reconstruction of mean July air temperature, as outlined in **Objective 3.**

In completing **Objective 3**, there are two main results, the first of which is that major July air temperature change in Papers I, II and III was associated with changes in northern Hemisphere July insolation. Papers I, II and III indicate three intervals in which mean July air temperature changes were associated with changing July insolation and vegetational turnover. Paper 1 (Bolland et al, 2020) describes July air temperature increase during the early Lateglacial interval on the Swiss plateau and indicates that early afforestation was a result of increasing July air temperatures. Paper II indicates that the largest temperature decrease occurred in the study interval ca. 49-99 ka, during the Odderade interstadial which is associated broadly with the transition from MIS 5a to MIS 4. Paper III indicated that the largest temperature decrease in the study interval ca. 125-100 ka was associated with the transition from the mid Eemian, to the late Eemian. In contrast, the second main result having completed **Objective 3** was to examine where temperature did not indicate major decreases. The new records from Füramoos indicate that the forest opening associated with stadial intervals A and B do not appear to have been driven primarily by changes in July air temperature. Rather, the available evidence suggests that they were been driven by other climatic variables, suggested to have been changes in mean temperature of the coldest month and/ or changes in precipitation.

Future work from Füramoos should be targeted at completing the chironomid assemblage record by sampling the Rissian Latelglacial and early Eemian sediments to make a continuous record from the Rissian Lateglacial to Bellamont 1. How the chironomid assemblage and lake environment developed during this interval remains an open question, and having shown the power of chironomids and other aquatic invertebrate remains to describe changes in lake ecology in this thesis, the completion of the record is essential to this end. Furthermore, as the Early Eemian chironomid assemblage has not been reconstructed, quantitative estimates of mean July air temperatures in the Eemian thermal maximum at Füramoos also remain unconstructed. Mean July air temperature estimates from the Early Eemian are essential for understanding regional climate dynamics in a world estimated to be globally 1-2 °C warmer than pre-industrial, and therefore this work is of upmost importance. This will be facilitated by a second area of future work that is especially relevant for completing the chironomid record of Füramoos which is to develop a more effective and time efficient method for the extraction of chironomid head capsules from highly compacted organic matter. Developing such a method would also facilitate the development of chironomid records in other locations that have similar sedimentary deposits to those described herein.

9. Appendix

Correlations of Fu15-2 to the Füramoos composite core

This section describes the correlation of the Fu15-2 core to the Füramoos composite core based on the FU1/3 and FURA core segments originally conducted at Institute of Earth Science, Heidelberg University (Kern et al., unpublished) and adjusted here. Correlations are plotted in relation to LOI in Appendix Figure 1. This correlation was necessary for plotting the composite core summary pollen data versus the chironomid inferred temperatures produced in Paper III of this thesis (Figure 2). To do this four tie points (used in the correlation of the FU15-2 core to Müller et al., 2003 in Paper III) were used based on LOI and palynostratigraphy. The following depths refer to the positions of the tie points on the Fu15-2 core. These were: the transition from an a *Corylus* dominated forest to a *Abies*/*Carpinus* forest 851.5 cm, a first decrease in LOI from 60 to 30% at 834.5cm, a second LOI decrease from 40 to 10% associated with the onset of Stadial A at 820cm and an LOI increase from ca. 15 to 60 % at 803cm associated with the onset of the Brörup (Appendix Figure 1). The core section 855 to 887cm is correlated to the Late Rissian glacial.

Dating of the Füramoos composite core

In order to determine the ages of the Füramoos composite core (Manuscript II, Kern et al, in progress) it was correlated to the classical Füramoos paper of Müller et al., (2003) from the same site (Appendix Figure 2). Correlations were based on vegetation changes associated with the transitions between palynostratigraphical units. LOI measurements from the Composite core and Total Organic Carbon from Muller et al., (2003) supported the decision making process in the correlations. Müller et al., (2003) previously developed an age depth model for their Füramoos core based on its correlation to climate-proxy records from the North Atlantic (McManus et al., 1994) and Greenland oxygen isotope records (Dansgaard et al. 1993), placing the Füramoos chronology within the MIS stratigraphy (Martinson et al, 1987). Specifically they correlate ice rafting episodes C24, C21 and C20 to Stadial A, Stadial B and Stadial C respectively and the last major peak in *Artemisia* during the Rissian Lateglacial to Heinrich Event 11 (McManus et al, 1994). Two later dates from the Middle Würmian are based on AMS ^{14}C and then all the dated tie points were linearly interpolated to provide an age depth model displayed Figure 4 in Müller et al., (2003).

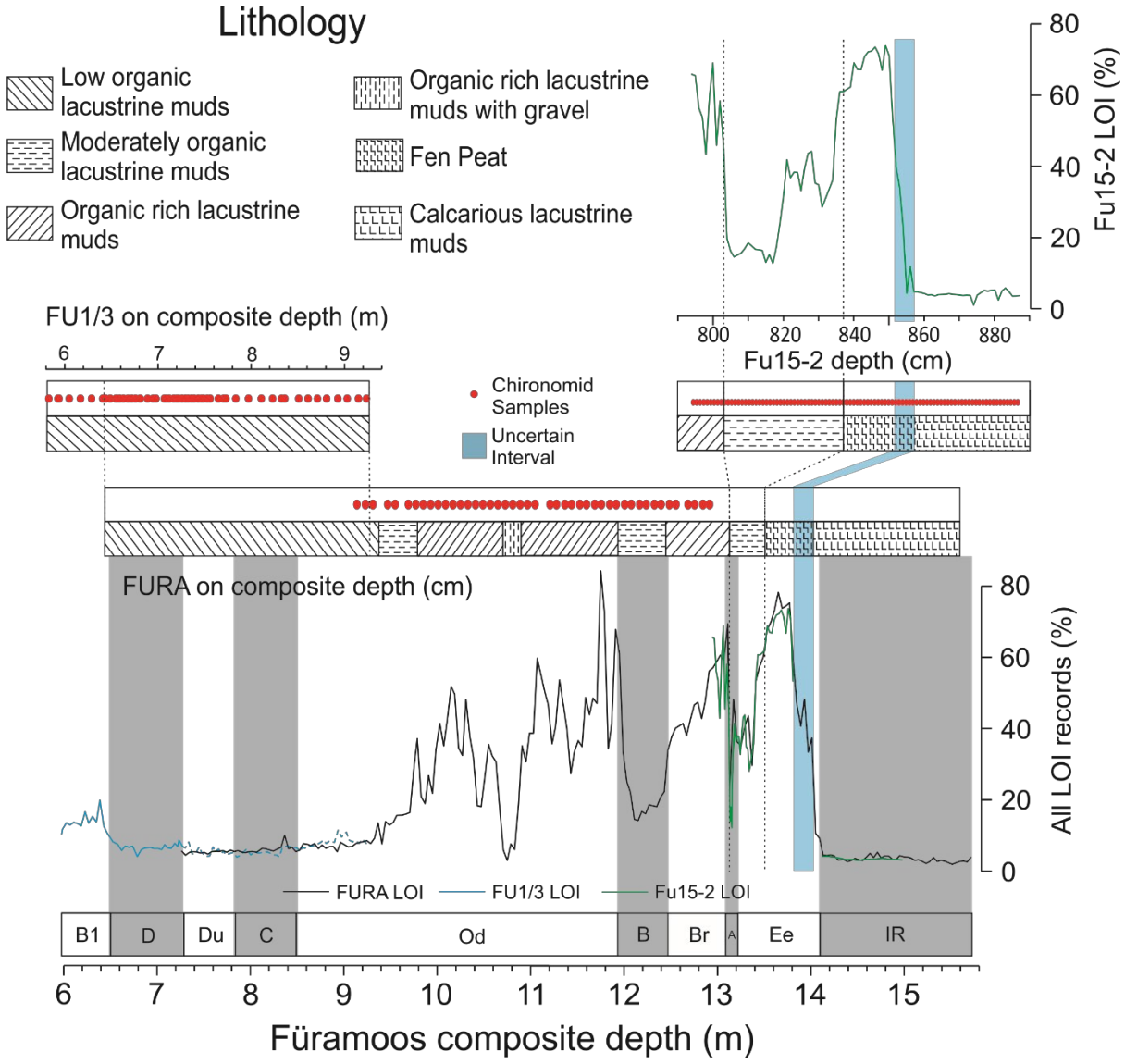

Appendix Figure 1: Correlation of the Fu15-2 core to the Füramoos composite sediment core (Manuscript II, Kern et al, 2019; in preparation) in relation to LOI (%). This correlation was based on four tie points described in text, *1, *2, *3 and *4 where *1 -*3 are based on changes in LOI (%) and *4 is based on the transition from a *Corylus* forest to an *Abies*/*Carpinus* forest. The stratigraphic position of FU 1/3 is also shown (Manuscript II; Kern et al, in preparation). Red circles indicate the chironomid samples that were taken and processed from the respective sediment cores to develop the Füramoos chironomid record. Time intervals represent: LR; Late Rissian glacial; Ee: Eemian interglacial; A: Stadial A; Br: Brörup; B: Stadial B; Od: Odderade; C: Stadial C; Du: Dürnten; D: Stadial D; B1: Bellamont 1.

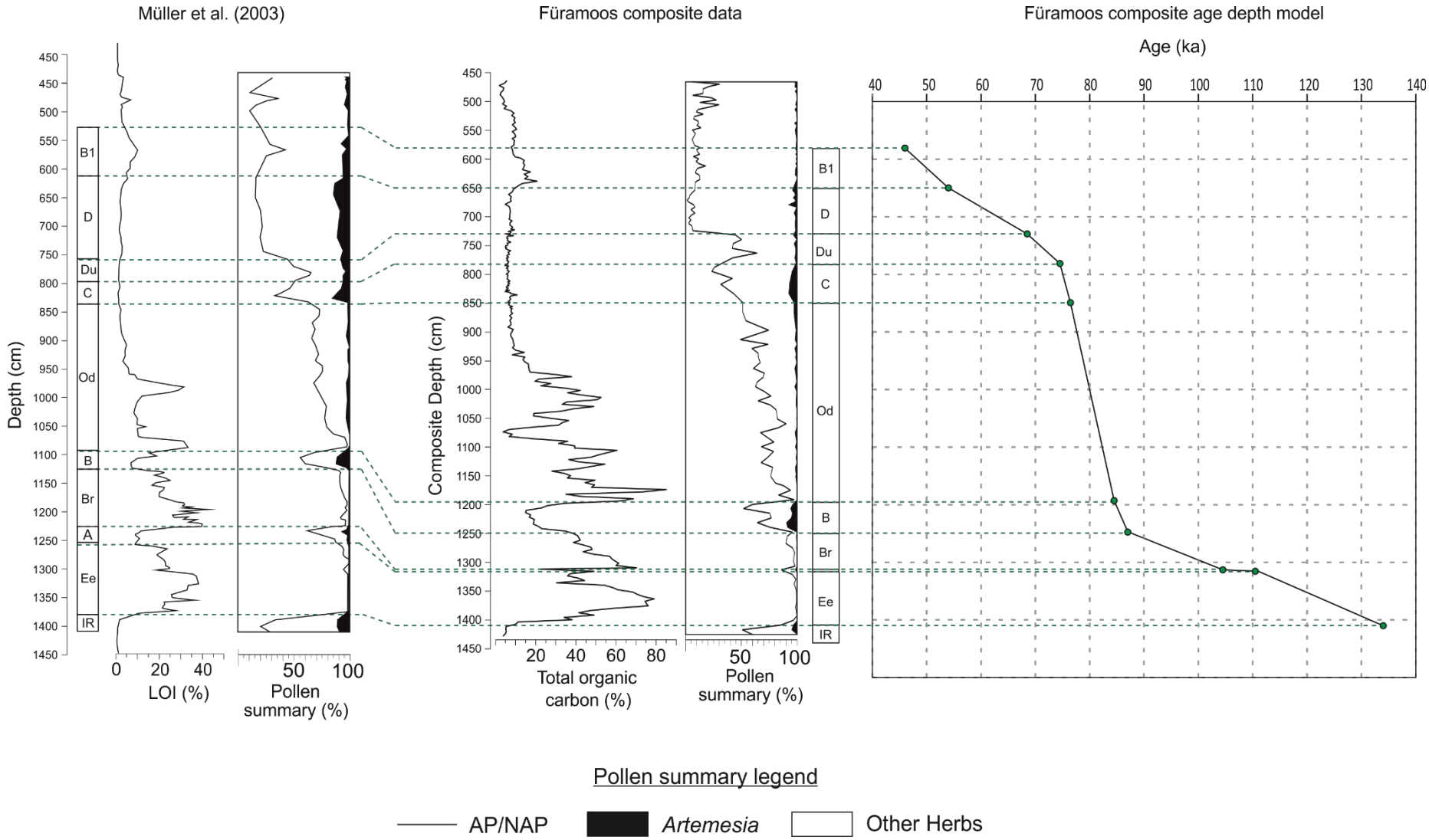
Müller et al. (2003)
Füramoos composite data
Füramoos composite age depth model
Depth (cm)
Composite Depth (cm)
Age (ka)
B1
D
Du
C
Od
B
Br
A
Ee
IR
LOI (%)
Pollen summary (%)
Total organic carbon (%)
Pollen summary legend
AP/NAP
Artemesia
Other Herbs

Appendix Figure 2: Füramoos composite core correlations to Müller et al., (2003) and the age depth model used in this thesis. Time intervals represent: LR; Late Rissian glacial; Ee: Eemian interglacial; A: Stadial A; Br: Brörup; B: Stadial B; Od: Odderade; C: Stadial C; Du: Dürnten; D: Stadial D; B1: Bellamont 1. Ages in the Müller et al., (2003) age model are based on correlations of pollen-inferred vegetation changes with changes in the North Atlantic (McManus et al, 1994) and two AMS ^{14}C dates from the middle Würmian. Ages produced for the Fu15-2 core with this age depth model differ slightly from those in Paper III. Where in Paper III the Fu15-2 core is correlated to the record of Muller et al., (2003) based on two tie points (onset of the Brörup and the *Corylus* to *Abies/Carpinus* pollen assemblage transition) here the Fu15-2 core is correlated to the Füramoos composite core based on the four tie points described in the appendix.

Delineation of a half and a full chironomid mentum

Appendix Figure 3 highlights an example chironomid mentum as well as what would be considered a half mentum and full mentum. More than half a mentum is considered to be a full mentum for counting purposes and less than a half mentum is disregarded. This is critical as chironomid mouthparts in fossil samples are often damaged and broken.

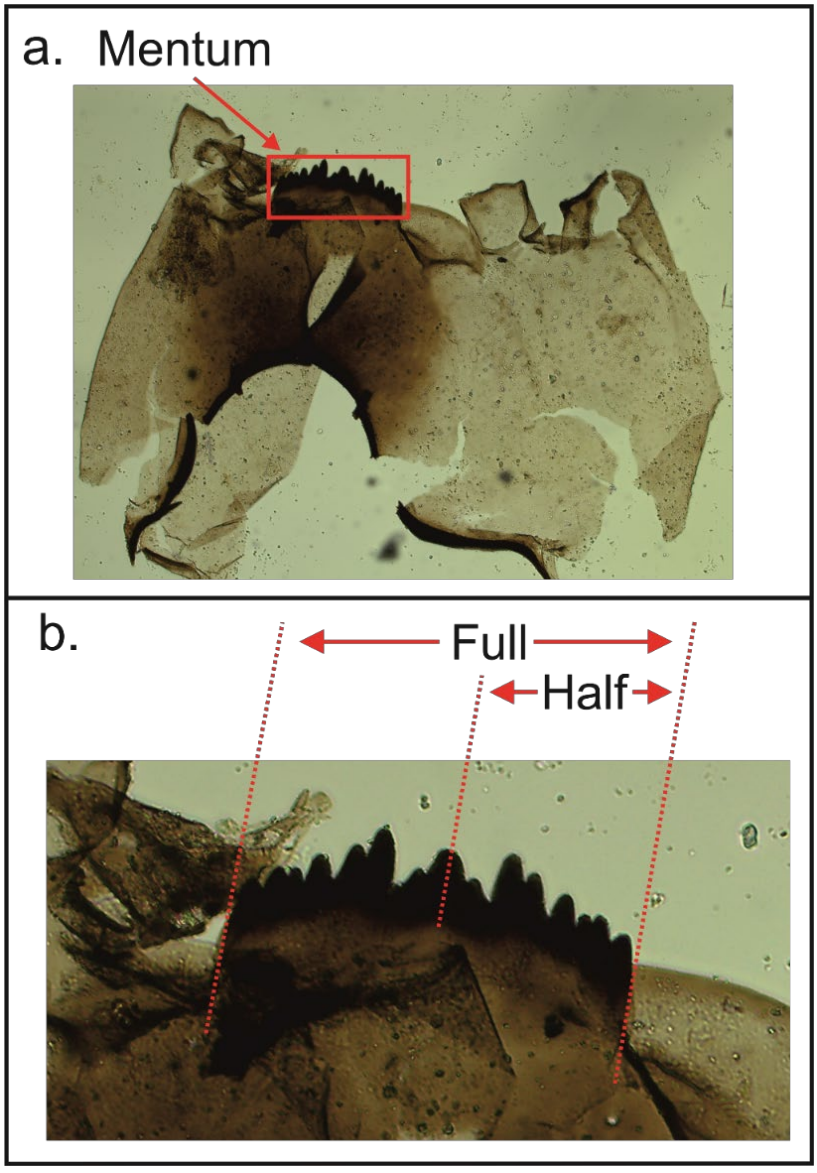

Appendix Figure 3: Illustration of the "Full" and "Half" mentum definitions referred to in text using a *Chironomus anthracinus*-type head capsule as an example. a. A full *Chironomus anthracinus*-type head capsule with the mentum identified and b. identification of the "Full" and "Half" head capsule categories described in text in regards to the mentum of *Chironomus anthracinus*-type head capsule. These categories remain even when only the mentum is preserved. A head capsule without a mentum is not counted.

10. Acknowledgements

Over the course of conducting this PhD project and compiling this thesis I, the author, have learnt many skills and techniques relative to being a chironomid analyst specifically as well as broader skills in relation to my progression as a young researcher. The first and foremost skill gained was the chironomid sample processing, picking and identification from which the vast majority of the data used in this thesis was derived. Furthermore I learnt how to produce statistics with which to describe and interpret that data, including zonation, ordination analysis, as well as how to implement a WAPLS model to reconstruct past July air temperatures and produce associated reconstruction statistics for that model. A second set of specific skills I developed while conducting this thesis was learning how to implement palynological and lithological changes, both within and without sites to correlate records. This was a skill that I repeatedly used over the course of this project, and I would not have been able to complete the thesis without it. Further skills gained include surface sediment coring, planning a field campaign and organising customs forms, teaching in a microscope lab and in the field, age depth modelling using CLAM, producing and presenting high quality presentations and the planning development and writing of original research manuscripts for publication. I also learnt that being a native English speaker does not necessarily make writing a manuscript easy.

I thank everyone who helped me with this, beginning with Oliver Heiri, who secured the funding for the project, gave me the opportunity to undertake the project and who tutored me throughout. I would also like to thank my co-authors Fabian Rey, Erika Gobet, Willy Tinner, Oliver Kern, Frederik Allstädt, Andreas Koutsodendris, Jörg Pross and Dorothy Peteet for all of their contributions and invaluable assistance. Jacqueline van der Knaap is also thanked for her work counting pollen for the Burgäschisee record. Although finishing my thesis at Basel University I spent the first two years of the project based at the University of Bern in the Institute of Plant Sciences with the Palaeoecology research group and would like to thank everyone there for providing such a welcoming environment for me to begin my PhD in. Furthermore, I would like to thank Oliver Kern, Andreas Koutsodendris, Jörg Pross and Dorothy Peteet for providing access to all three Füramoos sediment cores and all

members of the Institute of Earth Science, Heidelberg University for graciously hosting me when I went to visit and work there. In particular I would like to thank Oliver Kern who, alongside Frederik Allstädt, developed the initial interpretations and analysis of the Füramoos sediment cores, and kindly provided me with pollen, LOI and XRF data that he will be using in his own PhD thesis in the near future, enabling me to undertake this project.

I would also like to thank my friend and colleague Colin Courtney-Mustaphi who has provided me with a constant stream of advice and annoyance since he became part of our group. Ieva Grudzinska-Elsberga has provided much needed cake, chocolate and calories. Fabian Rey, who has helped me organise myself in the lab. Also Joshua Ebner, who has greatly expanded my knowledge of German beer. Finally I would like to thank my fiancé Janine, who has put up with me staying late at work and not spending as much time with her as she deserves.

This research has been funded by the Swiss National Science Foundation (SNSF grant 200021_165494).

11. References

Armitage, P.D., Pinder, L.C. and Cranston, P.S. eds., 2012. The Chironomidae: biology and ecology of non-biting midges. Springer Science & Business Media.

Bauch, H.A., Kandiano, E.S. and Helmke, J.P., 2012. Contrasting ocean changes between the subpolar and polar North Atlantic during the past 135 ka. *Geophysical Research Letters*, *39*(11).

de Beaulieu, J.L.D. and Reille, M., 1984. A long upper Pleistocene pollen record from Les Echets, near Lyon, France. Boreas, 13(2), pp. 111-132.

Beck. P., G. Caudullo, D. de Rigo, W. Tinner, *Betula pendula, Betula pubescens and other birches in Europe: distribution, habitat, usage and threats*. In J. San-Miguel-Ayanz, D. de Rigo, G. Caudullo, T. Houston Durrant, A. Mauri (Eds. 2016), European Atlas of Forest Tree Species. Publication Office of the European Union, pp. 70-73

Becker, C., 2018. Vegetations-und Klimaentwicklung in Süddeutschland während des Letzten Interglazial-Komplexes anhand neuer Bohrkerne aus Füramoos (Oberschwaben), MSc Thesis, Heidelberg University, Heidelberg.

Behre, K.E., Hölzer, A. and Lemdahl, G., 2005. Botanical macro-remains and insects from the Eemian and Weichselian site of Oerel (northwest Germany) and their evidence for the history of climate. *Vegetation History and Archaeobotany*, 14(1), pp. 31-53.

Berger, A. and Loutre, M.F., 1991. Insolation values for the climate of the last 10 million years. *Quaternary Science Reviews*, 10(4), pp. 297-317.

Beug, H.J., 1979. Vegetationsgeschichtlich-pollenanalytische Untersuchungen am Riß/Würm-Interglazial von Eurach am Starnberger See/Obb.

Bini, A., Buoncristiani, J. F., Couterrand, S., Ellwanger, D., Felber, M., Florineth, D., Graf, H. R., Keller, O., Kelly, M., Schlüchter, C., and Schoeneich, P., 2009. Switzerland During the Last Glacial Maximum (LGM) 1:500000. Swiss Topo

Bolland, A., Rey, F., Gobet, E., Tinner, W. and Heiri, O., 2020. Summer temperature development 18,000–14,000 cal. BP recorded by a new chironomid record from Burgäschisee, Swiss Plateau. *Quaternary Science Reviews*, 243, pp. 106-484.

Bond, G., Showers, W., Cheseby, M., Lotti, R., Almasi, P., DeMenocal, P., Priore, P., Cullen, H., Hajdas, I. and Bonani, G., 1997. A pervasive millennial-scale cycle in North Atlantic Holocene and glacial climates. *Science*, 278(5341), pp. 1257-1266.

ter Braak, C.J. and Juggins, S., 1993. Weighted averaging partial least squares regression (WA-PLS): an improved method for reconstructing environmental variables from species assemblages. In Twelfth International Diatom Symposium (pp. 485-502). Springer, Dordrecht.

ter Braak, C.J.F., Juggins, S., Birks, H.J.B. and Van der Voet, H., 1993. Weighted averaging partial least squares regression (WA-PLS): definition and comparison with other methods for species-environment calibration. In Multivariate environmental statistics (No. 6, pp. 525-560). Elsevier.

Brodersen, K.P. and Lindegaard, C., 1999. Mass occurance and sporadic distribution of Corynocera ambigua Zetterstedt (Diptera, Chironomidae) in Danish lakes. Neo-and palaeolimnological records. *Journal of Paleolimnology*, 22(1), pp. 41-52.

Brodersen, K.P. and Quinlan, R., 2006. Midges as palaeoindicators of lake productivity, eutrophication and hypolimnetic oxygen. *Quaternary Science Reviews*, *25*(15-16), pp. 1995-2012.

Brooks, S.J. and Birks, H.J.B., 2000. Chironomid-inferred late-glacial and early-Holocene mean July air temperatures for Kråkenes Lake, western Norway. *Journal of Paleolimnology*, 23(1), pp. 77-89.

Brooks, S.J., Langdon, P.G. and Heiri, O., 2007. The identification and use of Palaearctic Chironomidae larvae in palaeoecology. *Quaternary Research Association Technical Guide*, (10), pp. i-vi.

Caspers, G. and Freund, H., 2001. Vegetation and climate in the Early-and Pleni-Weichselian in northern Central Europe. Journal of Quaternary Science: Published for the Quaternary Research Association, 16(1), pp. 31-48.

Caudullo, G., Tinner, W., & de Rigo, D. Picea abies in Europe: distribution, habitat, usage and threats. European Atlas of Forest Tree Species. Publ. Off. EU, Luxembourg, San-Miguel-Ayanz, J., de Rigo, D., Caudullo, G., Houston Durrant, T., Mauri, A. (Eds. 2016)

Chapman, M.R. and Shackleton, N.J., 1999. Global ice-volume fluctuations, North Atlantic ice-rafting events, and deep-ocean circulation changes between 130 and 70 ka. *Geology*, *27*(9), pp.795-798.

Clark, P.U., Marshall, S.J., Clarke, G.K., Hostetler, S.W., Licciardi, J.M. and Teller, J.T., 2001. Freshwater forcing of abrupt climate change during the last glaciation. *Science*, *293*(5528), pp. 283-287.

Clark, P.U., Shakun, J.D., Baker, P.A., Bartlein, P.J., Brewer, S., Brook, E., Carlson, A.E., Cheng, H., Kaufman, D.S., Liu, Z. and Marchitto, T.M., 2012. Global climate evolution during the last deglaciation. *Proceedings of the National Academy of Sciences*, *109*(19), pp. E1134-E1142.

Dansgaard, W., Johnsen, S.J., Clausen, H.B., Dahl-Jensen, D., Gundestrup, N.S., Hammer, C.U., Hvidberg, C.S., Steffensen, J.P., Sveinbjörnsdottir, A.E., Jouzel, J. and Bond, G., 1993. Evidence for general instability of past climate from a 250-kyr ice-core record. *Nature,* 364(6434), pp. 218-220.

Dickson, T.R. and Walker, I.R., 2015. Midge (Diptera: Chironomidae and Ceratopogonidae) emergence responses to temperature: experiments to assess midges' capacity as paleotemperature indicators. *Journal of paleolimnology*, *53*(2), pp. 165-176.

Durrant T. H., de Rigo D, Caudullo. G., 2016. Pinus sylvestris in Europe: Distribution, habitat, usage and threats. In: European Atlas of Forest Tree Species, Publication Office of the European Union, Luxembourg. Publ. Off. EU Luxembourg, pp. 132–133.

Eggermont, H. and Heiri, O., 2012. The chironomid-temperature relationship: expression in nature and palaeoenvironmental implications. *Biological Reviews*, 87(2), pp. 430-456.

Engels, S., Bohncke, S.J., Heiri, O., Schaber, K. and Sirocko, F., 2008. The lacustrine sediment record of Oberwinkler Maar (Eifel, Germany): Chironomid and macro-remain-based inferences of environmental changes during Oxygen Isotope Stage 3. *Boreas*, 37(3), pp. 414-425.

Engels, S., Helmens, K.F., Väliranta, M., Brooks, S.J. and Birks, H.J.B., 2010. Early Weichselian (MIS 5d and 5c) temperatures and environmental changes in northern Fennoscandia as recorded by chironomids and macroremains at Sokli, northeast Finland. *Boreas*, 39(4), pp. 689-704.

Engels, S., Self, A.E., Luoto, T.P., Brooks, S.J. and Helmens, K.F., 2014. A comparison of three Eurasian chironomid–climate calibration datasets on a W–E continentality gradient and the implications for quantitative temperature reconstructions. *Journal of Paleolimnology*, 51(4), pp. 529-547.

Fletcher, W.J., Goni, M.F.S., Allen, J.R., Cheddadi, R., Combourieu-Nebout, N., Huntley, B., Lawson, I., Londeix, L., Magri, D., Margari, V. and Müller, U.C., 2010. Millennial-scale variability during the last glacial in vegetation records from Europe. *Quaternary Science Reviews*, *29*(21-22), pp. 2839-2864.

Greffard, M.H., Saulnier-Talbot, É. and Gregory-Eaves, I., 2011. A comparative analysis of fine versus coarse taxonomic resolution in benthic chironomid community analyses. *Ecological Indicators*, 11(6), pp. 1541-1551.

Grüger, E., 1979. Spätriss, Riss/Würm und Frühwürm am Samerberg in Oberbayern—ein vegetationsgeschichtlicher Beitrag zur Gliederung des Jungpleistozäns. *Geologica bavarica*, 80, pp. 5-64.

Guiot, J., Pons, A., de Beaulieu, J.L. and Reille, M., 1989. A 140,000-year continental climate reconstruction from two European pollen records. *Nature*, 338(6213), pp. 309-313.

Guthruf, J., Zeh, M. and Guthruf-Seiler, K., 1999. Kleinseen im Kanton Bern. Amt für Gewässerschutz und Abfallwirtschaft des Kantons Bern, Gewässer-und Bodenschutzlabor, pp. 32-34.

Heiri, O. and Lotter, A.F., 2001. Effect of low count sums on quantitative environmental reconstructions: an example using subfossil chironomids. *Journal of Paleolimnology*, 26(3), pp. 343-350.

Heiri, O. and Millet, L., 2005. Reconstruction of Late Glacial summer temperatures from chironomid assemblages in Lac Lautrey (Jura, France). *Journal of Quaternary Science*, 20(1), pp. 33-44.

Heiri, O. and Lotter, A.F., 2010. How does taxonomic resolution affect chironomid-based temperature reconstruction?. *Journal of Paleolimnology*, 44(2), pp. 589-601.

Heiri, O., Brooks, S.J., Birks, H.J.B. and Lotter, A.F., 2011. A 274-lake calibration data-set and inference model for chironomid-based summer air temperature reconstruction in Europe. *Quaternary Science Reviews*, 30(23-24), pp. 3445-3456.

Heiri, O., Koinig, K.A., Spötl, C., Barrett, S., Brauer, A., Drescher-Schneider, R., Gaar, D., Ivy-Ochs, S., Kerschner, H., Luetscher, M. and Moran, A., 2014a. Palaeoclimate records 60–8 ka in the Austrian and Swiss Alps and their forelands. *Quaternary Science Reviews*, 106, pp. 186-205.

Heiri, O., Brooks, S.J., Renssen, H., Bedford, A., Hazekamp, M., Ilyashuk, B., Jeffers, E.S., Lang, B., Kirilova, E., Kuiper, S. and Millet, L., 2014b. Validation of climate model-inferred regional temperature change for late-glacial Europe. *Nature communications*, *5*(1), pp. 1-7.

Helmens, K.F., Risberg, J., Jansson, K.N., Weckström, J., Berntsson, A., Tillman, P.K., Johansson, P.W. and Wastegård, S., 2009. Early MIS 3 glacial lake evolution, ice-marginal retreat pattern and climate at Sokli (northeastern Fennoscandia). *Quaternary Science Reviews*, 28(19-20), pp. 1880-1894.

Helmens, K.F., Väliranta, M., Engels, S. and Shala, S., 2012. Large shifts in vegetation and climate during the Early Weichselian (MIS 5d-c) inferred from multi-proxy evidence at Sokli (northern Finland). *Quaternary Science Reviews*, 41, pp. 22-38.

Helmens, K.F., 2014. The Last Interglacial–Glacial cycle (MIS 5–2) re-examined based on long proxy records from central and northern Europe. *Quaternary Science Reviews*, 86, pp. 115-143.

Hibbert, F.D., Austin, W.E., Leng, M.J. and Gatliff, R.W., 2010. British Ice Sheet dynamics inferred from North Atlantic ice-rafted debris records spanning the last 175 000 years. *Journal of Quaternary Science*, 25(4), pp. 461-482.

Hoek, W.Z. and Bohncke, S.J.P., 2002. Climatic and environmental events over the Last Termination, as recorded in The Netherlands: a review. *Netherlands Journal of Geosciences*, 81(1), pp. 123-137.

Hubbard, A., Sugden, D., Dugmore, A., Norddahl, H. and Pétursson, H.G., 2006. A modelling insight into the Icelandic Last Glacial Maximum ice sheet. *Quaternary Science Reviews*, 25(17-18), pp. 2283-2296.

Hughes, P.D., Gibbard, P.L. and Ehlers, J., 2013. Timing of glaciation during the last glacial cycle: evaluating the concept of a global 'Last Glacial Maximum' (LGM). *Earth-Science Reviews*, 125, pp. 171-198.

Hughes, P.D. and Gibbard, P.L., 2018. Global glacier dynamics during 100 ka Pleistocene glacial cycles. *Quaternary Research*, 90(1), pp. 222-243.

Johnsen, S.J., Dahl-Jensen, D., Gundestrup, N., Steffensen, J.P., Clausen, H.B., Miller, H., Masson-Delmotte, V., Sveinbjörnsdottir, A.E. and White, J., 2001. Oxygen isotope and palaeotemperature records from six Greenland ice-core stations: Camp Century, Dye-3, GRIP, GISP2, Renland and NorthGRIP. *Journal of Quaternary Science*, *16*(4), pp. 299-307.

Juggins, S., 2013. Quantitative reconstructions in palaeolimnology: new paradigm or sick science?. *Quaternary Science Reviews*, *64*, pp. 20-32.

Kaufman, D., McKay, N., Routson, C., Erb, M., Davis, B., Heiri, O., Jaccard, S., Tierney, J., Dätwyler, C., Axford, Y. and Brussel, T., 2020a. A global database of Holocene paleotemperature records. *Scientific data*, 7(1), pp. 1-34.

Kaufman, D., McKay, N., Routson, C., Erb, M., Dätwyler, C., Sommer, P.S., Heiri, O. and Davis, B., 2020b. Holocene global mean surface temperature, a multi-method reconstruction approach. *Scientific data*, *7*(1), pp. 1-13.

Kern, O.A., Koutsodendris, A., Mächtle, B., Christanis, K., Schukraft, G., Scholz, C., Kotthoff, U. and Pross, J., 2019. XRF core scanning yields reliable semiquantitative data on the elemental composition of highly organic-rich sediments: Evidence from the Füramoos peat bog (Southern Germany). *Science of The Total Environment*, *697*, 134110.

Klotz, S., Müller, U., Mosbrugger, V., de Beaulieu, J.L. and Reille, M., 2004. Eemian to early Würmian climate dynamics: history and pattern of changes in Central Europe. *Palaeogeography, Palaeoclimatology, Palaeoecology*, 211(1-2), pp. 107-126.

Kühl, N., Litt, T., Schölzel, C. and Hense, A., 2007. Eemian and Early Weichselian temperature and precipitation variability in northern Germany. *Quaternary Science Reviews*, 26(25-28), pp. 3311-3317.

Lambeck, K., Yokoyama, Y., Johnston, P. and Purcell, A., 2000. Global ice volumes at the Last Glacial Maximum and early Lateglacial. *Earth and planetary science letters*, *181*(4), pp. 513-527.

Langdon, P.G., Holmes, N. and Caseldine, C.J., 2008. Environmental controls on modern chironomid faunas from NW Iceland and implications for reconstructing climate change. *Journal of Paleolimnology*, 40(1), pp. 273-293.

Larocque, I., 2001. How many chironomid head capsules are enough? A statistical approach to determine sample size for palaeoclimatic reconstructions. *Palaeogeography, Palaeoclimatology, Palaeoecology*, 172(1-2), pp. 133-142.

Larocque-Tobler, I., Heiri, O. and Wehrli, M., 2010. Late Glacial and Holocene temperature changes at Egelsee, Switzerland, reconstructed using subfossil chironomids. *Journal of Paleolimnology*, 43(4), pp. 649-666.

Lisiecki, L.E. and Raymo, M.E., 2005. A Pliocene-Pleistocene stack of 57 globally distributed benthic δ18O records. *Paleoceanography*, 20(1).

Lischke, H., von Grafenstein, U. and Ammann, B., 2013. Forest dynamics during the transition from the Oldest Dryas to the Bølling–Allerød at Gerzensee—a simulation study. *Palaeogeography, Palaeoclimatology, Palaeoecology*, 391, pp. 60-73.

Liu, Z., Zhu, J., Rosenthal, Y., Zhang, X., Otto-Bliesner, B.L., Timmermann, A., Smith, R.S., Lohmann, G., Zheng, W. and Timm, O.E., 2014. The Holocene temperature conundrum. *Proceedings of the National Academy of Sciences*, *111*(34), pp. E3501-E3505.

Lotter, A.F., Walker, I.R., Brooks, S.J. and Hofmann, W., 1999. An intercontinental comparison of chironomid palaeotemperature inference models: Europe vs North America. *Quaternary Science Reviews*, 18(6), pp. 717-735.

Luoto, T.P., 2009a. Subfossil Chironomidae (Insecta: Diptera) along a latitudinal gradient in Finland: development of a new temperature inference model. *Journal of Quaternary Science*, 24(2), pp. 150-158.

Luoto, T.P., 2009b. A Finnish chironomid-and chaoborid-based inference model for reconstructing past lake levels. *Quaternary Science Reviews*, 28(15-16), pp. 1481-1489.

Magny, M., Aalbersberg, G., Bégeot, C., Benoit-Ruffaldi, P., Bossuet, G., Disnar, J.R., Heiri, O., Laggoun-Defarge, F., Mazier, F., Millet, L. and Peyron, O., 2006. Environmental and climatic changes in the Jura mountains (eastern France) during the Lateglacial–Holocene transition: a multi-proxy record from Lake Lautrey. *Quaternary Science Reviews,* 25(5-6), pp. 414-445.

Masson-Delmotte, V., M. Schulz, A. Abe-Ouchi, J. Beer, A. Ganopolski, J.F. González Rouco, E. Jansen, K. Lambeck, J. Luterbacher, T. Naish, T. Osborn, B. Otto-Bliesner, T. Quinn, R. Ramesh, M. Rojas, X. Shao and A. Timmermann, 2013: Information from Paleoclimate Archives. In: Climate Change 2013: The Physical Science Basis. Contribution of Working Group I to the Fifth Assessment Report of the Intergovernmental Panel on Climate Change [Stocker, T.F., D. Qin, G.-K. Plattner, M. Tignor, S.K. Allen, J. Boschung, A. Nauels, Y. Xia, V. Bex and P.M. Midgley (eds.)]. Cambridge University Press, Cambridge, United Kingdom and New York, NY, USA.

Marlon, J.R., Kelly, R., Daniau, A.L., Vannière, B., Power, M.J., Bartlein, P., Higuera, P., Blarquez, O., Brewer, S., Brücher, T. and Feurdean, A., 2016. Reconstructions of biomass burning from sediment charcoal records to improve data-model comparisons. *Biogeosciences*, *13*, pp. 3225-3244.

Martinson, D.G., Pisias, N.G., Hays, J.D., Imbrie, J., Moore Jr, T.C. and Shackleton, N.J., 1987. Age dating and the orbital theory of the ice ages: development of a high-resolution 0 to 300,000-year chronostratigraphy. *Quaternary research*, *27*(1), pp. 1-29.

Martrat, B., Grimalt, J.O., Shackleton, N.J., de Abreu, L., Hutterli, M.A. and Stocker, T.F., 2007. Four climate cycles of recurring deep and surface water destabilizations on the Iberian margin. *Science*, 317(5837), pp. 502-507.

McKay, N.P., Overpeck, J.T. and Otto-Bliesner, B.L., 2011. The role of ocean thermal expansion in Last Interglacial sea level rise. *Geophysical Research Letters*, 38(14).

McManus, J.F., Bond, G.C., Broecker, W.S., Johnsen, S., Labeyrie, L. and Higgins, S., 1994. High-resolution climate records from the North Atlantic during the last interglacial. *Nature*, *371*(6495), pp. 326-329.

van Meerbeeck, C.J., Renssen, H., Roche, D.M., Wohlfarth, B., Bohncke, S.J.P., Bos, J.A.A., Engels, S., Helmens, K.F., Sánchez-Goñi, M.F., Svensson, A. and Vandenberghe, J., 2011. The nature of MIS 3 stadial–interstadial transitions in Europe: new insights from model–data comparisons. *Quaternary Science Reviews*, 30(25-26), pp. 3618-3637.

Millet, L., Rius, D., Galop, D., Heiri, O. and Brooks, S.J., 2012. Chironomid-based reconstruction of Lateglacial summer temperatures from the Ech palaeolake record (French western Pyrenees). *Palaeogeography, Palaeoclimatology, Palaeoecology,* 315, pp. 86-99.

Mix, A.C., Bard, E. and Schneider, R., 2001. Environmental processes of the ice age: land, oceans, glaciers (EPILOG). *Quaternary Science Reviews*, *20*(4), pp. 627-657.

Müller, U.C., 2000. A Late-Pleistocene pollen sequence from the Jammertal, south-western Germany with particular reference to location and altitude as factors determining Eemian forest composition. *Vegetation History and Archaeobotany*, 9(2), pp. 125-131.

Müller, U., 2001. Die Vegetations-und Klimaentwicklung im jüngeren Quartär anhand ausgewählter Profile aus dem südwestdeutschen Alpenvorland. Geographisches Inst. der Univ. Tübingen.

Müller, U.C., Pross, J. and Bibus, E., 2003. Vegetation response to rapid climate change in Central Europe during the past 140,000 yr based on evidence from the Füramoos pollen record. *Quaternary Research*, 59(2), pp. 235-245.

Petit, J.R., Jouzel, J., Raynaud, D., Barkov, N.I., Barnola, J.M., Basile, I., Bender, M., Chappellaz, J., Davis, M., Delaygue, G. and Delmotte, M., 1999. Climate and atmospheric history of the past 420,000 years from the Vostok ice core, Antarctica. *Nature*, 399(6735), 429–436.

Olander, H., Birks, H.J.B., Korhola, A. and Blom, T., 1999. An expanded calibration model for inferring lakewater and air temperatures from fossil chironomid assemblages in northern Fennoscandia. *The Holocene*, *9*(3), pp. 279-294.

Otto-Bliesner, B.L., Rosenbloom, N., Stone, E.J., McKay, N.P., Lunt, D.J., Brady, E.C. and Overpeck, J.T., 2013. How warm was the last interglacial? New model–data comparisons. *Philosophical Transactions of the Royal Society A: Mathematical, Physical and Engineering Sciences*, 371(2001), 20130097.

Past Interglacials Working Group of PAGES, 2016. Interglacials of the last 800,000 years. *Reviews of Geophysics*, *54*(1), pp. 162-219.

Ponel, P., 1995. Rissian, Eemian and Würmian Coleoptera assemblages from La Grande Pile (Vosges, France). *Palaeogeography, Palaeoclimatology, Palaeoecology*, 114(1), pp. 1-41.

Quinlan, R. and Smol, J.P., 2001. Setting minimum head capsule abundance and taxa deletion criteria in chironomid-based inference models. *Journal of Paleolimnology*, 26(3), pp. 327-342.

Rasmussen, S.O., Bigler, M., Blockley, S.P., Blunier, T., Buchardt, S.L., Clausen, H.B., Cvijanovic, I., Dahl-Jensen, D., Johnsen, S.J., Fischer, H. and Gkinis, V., 2014. A stratigraphic framework for abrupt climatic changes during the Last Glacial period based on three synchronized Greenland ice-core records: refining and extending the INTIMATE event stratigraphy. *Quaternary Science Reviews*, 106, pp. 14-28.

Renssen, H. and Isarin, R.F.B., 2001. The two major warming phases of the last deglaciation at∼ 14.7 and∼ 11.5 ka cal BP in Europe: climate reconstructions and AGCM experiments. *Global and Planetary Change*, 30(1-2), pp. 117-153.

Rey, F., Gobet, E., van Leeuwen, J.F., Gilli, A., van Raden, U.J., Hafner, A., Wey, O., Rhiner, J., Schmocker, D., Zünd, J. and Tinner, W., 2017. Vegetational and agricultural dynamics at Burgäschisee (Swiss Plateau) recorded for 18,700 years by multi-proxy evidence from partly varved sediments. *Vegetation History and Archaeobotany*, *26*(6), pp. 571-586.

Samartin, S., Heiri, O., Kaltenrieder, P., Kuehl, N. and Tinner, W., 2016. Reconstruction of full glacial environments and summer temperatures from Lago della Costa, a refugial site in Northern Italy. *Quaternary Science Reviews*, *143*, pp. 107-119.

Sánchez Goñi, M.F.S., Landais, A., Fletcher, W.J., Naughton, F., Desprat, S. and Duprat, J., 2008. Contrasting impacts of Dansgaard–Oeschger events over a western European latitudinal transect modulated by orbital parameters. *Quaternary Science Reviews*, 27(11-12), pp. 1136-1151.

Schreiner, A., 1992. Einführung in die Quartärgeologie. Schweizerbart'sche Verlagsbuchhandlung

Seguinot, J., Ivy-Ochs, S., Jouvet, G., Huss, M., Funk, M. and Preusser, F., 2018. Modelling last glacial cycle ice dynamics in the Alps. *The Cryosphere*, 12(10), pp. 3265-3285.

Shackleton, N.J., Sánchez-Goñi, M.F., Pailler, D. and Lancelot, Y., 2003. Marine isotope substage 5e and the Eemian interglacial. *Global and Planetary change*, 36(3), pp. 151-155.

Spahni, R., Chappellaz, J., Stocker, T.F., Loulergue, L., Hausammann, G., Kawamura, K., Flückiger, J., Schwander, J., Raynaud, D., Masson-Delmotte, V. and Jouzel, J., 2005. Atmospheric methane and nitrous oxide of the late Pleistocene from Antarctic ice cores. *Science*, 310(5752), pp. 1317-1321.

Spratt, R.M. and Lisiecki, L.E., 2016. A Late Pleistocene sea level stack. *Climate of the Past*, 12(4), pp. 1079-1092.

Stern, J.V. and Lisiecki, L.E., 2013. North Atlantic circulation and reservoir age changes over the past 41,000 years. *Geophysical Research Letters*, 40(14), pp. 3693-3697.

Thienemann., A. (1921) Biologische seetypen und die gründung einer hydrobiologischen anstalt am bodensee. *Archiv für Hydrobiologie*, 13, pp. 347–370.

Tóth, M., Magyari, E.K., Brooks, S.J., Braun, M., Buczkó, K., Bálint, M. and Heiri, O., 2012. A chironomid-based reconstruction of late glacial summer temperatures in the southern Carpathians (Romania). *Quaternary Research*, 77(1), pp. 122-131.

Turner, C. and West, R.G., 1968. The subdivision and zonation of interglacial periods. *Eiszeitalter und Gegenwart*, 19(93), p. 93–101.

Turney, C.S. and Jones, R.T., 2010. Does the Agulhas Current amplify global temperatures during super-interglacials?. *Journal of Quaternary Science*, 25(6), pp. 839-843.

Verbruggen, F., Heiri, O., Meriläinen, J.J. and Lotter, A.F., 2011. Subfossil chironomid assemblages in deep, stratified European lakes: relationships with temperature, trophic state and oxygen. *Freshwater Biology*, *56*(3), pp. 407-423.

Waelbroeck, C., Labeyrie, L., Michel, E., Duplessy, J.C., McManus, J.F., Lambeck, K., Balbon, E. and Labracherie, M., 2002. Sea-level and deep water temperature changes derived from benthic foraminifera isotopic records. *Quaternary Science Reviews*, 21(1-3), pp. 295-305.

Walker, I.R., 2001. Midges: Chironomidae and related diptera. In *Tracking environmental change using lake sediments* (pp. 43-66). Springer, Dordrecht.

Walkling, A.P. and Coope, G.R., 1996. Climatic reconstructions from the Eemian/Early Weichselian transition in Central Europe based on the coleopteran record from Gröbern, Germany. *Boreas*, 25(3), pp. 145-159.

WCRP Joint Scientific Committee (JSC), 2019. World Climate Research Programme Strategic Plan 2019–2028. WCRP Publication 1/2019.

Wegmüller, S., 1992. *Vegetationsgeschichtliche und stratigraphische Untersuchungen an Schieferkohlen des nördlichen Alpenvorlandes* (Vol. 102). Birkhäuser, Basel.

Wehrli, M., Tinner, W. and Ammann, B., 2007. 16 000 years of vegetation and settlement history from Egelsee (Menzingen, central Switzerland). *Holocene*. 17(6), pp. 747-761.

Welten, M., 1988. Neue pollenanalytische Ergebnisse über das jüngere Quartär des nördlichen Alpenvorlandes der Schweiz (Mittel-und Jungpleistozän). Beiträge zur geologischen Karte der Schweiz, 162, pp. 9-40.

Woillard, G.M., 1978. Grande Pile peat bog: a continuous pollen record for the last 140,000 years. *Quaternary Research*, 9(1), pp. 1-21.

Alexander William Bolland

Home:
Address: Bruggstrasse 12a, 4153 Reinach BL, Switzerland
Email: alexander.bolland@hotmail.co.uk
Phone: +41 78 679 90 71

Work (Guest status):
Address: Geoecology, Department of Environmental Sciences, University of Basel, Klingelbergstrasse 27, CH-4056 Basel, Switzerland
Email: alexanderwilliam.bolland@unibas.ch
Phone: +41 31 631 38 68

3/1/2017 - 27/1/2021	**PhD Geoecology** Basel University
Thesis project:	Chironomid-inferred summer temperature and lake development during the last interglacial-glacial cycle in central Europe
Key skills Developed:	Chironomid sample processing, identification and numerical analysis; Palynostratigraphical correlation of sediment cores within and without site; Manuscript development and writing; Development and planning of field campaigns; Field work in adverse conditions; Teaching students in class and in the field; BSc and MSc student supervision.
Teaching:	-Teaching assistant: Advanced plant biology (1/2/1018 – 1/3/2018) -Teaching assistant: Methods in palaeolimnology and palaeoecology (25 – 28/6/2019). -Teaching assistant: Lectures and practicals: Terrestrial Palaeoenvironments and Long-Term Ecology (08/2019 – 01/2020) -Blockcourse: Ecology and Conservation Biology (06 – 28/05/2019) -Assisted supervision of two MSc students and one BSc Students
Field Campaigns:	- Surface sampling, Italy (March 2018): Campaign leader and primary organiser; Planning a surface coring campaign; Organising customs forms, Surface sediment coring; Driving; managing accommodation - Long coring campaign, Italy (June 2018): Technical assistant; Sediment coring at Lake Mergozzo and Lake Monato; Using a UWITEC Sediment corer. - Long coring campaign, Tanzanea (October 2018): Technical assistant; Using a UWITEC Sediment corer; Manual deployment of sea anchors; Driving support power boat
Academic courses Taken:	Achieved a total of 38.5 ECTS during the PhD. The following are selected courses: Writing Workflow – Forming Your Next Research Article; Quantitative analysis of palaeoecological analysis using R; Palaeoecology – Numerical tools and approaches; Palaeoecology and Palaeoclimatology of the Alps and their Forelands; Advanced Plant Biology – Paleoecology.

9/2015-9/2016:	**MSc Environmental Monitoring Modelling and Reconstruction, Distinction and Highly commended performance.** University of Manchester
Dissertation:	The chironomid palaeoecological archive of Morocco: a novel contribution to the palaeoclimate of North Africa.

Course content:	Paleoenvironmental reconstruction; Environmental monitoring and modelling concepts and practice; GIS and environmental applications; Environmental impact assessment; Peatlands and hydrology; Glacial, sea ice and sheet ice mapping.
Skills taught:	Analytical laboratory techniques including ICP-MS sample preparation, X-ray fluorescence and Magnetic susceptibility analysis; Assessment of environmental change; Matlab; Development, calibration and implementation of environmental models; GIS modelling; TAS (Terrain analysis system) modelling; River and flood modelling; Risk assessment preparation; Remote sensing analysis; Adobe illustrator.

2020-2013:	**BSc (Hons) Marine Biology and Oceanography, 2:1.** University of Newcastle-Upon-Tyne
Dissertation:	Photodissolution of River Tyne Suspended Particulate Matter and Subsequent Photobleaching of Coloured Dissolved Organic Matter
Course content:	Marine Ecology and Biodiversity; Biogeochemistry; Physical Oceanography; Marine Chemistry; Fisheries and Aquaculture; Marine Policy and Conservation; Marine Toxins, Microbiology; Marine Habitats.
Skills taught:	Ecosystem modelling; Spatial Mapping; Spectrophotometer use; Ability to conduct research at sea; Statistical analysis; Good fieldwork practice in ecological studies; Good lab practice in an analytical setting; Risk assessment preparation; Minitab software usage.

Additional Scientific Conferences / Courses

25-7/2019 - 31/7/2019	INQUA Dublin: Oral presentation to the INTIMATE session
18/6/2018 - 21/6/2018	International Palaeolimnology Association – International association of Limnology Joint conference - 2nd place in IPA poster competition - Runner up to become Young Scientist Representative in IPA committee
26/8/2018 - 31/8/2018	17th International Swiss Climate Summer School 2018 "Earth system variability through time – processes, observations and models!
5/6/2016 - 11/6/2016	Integrating ice core, marine and terrestrial records (INTIMATE) training school, Poland

---

Licences / Certifications

- Full clean Swiss driving licence.
- Powerboat licence level II – RYA.
- Maritime Radio Operator Certificate of Competence- Short Range- RYA.
- Personal Sea Survival Techniques Training (Oct 2012).

Publication List

Bolland, A., Rey, F., Gobet, E., Tinner, W. and Heiri, O., 2020. Summer temperature development 18,000–14,000 cal. BP recorded by a new chironomid record from Burgäschisee, Swiss Plateau. *Quat. Sci. Rev.*, *243*, p.106484.

Bolland, A., Kern, O. A., Allstädt, F. J., Peteet, D., Koutsodendris, A., Pross, J., and Heiri, O. 2021a (In Press). Summer temperatures during the Last Glaciation (MIS 5c to MIS 3) inferred from a 50,000-year chironomid record from Füramoos, southern Germany. *Quat. Sci. Rev*.

Bolland, A., Oliver, K., Andreas, K., Pross, J., and Heiri, O., 2021b (Submitted). Chironomid-inferred summer temperature development during parts of the late Rissian, Eemian and earliest Würmian glacial at Füramoos, southern Germany. *Boreas*.